Association between RyR and FKBP in experimental preparations: evidence for negative cooperativity

Spencer Richardson

October 2021

A thesis submitted for the degree of Doctor of Philosophy of The Australian National University

Declaration

This thesis contains no material which has been accepted for the award of any other degree or diploma in any university. To the best of the author's knowledge, it contains no material previously published or written by another person, except where due reference is made in the text.

Spencer Richardson

October 2021

Acknowledgements

To Suzy Pace and Joan Stivala for their invaluable assistance with muscle preparations, without which this thesis would not be possible, and for kindly sharing with me the benefit of their experience.

To Chris Thekkedam, for your true friendship, without which the long afternoons at the lab bench would have been much lonelier.

To Nikki Beard, Marco Casarotto, and Damien Hall, for their enormous generosity in teaching me experimental techniques, guiding my research, and supporting me in finding my path as a researcher.

And finally, to Angela Dulhunty, for her vast wisdom, steady guidance, and endless patience. I simply could not have asked for a better supervisor. I consider myself truly lucky to have had the opportunity to work with you; the years I have spent in your laboratory have been some of the most rewarding (and challenging!) of my life, and while completing this thesis took a little longer than either of us were planning, I wouldn’t trade the experience for anything!

Abstract

Ryanodine receptors (RyR), a class of massive tetrameric intracellular ion channels, are an indispensable element of excitation-contraction coupling, governing the release of Ca^{2+} from the sarcoplasmic reticulum (SR). FK506-binding proteins (FKBP), a class of soluble proteins named for their affinity to the immunosuppressant drug FK506, have long been known to bind RyR endogenously, at a stoichiometry of one FKBP per RyR monomer. Much is unknown regarding the relationship between the two species, however: for example, it is not known whether FKBP-binding sites on the RyR are fully occupied in normal physiology, or whether instead there might be a dynamic aspect to the association between the two proteins.

In this thesis, the relationship between the two most prominent isoforms of RyR, RyR1 and RyR2, and their endogenous ligands, FKBP12 and FKBP12.6, is examined via biochemical experiments. The effects of FKBP-dissociating treatments, saturation of RyR by exogenous FKBP, and the effects of the FKBP-RyR stabilising drug S107 are all examined in depth, with additional observations made on the dimerisation of GST-FKBP12 and FKBP12 and the effects of SR vesicle processing on the association between RyR and FKBP. These experiments give rise to some surprising results: FKBP-dissociating treatments have very different effects on RyR1 and RyR2, and while considerable FKBP is lost from RyR during the preparation of SR vesicles, it appears that RyR may not be endogenously saturated with FKBP.

Finally, drawing on observations made during the biochemical experiments comprising this thesis, one particularly intriguing model of a relationship between RyR and FKBP will be explored in greater depth: negative cooperation between the two species, wherein each molecule of FKBP binding to a RyR tetramer renders any subsequent binding less likely. This model is reconciled with the existing literature, and intriguing preliminary data is presented in support of negative cooperativity.

Table of Contents

List of Figures

Chapter 1: Introduction

1.0 Introduction

The general physiology of muscular contraction has been fairly well-characterised after more than a century of dedicated scientific inquiry, but on the smallest scale, as we examine the molecular machinery which underlies muscle function, many questions yet remain. This uncertainty invites inquiry, not only to “fill in” our picture of human physiology, but also because dysfunction in how this molecular machinery operates is only able to be effectively addressed when its normal functioning is well-understood. Given the potentially serious consequences of muscle dysfunction, this lends work into the fundamental processes of muscle physiology a particular urgency.

A relationship between two of the components of our muscle’s molecular machinery about which much is still uncertain is that between the ryanodine receptors (RyR), a class of massive intracellular ion channels, and the FK506-binding proteins (FKBP), so named for their affinity to the immunosuppressant drug FK506, and which perform a wide variety of functions in the cell. RyR are an indispensable element in the physiological process of “excitation-contraction (EC) coupling”, a key step in muscle contraction, and FKBP, alongside many other RyR-associated proteins, have long been known to bind to RyR endogenously. Beyond the existence of this binding relationship, however, much uncertainty still attends the question of just how FKBP regulates the behaviour of RyR – or indeed, if they do at all. In this thesis, I present a primarily biochemical investigation of several of the dimensions of the relationship between these two molecules, RyR and FKBP, with an aim towards presenting a model of their relationship that may be compared against – and possibly synthesised with – existing electrophysiological data on their interaction.

As mentioned above, despite the lack of a clear narrative about the role played by FKBP in regulating RyR activity, much work has nevertheless gone into the topic. Further, to understand the broader significance of FKBP regulation of RyR, it is necessary to contextualise their interaction within the broader physiological process – muscle contraction – that they help to effect. Therefore, the majority of this introductory chapter will be dedicated to a comprehensive review of the current state of knowledge

of FKBP interactions with RyR, all situated within the context of the current state of knowledge regarding the broader physiology of muscle tissue.

This review will begin with a broad scope, exploring the structure and function of muscle tissues, from the scale of whole muscle tissues down to the most relevant molecular interactions which enable muscle function (**1.1**). Among these interactions, in particular, the physiological process of excitation-contraction (EC) coupling will be closely detailed (**1.2**). Then, the properties of the two specific classes of molecules with which we are concerned will each in turn be examined: first, those of RyR (**1.3**); and then, those of their putative regulators, the FK506-binding proteins (**1.4**). Finally, the aims of this thesis, arising from uncertainties attending the relationship between RyR and FKBP, will be explicitly presented (**1.5**); these aims will then be addressed by the experiments presented in following chapters.

1.1 Muscle

The majority of animals on Earth rely on muscle tissue to enable locomotion, the operation of the circulatory system, the digestion of food – indeed, almost any physiological process involving “movement” is generally muscle-dependent. In mammals, muscle tissue is found in three different forms: cardiac muscle, which makes up the heart; skeletal muscle, all the muscle which is under voluntary nervous control; and smooth muscle, which is found in the gut and other internal organs, and is under involuntary control. As the aims in this thesis focus on muscle of the mammalian skeletal and cardiac systems, detailed context will be provided only for these tissue types, although interesting contrasts between cardiac or skeletal and smooth muscle function will occasionally be explored, as will differences between mammalian and non-mammalian muscles.

1.1.1 Skeletal muscle

The principle function of skeletal muscle is to effect the voluntary movement of an organism, and complementarily, to provide structural support in order to maintain posture. Skeletal muscle must therefore be able to rapidly contract while also maintaining fine control over contractile strength.

The motor neurons which innervate skeletal muscle are one of the critical factors which enable this modulation, allowing for both sufficiently frequent excitatory stimulation of muscle tissues and delicate control over fibre recruitment. A single motor neuron innervates many individual muscle fibres, forming together a single “motor unit”. These motor neurons will branch along their axon, each branch connecting to a particular muscle fibre via a structure called the motor end plate. This arrangement is illustrated in Figure **1.1**. Here, at the neuromuscular junction, the action potential conducted by the innervating axon branch causes voltage dependant calcium channels to open on the neuronal axon terminal, allowing extracellular Ca^{2+} to bind to intra-neuronal chemoreceptors, which in turn prompt acetylcholine release from the axon terminals into the space between the axon and the fibre: the synaptic cleft. Acetylcholine diffuses across the cleft and binds to nicotinic acetylcholine receptors on the fibre sarcolemma, which upon binding acetylcholine allow a Na^{+} and K^{+} influx. This ionic current depolarizes the fibre sarcolemma and initiates the process of EC coupling, which ultimately results in contraction of the fibre – much more on EC coupling can be found in section **1.2**, below.

Exactly how many muscle fibres are innervated by a given motor neuron varies from muscle to muscle, ranging from one neuron per ~10 fibres in extraocular muscles to one neuron per ~1500 fibres in large muscles such as the medial gastrocnemius of the thigh; the lower this ratio, the finer the degree of control available over muscle contraction.

Figure 1.1: Immunofluorescent stain of the neuromuscular junction in rabbit triangularis sterni muscle (adapted from Court, 2008). Motor neurons can be seen in green branching to innervate two muscle fibres, contributing to a single motor unit, or innervating only a single fibre. Axons terminate on the surface of muscle fibres in a characteristic motor end plate. Muscle fibres (**red**) are imaged by anti-laminin immunofluorescence, neurons (**green**) by anti-neurofilament immunofluorescence, and motor end plates (**purple**) by Alexa Fluor 647-conjugated α-bungarotoxin. Scale bar, ~10 μm.

The fibres of skeletal muscle are generally between 10 to 100 μm in diameter and typically between 40-60% the length of the whole muscle, occasionally spanning the full length of the muscle. Each fibre is composed principally of longitudinally-oriented contractile elements, myofibrils, which compose about 80% of the cellular volume, distinctly visible in both Figures **1.1** and **1.2**. Myofibrils are composite structures, with overlapping thick and thin microfilaments, composed respectively by myosin and actin molecules; these myofibrils are themselves organised into discrete contractile segments, called sarcomeres.

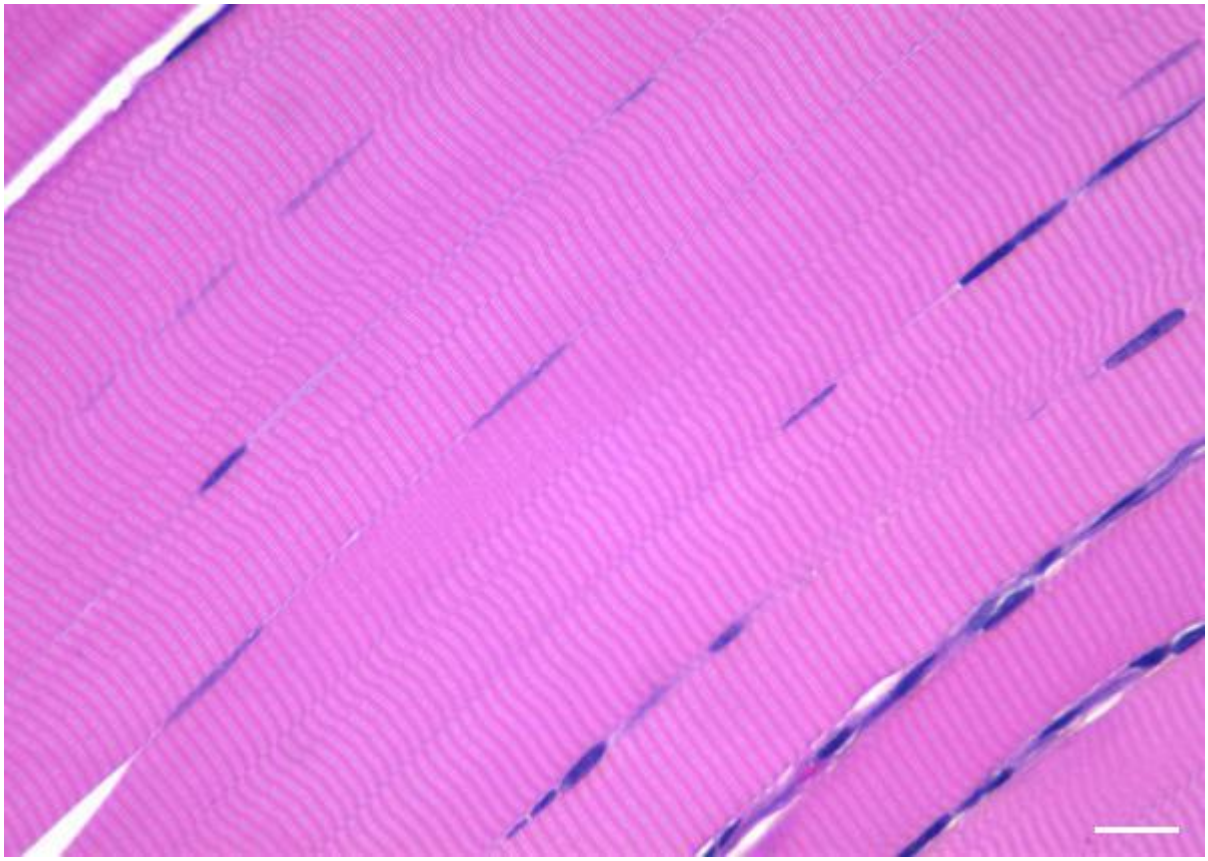

Figure 1.2: Longitudinal sections of human gastrocnemius muscle, stained with hematoxylin and eosin (adapted from Seidman, 2017). Longitudinal sections demonstrate the striated appearance of skeletal muscle. Scale bar, ~12 μm.

Each sarcomere is bounded by two “Z-lines”, to which actin attaches, and adjacent to these two Z-lines can be seen via light microscopy two faint regions, the “I-bands”, where only thin microfilaments are visible. Between these I-bands, at the centre of the sarcomere, is a darker region, the “A-band”, where thick and thin microfilaments overlap. This pattern of a dark Z-line – faint I-band – dark A-band – faint I-band – dark Z-line gives skeletal muscle its characteristic striated appearance, and is demonstrated in the electron micrograph of Figure **1.3**.

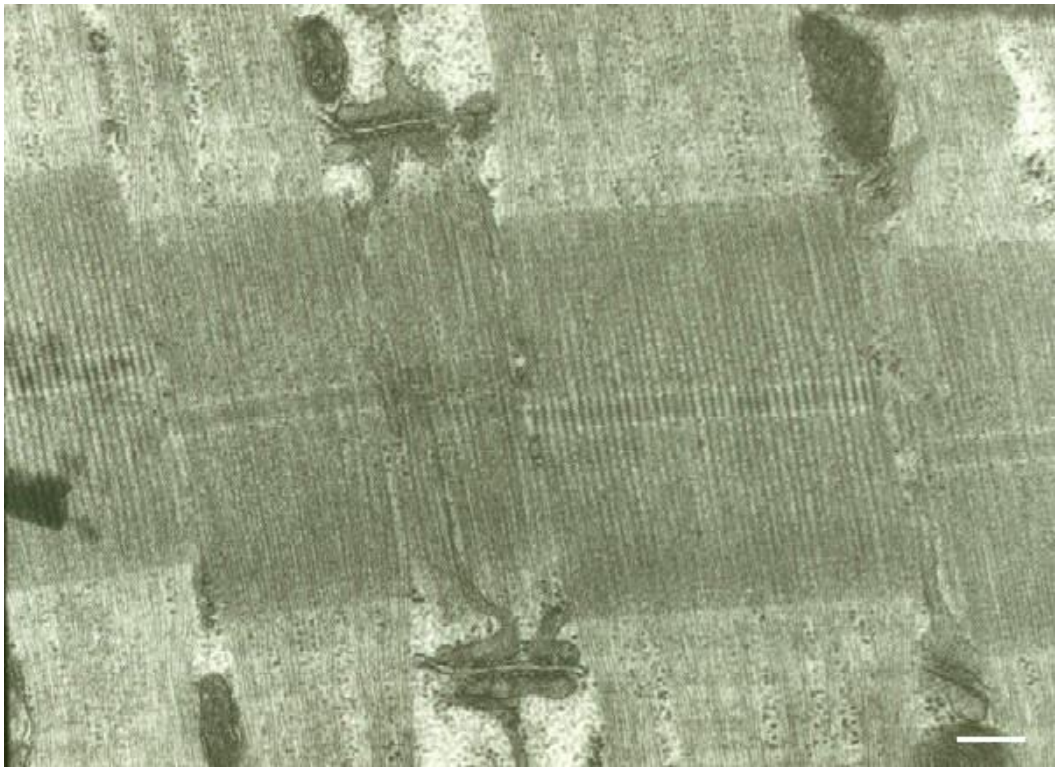

Figure 1.3: Electron micrograph of human gastrocnemius muscle (adapted from Seidman, 2017). Two triads are visible in the middle top and bottom of the micrograph, at the junction of the pale grey I-bands and the dark grey A-bands. Scale bar, ~200 nm.

As excitable tissues, muscle fibres possess a specialised plasma membrane, the sarcolemma, containing voltage-gated ion channels that effect membrane depolarisation and repolarisation in order to propagate action potentials. This sarcolemma, as well as covering the surface of the fibre, penetrates into the muscle fibre with structures called transverse tubules, or T-tubules (Franzini-Armstrong & Porter, 1964). These T-tubules run along the I-band and A-band interface in mammalian skeletal muscle (or along the Z-line in amphibia) enabling action potential propagation transversal through the cross-section of the fibre. Early experiments involving assembly of electron micrographs of slices of the frog T-tubule network revealed tubes with a dimension of ~40 x 80 nM arranged in a characteristically "tortuous" networked mesh (see **Figure 1.4** from Peachey & Eisenberg, 1978, below; Franzini-Armstrong, 1975). In mice and rats, the arrangement of T-tubules is similar, although generally narrower and longer; this varies considerably according to the muscle under examination. For example, mice and rat soleus T-tubules (18.0 nm x 78.0 nm and 16.4 nm x 75.1 nm) are significantly broader than T-tubules from rat

sternomastoid muscle (8.5 nm x 55.2 nm) (Dulhunty, 1984). Human T-tubules follow this general pattern, being somewhat narrower than in amphibians (20 – 40 nm x ~2 µm – 400 nm, Hong, 2017). Regardless of species, each T-tubule is generally flanked by the terminal cisternae of a specialised tube-shaped endoplasmic reticulum network, the sarcoplasmic reticulum, or SR (Franzini-Armstrong, 1972). This arrangement of structures – a T-tubule bounded on either side by SR – is known as a triad, and plays a critical role in contractile function, as it brings into close association several elements necessary for transforming the depolarisation of the sarcolemma into an increase in cytoplasmic calcium ion, with contraction. This interplay of elements is expanded upon further in section **1.2**, “Excitation/contraction coupling”.

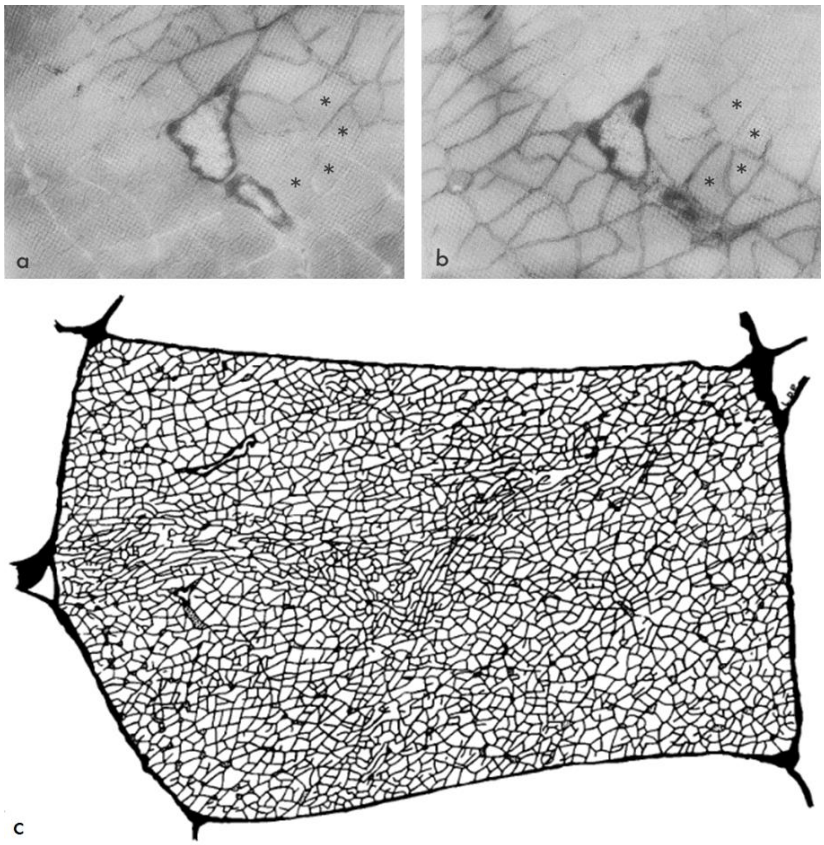

Figure 1.4: The “torturous” arrangement of T-tubule networks throughout a single myocyte (Peachey & Eisenberg, 1978). A and **B** are electron micrographs of localised areas of the T-tubule network in slices of frog skeletal muscle; **C** shows reconstruction of these slices into a complete T-tubule network map of a single fibre cross-section. No scale is given in the original, but the micrograph is at a magnification of 1400x, so 1 cm on the figure = ~7 µm.

Finally, it is worth noting that skeletal muscle fibres present (in mammals) as two physiologically distinct populations: fast or slow-twitch. Most skeletal muscle tissues possess both fibre types, with a greater relative proportion of fast-twitch muscle fibres found in muscles subject to sporadic contraction, e.g., the biceps brachii. Slow-twitch, or type I, muscle fibres contract more slowly than fast-twitch fibres and rely on aerobic metabolism. They have a higher content of mitochondria and myoglobin, the latter contributing to their darker colour when compared to fast-twitch, or type II, muscle fibres. Fast-twitch fibres are further subdivided into populations that present with higher or lower levels of mitochondria and myoglobin, the former functionally aerobic and the latter relying on glycolysis. Figure **1.5** employs fibre-specific stains to emphasise these distinctions between fibre types. Notably, motor units are composed solely of fibres of a single type, allowing for fibre-type specific contractions.

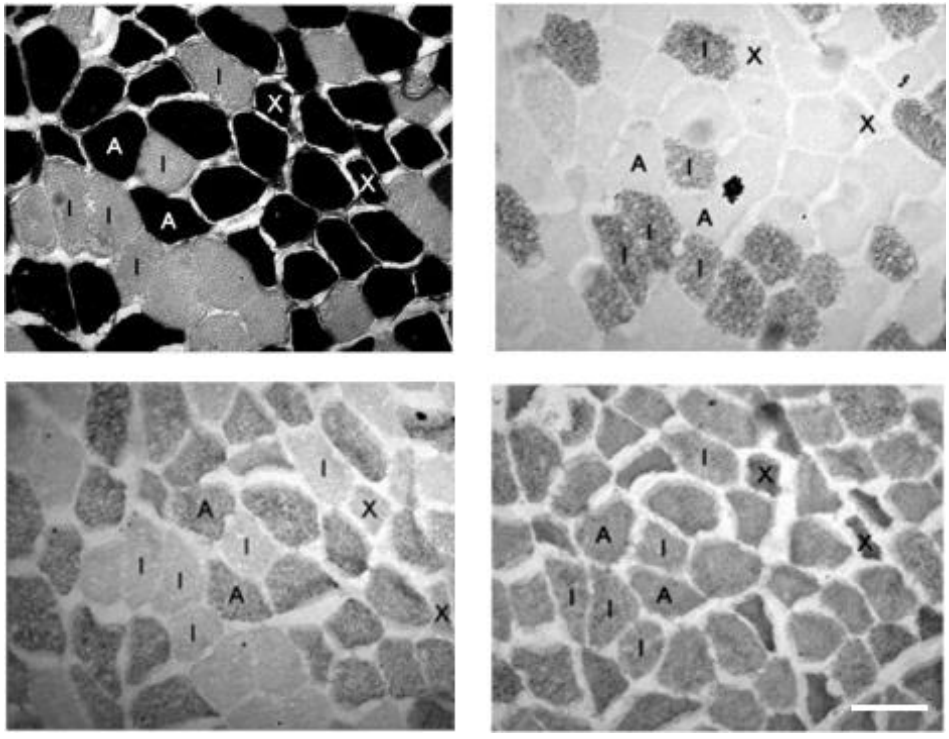

Figure 1.5: Cross-section of human vastus lateralis muscle with various stains demonstrating contrast between fibre types (adapted from Kohn, 2011). I indicates type I fibres, **A** indicates aerobic type II fibres, and **X** indicates glycolytic type II fibres. Clockwise from top left: ATPase stain affects only type II fibres; BA-D5 specifically stains type I fibres; 2F7 specifically stains aerobic type II fibres; and 6H1 specifically stains glycolytic type II fibres. Scale bar, ~80 μm.

1.1.2 Cardiac muscle

The principal mass of cardiac muscle makes up the contractile walls of the heart, or myocardium, the rhythmic pulsation of which enables the movement of blood around the body. Small papillary cardiac muscles also extend from the ventricular walls and regulate the opening and closure of heart's valves.

The innervation of cardiac muscle is somewhat more complex than that of skeletal muscle, consequent to its contraction being an entirely involuntary process, with both sympathetic and parasympathetic innervation (notably by the vagal nerves) enabling bi-modal control of conduction velocity, heart rate, and contractile force. However, unlike skeletal muscle, innervation of the heart is not what drives the cardiac action potential. Instead, these action potentials are generated by specialised myocyte clusters in the sinoatrial node and right atrium, and from there propagated rapidly across the whole of the heart.

Morphologically, cardiac myocytes are considerably smaller than skeletal muscle fibres – in particular, much longitudinally shorter, with an average size of around 125 μm x 20 μm. Each cardiac myocyte typically contains one or two centrally-located nuclei, in contrast to multinucleate skeletal muscle fibres. Cardiac myocytes also differ from skeletal fibres in their organisation: cardiac myocytes branch and interconnect, both structurally and electrically, unlike skeletal fibres which while arranged in bundles, have no inter-fibre connections. This difference in morphology is evident in Figure **1.6**. Amidst this interconnectivity, the sarcolemmae of cardiac fibres merge at junctions called "intercalated discs". These areas of intercalation are structurally and functionally heterogeneous, and can be categorised as intermediate junctions, desmosomes, or gap junctions. Intermediate junctions and desmosomes provide mechanical support and enable electrical coupling of adjacent cells, preventing their disassociation during contraction, while gap junctions, generally found parallel to the longitudinal axis of the cell, provide low-resistance pathways for the rapid propagation of action potentials through the myocardium. Together, these cellular mechanisms enable both mechanical and electrical coordination of the myocardium, such that it behaves as a single functional unit, or "syncytium"; this synchronous action is critical for fulfilling its primary physiological function of pumping blood.

A further adaption to the unique physiological demands of cardiac function is that cardiac cells have ~10 times the amount of mitochondria as compared to skeletal muscle fibres, with about 25-35% of their cellular volume taken up by mitochondria, compared to ~3-8% in skeletal muscle (Larsen, 2012). This protects against fatigue, essential for the non-stop activity of the heart. However, just as with skeletal muscle, sarcomeres occupy the greater portion of the cardiac muscle cell. While sarcomeres in cardiac cells still exhibit the Z-line / A-band / I-band morphology of skeletal sarcomeres (see Figure **1.7**, for example), the relative disorganisation and branching of their constituent myofibrils make this harder to detect, and cardiac muscle therefore typically lacks the striated appearance of skeletal muscle.

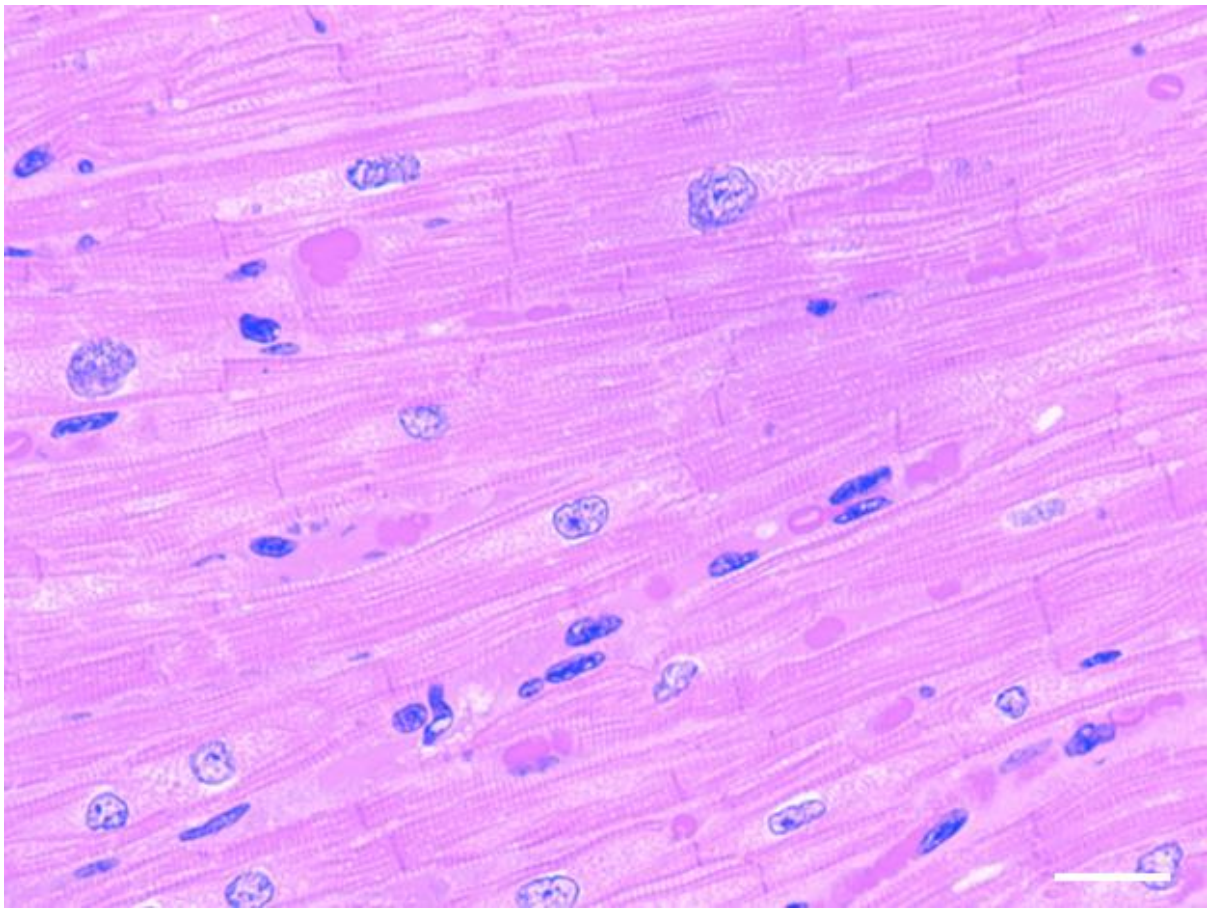

Figure 1.6: Human cardiac muscle tissue, stained with hematoxylin and eosin (adapted from Takizawa, 2018). Compared to skeletal muscle tissue (**Figure 1.2**), branching and disorganisation of individual cells is evident, as well as generally more squat and flexible cell morphology. Scale bar, ~40 μm.

Finally, the T-tubule / SR network is somewhat less complex in cardiac tissue. The SR networks themselves are typically less extensive than in skeletal cells, and their terminal cisternae present a smaller surface at T-tubule interface zones. Cardiac T-tubules are generally four to five times broader than skeletal T-tubules, with an average luminal diameter of ~300 nm in rat cardiomyocytes (Page, 1971; Page, 1979) – the diameter of cardiac T-tubules varies widely, however, with two-photon imaging of intact rabbit cardiac T-tubule networks revealing diameters from 20 to 450 nm (Savio-Galimberti, 2008). Cardiac T-tubules are also more sparsely distributed: they penetrate into the cell only once per sarcomere, proximate to the Z-line – similar to what is observed in amphibian skeletal muscle. In terms of the T-tubule / SR interface, as implied, generally a single terminal cisternae will align with or partially envelop a particular T-tubule, forming a “dyad” rather than a skeletal triad. Cardiac triads do rarely manifest, but appear and function distinctly from skeletal triads due to the width of the cardiac T-tubules and the narrowness of cardiac terminal cisternae. Further, an additional interface type, a “peripheral coupling”, may occur when junctional SR is adjacent to the sarcolemmal surface (Franzini-Armstrong 1998, 1999).

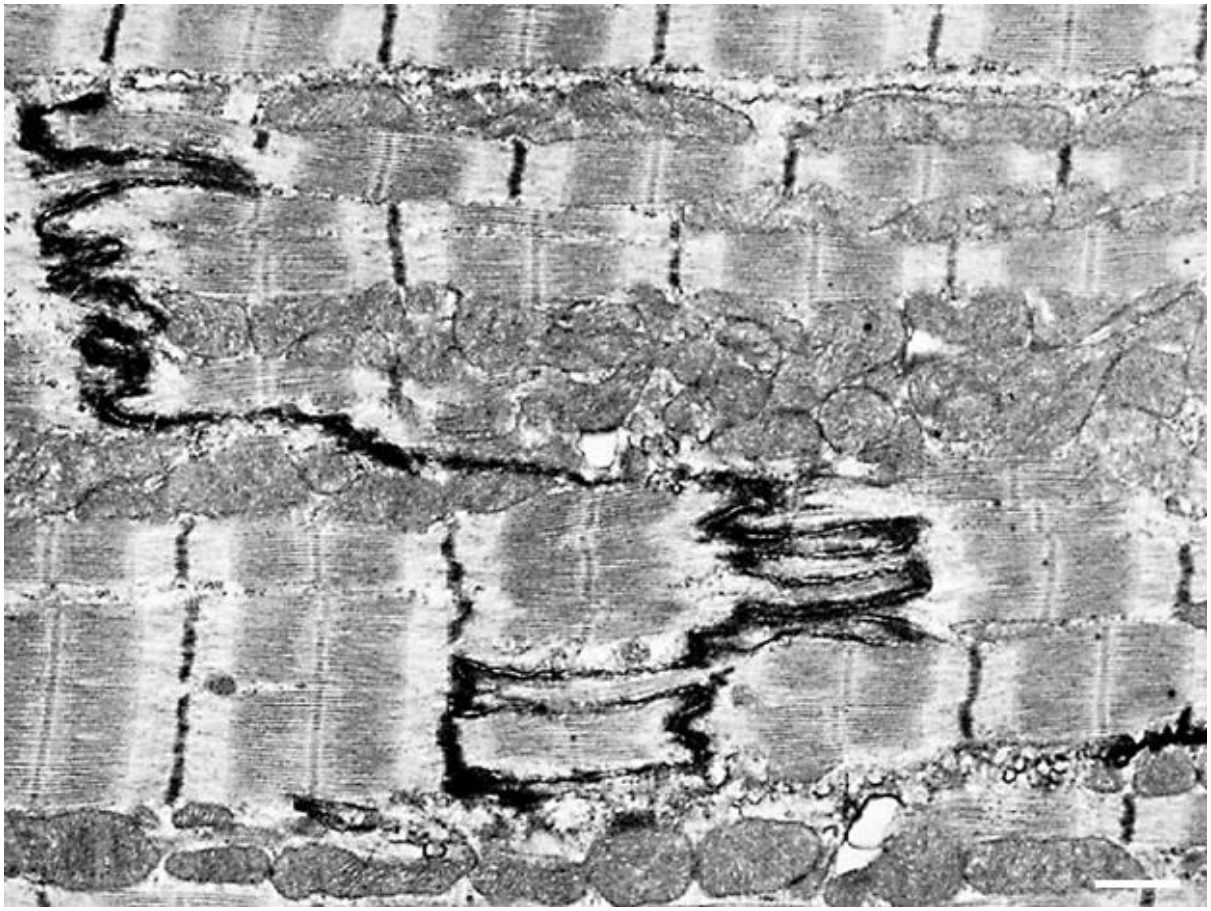

Figure 1.7: Electron micrograph of human cardiac muscle tissue (adapted from Takizawa, 2018). Contractile machinery between Z-discs is evident, but far more disorganised as compared to that in skeletal muscle (Figure **1.3**). Thickest dark portions of the micrograph indicate intercalated discs. Scale bar, ~500 nm.

1.2 Excitation/contraction coupling

As alluded to previously, the series of events between the arrival of an action potential at the dyadic or triadic junction and the contraction of muscle tissue is known as excitation/contraction (EC) coupling. The membrane and protein structures which compose the dyads or triads – and therefore, which enable the EC coupling process – are collectively referred to as calcium release units, or CRUs (Franzini-Armstrong, 1999, 2005). These constituent elements will be reviewed below, and following this, the “mechanism” of EC coupling will be examined in greater detail.

1.2.1 The calcium release unit

The CRU refers to a particular “zone” in which most of the complexity of the process of EC coupling occurs: taken broadly, junctional SR domains and their opposing T-tubule domain. These CRU interfaces are found adjacent the Z-lines of sarcomeres, in one “band” in cardiac myocytes and the non-mammalian skeletal muscle, or two bands proximate to the A-I junction in mammalian skeletal muscle.

CRUs have a characteristic proteome that supports their unique functionality, including regulatory molecules such as calmodulin or protein kinase A (in addition to FKBP) several of which will be reviewed in **1.3** and **1.4** below, but by far the two most important of these constituent proteins are: first, L-type calcium channels, sometimes referred to with the nomenclature $Ca_v1.x$, were x denotes one of the four isoforms, and also referred to as dihydropyridine receptors (DHPR). Second of these crucial proteins are the ryanodine receptor calcium release channels (RyR). Briefly, these two proteins are critical to the process of EC coupling; in particular, the transduction of an action potential into muscular contraction: DHPR respond to sarcolemmal voltage changes and transduce this signal to RyR, which in turn release SR Ca^{2+}. The pairing of these two proteins, along with the rest of the cellular transduction apparatus at a given junction, may be referred to collectively as a “couplon”; this couplon unit acts essentially synchronously with other couplons during EC coupling, due to their effectively simultaneous triggering by rapid depolarisation across the entire cross-section of the muscle fibre propagated by the T-tubule network (Stern, 1997).

The geometric arrangement and stoichometry of DHPR and RyR at the couplon differs significantly between skeletal and cardiac muscles; these differences are worth expanding upon, as they are directly related to the different modes of signal transduction seen in skeletal and cardiac excitation-contraction coupling. This, in turn, reflects the unique physiological demands of each tissue type.

In skeletal muscle, the DHPR are arranged into a “tetrad”, with each DHPR sitting at the vertex of a hypothetical square, corresponding to the geometry of the RyR tetramer. These tetrads are organised into larger arrays, and there exists a consistent stoichiometric relationship between the tetrads and their associated RyR, such that every other RyR tetramer is matched to a tetrad, leaving one RyR uncoupled for each that is paired to a tetrad (Paolini, 2004; see Figure **1.8**). This pattern of association is

unique to skeletal muscle, and the close proximity of every other RyR to a DHPR allows for mechanical interaction – whether direct or via intermediary protein structures – between the two molecules, another EC coupling property characteristic of skeletal muscle (expanded upon below, **1.2.2**).

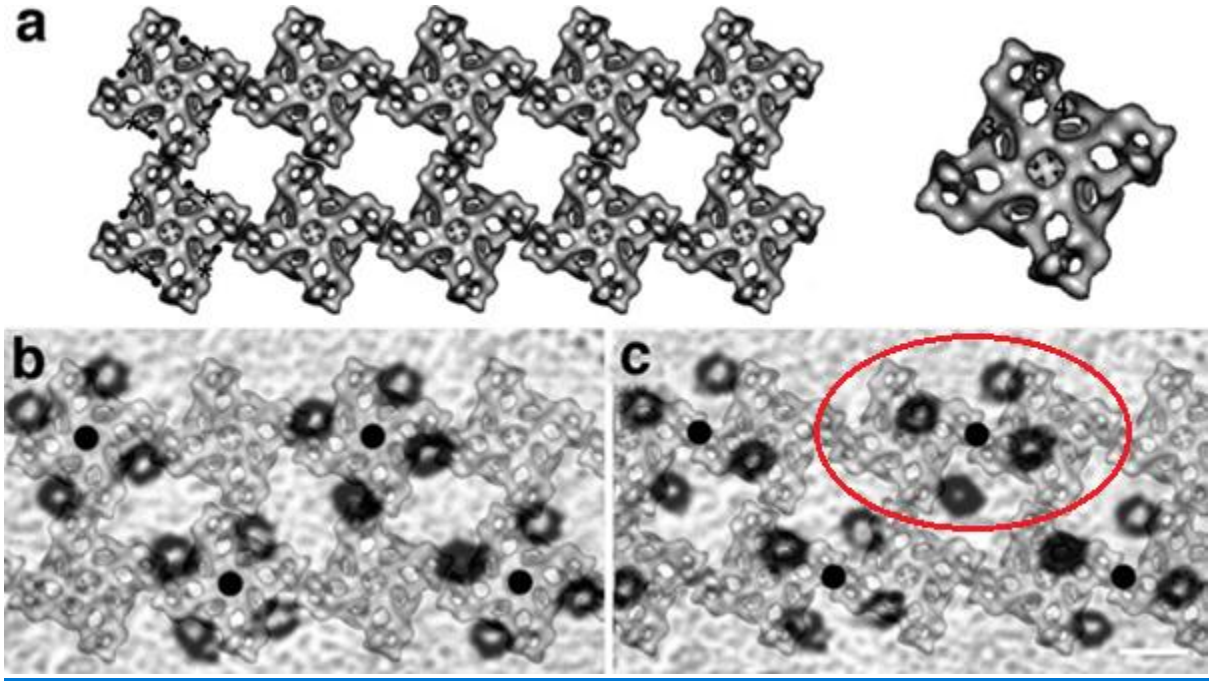

Figure 1.8: Overlay of RyR1 3D structure upon rotary shadowed micrograph of DHPR array (adapted from Paolini, 2004). DHPRs are ringed with platinum which appears dark on the micrograph. Overlay of RyR 3D structure from panel **A** (from Serysheva, 1995) shows the spatial relationship of the two CRU elements. **B** and **C** both depict possible overlay geometries; however C depicts the "sharing" of a DHPR by two RyR1s (shown in area circled in red) which is physiologically unlikely, and was therefore rejected by the authors as a potential fit. Scale bar, ~10 nm.

By contrast, cardiac DHPRs within the CRU area are rarer and not found in set groupings or geometries. The stoichiometry of a cardiac couplon is roughly 100 RyR tetramers against 10-25 DHPRs (Bers, 2002), compared to 2 DHPRs per RyR tetramer skeletal muscle; however, unlike in skeletal muscle, cardiac DHPR do not appear to be proximately matched with RyR (Sun, 1995). At the dyadic level, between 4-10 RyRs (dependant on species) are associated with each DHPR (Bers, 2002). Again, however, the arrangement of these elements of the cardiac CRU is suitable for

their mode of interaction: chemical, rather than directly mechanical, via transient extracellular Ca^{2+} fluxes through the DHPR – this mechanism is expanded upon in the following section, **1.2.2**.

1.2.2 Excitation/contraction mechanism

The initiating factor of EC coupling is the inception of an action potential, downstream from innervating neurons in the case of skeletal muscle, or from the SA node in cardiac muscle, which depolarises the muscle sarcolemma from a resting potential of ~-90 mV to an action potential threshold potential of ~-54 mV (Bers, 2002). In skeletal muscle, membrane depolarisation activates voltage-gated Na^+ channels on the sarcolemma, allowing signal propagation along the sarcolemma and down into the T-tubule network. Na^+ channels are rapidly deactivated following activation to prevent reverse propagation of the signal; additionally, voltage-activated K^+ channels repolarise the depolarised membrane via K^+ efflux (Kandel, 2013). The total duration of a skeletal muscle action potential is in the order of 2-5 ms. In cardiac muscle, the action potential initiated by the SA node is much more prolonged, typically in the order of 200-400 ms. Further, while non-pacemaking cells in the heart do activate Na^+ channels as in skeletal muscle, Ca^{2+} flux into cardiac pacemaker cells constitutes a key step in the propagation of membrane depolarisation, and subsequent to this initial depolarisation, Ca^{2+} flux into non-pacemaking cells prolongs the duration of the action potential, contributing the characteristic plateau phase (Bers, 2002).

As the depolarisation signal reaches the DHPR, they undergo a conformational change (Schneider & Chandler, 1973; Rios & Brum, 1987), which in turn induces the activation of RyR. In skeletal muscle, this signal transduction from DHPR to RyR is accomplished through mechanical interaction, presumably mediated by intermediary protein structures, while in cardiac muscle, the transduction is achieved chemically, via an influx of RyR-activating concentrations of Ca^{2+} through the DHPR from the extracellular space. In both cases, Ca^{2+} is released through the RyR from the SR, increasing cytoplasmic Ca^{2+} from 100 nM to the low micromolar range, thereby inducing myofibril shortening (Szent-Gyorgyi, 1975). This cascade of events – from membrane depolarisation to Ca^{2+} release from the SR – is generally taken to encompass EC coupling, but achieving muscle contraction requires a few more

chemical and mechanical processes that are covered below in section **1.2.3**, **Contractile machinery**.

As mentioned above, the mechanism of EC coupling differs significantly between skeletal and cardiac muscle. The nature of the "mechanical" interaction between DHPR and RyR in skeletal muscle is the subject of much investigation and is yet to be precisely resolved despite intense research efforts, but nonetheless, several aspects of this interaction have been successfully characterised. Primarily, the transduction signal appears to be communicated through a flexible, unstructured region of the α_{1S} subunit of the DHPR, the II-III loop (Nakai, 1998; Dulhunty, 1999; Grabner, 1999; Kugler, 2004; Takekura, 2004; Casarotto, 2006; Cui, 2009). However, direct interactions between the RyR1 and II-III loop have not been successfully detected (Beam, 2010; Rebbeck, 2014). Indeed, even after years of experimentation, the only evidence which might suggest a direct interaction consists of weak binding shown between the critical domain and an RYR1 fragment in a yeast two-hybrid assay (Proenza, 2002). Arguing against the possibility of a direct RyR1:II-III loop interaction, a degree of EC coupling in dysgenic myotubes was restored by a modified α1S subunit lacking both the peptide A domain and the critical domain (Ahern, 2001). Further, tetrads are not formed in relaxed-phenotype zebrafish junctions despite the presence of the intact α1S II-III loop (Schredelseker, 2005).

This lack of evidence for direct interaction between RyR1 and the II-III loop has prompted speculation that an additional protein – or proteins – may be involved in the transduction cascade, positioned between the II-III loop and RyR1. A potential candidate for this intermediary is the β_{1a} subunit of the DHPR. The β_{1a} subunit has been established to bind to residues 3201-3661 of the RyR1 (Cheng, 2005) with nanomolar affinity; specifically, 35 residues from its C-terminal have been shown to have the same interaction (Rebbeck, 2011). While binding of the β_{1a} subunit to the II-III loop has not been fully established, data, including as yet unpublished data (Casarotto, personal communication) suggests that it may be plausible. Cryo-EM structures of the DHPR indicate that such binding may be geometrically possible (Wu, 2015), and FRET experiments show a change in II-III loop conformation upon binding of the whole β_{1a} subunit to the α_{1S} subunit (Mahalingam, 2016). Recently, the protein STAC3 has emerged as another essential element of the EC coupling machinery, first identified due to a point mutation in STAC3 contributing to a rare myopathy, STAC3-

related congenital myopathy (Horstick, 2013; Nelson, 2013; Zahareiva, 2018). Intriguing evidence points towards STAC3 playing at least a mediating role between skeletal RyR and DHPR. First, simply that STAC3 lacks any paralog in cardiac muscle indicates a function for STAC3 that relates to some physiological function that is unique to skeletal muscle: the mechanical coupling of RyR and DHPR is one likely such element. STAC3 has been demonstrated to stably associate with DHPR in skeletal muscle myotubes, and interestingly, cardiac muscle myotubes also (Campiglio & Flucher, 2017). Specifically, STAC3 associates with the C-terminal EF-hand domain of the DHPR (Niu, 2018; Niu, 2018b). STAC3 is shown to localise to triads even in the absence of DHPR, indicating a potential interaction with RyR1 (Campiglio, 2018) – however, as yet, the exact mechanism of this interaction has not been characterised.

In cardiac muscle, the chemical transduction mechanism between the DHPR and RyR is responsible for a number of functional differences in EC coupling when compared with the skeletal muscle DHPR:RyR transduction mechanism. When it detects the depolarisation of the sarcolemma, the cardiac DHPR undergoes a conformational change that allows an influx of extracellular Ca^{2+} into the junctional cytoplasm. While this increase in local [Ca^{2+}] is too transient to drive contraction alone, it does activate the cardiac RyR (see below, **1.3.4.1**), enabling the release of sarcoplasmic Ca^{2+} into the cytoplasm, thereby bringing [Ca^{2+}] to a level sufficient to enable contraction. This process of chemical signal transduction is referred to as Ca^{2+}-induced Ca^{2+} release, or CICR (reviewed in Dulhunty, 2002). As the cytoplasm during contraction contains both extracellular and sarcoplasmic Ca^{2+}, to return to resting conditions and preserve homeostasis, both must be removed at a ratio of their origin, roughly 3:7 respectively (reviewed in Bers, 2002).

1.2.3 Contractile machinery

The mechanism by which Ca^{2+} released by the SR into the cytoplasm induces myofibril shortening involves the interaction of myosin protein heads and actin. Actin filaments possess a myosin-binding site that under resting cytoplasmic conditions is occluded by interaction with two other proteins, troponin and tropomyosin; as the cytoplasmic Ca^{2+} increases, it binds to troponin, which in turn dissociates troponin from actin; this

disassociation alters the tropomyosin-actin binding conformation, and as tropomyosin rotates about the actin filament, the myosin-binding site is exposed (Narita, 2001; and see Figure **1.9**).

With the hydrolysis of ATP providing energetic impetus, myosin binds to actin, which binding event causes the actin filament to be pulled longitudinally ~7 nm as the myosin head rotates. This dislocation causes disassociation of the ATP-hydrolysis products, ADP and orthophosphate, and their replacement by fresh ATP, which in turn rapidly dissociates myosin from actin. The aggregate effect of these binding and pulling cycles is to enable mass muscle contraction. Contraction ceases as cytoplasmic Ca^{2+} drops to resting as it is taken back into the SR, principally via the sarco/endoplasmic reticular Ca^{2+} ATPase, or SERCA (Sandow, 1952; Fill & Copello, 2002).

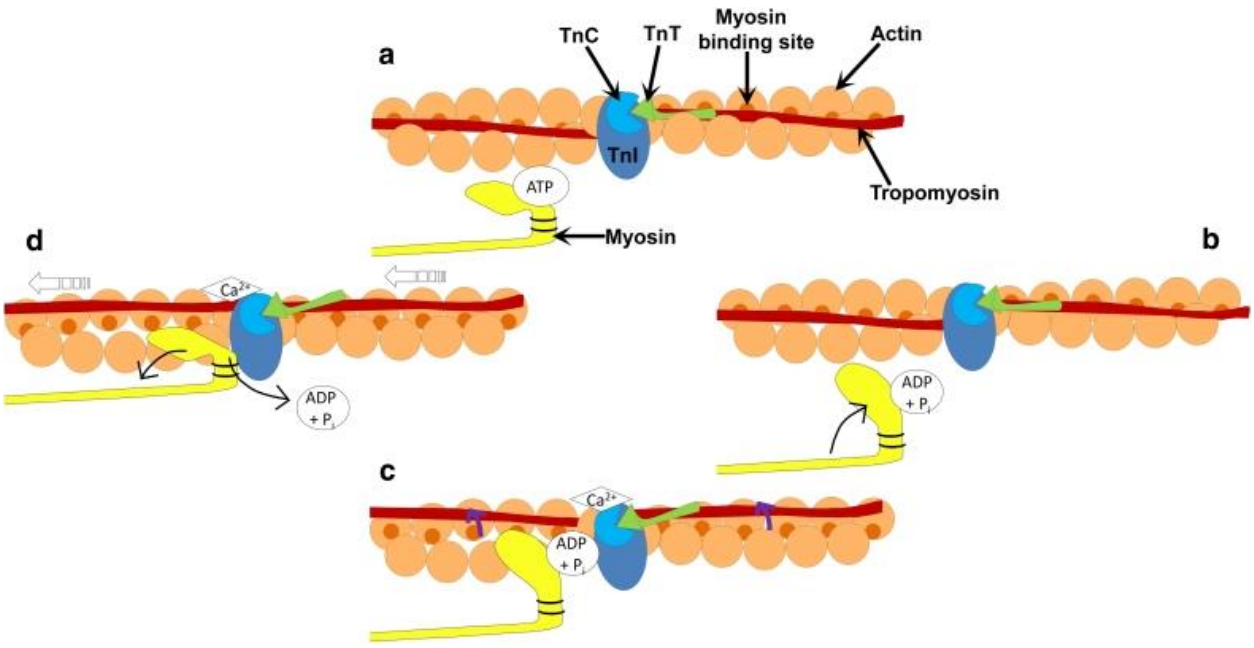

Figure 1.9: Calcium-induced myofibril shortening (modified from England, 2013). The Sliding Filament Hypothesis. **A**, ATP binds to the ATP-binding domain on the myosin head. **B**, ATP is hydrolyzed to ADP and a phosphate allowing the myosin head to move towards the actin filament. **C**, binding of Ca^{2+} to troponin C (TnC) results in a conformational change in the troponin complex, allowing the movement of tropomyosin around the actin filament. **D**, release of the hydrolyzed nucleotides results in the extension of the myosin head permitting the sliding of the filaments.

1.3 The ryanodine receptor

What would come to be known as the ryanodine receptor protein was first observed in skeletal muscle in the 1970s, seen as an electron dense protrusion from the SR membrane, forming “junctional feet”, immediately proximate to the T-tubule network of the sarcolemma (Franzini-Armstrong, 1970). The ryanodine receptor was so named for its high affinity to a particular botanical alkaloid and now-banned natural insecticide – ryanodine – which enabled its intial isolation and characterisation (Fleischer, 1985). The RyR family are homotetramers with each monomer massing ~550 kDa and the complete unit massing ~2.2 MDa, making them the largest known ion channels (Inui, 1987).

Structurally and functionally, the RyRs are broadly similar to the inositol 1.4.5-triphosphate receptors, or IP3Rs, which are ubiquitously found in the ER of all different cell types – although at low levels in muscle cells, where they are involved in regulation of gene expression rather than contractile Ca^{2+} signaling (Berridge, 2000). Much like the RyR, their main function is to effect intracellular Ca^{2+} release (Foskett, 2007). Despite broad structural and functional similarity, RyR and IP3R exhibit only ~40% homology, mostly notably across their pore domains, with the most notable structural difference between the two channel classes being the much smaller cytoplasmic domain of the IP3R.

Since IP3R and RyR may be expressed in the same endoplasmic / sarcoplasmic reticuli and are regulated by some of the same factors – notably, cytoplasmic [Ca^{2+}], which agonises IP3R synergistically with the endogenous IP3R ligand IP3 – a degree of functional coupling may exist between the two channels. In muscle, such coupling, whereby IP3R synergistically effect Ca^{2+} release from the SR alongside RyR, has been observed in skeletal muscle (Volpe, 1985; Valdivia, 1992), smooth muscle (Gordienko, 2002), and in the heart (Zima, 2004). In general, the expression levels of IP3Rs in muscle tissue are 1-2 magnitudes lower than that of RyR isoforms (Perez, 1997) and so their contribution to the Ca^{2+} efflux necessary for contraction is generally minimal. Rather, the fact that IP3R are agonised by IP3 as well as Ca^{2+}, as well as their somewhat different response range to [Ca^{2+}], means that they can effectively modulate RyR function by independently altering cytoplasmic [Ca^{2+}]. For example, in the heart, is it speculated that IP3R may enhance and stabilise CICR (Domeier, 2008).

1.3.1 RyR genetics, isoforms, and distribution

Three isoforms of the RyR are found in mammals: RyR1, RyR2, and RyR3, each encoded by a separate gene on separate chromosomes (Mattei, 1994). RyR1 was first identified in skeletal muscle (Takeshima, 1989; Zorzato, 1990); RyR2 was first identified in cardiac muscle (Nakai, 1990; Otsu, 1990); and RyR3 was first identified in brain tissue (Hakamata, 1992). Subsequently, however, RyRs have been found not to be tissue-specific. RyR1 may be found generally throughout the brain (specifically in the cerebellum and Purkinje cells), cardiac muscle, and smooth muscle, as well as in the adrenal glands, ovaries, and testes. RyR1 has also been shown to be expressed in B-lymphocytes. (Furuichi, 1994; Giannini, 1995; Lee, 2002; Nakai, 1990; Neylon, 1995; Vukcevic, 2010). RyR2 is the most common isoform found in the brain and is also expressed at low levels in many other tissues, including the stomach, kidneys, adrenal glands, thymus, lungs, and ovaries (Furuichi, 1994; Giannini, 1995; Kuwajima, 1992; Lai, 1992; Nakanishi, 1992). Finally, RyR3, contra to its original designation as the “brain isoform”, seems to play a developmental function in the genesis of striated muscle tissue, and is ubiquitously distributed in various tissue types throughout the body, with small amounts present in mature skeletal muscle (especially the diaphragm) and cardiac muscle (Neylon, 1995; Marks, 1989), as well as in the smooth muscle of the vasculature and many different organs (Giannini, 1995; Ottini, 1996). In the brain, RyR3 is primarily expressed in hippocampal neurons, Purkinje cells, the thalamus, and the corpus striatum (Hakamata, 1992; Lai, 1992; Furuichi, 1994).

These three mammalian isoforms are roughly 65% homologous in sequence, with three main regions of divergence: D1, between residues 4254 and 4631 in the skeletal sequence and 4210 and 4562 in the cardiac sequence, which in skeletal muscle appears to regulate Ca^{2+} sensitivity (Du, 2000); D2, between residues 1342 and 1403 in the skeletal sequence and residues 1353 and 1397 in the cardiac sequence, which may underlie the differences in DHPR interaction between the isoforms (Perez, 2003); and D3, between residues 1872 and 1923 in skeletal sequence and 1852 and 1890 in the cardiac sequence, which may code for Ca^{2+}-regulated inhibition sites (Hayek, 1999).

Non-mammalian vertebrates express analogous isoforms: RyRa is roughly equivalent to RyR1; RyRb to RyR3, and the “cardiac type” RyR to RyR2 (Oyamada, 1994; Ottini,

1996). In invertebrate tissues, only a single isoform has been identified, across organisms such as Drosophilia melanogaster (Takeshima, 1994), Caenorhabditis elegans (Maryon, 1996), and Homarus americanus (Quinn, 1998). In general, the invertebrate isoform exhibits strong homology across different inveterbrate species, with 82.3% homology between the Anopheles gambiae and Drosophilia melanogaster isoforms, but only very distant homology with mammalian isoforms – 46.7% homology between Drosophilia melanogaster RyR and rabbit RyR2 (Gutteridge, 2003). These differences between the insect isoform of RyR and mammalian RyR have enabled the development of insecticides targeting sites specific to the insect RyR (Sattelle, 2008). Previously, ryanodine itself was used as an insecticide, but its mammalian toxicity has precluded continued use; currently, two classes of insect-RyR-specific agonists are used, phthalic diamides (Ebbinghaus-Kintscher, 2006) and anthranilic diamides (Lahm, 2007), both of which are potent RyR agonists that act at sites found only in the insect RyR isoforms.

1.3.2 RyR structure and domains

The majority of RyR mass extends into the cytoplasm, with 80% of the protein comprising cytoplasmic domains and the remaining proportion luminal or transmembrane domains. This gives the RyR a characteristic mushroom shape, with the dimensions of the cytoplasmic portion roughly a square prism 280 Å wide and long and 120 Å deep, and the transmembrane region a cylinder of diameter 120 Å and 60 Å in length. Examination of the RyR sequence reveals several functional motifs common to other proteins, but the role that most of these motifs play in RyR function is yet to be discovered (reviewed in Samsó, 2017 and Hamilton & Serysheva, 2009). Structural examination of RyR has been impeded by several factors, most significantly the sheer size of the protein, coupled with its relative mobility in solution. However, the advent of the cryo-electron microscopy (cryo-EM) revolution in large molecule imaging has meant that near-atomic resolution structures are now available to supplement those structures previously obtained.

Three high-resolution structures of the RyR1 were obtained via cryo-EM (Yan, 2015; Zalk, 2015; Efremov, 2015), the best-resolved of which gives the structure of the molecule at an average resolution of 3.8 Å (Figure **1.10**). Even in these high-resolution

structures, the peripheral domains of RyR1 are still somewhat poorly resolved, and so it is useful to compare the various structures against one another in order to tease out their commonalities. Regardless, these three structures, together with much previously published work on both the structure of the whole RyR1 and on specific RyR1 domains, mean that we are able to confirm with high confidence much of the sequence-structure relationship of RyR1. Notably, two of the CryoEM structures (Yan, 2015 and Zalk, 2015) were obtained by capturing RyR1 with FKBP12 immobilised on a column, which was subsequently eluted with excess of either FKBP12 or FKBP12.6, meaning that structures are shown saturated with FKBP. Whether this full saturation represents the endogenous stoichiometry of FKBP12 bound to RyR1 is uncertain – more on this in section **1.4** below. By interesting contrast, and particularly feeding into the data regarding incomplete occupancy of RyR by FKBP in Chapter 4 of this thesis, the remaining study (Efremov, 2015), did not rely on FKBP-based elution of the RyR1 molecule, but nonetheless observed endogenous FKBP12 bound to the RyR at low levels of occupancy.

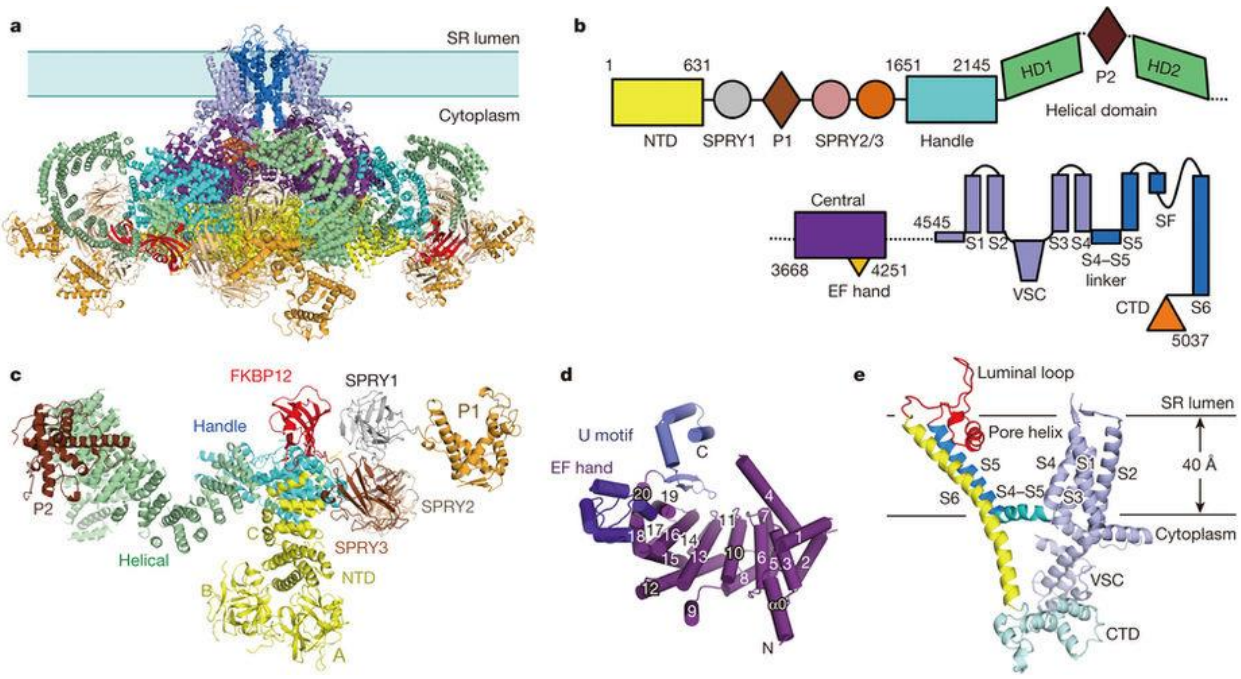

Figure 1.10: Structure of rabbit RyR1 in complex with FKBP12, and a diagrammatic representation of significant domains (Yan, 2015). **A**, Structure of RyR1 in complex with FKBP12. **B**, schematic of domain organization in a single RyR1 protomer. Domain annotations and arrangement are covered further below. **C**, Spatial arrangement of the cytoplasmic domains preceding the central domain within one RyR1 protomer. **D**, Structure of the central domain. The central domain comprises an armadillo repeat-like superhelical assembly of 20 α-helices, an EF-hand domain on the ridge of the assembly, and a U-motif at the C terminus. **E**, Structure of the channel domain from one RyR1 protomer.

A high-resolution structure for RyR2 (Peng, 2016; Figure **1.11**) followed that obtained for RyR1, revealing a high degree of homology in presentation of domains despite only 65% sequence similarity between the isoforms: this homology may be seen in panel **C** of the figure below. Notably, in this instance, structures were resolved for both the open and closed states of RyR2, illuminating the roles of non-central domains in the pore dilation process. Here, again, RyR2 destined for EM imaging was purified from muscle tissue by exploiting the affinity of RyR2 for FKBP12; however, upon size-exclusion purification, this complex apparently fell apart, resulting in RyR2 structures completely absent any associated FKBP, with a potential concomitant increase in RyR2 flexibility resulting in some motifs (e.g. armadillo repeats in the HD2 domain) appearing invisible. Complementary to these data, a cryo-EM structure for RyR2 in complex with FKBP12.6 quickly followed (Dhindwal, 2017), which similarly exploited the affinity of RyR2 for FKBP12.6, but preserved FKBP12.6 binding to the RyR2 for cryo-EM analysis, resulting in a structure with all FKBP-binding sites saturated with FKBP12.6. Two conformations were observed for the FKBP12.6-saturated RyR2, likely corresponding to the heterogenous degree of RyR2 phosphorylation in the experimental dataset. In comparison to the RyR2 structures of Peng et al. (2016), these FKBP12.6-saturated RyR2 structures had a less-flexible and thus better-resolved HD2 domain; given the posited role of FKBP12.6 in stabilisation of RyR2 gating (see **1.4.4.2** below), this indicates the HD2 domain as a potential determinant of channel stability.

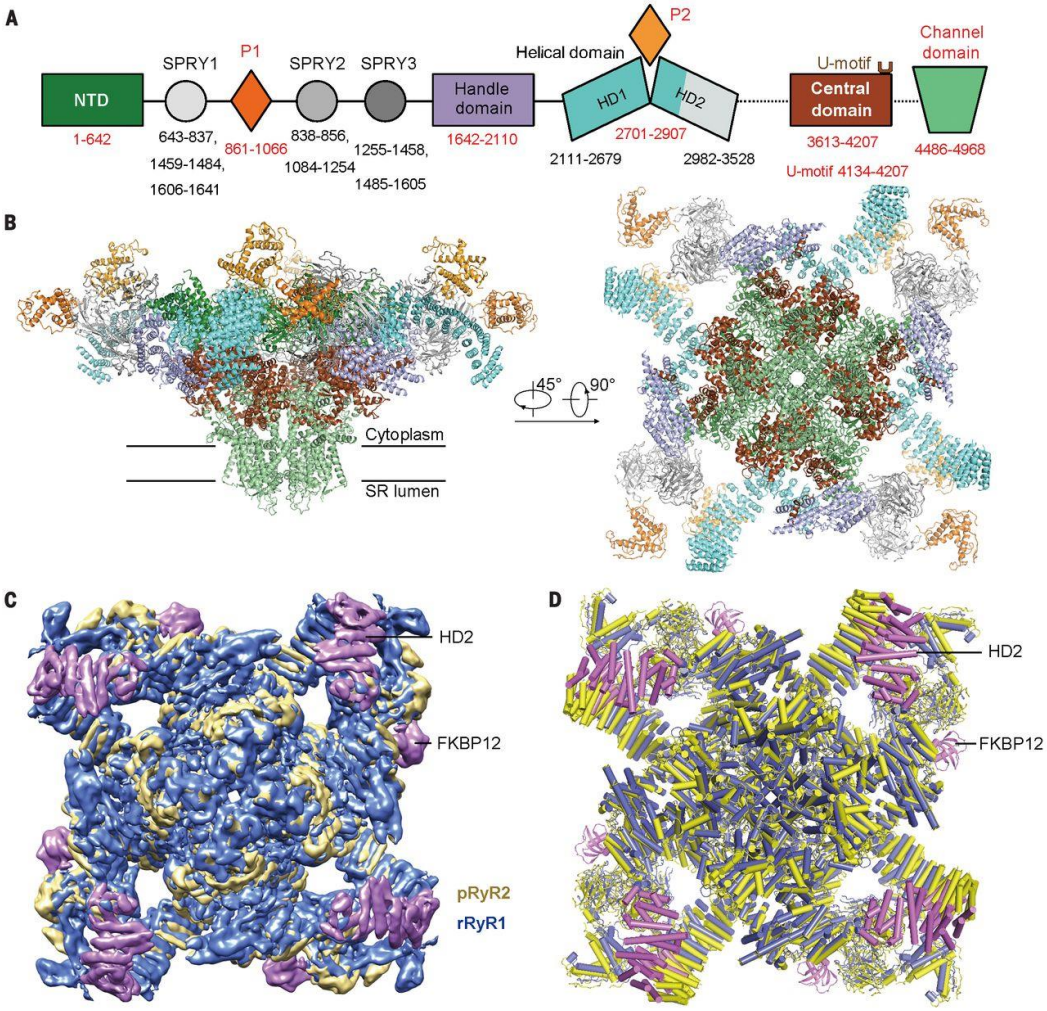

Figure 1.11: Structure of the closed porcine RyR2 and a diagrammatic representation of significant domains (Peng, 2016). A, schematic of domain organisation in a single RyR2 protomer. Domain annotations and arrangement are covered further below. **B**, structure of the closed RyR2. **C**, comparison of the EM maps of RyR2 and RyR1 structures. **D**, structural comparison of RyR2 (yellow) with RyR1. Note that all FKBP12 annotations refer to FKBP12 bound to RyR1, as no FKBP12 was apparent in the RyR2 structures.

Figures **1.10** and **1.11** give a useful basis for discussion of the labelling of the various structural features evident in the figures. Previous work on the structure of RyR, using mostly cryo-EM derived structures with an average resolution of ~10 Å, generated a generally-agreed upon nomenclature for discussing the different regions of the RyR, which has since been replaced by a newer nomenclature based on the recent more highly-resolved structures. Lanner (2010) reviews the regions of the RyR in the old-form nomenclature as follows: first, the vast cytoplasmic portion of the RyR is broadly

referred to as the “foot” domain. The highly-mobile edges of the foot are referred to as “clamps”, connected via “handle” domains at the RyR vertices that surround the “central rim” of the foot domain. The central rim then connects to the transmembrane portion of the protein via the “column” region. These broad structural divisions were further divided into 15 separate subdomains. Perhaps one of the most important revisions of this nomenclature is in labelling elements of the “clamp” and “handle” domains specifically as SPRY domains: precisely, subdomains 9 and 5 become SPRY1 and SPRY3 respectively, with SPRY2 assigned to a previously undistinguished region proximate these two subdomains. SPRY domains were first identified in *Dictyostelium discoideum* tyrosine kinase spore lysis A, and soon after found also in mammalian RyR, hence their name, a portmanteau of **SP**ore lysis and **RY**anodine receptor (Ponting, 1997). Subsequently, SPRY domains have been found in many proteins and to be involved in myriad cellular processes (reviewed in Rhodes, 2005). Characteristic of SPRY domains is their β-sandwich structure, rather than any particular amino acid sequence. In RyR, SPRY domains form a critical binding determinant for FKBP – more on this in section **1.4**, below. Further significant revisions of nomenclature include subdomains 3 and 4 of the clamp area becoming concatenated into helical domain 1, and subdomains 7 and 8 into helical domain 2. These nomenclature changes are summarised in Figure **1.12** overleaf:

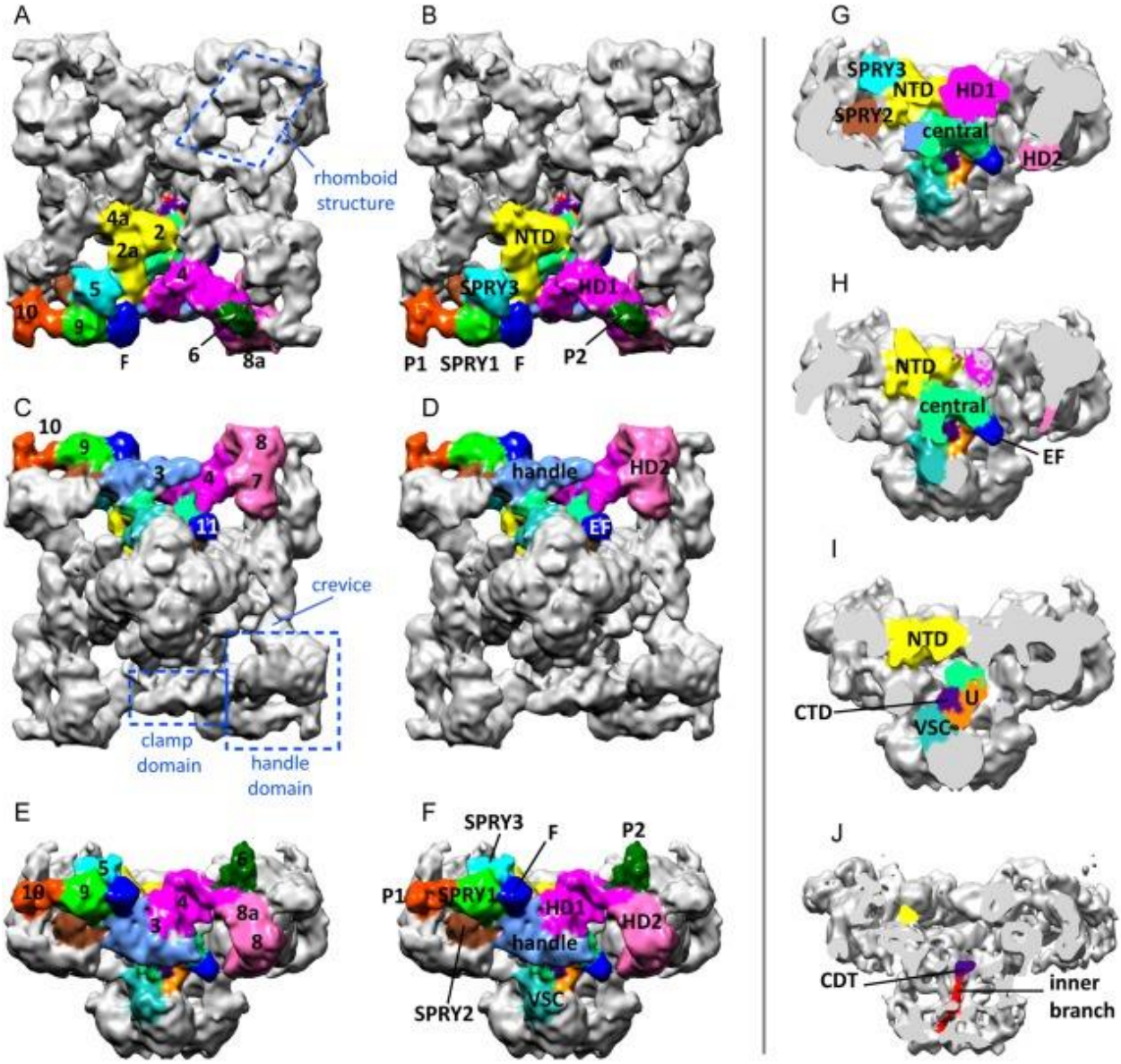

Figure 1.12: Multi-domain structure of the cytoplasmic domain of RyR1 with comparison of old and new nomenclatures (Samsó, 2017). Panels on the left show numerical designations and on the right show new domain names. **A, B,** cytoplasmic view. **C, D,** sarcoplasmic reticulum luminal view. **E, F,** side view. **G-J,** successive slices towards the fourfold axis showing the internal domains; only new domain names are here given.

Finally, quite recently, high resolution cryo-EM structures have been generated showing conformational changes undergone by the RyR in the presence and absence of various physiological modulators, such as Ca^{2+}; these will be more fully explored later in this chapter.

1.3.3 Function

The essential “functionality” of the RyR is as an ion channel, releasing Ca^{2+} from the SR to the cytoplasm. The ion conductance properties of the RyR are similar across isoforms, and indeed, were observed before the RyR itself was identified, with Smith (1985) identifying that there existed a sarcoplasmic reticulum ion channel with a Ca^{2+} conductance of 125 pS. The predicted structure of the RyR ion channel pore is similar to that of K^+ channels (Balshaw, 1999; Zhao, 1999; Gao, 2000), but with the important difference that the RyR readily conducts both mono and divalent cations. Further, the minimum radius of the RyR pore, as established in single channel experiments, is 3.3-3.5 Å (Tinker & Willams, 1993), more than twice the minimal radius of a K^+ channel pore. In general, RyR are permeable to many different monovalent and divalent cations, but exhibit little selectivity for specific mono- or divalent cations, and only moderate selectivity between mono- and divalent cations. However, they are highly selective for cations over anions. The specificity for which particular cations the RyR conducts is as follows, but again, the degree of selectivity is slight: $K^+ > Rb^+ > Na^+ \approx Cs^+ > Li^+$, and $Ba^{2+} > Sr^{2+} > Ca^{2+} > Mg^{2+}$ (Lindsay, 1991; Tinker & Williams, 1992).

The phenomena of subconductance, where RyR channels open to discrete levels below that of their maximum conductance, has been observed in both native and expressed RyR in lipid bilayer studies. In addition to a fully open state, three distinct subconductance levels have been observed, at 25%, 50%, and 75% of maximal conductance (Ahern, 1997). It was originally uncertain whether these states were consequent to the uncoordinated activation of pores present in each individual monomeric subunit of the RyR tetramer, or were a single discrete pore exhibiting multiple conductance states (reviewed in Meissner, 1994; Dulhunty, 1996). The cryo-EM images obtained of RyR (Yan, 2015; Zalk, 2015; Efremov, 2015) appear to have settled this uncertainty, showing only a single pore. The four “steps” in conductance that have been observed may correlate to the action of individual RyR monomers, or perhaps to the effect on either the whole RyR or individual subunits of regulatory molecules which are also present in quaternary stoichiometries – for example, FKBP (further discussed in **1.4.4**).

1.3.4 Regulation of function

RyR function is regulated or influenced by many different small molecules, proteins, cellular processes, and exogenous compounds – indeed, the sheer bulk of the RyR, particularly cytoplasmically, means that it presents a uniquely large surface for regulators to interact with. This can make discrete analysis of the role of a given regulatory factor difficult, as regulators may work both synergistically or indirectly, by influencing the behaviour of another regulator more so than the RyR directly. Below, a few of the most relevant of these regulatory factors will be summarised.

1.3.4.1 Small molecules

Among the endogenous small-molecule regulators of the RyR, the most critical are Ca^{2+}, Mg^{2+}, and ATP (Laver, 2018). Importantly, each RyR isoform is regulated differently by these molecules, reflecting the different ways in which they engage in EC coupling (**1.2.**). Four Ca^{2+} interaction sites across the RyR provide the primary targets for Ca^{2+} (and Mg^{2+}) regulation: two sites, one cytoplasmic and one luminal, induce activation of the RyR upon binding Ca^{2+}, while two cytoplasmic sites of differing affinity decrease RyR activity upon binding Ca^{2+}. Mg^{2+} is involved in this regulatory system primarily as a competitor for Ca^{2+} at either activation site, or at the cytoplasmic inhibition site. Finally, ATP agonises RyR, although somewhat differently between RyR isoforms, with Ca^{2+} a necessary cofactor in ATP agonism of RyR2, but ATP agonism of RyR1 possible with only trace concentrations of Ca^{2+} present (Kermode, 1998; Laver, 2001).

The best-characterised of these Ca^{2+} interaction sites is perhaps the cytoplasmic activation site. Activation of the RyR by cytoplasmic Ca^{2+} has been long-established (Meissner, 1986; Hymel, 1988), and notably, increased concentrations of cytoplasmic Ca^{2+} are sufficient to drive a large increase in channel open probability independent of any other activating ligand. Subsequently, it has been shown that RyR activity actually follows a bell curve in response to increasing levels of cytoplasmic Ca^{2+} (Tripathy & Meissner, 1996). This observation of biphasic regulation of RyR by cytoplasmic Ca^{2+} suggested that there existed also a mechanism for cytoplasmic inhibition of RyR by Ca^{2+}. That is, activation of the RyR is triggered by low micromolar

Ca^{2+} concentrations, with the threshold of this effect at around 100 nM (Zahradník, 2005), but at much higher concentrations (beginning at 100 µM for RyR1, and beginning at 1 mM for RyR2 (Bezprozvanny, 1991)), RyR are inhibited. Full inhibition of RyR1 is observed at ~1 mM cytoplasmic [Ca^{2+}], while full inhibition of RyR2 occurs at ~10 mM to ~100 mM, with an IC50 for inactivation of ~40 mM [Ca^{2+}] (Laver, 1995).

Inhibition of the RyR by very high concentrations of cytoplasmic Ca^{2+} was observed in the first experiments that established its activation by cytoplasmic Ca^{2+} (Meissner, 1986). The site at which this inhibition occurs has, as expected, been characterised to have a considerably lower affinity for Ca^{2+} than the cytoplasmic activation site, about 1 mM in RyR2 (Laver, 2007). Complicating this picture, an additional, more subtle inhibitory modulation of the RyR2 by cytoplasmic Ca^{2+} interacting with a high-affinity site has also been observed (Laver, 2007). Here, cytoplasmic [Ca^{2+}] greater than ~1 µM reduces the mean channel open time, while not, however, significantly affecting the net channel open probability due to the concurrent decrease in channel closed times caused by the action of Ca^{2+} at the cytoplasmic activation site. The subtlety of this inhibitory effect on mean channel open times means that while this mode of regulation may have an important physiological role, particularly as cytosolic [Ca^{2+}] cycles from 100-150 nm at rest to micromolar levels during contraction, it does not contribute to the broadly biphasic pattern of RyR regulation caused by Ca^{2+} interacting with the cytoplasmic activation and low-affinity inhibition sites.

RyRs have also been shown to be regulated by luminal Ca^{2+}: the susceptibility of RyRs to activation by luminal Ca^{2+} was first demonstrated in single channel bilayers by Sitsapesan and Williams (1994). Complicating this picture, however, were later findings that luminal Ca^{2+} activation is difficult to disentangle from Ca^{2+} passing through the channel and subsequently participating in cytoplasmic activation (Laver, 2007). Distinguishing the independent and synergistic effects of the luminal activation required observation of open and closed channel states separately; these studies concluded independent luminal activation may occur at ~40 µM [Ca^{2+}] in RyR2. When considered in a synergistic “physiological” context, however, luminal activation was only observed when cytoplasmic [Ca^{2+}] was sub-micromolar. As RyR1 are not physiologically activated by cytoplasmic [Ca^{2+}] during excitation-contraction coupling, it might be supposed that luminal Ca^{2+} sensitivity is more significant a factor in RyR1 regulation; however, in terms of sensitivity to luminal Ca^{2+}, RyR2 are up to ten times

more sensitive than RyR1 (Jiang, 2004; 2005). Indeed, this sensitivity to luminal Ca^{2+} activation underlies store-overload induced calcium release (SOICR), a mechanism of aberrant RyR2 activation and subsequent Ca^{2+} release that underlies a number of RyRopathies – more on this in section **1.3.5, Pathology** below. Importantly, it has been established that the sensitivity of RyR2 to luminal Ca^{2+} is highly mediated by the presence of luminal CSQ2 (Györke, 2004; Wei, 2009; Hanna, 2017), but that this is not the case for RyR1 and CSQ1 (Qin, 2009). More on this in section **1.3.4.2, Proteins**, below.

Cytoplasmic Mg^{2+} is a critical endogenous inhibitor of RyR activity (Lamb & Stephenson, 1991, 1994). Three specific mechanisms for Mg^{2+} inhibition have been presented, which are common to both the skeletal and cardiac contexts, but with the important caveat that since RyR1 has nearly a 10-fold greater affinity for both Mg^{2+} and Ca^{2+} at its cytoplasmic inhibition sites, Mg^{2+}-based inhibition plays a different physiological role in the regulation of the two isoforms. The proposed mechanisms for Mg^{2+} inhibition are as follows: first, Mg^{2+} inhibits RyR activity by competing with Ca^{2+} for binding to the high-affinity cytoplasmic activation site on the RyR (Laver, 2004). In cardiac muscle, the Ka for Ca^{2+} association is increased almost tenfold when Mg^{2+} is present at lower-than-physiological-concentrations of 220 µM, indicating an affinity for Mg^{2+} at activation site of roughly 20-60 µM, some 50 times weaker than the site's affinity for Ca^{2+}; a similar ratio obtains in skeletal muscle. Consequently, Mg^{2+} inhibition via competition with Ca^{2+} for binding to an activation site is only effective at low cytoplasmic [Ca^{2+}] levels, i.e., when the muscle is at rest. This mode of regulation may therefore be interpreted as a "brake" upon Ca^{2+} release in resting muscle. The second mode of regulation is that Mg^{2+} may compete for binding to the RyR's luminal activation site in a similar fashion that it competes for binding to the cytoplasmic activation site (Laver, 2008). Much as with the RyR's activation by luminal Ca^{2+}, its inhibition by luminal Mg^{2+} is synergistic in fashion, with Mg^{2+} competing with nearly equal affinity to Ca^{2+} for the luminal activation site. Notably however, when non-physiological Mg^{2+} gradients are introduced, a far greater impact is observed from Mg^{2+} flowing through the channel to subsequently inhibit the cytoplasmic activation site. Finally, and significantly, at sufficiently high concentrations, Mg^{2+} may bind to the low-affinity cytoplasmic inhibition site, with a similar effect to Ca^{2+} binding (Laver, 1997; these relationships are summarised in Figure **1.13**). Here, the isoform-specific differences in

affinity for divalent ions at the cytoplasmic inhibition sites result in the major physiological difference in Mg^{2+}-based regulation of RyR. In the heart, the elevated cytoplasmic [Ca^{2+}] levels during contraction are sufficient to overcome inhibition caused by Mg^{2+} binding to the cytoplasmic inhibition sites, while in skeletal muscle, this Mg^{2+}-inhibition still counteracts the increased cytoplasmic [Ca^{2+}]. This difference is a factor in the fundamental difference between the modes of EC coupling between the two isoforms (**1.2**). The persistent Mg^{2+}-inhibition observed in skeletal muscle is naturally not constitutive, however: during T-tubule depolarization and subsequent EC coupling, the affinities of RyR1 for Mg^{2+} at both inhibition and activation sites are reduced almost tenfold, relieving inhibition of RyR1 by Mg^{2+} and permitting its activation by normal concentrations of cytoplasmic ATP, synergistically assisting in EC coupling promoting mechanisms, i.e. mechanical signal transduction from the DHPR (Dutka and Lamb, 2004).

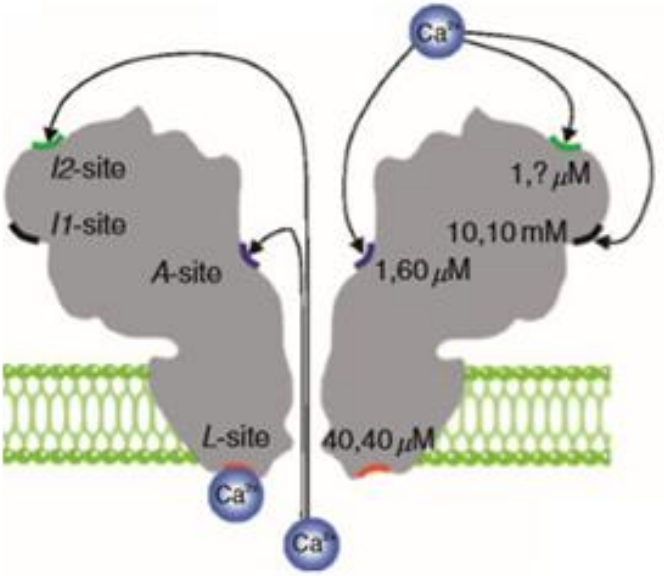

Figure 1.13: Ca^{2+}/Mg^{2+} regulatory sites on the cardiac RyR (from Laver, 2010; in turn adapted from a silhouette by Samsó, 2005). The four small-molecule interaction sides are shown on the left RyR subunit, with the nomenclature developed by Balog, 2001, and their affinities for first Ca^{2+}, and then Mg^{2+}, are shown on the right RyR subunit. A-site is the cytoplasmic activation site, L-site is the luminal activation site, I2-site is the low-affinity cytoplasmic inhibition site, and I1-site is the high-affinity cytoplasmic inhibition site.

Finally, cytoplasmic ATP is an endogenous agonist of RyR1 and RyR2 (Meissner, 1984; Smith, 1986) with two different mechanisms of action. Primarily, ATP can activate the RyR1 by interacting with a specific adenosine nucleotide binding site (Smith, 1986; Laver, 2001) located at the mutual junction of the S6c, CTD, and TaF domains, near the RyR1 pore (des Georges, 2016). Secondly, ATP can indirectly activate RyR1 by providing a substrate for the activity of calcium calmodulin kinase II, thereby effecting the phosphorylation of the RyR and increasing its activity (Sonnleitner, 1997; Dulhunty, 2001); notably, this phenomenon was first observed in the amphibian skeletal RyR (Wang & Best, 1992). ATP alone is insufficient to strongly activate RyR2, although it strongly increases RyR2 sensitivity to Ca^{2+}-induced activation (Kermode, 1998), while ATP is sufficient to activate RyR1 when only trace amounts of Ca^{2+} are present (Laver, 2001). Notably, synergistic activation of RyR2 through the combination of ATP and Ca^{2+} binding is observed at both cytoplasmic and luminal Ca^{2+}-binding sites (Tencerová, 2012). More on the regulation of RyR by phosphorylation can be found below, in section **1.3.4.3**, Post-translational modifications.

1.3.4.2 Proteins

The vast size of the RyR, particularly its cytoplasmic domain, enables regulation by a number of different proteins simultaneously. Among these are the calcium-binding proteins calmodulin and S100A1, and the FK506-binding proteins, or FKBP. Due to their importance to this thesis, FKBP will be covered separately in section **1.4**. The RyR luminal surface binds the regulatory proteins calsequestrin, triadin, and junctin, which together with the RyR form a quaternary membrane-bound complex (Guo & Campbell, 1995; Zhang, 1997; Shin, 2000; Wei, 2006; Beard & Dulhunty, 2015).

Of the other RyR-regulatory proteins, perhaps the most examined is calsequestrin, or CSQ; some controversy, however, still remains as to its mode of regulation. It was first isolated from the SR of skeletal muscle by several groups in the 1970s (Ikemoto, 1972; Meissner, 1973) and was described as a Ca^{2+} storage and buffering protein with a MW weight of approximately 44 kDa. Subsequently, a cardiac isoform was identified in cardiac tissue (Campbell, 1983), and so the two isoforms have been named respectively CSQ1 and CSQ2. CSQ is found in high abundance adjacent to the SR

junctional regions in which RyR is concentrated and appears to be anchored to the SR by filamentous accessory proteins – likely triadin and junctin (Franzini-Armstrong, 1987). In general, the importance of CSQ-regulation of RyR is clearly demonstrated in knockout and overexpression studies, with CSQ deficiency in cardiac tissue resulting in improper Ca^{2+} handling and subsequent susceptibility to CPVT (Postma, 2002; Lahat, 2004), and CSQ2 overexpression suppressing SR Ca^{2+} transients and causing severe cardiac hypertrophy in mouse models (Jones, 1998; Sato, 1998; Terentyev, 2003). CSQ1 knockout in mice results in significant remodelling of calcium release units, with multilayered junctions, an increase in mitochondria and RyR1 density, and more constricted junctional SR (Protasi, 2009). Physiologically, CSQ1 knockout increases susceptibility to malignant hypothermia (Protasi, 2009). Importantly, the mode of CSQ regulation appears to differ between isoforms, with CSQ1 inhibiting RyR1, while CSQ2 increases the open probability of both RyR1 and RyR2 (Wei, 2009).

Triadin was first identified as a 95 kDa protein associated with the skeletal muscle triad – hence its name – and was initially thought to connect the DHPR to the RyR (Kim, 1990). Subsequently, this time as a 32 kDa protein, it was also identified in cardiac muscle (Peng, 1994). Now, however, it is known that the triadin gene may be multiply spliced, resulting in different-sized triadin products. In rodent skeletal muscle, four splice variants exist, Trisks 95, 51, 49, and 32, the number denoting their molecular weight in kDa (Marty, 2000; Vassilopolous, 2005). Curiously, no particular muscle or fibre specificity in terms of the expression of these splice variants has been noted. Trisk 32 is in fact also the 32 kDa triadin which was first noted in cardiac tissue, and in the cardiac context may be referred to as CT1 (Kobayashi & Jones, 1999), where it is the predominant isoform. Two other isoforms have been identified in cardiac tissue, CT2 and CT3 (Guo, 1996; Hong, 2001).

In terms of regulation of RyR, overexpression of Trisk 95 in skeletal myotubes was observed to subvert depolarisation-induced Ca^{2+} release from the SR (Rezgui, 2005). Curiously, suppression of triadin, whether by mutation of triadin-interacting residues on the RyR (Lee, 2004; Goonasekera, 2007) or by siRNA interference with triadin expression (Wang, 2009), also inhibited depolarisation-induced Ca^{2+} release from the SR. A mouse model with a total deletion of triadin proved not to be fatal, and indeed, exhibited mostly normal skeletal muscle function (Shen, 2007). There was observed a concomitant reduction in calsequestrin expression in the KO model, and here, again,

the loss of triadin inhibited depolarisation-induced Ca^{2+} release (Shen, 2007). None of these studies suggest an exact regulatory mechanism by which this activity is exercised, but it is likely due to the removal of triadin resulting in a general disorganisation of the triad – in the mouse KO model, up to 30% of triads in EDL muscle were observed to be disordered (Shen, 2007). Triadin has also been demonstrated to have a specific effect on the activity of the RyR, with luminal triadin added to RyR in single channel experiments increasing RyR open probability up to twofold (Györke, 2004; Wei, 2009; Wium, 2012).

Junctin was first identified in the 1980s as a CSQ-binding protein of approximately 26 kDa, present in the junctional SR membranes of both cardiac and skeletal muscle (Mitchell, 1988). The membrane topology and structure of junctin is broadly similar to that of triadin: it is an integral membrane protein, with a short cystoplasmic N-terminal protrusion, a hydrophobic helix that spans the SR membrane, and the bulk of the protein protruding into the lumen as a highly-charged C-terminal length (Jones, 1995). The function of junctin was initially speculated to be solely a CSQ-anchoring protein, but has since been somewhat expanded to encompass a degree of regulatory action upon the RyR (Li, 2015; Gergs, 2007; Yuan, 2007). In general, junctin exists as a single isoform; however, an additional splice-variant, with a 15 amino acid insertion, has been identified in human cardiac tissue, although not yet in the cardiac tissue of any other organism – the functional difference of this splice variant is yet to be characterised (Lim, 2000).

Junctin has long been shown to interact with RyR (Zhang, 1997), but the purpose of this interaction and the role played by junctin in regulating the RyR is not well understood. Knockdown and knockout experiments have, in cardiac muscle, demonstrated irregular Ca^{2+} release, greater in both frequency and magnitude as compared to wild-type cells, with the degree of irregularity proportional to the degree of junctin ablation (Yuan, 2007); however, the nature of these experiments means that it is difficult to state whether this irregularity is caused by a lack of junctin interacting directly with RyR, or just the lack of junctin interacting with a different modulator of RyR, such as CSQ. Lipid bilayer experiments (Györke, 2004) have demonstrated that luminal junctin significantly increases RyR open probability, but again point to the primary role of junctin as a constituent element of the quaternary RyR-CSQ-junctin-triadin membrane complex (Li, 2015).

Calmodulin (CaM) and S100A1 are both small cytoplasmic proteins that bind Ca^{2+} via EF-hand motifs. These motifs are active at contractile cytoplasmic [Ca^{2+}], but not at resting [Ca^{2+}]. When occupied with Ca^{2+}, the motifs induce a conformational change in their proteins, enabling the exposure of a hydrophobic pocket implicated in protein binding (Maier & Bers, 2002). CaM binds directly to RyR with a stoichiometry of 4 per homotetramer, or one per subunit (Moore, 1999). All three isoforms of RyR are regulated by CaM, both in its Ca^{2+}-free and Ca^{2+}-bound conformations (Tripathy, 1995; Yamaguchi, 2005). Ca^{2+}-free (when cytoplasmic [Ca^{2+}] is <1 µM) CaM acts as a partial agonist of RyR1 and RyR3, while inhibiting RyR2, whereas with Ca^{2+}-bound, CaM inhibits all isoforms of the channel, suppressing SR Ca^{2+} release (Ikemoto, 1998; Fruen, 2000; Balshaw, 2001; Yamaguchi, 2005). Crucially, CaM inhibition of RyR2 is dependent upon phosphorylation of either residues S2808 or S2814 (Walweel, 2019). In general, CaM appears more critical for regulation of RyR2 than RyR1. A study of CaM deficient skeletal muscle showed only a modest impact on RyR1 function (Yamaguchi, 2011), while mutation or ablation of CaM in cardiac muscle resulted in RyR2-mediated cardiac arrythmias, chiefly CPVT-type arrythmias (Nyegaard, 2012; Nomikos, 2014; Søndergaard, 2015 & 2017). This critical role for CaM in the regulation of RyR2 is supported by findings in bilayer studies, where CaM prolonged RyR2 close times, allowing Ca^{2+} to diffuse away and prevent cyclic CICR-type channel activation (Xu & Meissner, 2004).

S100A1, as mentioned above, is like CaM, a small Ca^{2+}-binding protein. S100A1 was thought to compete with CaM for the same binding site in RyR1 (Wright, 2008; Prosser, 2008) and thereby modulate RyR activity, but more recently, concurrent modulation of the RyR1 by both S100A1 and CaM has been observed in FRET studies, where S100A1 regulation of the channel is independent of its competition for the CaM binding site (Rebbeck, 2016). Single channel studies of S100A1 point towards an inhibitory mode of S100A1 regulation, at least for RyR2 (Yamaguchi, 2013). However, the effects of S100A1 across the RyR isoforms have yet to be fully characterised.

1.3.4.3 Post-translational modifications

RyR have been shown to be significantly affected by post-translational modifications such as phosphorylation and thiol modification by ROS/RNS: these modifications are

important in normal physiology, but abnormal modifications also play a significant role in RyR dependent disorders.

RyR modulation consequent to phosphorylation was first identified in the 1980s in cardiac muscle (Takasago, 1989), yet the functional impact of phosphorylation on RyR activity remains somewhat controversial. In total, three serines on RyR2 (S2808, S2814, and S2030) and one on RyR1 (S2843) have been identified as phosphorylation targets, with three different potential kinases acting upon them: protein kinase A (PKA), calmodulin-dependent protein kinase II (CaMKII), and protein kinase G (PKG) (Benkusky, 2007; Camors & Valdivia, 2014; Huke & Bers, 2008; Marx, 2000; Reiken, 2003; Respress, 2012; Rodriguez, 2003; Shan, 2010; Walweel, 2017; Wehrens, 2006, 2004; Xiao, 2006). The specificity of kinase action is the subject of some debate – while for example, Ser2814 in RyR2 is generally agreed to be only available to CaMKII, S2808 in RyR2 was initially characterised as available only to PKA (Marx, 2000; Wehrens, 2006), but subsequently has been shown to be phosphorylated by CaMKII and PKG (reviewed in Camors & Valdivia, 2014).

In healthy physiology, phosphorylation of the RyR assists in effecting flight or fight responses to stress: B-adrenergic stimulation of muscles results in the downstream activation of PKA, which phosphorylates the RyR, enabling greater and more rapid Ca^{2+} transients, resulting in stronger and faster muscle contraction (Bers, 2002). In pathology, also, abnormal phosphorylation plays a role: one model suggests that hyper-adrenergic conditions occurring during heart failure encourage the PKA-mediated phosphorylation of RyR2 serine residues, disrupting the association of regulatory molecules such as FKBP (see also section **1.4.5**) and thereby encouraging a “leaky” phenotype that may cause arrhythmias (Marx, 2000; Reiken, 2003). Against this hypothesis, some groups have found no evidence of PKA hyperphosphorylation in heart failure (Xiao, 2005). Other groups have identified a role for CaMKII in hyperphosphorylation subsequent to heart failure causing a similar “leaky” phenotype, although the multiple possible targets for CaMKII make it difficult to consider the phenotype consequent to RyR2 phosphorylation alone (Ai, 2005; Neef, 2010; Denniss, 2018).

The function of the RyR has also been established to be sensitive to redox conditions, with alterations in the redox state capable either of activating (Stoyanovsky, 1997;

Eager & Dulhunty, 1998) or inhibiting (Marengo, 1998) the channel. Typically RyRs have nitric oxide (NO) covalently yet reversibly bound to their exposed cysteine residues; it is this association that changes in the cellular redox state are able to disrupt (Sun, 2008). Of the ~100 cysteines in each RyR monomer, around ~20 are available for redox modification, whether via oxidation, nitrosylation, or glutathione alkylation (Zable, 1997; Xu, 1998). These cysteines are distributed fairly evenly across the RyR cytoplasmic domains.

1.3.4.4 Exogenous compounds

Exogenous compounds affecting RyR function are of both medical and experimental interest, as they are able to inhibit or activate the channel, both giving rise to pathology and relieving symptoms associated with RyR-related pathologies. A large number of compounds have been demonstrated to affect RyR function, with one review (Xu, 1998) listing, among others, ryanoids, toxins, xanthines, anthraquinones, phenol derivatives, adenosine and purinergic agonists and antagonists, NO donors, oxidizing reagents, dantrolene, local anesthetics, and polycationic reagents all as possible modulators of RyR. Of these, of most experimental significance are the ryanoid ryanodine and the methylxanthine caffeine; and of most significance medically are perhaps the volatile anaesthetics, along with dantrolene. Not mentioned above, but studied extensively in recent years is the sodium channel blocker flecainide, which finds clinical use in the treatment of CPVT (Watanbe, 2009; Biernacka & Hoffman, 2011; Pott, 2011; van der Werf, 2011; Hwang, 2019), a condition discussed further below in **1.3.5, Pathology**.

Ryanodine, the toxic plant alkaloid for which the ryanodine receptor was named, is a potent bimodal modulator of RyR activity. In single channel experiments, when added to the cytosolic side of a RyR in micromolar quantities, ryanodine activates RyR, promoting long-lived subconductance levels and a consequent increase in overall P_o. When added in millimolar quantities, however, ryanodine completely inhibits channel activity (Lai, 1989; Pessah & Zimanyi, 1991). Characteristic of both modes of modulation by ryanodine is that affected channels are resistant to additional regulation by Ca^{2+}, Mg^{2+}, or ATP (as in **1.3.4.1**).

Caffeine has long been recognised as a promotor of Ca^{2+} release from the SR (Endo, 1977). Specifically, it is known now to bind to a site on the RyR adjacent the S2-S3 linker domains (des Georges, 2016), and then to strongly positively affect RyR channel open probability, while not significantly affecting pore conductance (Rosseau, 1988; Sitsapesan & Williams, 1990). At low concentrations, up to 2 mM, caffeine has a Ca^{2+}-sensitising action, whereby in the presence of high nanomolar to low micromolar [Ca^{2+}], channels dwell much less in closed states. Higher concentrations, up to 10 mM, activated channels even at picomolar [Ca^{2+}], and increased the duration of open states as well as decreasing the duration of closed states. Unlike ryanodine, channels modulated by caffeine remained sensitive to other modulators, including Mg^{2+} and ATP.

A “set” of RyR modulators of significant medical interest are volatile anaesthetics, including halothane, enflurane, and isoflurane, and the drug dantrolene. This is due to their involvement in malignant hyperthermia, a potentially fatal condition experienced by those with certain RyR1 mutations after administration of volatile anaesthetics (more details in **1.3.5, Pathology**, below). Broadly, halothane has been shown to increase SR Ca^{2+} release at gas concentrations ranging from ~4% down to 0.002% (Frazer & Lynch, 1992; Beltran, 1996). Single channel experiments (Connelly & Coronado, 1994; Bull & Marengo, 1994) confirmed that halothane acted to increase channel open probability, and further, that this activation was highly dependant on both pH and cytoplasmic [Ca^{2+}]. The largest effects of halothane were seen at cytoplasmic [Ca^{2+}] between 1 and 10 µM, with few effects observed at concentrations an order of magnitude different in either direction. Reducing cytoplasmic pH from physiological levels to 7.1 induced activation at lower [Ca^{2+}]; reducing pH further to 6.8 abolished all spontaneous Ca^{2+} release, although Ca^{2+} release was still able to be stimulated by halothane independent of cytoplasmic [Ca^{2+}]. While the impact of volatile anaesthetics on RyR function appears to the be primary driver of malignant hyperthermic pathology, it is likely that their effect on other Ca^{2+} homeostasis systems – for example, the function of SERCA – also contributes to the pathology (Beltran, 1996).

Dantrolene is a derivative of hydantoin with postsynaptic muscle relaxant action, and since 1975 (Harrison, 1975) has been recognised as the primary pharmaceutical treatment for malignant hyperthermia. At therapeutic concentrations greater than 10 µM, dantrolene reduces the maximum rate of Ca^{2+} release via RyR without affecting

RyR Ca^{2+} sensitivity (Tian, 1991); this effect is fairly subtle, but more discernable when examined along with potent RyR activators, for example caffeine and ATP. One single-channel study confirmed this antagonistic effect of dantrolene upon RyR function (Nelson, 1996), but many subsequent studies were unable to replicate this result (Szentesi, 2001; Diaz-Sylvester, 2008; Wagner, 2014). Recently, it has emerged that calmodulin (see section **1.3.4.2, Proteins**) is an essential cofactor for dantrolene's inhibitory action, explaining the lack of observed dantrolene action in single channel experiments, as calmodulin typically dissociates from the RyR complex upon purification (Oo, 2015).

Flecainide, a class IC anti-arrhythmic drug, was first synthesised in 1972 (Hudak, 1984), the result of an attempt to create new fluorinated anaesthetic agents. The primary action of flecainide is the selective and potent blockade of cardiac Na^+ channels, resulting in slowing of cardiac conduction (Holmes & Heel, 1985); further, flecainide inhibits K^+ channel opening, resulting in prolongation of the action potential in ventricular and atrial fibres. In addition to this well-characterised activity, flecainide is posited to block the RyR2, as flecainide treatment is observed to reduce spontaneous Ca^{2+} waves in CPVT (see **1.3.5, Pathology**) model organisms such as CASQ2-null mice (Watanabe, 2009) and mice heterozygous for the CPVT mutation R4496C in RyR2 (Hwang, 2019). Whether this action is consequent to RyR2 blockade or to Na^+ channel blockade alone is disputed (Sikkel, 2013), with at least one group finding little effect of flecainide on RyR2 channel activity (Bannister, 2015). However, that flecainide is observed to suppress Ca^{2+} efflux from RyR2 in permeabilised cardiomyocytes in conditions that render Na^+ channels inactive (Hilliard, 2010; Savio-Galimberti & Knollmann, 2015; Batiste, 2019) would seem to point towards flecainide directly blocking the RyR2 as at least a parsimonious explanation of its observed activity in Ca^{2+} wave suppression.

1.3.5 Pathology

Mutations in the RYR1 and RYR2 genes have been implicated in several diseases of skeletal and cardiac muscle respectively – currently, over 300 different mutations are associated with the development of pathologies. Generally, these diseases emerge due to abnormal calcium handling by the RyR, which in turn disrupts the normal

functioning of EC coupling (**1.2**) and consequently, the function of muscles (**1.1**). Any particular “RyRopathy” may be caused any of a number of potential mutations, which may be domains apart on the RyR. Consequently, RyRopathies are distinguished on the basis of symptoms, rather than the localisation of mutations. In RyR1, mutations have been associated with malignant hyperthermia (MH) (MacLennan, 1990), central core disease (CCD) (Zhang, 1993), multiminicore disease (MmD) (Ferreiro, 2002), atypical periodic paralyses (APP) (Zhou, 2010), and exertional rhabdomyolysis (Capacchione, 2010). Recently, RyR1 mutations have even been associated with a novel bleeding disorder consequent to smooth muscle contractile dysfunction (Lopez, 2016). In RyR2, mutations have been implicated in the development of catecholaminergic polymorphic ventricular tachycardia (CPVT) (Marks, 2002; Laitinen, 2003), arrhythmogenic right ventricular dysplasia type 2 (ARVD2) (Volta, 1961; Fontaine, 1984), and atrial fibrillation (Shan, 2012). Further, although it is something of a case of “the chicken and the egg”, post-translational modification of the RyR2 (see **1.3.4.3**), particularly oxidation and phosphorylation, is strongly associated with heart failure.

Of the RyR1 pathologies, MH is perhaps the best-characterised, largely because of its potential fatality. MH manifests in sustained muscular contraction when susceptible individuals are treated with inhaled anaesthetics such as halothane, or with muscle relaxants such as succinylcholine, as described above in **1.3.4.4** (Mickelson & Louis, 1996). This sustained muscle contraction is consequent to a dysregulation of the normal Ca^{2+} homeostasis, with the RyR1 becoming more sensitive to excitatory stimuli (Tong, 1999). MH is moderately rare, and significantly more common in children, with symptoms apparent in ~1 in 15000 anaesthetised children and ~1 in 50000-100000 adults (Rosenberg, 2007). Over 200 different mutations in RyR1 are associated with MH, clustered mainly in the cytoplasmic domain, although a population of MH-causing mutations exist near the carboxyl terminus (Philips, 1994; Quane, 1994; Monnier, 2000; Scacheri, 2000; Tilgen, 2001; Lawal, 2020). MH can be fatal if not treated immediately, with the commonest treatment method being administration of dantrolene, which acts as a strong RyR1 antagonist (Ward, 1986). Symptoms consequent to the sustained contractions induced by MH include elevation in body temperature, metabolic acidosis, tachycardia, and hypoxia (Ryan & Tedeschi, 1997). These symptoms may be treated in addition to administering dantrolene, via ice bath

to lower body temperate, diuresis / administration of Tris buffer etc to prevent metabolic acidosis, and administering beta-blockers or amiodarone to address persistent tachycardias. Somewhat related to MH is exertional rhabdomyolysis: here, Ca^{2+} dysregulation causing elevated body temperature, manifesting after sustained exertion, results in the breakdown of striated muscle, with muscle breakdown products potentially causing renal failure (Capacchione, 2010).

CCD, and the related diseases MmD, nemaline myopathy, and centronuclear myopathy, are distinct from MH in that they manifest slowly over time rather than as a single acute episode. Their symptoms are somewhat different, though all involve a gradual loss of skeletal muscle function: CCD, for example, presents as hypotonia and weakness in the lower limbs, generally leading to delayed acquisition of motor skills (Dirksen & Avila, 2002). These diseases are considered to be related due to their common feature of the development of “cores” of tissue in the centre of muscle fibres in affected patients which are metabolically inactive due to a lack of mitochondria and oxidative enzyme activity (Shuaib, 1987). In some cases, structural CRU elements such as the junctional SR and T-tubules may disorganise and deteriorate, causing further Ca^{2+} dysregulation (Tong, 1999). MmD contrasts with CCD in that smaller “mini cores” are the primary driver of pathology in affected muscles, but these exhibit an analogous lack of oxidative enzyme activity, causing limb weakness and potentially tissue hypoxia (Jungbluth, 2007; Sharma, 2007).

Many patients with “core” diseases may also present MH symptoms when subject to the relevant stimulus, indicating some overlap in the conditions (Jungbluth, 2003). CCD, although perhaps the commonest of the core diseases is nevertheless rare, with an incidence of ~1 in 100000 births (Jungbluth, 2007). CCD inherited in an autosomal dominant fashion was found to be mostly caused by mutations around the C-terminus of the RyR1, while CCD inherited recessively showed no particular clustering of RyR1 mutations, again illustrating the variety of potential pathogenic RyR1 mutations (Jungbluth, 2007).

APP is perhaps the most recently characterised RyR1 pathology, presenting as paralysis generally consequent to common triggers such as cold, heat, stress, or physical exertion: this may cause delays in motor skill acquisition, as in the core pathologies (Zhou, 2010). A related and more common condition, congenital periodic

paralysis, is caused by mutations in the CACNA1s gene which codes for the skeletal DHPR isoform / Cav1.1; however, atypical periodic paralysis is caused by RyR1 mutation instead. While only a handful of APP patients have thus far been identified (Matthews, 2018), it is likely that many more exist and may be miscategorised as having “typical” DHPR-dependant periodic paralysis instead, due to the close overlap of the two phenotypes.

In the heart, mutations in RyR2 are associated with often fatal arrhythmia; indeed, with the advent of effective therapies for MH episodes, arrhythmogenic mutations in RyR2 may be considered the deadliest, and hence most serious of the RyRopathies. CPVT is the most common of these arrhythmias, and as the name suggests, describes a class of stress-induced ventricular tachycardias (Marks, 2002; Laitinen, 2003). More than 300 different RyR2 mutations are associated with CPVT, and are spread across the full length of the protein, although significantly clustered around residues 3949–4332 and 4867–4967 (Olubando, 2020). Interestingly, but logically, CPVT may also be caused by mutations in CSQ2 and CaM (see **1.3.4.2**). A number of different RyR2 regulators are implicated in the progression of CPVT symptoms: notably, PKA and CaMKII phosphorylation has been suggested as a triggering factor in the RyR2 hyperactivity seen in CPVT (Valdivia, 1995; Wehrens, 2004a). Normally, phosphorylation of the RyR2 is functionally useful in that, in response to catecholaminergic stimulation, it acts to increase the magnitude of the Ca^{2+} transient, allowing stronger systolic contraction and for SR Ca^{2+} stores to be more quickly refilled during brief diastolic phases (Callewaert, 1988). In CPVT, aberrant release of Ca^{2+} from the SR during diastole is then synergistically enhanced by this situational phosphorylation. In CPVT-susceptible patients, elevation in cystolic Ca^{2+} levels is thought to activate NCX, with the downstream effect of causing delayed afterdepolarisations and VT due to the unequal exchange of 3 Na^{+} ions for one Ca^{2+} ion (Fozzard, 1992). Certain interventions for CPVT-vulnerable patients have been proposed, including flecainide (Watanbe, 2009; Biernacka & Hoffman, 2011; Pott, 2011; van der Werf, 2011; Hwang, 2019) and 1,4-benzothiazepine derivatives such as JTV519 and S107 – more on these, and the potential link between FKBP and CPVT in section **1.4.5**, below.

ARVD2 is characterised by the replacement of cardiac myocytes with fatty and fibrous tissue, resulting in ventricular arrhythmias (Corrado, 2000). Mutations in RyR2 leading

to ARVD2 are found in regions roughly homologous to those in RyR1 where mutations may cause MH and CCD, indicating a similar “disorganisation” etiology for the diseases. Alongside these structural symptoms, irregular Ca^{2+} handling by RyR2 in ARVD2 has been implicated in directly causing ventricular arrhythmia (Tiso, 2001). ARVD2 is somewhat more common than CPVT, with an incidence of ~1 in 10000 (Fontaine, 2001).

1.4 FK506-binding proteins

The questions that I will address in this thesis all concern the role played by the FK506-binding proteins – or FKBP – in binding to RyR and regulating RyR behaviour, so a thorough examination of the literature concerning FKBP is essential.

FKBP belongs to an immunophilin family of peptidyl-prolyl cis-trans isomerases. As the name suggests, these proteins convert proline bonds from cis to trans configurations – hence, they play a key role in regulating the rate of folding of certain proteins. Also in the immunophilin family together with FKBP are the cyclophilins, which exhibit similar isomerase functionality. FKBP and cyclophilins are distinguished by their primary pharmacological binding partners. While cyclophilins bind to cyclosporin, FKBP bind to drugs analogous to FK506 and rapamycin, members of a class of immunosuppressant drugs used primarily to supress innate immunity in organ transplantations. This immunosuppressant activity is effected by the interaction between the drugs and FKBP12 – more on this in section **1.4.3** below.

FKBP isoforms are found throughout all taxa: in humans, 15 isoforms have been identified (Rulten, 2006). The various isoforms may be categorised by reference to either their parent genes, or their molecular weight; for example, “FKBP4”, referencing the given FKBP gene, may also be called “FKBP52”, in reference to the FKBP’s molecular weight. For the purposes of this thesis, isoforms are categorised by molecular weight. In addition to their isomerase functionality, many FKBP isoforms perform additional cellular roles; some examples follow. FKBP25 may be involved in signalling for nuclear localisation, and possesses nucleic acid binding domains (Prakash, 2016). Another group of FKBP contain functional motifs called tetratricopeptide repeats, which enable them to transport and regulate large molecular

structures such as steroid receptor complexes: for example, FKBP52 and FKBP54 are implicated in the transport and regulation of gluco-corticoid and progesterone receptors (Johnson, 1996). A large subclass of FKBP (FKBP13, FKBP19, FKBP22, FKBP23, and FKBP65) are localised to the endoplasmic reticulum. While their precise role is uncharacterised, they are speculated to play a part in protein folding and expression, and in particular, the biosynthesis of collagens. Of these FKBPs, several possess Ca^{2+}-binding EF hand motifs, implying that their functionality is somehow Ca^{2+}-sensitive (Ishikawa, 2017).

Finally, two isoforms, FKBP12 and FKBP12.6, have been shown to be key regulatory factors of the RyR isoforms (**1.3.3**), although the precise nature of this regulation remains somewhat controversial. It is this "secondary" function of these two FKBP isoforms with which this thesis is primarily concerned; therefore, the following review concerns them alone.

1.4.1 FKBP genetics, isoforms, and distribution

FKBP12 and FKBP12.6 are encoded in humans by two unique genes, FKBP1A and FKBP1B respectively. Given their structural homology (covered further below in **1.4.2**, with Figure 1.14 below showing their alignment), it is perhaps unsurprising that the proteins also share ~83% sequence homology, with the two isoforms differing only by 18 residues, all but 5 of which are conservative substitutions, as shown in Figure **1.14**.

```
FKBP12.6  1 GVEIETISPGDGRTFPKKGQTCVVHYTGMLQNGKKFDSSRDRNKPFKFRIGKQEVIKGFE  60
            ||..|||||||||||||.||||||||||..|||||||||||||||| .|||||||.|.|
FKBP12    1 GVQVETISPGDGRTFPKRGQTCVVHYTGMLEDGKKFDSSRDRNKPFKFMLGKQEVIRGWE  60

FKBP12.6 61 EGAAQMSLGQRAKLTCTPDVAYGATGHPGVIPPNATLIFDVELLNLE 107
             || ||||.||||||| .|| |||||||||.|||.|||.|||||| ||
FKBP12   61 EGVAQMSVGQRAKLTISPDYAYGATGHPGIIPPHATLVFDVELLKLE 107
```

Figure 1.14: Sequence alignment of FKBP12.6 and FKBP12. Cyan highlights the FKBP12.6 sequence; magenta highlights the FKBP12 sequence. Identical paired residues are marked with a dash, similar paired residues with a dot, and non-similar paired residues with a gap, aligned via Smith-Waterman algorithm (Smith, 1981).

The different roles played by these two FKBP isoforms in regulating RyR is a matter of some controversy – more on that in section **1.4.4**, below – however, some general observations on the differences between the two isoforms can nevertheless be made. It is accepted that FKBP12.6 binds to both RyR1 and RyR2 with a substantially higher affinity than does FKBP12. For example, Guo (2010) found that FKBP12.6 bound to RyR2 with a Kd of ~0.7 nM, while FKBP12 bound to RyR2 with a Kd of ~206 nM. Similar differences, i.e. approximately 2 orders of magnitude, are observed in FKBP12 and FKBP12.6 binding to RyR2 in SPR experiments (Blayney, 2010). Additionally, while FKBP12 is ubiquitously expressed in most tissue types, FKBP12.6 appears to be expressed only in neuromuscular tissues. Initial work on these two isoforms pointed towards strict tissue-specificity in their expression as RyR regulators, with FKBP12 being the "skeletal" isoform and FKBP12.6 the "cardiac" isoform. More recently, however, both FKBP12 and FKBP12.6 have been shown to be expressed in cardiac tissue in various species-specific ratios, with for example, mouse RyR2 associating with FKBP12 100-fold more than FKBP12.6 (Zissimopolous, 2012), likely indicating far higher expression levels of FKBP12 as compared to FKBP12.6. Given this species-dependant expression of the two isoforms, it is therefore worth noting that the sheep hearts used in this thesis exhibit a roughly "human" ratio of FKBP isoforms: i.e., a mixed population of FKBP12 and FKBP12.6 associated with cardiac RyR, favouring FKBP12 over FKBP12.6 (see Chapters 3 and 4 especially later in this thesis for data on sheep FKBP ratios; Walweel, 2017 for data on human heart FKBP expression).

1.4.2 FKBP 3D structures

FKBPs have been structurally resolved both in isolation and as accessory proteins bound to RyRs, these latter structures providing evidence for the RyR domains involved in FKBP-mediated regulation. Crystallogaphic studies (Deivanayagam, 2000; Fulton, 2003; Wilson, 1995) reveal a high degree of structural homology between FKBP12 and FKBP12.6, with their structures superposing with an atomic positioning root-mean-square deviation of just 0.47 Å. In terms of secondary structure, both FKBP are amphiphilic β-sheet proteins containing five antiparallel strands and a central helix, as well as a hydrophobic binding pocket which interacts with the rapamycin/FK506 class of immunosuppressant drugs (Figure **1.15**).

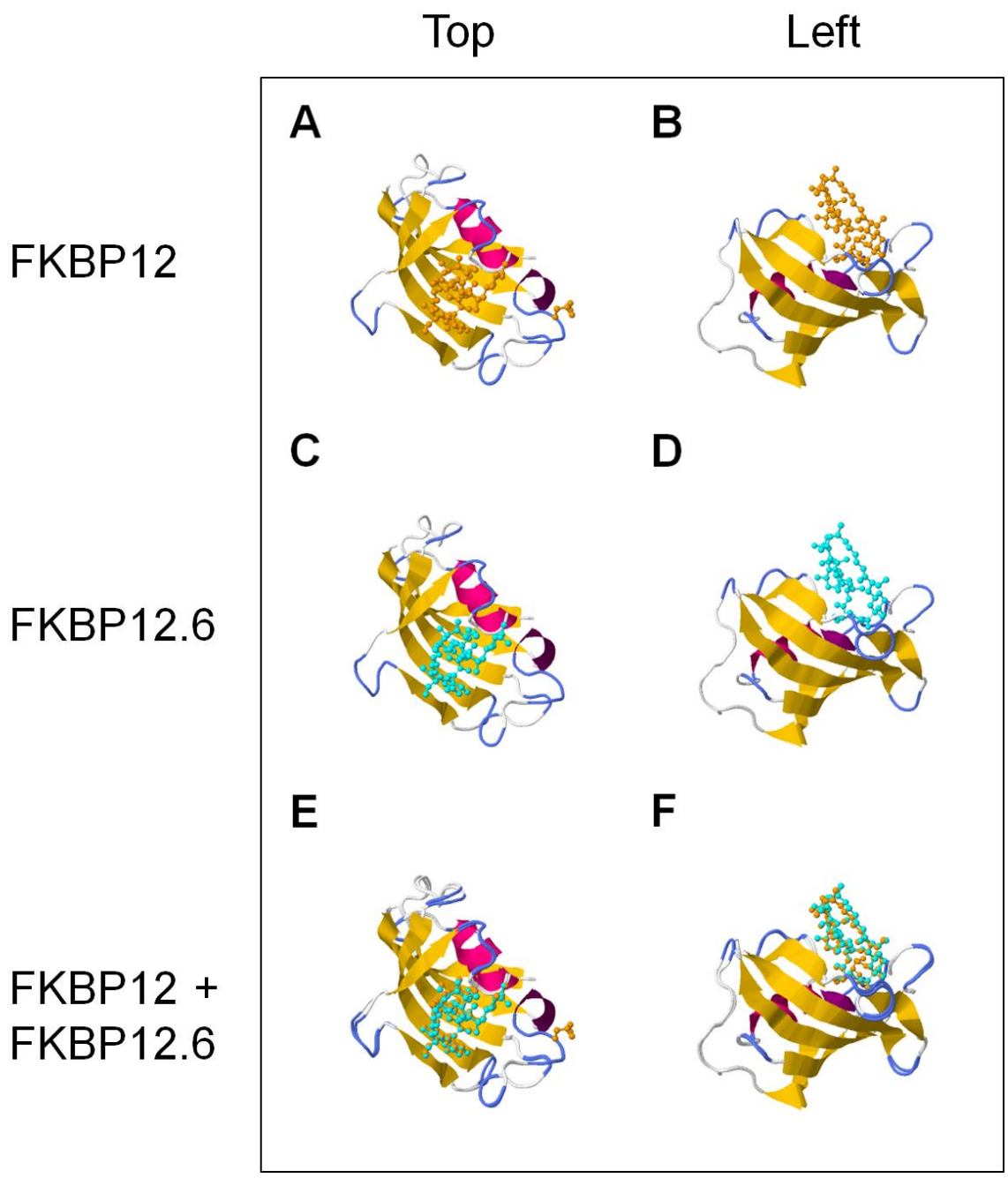

Figure 1.15: FKBP12 and FKBP12.6 structures shown separately, and also overlaid with structures aligned to demonstrate similarity. **A**, **C**, and **E** shows the molecules from one perspective, while **B**, **D**, and **F** shows the molecules rotated 90 degrees clockwise through both the x- and z-axes. FKBP12 is shown in complex with FK506 (in ochre) and FKBP12.6 in complex with rapamycin (in cyan); yellow denotes beta sheets and pink, the central helix. Figure was constructed in Jmol from PDB data based on crystallographic structures (PDB accession codes 2DG3 and 1C9H for human FKBP12 and FKBP12.6 respectively). Structures were aligned via the rigid FATCAT method (Ye & Godzik, 2003).

As mentioned in **1.3.2**, the high-resolution cryo-EM RyR structures have generally (with the exception of those in Efremov, 2015 and Peng, 2016) been generated with saturating concentrations of FKBP12 or FKPBP12.6 bound to the RyR. This saturating concentration of FKBP serves to elute RyRs from immobilisation on chromatographic columns, but the binding of four FKBP molecules also stabilises the RyR in a single fixed visualisable conformation. While the resolution for these FKBP structures is somewhat inferior to that obtained in crystallographic studies (4-6 Å, as compared to 1-2 Å) due to their binding position on the periphery of the RyR structure, these images are nonetheless highly useful in that they show physiological conformations and provide strong evidence for RyR binding determinants – see Figure **1.16**, but more on this in section **1.4.4** below.

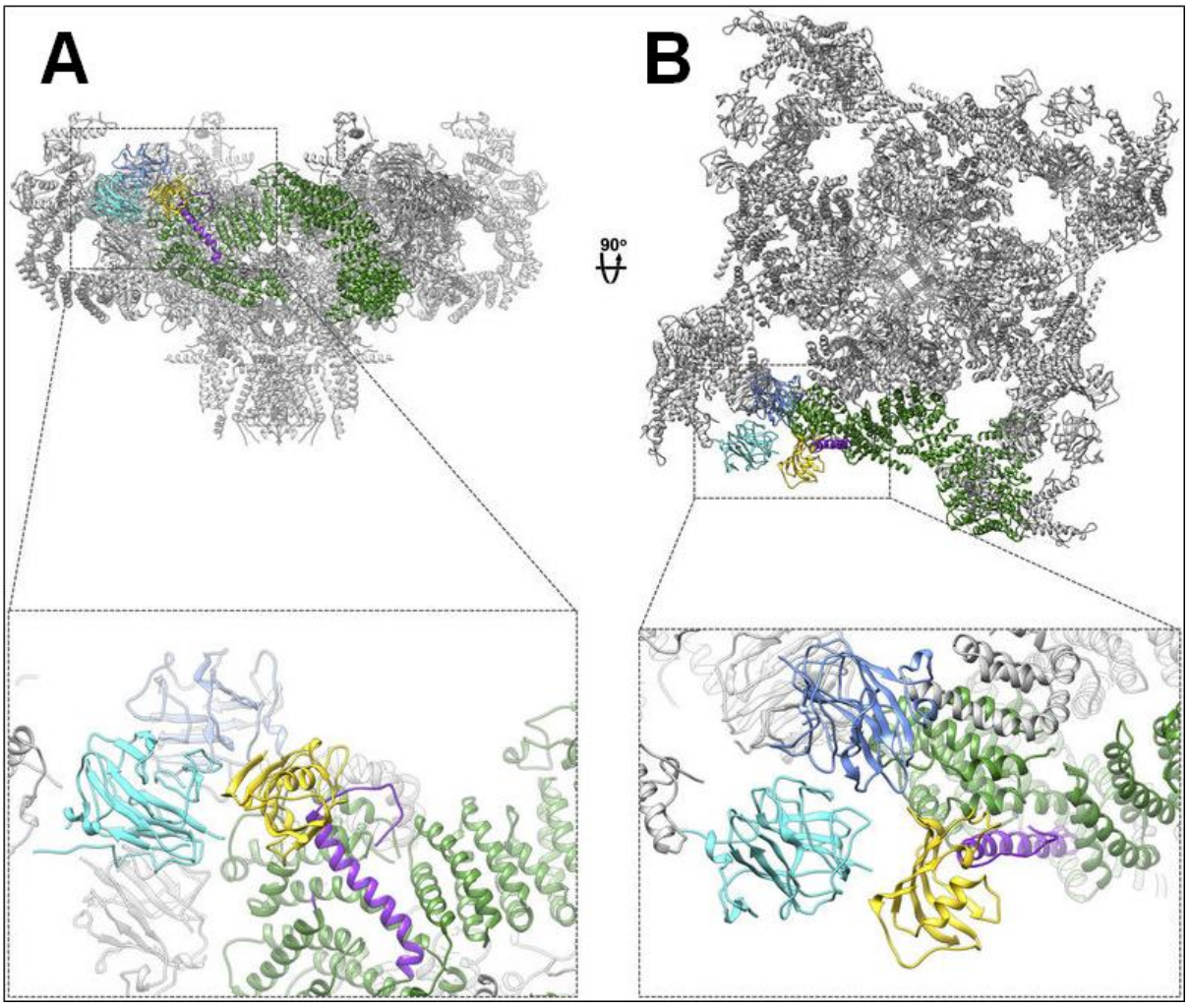

Figure 1.16: Structure of RyR1, viewed from the membrane plane (**A**) and the cytosol (**B**), with enlarged views of bound FKBP12.6, shown in yellow (Zalk, 2015). In association with FKBP12.6, SPRY1 is depicted in light blue, SPRY2 in cyan, the bridging solenoid in green and the FKBP-binding helix in purple. It is worth reiterating that FKBP12.6 bound to RyR1 is non-physiological, and solely an artefact of the RyR1 purification process, but may be assumed to be analogous to FKBP12's binding relationship to RyR1.

1.4.3 Immunomodulatory and enzymatic function of FKBP

FKBP12 and FKBP12.6, through their interaction with exogenous immunosuppressant compounds such as FK506 and rapamycin, can play a role in regulating T-cell behaviour – indeed, it is via these interactions that FK506 and rapamycin exert their clinical immunosuppressant activity. Somewhat unexpectedly, this T-cell regulation is

achieved through two different highly specific mechanisms, depending on whether FKBP is complexed to FK506 or rapamycin. As shown above (**1.4.2, Figure 1.15**), both drugs are structurally very similar, but the fine differences in their structure when complexed with FKBP nevertheless result in very different modes of action. Notably, much work has considered the FKBPs to be interchangeable as complex partners for FK506 and rapamycin. Considering their structural similarity (**1.4.2**, above), this is perhaps a reasonable assumption, but the question of whether FKBP12 and FKBP12.6 immunosuppressant complexes behave somewhat differently remains open.

Broadly, the complex of an FKBP and FK506 has been shown to inhibit the activity of the phosphatase calcineurin (Liu, 1991; Fruman, 1992; Sewell, 1994; Wu, 2011). This inhibition of calcineurin prevents effective translocation of T-lymphocytes, thereby preventing the production of downstream T-cell derived mediators such as interleukin-2, resulting in immunosuppression (Huai, 2002; Ke & Huai, 2003).

The complex of FKBP and rapamycin, by contrast, interacts with the protein mTOR (mammalian target of rapamycin), a kinase whose role is to regulate the cell growth and the progression of the cell cycle (Lawrence, 2004; Panwalker, 2004). The FKBP-rapamycin complex blocks the function of mTOR (Heitman, 1991; Sabatini, 1994; Brown, 1995; Peterson, 2000), which inhibits the further production and proliferation of T-cells, thereby causing immunosuppression (Kay, 1991; Sharma, 1994; Law, 2005).

Unusually, these two highly-specific physiological targets for FKBP12 first require the complexation of an exogenous drug. Whether a cellular role for cytoplasmic FKBP12 exists beyond regulation of RyR (**1.4.4**, below) is yet unknown, although certain studies strongly suggest the possibility: for example, mice with FKBP12 deficiency manifested cell cycle arrest in the G1 phase (Aghdasi, 2001). This “native” role for FKBP12 likely involves its inherent cis-trans prolyl isomerase activity, the substrate/s for which are yet to be identified, but are likely proteins requiring isomerase transformation for proper folding. Timerman (1995) mutated F36Y, W59H, and F99Y in FKBP12, finding a substantial loss in its enzymatic activity; however, these mutant FKBP12 still regulated RyR1 in the same manner as wild-type FKBP12, indicating that FKBP regulation of RyR (**1.4.4**, below) is independent of their enzymatic activity.

Whether these mutant FKBP12 would cause disruption of the cell cycle as in Aghdasi (2001), above, is an interesting but as yet currently unanswered question that would address whether FKBP12's "native" activity is enzymatic in nature. FKBP12.6, by contrast, is unlikely to have a "native" cellular role beyond RyR regulation, given its limited and tissue-specific expression.

1.4.4 RyR-regulatory function of FKBP

FKBP binds the RyR tetramer with a stoichiometry of 4:1, i.e. 1 FKBP per RyR monomeric subunit (Jayaraman, 1992; Lam, 1995; Qi, 1998; Timerman, 1993), although whether this potential maximal stoichiometry accurately reflects the physiological stoichiometry is addressed in Chapter 4 of this thesis. As briefly covered in **1.4.2.**, cryo-EM studies of RyR1 in complex with FKBP reveal that FKBP primarily binds to the interface of the SPRY1, SPRY2, and solenoid domains of RyR (Zalk, 2015; Yan, 2015), yet much uncertainty still attends the precise binding determinants of the FKBP:RyR interaction.

Work on the FKBP:RyR binding interface began with various mutagenesis and protein:protein interaction studies. Using RyR2 fragments, I2427 and P2428, located in the α−solenoid 2 domain, were identified via co-immunoprecipitation and co-sedimentation experiments as forming a binding pocket for FKBP12.6 by Marx et al. (2000), but later work (Masumiya, 2003), also using co-immunoprecipitation techniques, found that mutation of these residues did not alter FKBP12.6 pulldown of RyR2. Instead, that study found that the sequence spanning residues 305-1937 was critical for FKBP12.6 binding. Later the same year Zhang et al. (2003), through immunoprecipitating terminal truncation mutants of RyR2 with FKBP12.6, narrowed the binding region to the 40 residues between 1815-1855, part of the RyR handle domain. In terms of RyR:FKBP12 interaction, Gaburjakova et al. (2001) identified via attempted immunoprecipitation of point mutation variants of V2461 (and successful immunoprecipitation of the wild-type) that the α−solenoid 2 domain of RyR1 is a critical binding determinant for FKBP12, broadly in agreement with the findings of Marx et al. (2000). A somewhat "left-field" finding by Zissimopolous & Lai (2005) indicated that in addition to an interaction with the handle domain, FKBP12.6 was able to interact with weaker affinity to the C-terminal region (3788-4756) of RyR2, with this C-terminal able

to displace FKBP12.6 from native RyR2 in competition assays, implying a potential secondary lower-affinity binding site for FKBP12.6 on the RyR2. This study also joined Masumiya et al. (2003) in rejecting the hypothesis proposed by Marx et al. of an interaction with the second α−solenoid domain.

Cryo-EM and crystallographic studies, both of the whole RyR and of segments, revolutionised the study of the RyR:FKBP binding site. Crystal structures of the RyR2 SPRY1 domain docked with the FKBP12 crystal structure (Yuchi, 2015) reveal that the two are plausibly proximate enough to support a potential binding relationship, and further, that a hydrophobic pocket in SPRY1 may be the critical determinant of FKBP12 binding, most likely between F674 (in the rabbit RyR1 sequence) and R40 in FKBP12. Interestingly, this study also shows that an unstructured region in SPRY1 becomes structured upon FKBP12 binding, supporting a FKBP12 “stabilisation” hypothesis of RyR regulation (see section **1.4.4.1**). The three cryo-EM structures of RyR1 (covered previously in section **1.3.2**) provide support for some of these previously mentioned FKBP12 binding hypotheses. Zalk et al. (2015) show FKBP12.6 interacting with RyR1 in a similar location on the handle as was proposed by Zhang (2003); specifically, FKBP12.6 sits between SPRY1 and SPRY2, and primarily interacts with the bridging solenoid. Again in support of the FKBP “stabilisation” hypothesis, a helix extending from the RyR1 BrA subdomain also is proximate to the FKBP12 binding site, and so it was hypothesised that FKBP12 interaction with this helix restricts the mobility of the SPRY1-SPRY2-BrA interface. The other cryo-EM studies find much the same geometry of interaction, with the critical difference that the studies do not agree on the assignment of locations for the different SPRY domains, due to poor local resolution at the periphery of the RyR1 structures. In general, the studies support the notion that multiple sites across the SPRY domains may contribute to the FKBP12 binding site, throughout the N-terminal region of RyR1, and interact also with the first α−solenoid domain as was proposed by Zhang et al. (2003); however, they fail to provide much support for the hypothesis that FKBP also binds to the second α−solenoid domain, as was initially proposed by Marx et al. (2000). Subsequent cryo-EM studies of RyR2 structure (Peng, 2016; Dhindwal, 2017) appear analogous to RyR1 in terms of potential interaction surfaces presented to the FKBPs.

Much as the nature of FKBP binding to the RyR has been extensively investigated, but has yet to be conclusively settled, the functional significance of the association

between FKBP and RyR has been the subject of much research, but several open questions remain. Specifically, while the nature of FKBP12 regulation of RyR1 in skeletal muscle is fairly settled (see **1.4.4.1**, below), the exact mode of the FKBP regulation of cardiac RyR2 (**1.4.4.2**) is considerably more controversial, with evidence for a wide range of effects upon channel function. In the subsections below, the previous work on FKBP regulation of both RyR1 and RyR2 is summarised; following this, a brief summary of some of the less well-characterised contexts in which FKBP and RyR interact is also presented.

1.4.4.1 FKBP regulation of RyR1 function in skeletal muscle

The association between FKBP12 and RyR1 is well-established, and was the first FKBP-RyR interaction identified (Collins, 1991; Jayaraman, 1992; Ahern, 1994; Carmody, 2001; Samsó, 2006; Wen, 2012). Consequently, the FKBP12-RyR1 interaction is perhaps the best characterized of all FKBP-RyR interactions.

It is generally agreed that binding of FKBP12 to RyR1 stabilises the channel in a closed conformation (Timerman, 1993; Ahern, 1994 & 1997; Brillantes, 1994; McCall, 1996; Ondrias, 1998; Marx, 1998 & 2001; Avila, 2003). Corollary to this, removal of FKBP12 from RyR1, generally by treatment with FK506 or rapamycin, will result in both increased channel open probability, increased duration of channel openings, increased probability of submaximal subconductance channel openings, and a concomitant increase in Ca^{2+} release from SR stores (Timerman, 1993; Brillantes, 1994; Mayrleitner, 1994; Ahern, 1997; Marx, 1998; Gaburjakova, 2001). Notably, as shown in several of the above studies, this increase in channel activity may be reversed by treatment with exogenous FKBP12, providing strong evidence for FKBP12's role as a stabilizer of RyR1 function. The structural basis of FKBP12 stabilisation of RyR1 is examined in Samsó (2017), which compares previously determined (Samsó, 2005; Samsó; 2009) structures of closed-state RyR1 without associated FKBP12 to structures of both open- and closed-state RyR1 with FKBP12 bound (Figure **1.17**). FKBP12 is revealed to significantly impact the conformation of closed-state RyR1: two different conformations for closed RyR1 are revealed, subject to the presence or absence of bound FKBP12. Without FKBP12 associated, closed-state RyR1 is found in a "relaxed" conformation, intermediate between the open-state

and closed-state conformations, although with the ion gate still occluded. This “relaxed” conformation requires much less energy to shift into an open conformation, perhaps indicating the structural basis underlying the subconductance phenomena observed in the absence of FKBP12.

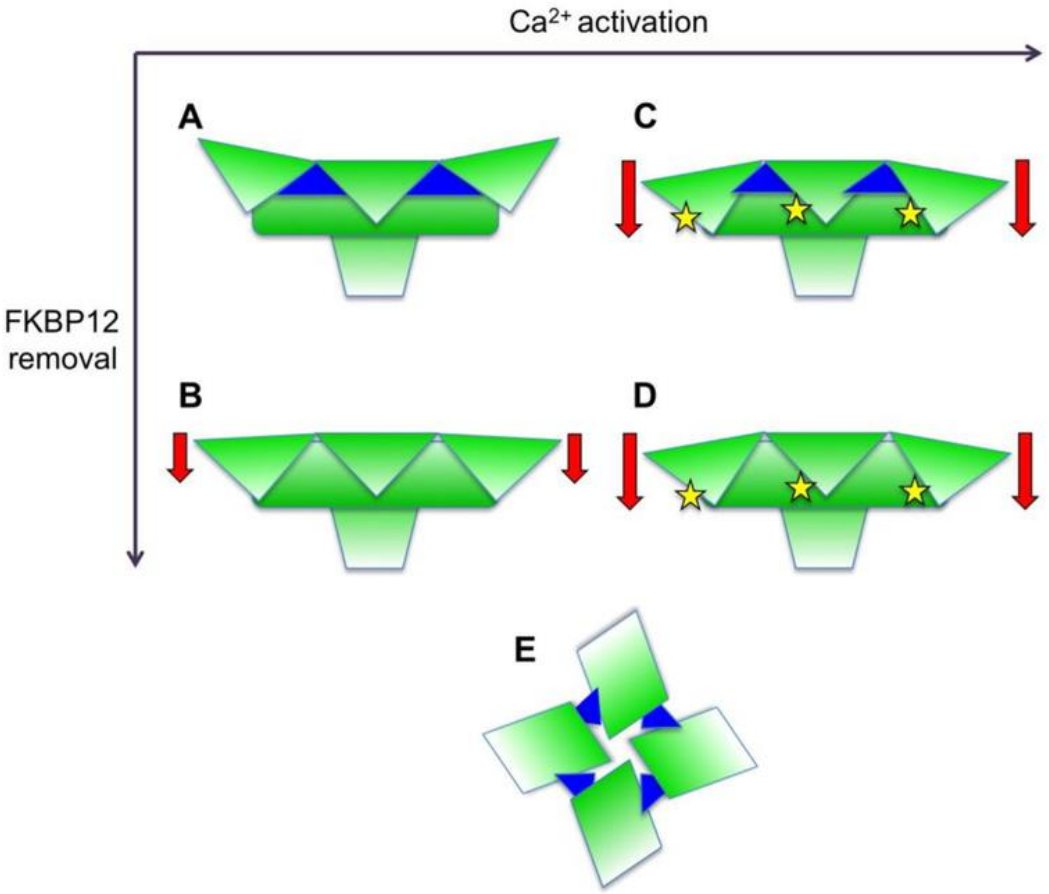

Figure 1.17: Conceptual diagram illustrating the effects of both FKBP12 association and maximally activating [Ca^{2+}] on RyR1 (Steele & Samsó, 2019). RyR1 is represented in green, FKBP12 in blue, and Ca^{2+} ions in yellow. Panels **A**-**D** give a side view of RyR1 under different conditions: **A**, RyR1-FKBP12 closed with FKBP12 buttressing the upward conformation; **B**, RyR1 closed; **C**, RyR1-FKBP12 open; **D**, RyR1 open. **E** shows a fourfold view illustrating how FKBP12 promotes the coordination of the four subunits.

The role of FKBP12 as a regulator of RyR1 function in skeletal muscle has been confirmed by studies examining the physiological consequences of skeletal-specific alterations to FKBP12 expression. It is important to note that all studies involving

FKBP12 knockout must necessarily be tissue-specific, as universal knockout of FKBP12 proves embryonically fatal due to defects in cardiac conduction (Shou, 1998) – this is examined in greater detail in the following section, **1.4.4.2**. Briefly, however, in these embryonically fatal mutants, no particular disorganisation of skeletal muscle was observed. Tang (2004) generated the first skeletal-specific FKBP12 knockout mouse model. Here, it was observed that the knockout mice exhibited reduced voltage-gated SR Ca^{2+} release; this observation was correlated with a reduction in maximum tetanic force in the EDL of FKBP12-deficient mice, although force reductions were not observed in myotubes from the soleus or diaphragm. Researchers therefore concluded that FKBP12 is somehow involved in modulating the gain of EC coupling. Subsequent tissue specific FKBP12 knockout work (Corona, 2008) showed a correlated "improved" phenotype for FKBP12-deficient mice, in that despite being smaller and weaker, they more quickly recovered contractile strength after multiple injuries, and exhibited considerably less muscle damage upon histological examination. Unusually, researchers noted a strong sex-dependent difference in their results, with female mice exhibiting a more markedly "improved" phenotype. Lee et al. (2014) confirmed this previous work, showing also a compensatory increase in the generation of type I muscle fibres, perhaps accounting for the "positive" aspects of the FKBP12 knockout phenotype.

The generally mild phenotype of FKBP12 knockout in skeletal muscle is somewhat puzzling, given the apparent serious dysregulation observed in electrophysiological studies of FKBP12-stripped RyR1. Corona (2008) suggested that in knockout models, FKBP12.6 may be expressed in increased levels in skeletal muscle and hence play a compensatory role; alternatively, despite reductions in FKBP12 levels of between 80-90% in knockout-affected tissues (Lee, 2014), this small remainder may be sufficient to protect against grievously pathological consequences. Indeed, based on their calculation of a high affinity of FKBP12 for RyR1 (~30 nM) and the relative tissue concentrations of FKBP12 and RyR1, the researchers in Lee et al. (2014) estimated that up to 50% of available RyR1 binding sites for FKBP12 may be occupied even in their knockout model.

Further support for FKBP12 as a key regulator of skeletal muscle RyR1 can be found in a study by Baumann et al. (2014). Here, anterior crural muscles in mice were stressed via eccentric contractions, and the muscle subsequently homogenised and

centrifuged to obtain a pellet and supernatant. While not specifically shown to be associated with RyR1, the amount of FKBP12 in the pelleted membranous fraction – i.e., the fraction most likely to contain RyR1– was found to be decreased in proportion to the degree of muscle injury, and the quantity of free cytoplasmic FKBP12 in the supernatant fraction was increased for up to three days post-injury. Muscle function tests were also carried out, with regression analysis showing that ~38% of variability in isometric tetanic torque measured immediately after the eccentric contraction trials could be accounted for by changes in RyR1-associated FKBP12 levels, providing strong evidence for FKBP12 as a functional regulator of normal RyR1 activity.

FKBP12.6 has not been shown to be expressed at significant levels in skeletal muscle, and hence the RyR1-FKBP12.6 interaction is not of physiological relevance; regardless, it is of interest, and so will be covered briefly. FKBP12.6 has been shown to bind RyR1 in vitro (Barg, 1997; Cornea, 2009) and with an affinity greater than that of FKBP12 (Galfré, 2012; Venturi, 2014); this increased affinity has subsequently been exploited for affinity-based purification of RyR1 from skeletal muscle, notably in Zalk et al., 2015, where FKBP12.6 was used to elute RyR1 captured by immobilised FKBP12. Functionally, Venturi et al. (2014) observed that while FKBP12 inhibits RyR1 activity, FKBP12.6 activates it. If the two isoforms do indeed have opposing effects on RyR1, this would contradict the suggestion of Corona et al. (2008), above, that FKBP12.6 may potentially be upregulated and hence play a physiological role in skeletal muscle RyR1 regulation where tissues are FKBP12 deficient.

1.4.4.2 FKBP regulation of RyR2 function in cardiac muscle

The role of FKBP in regulating RyR2 function in the heart is still quite uncertain, with contradictory evidence for the roles played by both FKBP isoforms. Below, the evidence for the various modes of regulation observed is presented, along with some possible explanations for this disparity of results between groups.

First, however, it is important to note that RyR2 is not the sole RyR isoform found in cardiac tissue. Jeyakumar et al. (2002) found RyR1 localised in the intercalated disks of human and mouse hearts, and RyR3, although not identified in cardiac muscle, is abundantly present in cardiac vascular smooth muscle. However, RyR2 is the

predominant cardiac RyR isoform in many species, and hence, its regulation is of great interest when considering cardiac muscle function.

Furthermore, as mentioned above in **1.4.1**, an additional complication in assessing the nature of FKBP regulation of RyR2 is the strong species-dependence of cardiac FKBP isoform expression. Zissimopolous et al. (2012) present evidence for dramatic variability in expression patterns, ranging from primarily FKBP12.6 associated with RyR2 in the rat heart, to primarily FKBP12 associated with RyR2 in the rabbit and mouse heart. Intermediate between the two extremes were pigs, in whose hearts both isoforms were detected, with FKBP12 dominating. Our group has previously published work (Richardson, 2017) demonstrating that sheep cardiac RyR2 binds FKBPs in a similar ratio, with both isoforms present but FKBP12 dominating; Walweel et al. (2017) also demonstrates this ratio obtains for human cardiac RyR2. This species-specific FKBP ratio is of key importance in assessing studies that attempt to measure the effect of disruptions in FKBP binding to RyR2 – for example, Su et al. (2003) observed an effect of FK506 in reducing SR Ca^{2+} stores in mice, but not rabbits; in the light of Zissimopolous et al.'s work, this is likely consequent to the two species' differential expression and binding of the FKBP isoforms (Richardson, 2017, and also see Chapter 3 of this thesis for data supporting this hypothesis of FKBP isoform specificity of FK506 action).

Some early parallel experiments to those in skeletal muscle, where FKBP is removed from RyR2 via treatment with FK506 or rapamycin, showed a similar increase in channel open probability or Ca^{2+} spark duration (Kaftan, 1996; Xiao, 1997) after FKBP removal. Against this, Barg (1997) showed that stripping of FKBP from RyR2 did not significantly alter channel function, and although FKBP12.6 (but not FKBP12) re-bound to RyR2 subsequent to stripping, it did not significantly alter channel gating properties. In support of FKBP12 not associating with RyR2, Carmody et al. (2001) failed to observe an association of exogenous FKBP12 to cardiac microsomes. Following Barg et. al. (1997), Xiao et al. (2007) found similarly that removal of FKBP12.6 from RyR2 had no significant effect on channel function. However, in an inverse experiment, Guo et al. (2010) observed that the introduction of exogenous FKBP12.6 to RyR2 in permeabilised rat and mouse cardiac myocytes inhibited channel activity, but exogenous FKBP12 did not, although both associated with RyR2. Importantly, the researchers there observed that only 10-20% of native RyR2 were

occupied by FKBP12.6, concurring with the findings of Zissimopolous et al. (2012), at least as regards mice. Complicating matters further, an alternative model of FKBP regulation of RyR2 was proposed by Galfré et al. (2012), where the researchers observed that physiological concentrations (~3 μM) of FKBP12 activated sheep heart RyR2, and that this activation was antagonised by FKBP12.6.

Turning to in vivo examination of the cardiac function of FKBP, as alluded to in **1.4.4.1**, above, the first FKBP12 knockout models (Shou, 1998) proved fatal between embryonic day 14.5 and birth. Mice developed multiple cardiac defects, including ventricular septal defects, noncompaction of the ventricular myocardia, and thin ventricular compact walls, likely the main cause of embryonic fatality. This work was followed by a similar FKBP12.6 knockout study (Xin, 2002). Here, FKBP12.6 deficient mice exhibited a far less dysfunctional (although still pathological) phenotype, as compared to the FKBP12-deficient cohort. Increases in Ca^{2+} spark duration and CICR gain were observed, leading to increased Ca^{2+} load in cardiac ventricular myocytes. Unexpectedly, these calcium-handling alterations led to cardiac hypertrophy in male mice, but not in female mice, leading the researchers to posit a role for oestrogen in modulating cellular response to Ca^{2+} overload. Complementary to this study, Wehrens et al. (2003) found an increased probability for FKBP12.6 deficient mice to suffer fatal ventricular arrhythmias subsequent to exercise, although in contrast to Xin's (2002) study, Wehrens found no cardiac remodelling in response to FKBP12.6 knockout in either male or female mice. Confounding both these studies, a further investigation by Xiao et al. (2007) found no increase in stress-related arrhythmia or any alterations in RyR-mediated Ca^{2+} handling in FKBP12.6 deficient mice. This lack of congruity between studies matches that seen in electrophysiological studies, where different groups have observed both significant and negligible consequences of stripping FKBP12.6 from RyR2 channels. In general, as all these studies were on mice, it is worth again mentioning that in Zissimopolous's (2012) survey of the FKBP isoforms associated with RyR2 in various species, mice had only a small amount of FKBP12.6 associated with their RyR2, with the preponderance of associated FKBP being FKBP12 – the deletion studies in particular, may have produced less equivocal results were they performed on a species with greater FKBP12.6 dependence, such as rats.

A pair of studies from Loughrey (2004) and Seidler (2007) examined the consequences of overexpressing respectively FKBP12.6 and FKBP12 on several

measures of function in adult rabbit cardiomyocytes. Both studies present the rabbit model as closely matching the human heart in terms of affinities of their respective RyR2 variants to FKBP12 and FKBP12.6, although as mentioned above, the study of Zissimopolous et al. (2012) appears to indicate that rabbit hearts have extremely low levels of FKBP12.6 associated with their RyR2. Regardless, the studies showed that FKBP12.6 overexpression resulted in higher SR Ca^{2+} store loads alongside reduction in metrics of Ca^{2+} spontaneous spark properties (amplitude, width, and frequency), and consequently, Ca^{2+} whole-cell transients of greater amplitude, due to greater quantities of Ca built up in SR stores. Intriguingly, a possible role for FKBP12.6 in coordinating activity of proximate RyR2 was also proposed in the study of Loughrey et al. (2004), with much more synchronous Ca^{2+} release events being seen in the study's overexpression model. Much more attenuated results were seen from FKBP12 overexpression: while store Ca^{2+} loads were likewise increased, there was no increase in Ca^{2+} spark transient amplitude observed, and indeed, contrary to what was observed with overexpression of FKBP12.6, overexpression of FKBP12 appeared to increase Ca^{2+} spark amplitude. Taken together, these rabbit studies generally support the electrophysiological observations in Guo (2010), where FKBP12.6 overexpression resulted in stabilisation of RyR2 gating, but FKBP12 overexpression had little impact on RyR2 behaviour.

Maruyama et al. (2011) then re-examined the cardiac phenotype of FKBP12 mutant mice, by both overexpressing and conditionally knocking out FKBP12. Again, FKBP12 knockout proved fatal, due to cardiac conduction defects. Ventricular myocytes isolated from deficient mice showed faster than normal action potential upstrokes and a doubled peak sodium current density. Contrasted with this, FKBP12-overexpressing mice showed a ~80% reduction in peak sodium current density, as well as abnormalities in current recovery and late current. The phenotype of the FKBP12-overexpressing myocytes was able to be replicated in the FKBP12-deficient mice by addition of exogenous FKBP12. Interestingly, this suggests the possibility of serious arrhythmogenic pathology consequent not just to FKBP12 deficiency, but also to FKBP12 overload.

Taken together, these studies fail to present a clear model for FKBP regulation of RyR2. The model with the most weight of evidence appears to present FKBP12.6 acting on RyR2 much as FKBP12 does on RyR1, reducing the frequency of channel

openings in a “stabilising” manner; alongside this, no real “effect” of FKBP12 on RyR2 is observed, save that their total absence is fatal. The model of Galfré et al. (2012) where FKBP12 was found to be excitatory on RyR2 function and this excitatory action antagonised by FKBP12.6, must be granted consideration, however, especially as it is one of the few studies to consider the FKBP isoforms acting upon RyR2 in a competitive rather than independent manner. The lack of support for this model from overexpression studies may be consequent to endogenous levels of FKBP12 or FKBP12.6 confounding analysis of competitive effects; alternatively, the lack of control over FKBP concentrations in overexpression studies may result in analysis primarily of supraphysiological concentrations of FKBP, with limited physiological pertinence. Finally, as regards discrepancy between studies, it is important to reiterate the significance of species-specific expression of FKBP – this evidence alone points to differential modes of regulation of RyR2 by FKBP in different species, and so conclusions derived from a particular cardiomyocyte population may not be generalisable across species.

1.4.4.3 FKBP regulation of RyR in other contexts

While the preponderance of work on FKBP regulation of RyR has been in skeletal and cardiac muscle, important research has also been conducted on how FKBP regulates RyR in other tissues. Following are brief summaries of how FKBP regulates the somewhat-neglected RyR3 isoform; how FKBP regulates RyR present in certain smooth muscle tissues; how FKBP regulates neural RyR; and finally, how FKBP mediates the relationship between RyR and other proteins of the CRC.

1.4.4.3.1 FKBP regulation of RyR3

Due to its relatively low expression level, RyR3 has been somewhat neglected in comparison to the other RyR isoforms. Studies on RyR3 have generally been undertaken using RyR3 expressed in HEK293 cells, rather than purified from tissues, again due to the difficulty of separating RyR3 from other natively co-expressed RyR isoforms. As with RyR1 and RyR2, RyR3 has been shown to tightly associate with

both FKBP12 and FKBP12.6 (Bultynck, 2001a & 2001b). FKBP12 associates with RyR3 preferentially over RyR2, but not over RyR1 (Chelu, 2004).

In terms of regulatory behaviour, Van Acker et al. (2004) showed that a mutation disrupting association of FKBP12 to RyR3 increased Ca^{2+} efflux and sensitivity to caffeine. Spontaneous Ca^{2+} release was about 50% more likely to occur in cells with disrupted FKBP12 binding. Overexpressing FKBP12 induced the reverse effect in wild-type cells, reducing the number of spontaneous Ca^{2+} release events, while not affecting the spark frequency of mutant cells. Broadly, therefore, RyR3 appears to be regulated by FKBP12 in much the same manner as RyR1; however, whether physiologically it is regulated by FKBP12 alone or by FKBP12.6 also is unknown – given the broad expression of RyR3, this is likely to be tissue-specific.

1.4.4.3.2 FKBP regulation of RyR in smooth muscle

While the function of smooth muscle is outside the scope of this thesis, the regulation of RyRs by FKBP in this tissue is nevertheless of interest, as the interacting FKBP and RyR isoforms are the same as found in other tissues, and indeed, may be found interacting in novel combinations.

In general, smooth muscle exhibits a high degree of tissue specificity in its expression of both RyR and FKBP; perhaps to be expected, given the diversity of tissues in which smooth muscle operates. Initial evidence that FKBP played a key role in smooth muscle RyR regulation came from a study by Bielefeldt et al. (1997) which demonstrated that FK506 treatment modulated the Ca^{2+} release properties of intestinal myocytes. In terms of specific tissues, groups have examined the FKBP-RyR relationship in smooth muscle from the trachea (Wang, 2004), colon (MacMillan, 2005 & 2008), pulmonary artery (Wang, 2004; Liao, 2011), and bladder (Weidelt & Isenberg, 2000; Wang, 2004; Ji, 2004; Fritz, 2007; Zheng, 2010).

In all tissues, FKBP12 was found – unsurprisingly, due to its ubiquity of expression – but FKBP12.6 was not detected in colonic smooth muscle. RyR2 was the predominant isoform in all tissues, although Fritz (2007) found the presence of RyR1 in bladder smooth muscle essential to the propagation of depolarisation-induced Ca^{2+} sparks, and Coussin (2000) had previously shown a similar dependence on the expression of

multiple RyR isoforms for CICR in vascular tissues. In all tissues bar the colon, FKBP12.6 was identified as the primary regulatory isoform of RyR, with, for example, FKBP12.6 null mice exhibiting a substantial increase in spontaneous Ca^{2+} release events in urinary bladder myocytes. By contrast, MacMillan (2008) demonstrated an unusual case of RyR2 regulated by FKBP12 alone in colonic myocytes. In all cases, FKBP regulation of RyR was similar to that of FKBP12 regulation of RyR1, i.e. a stabilisation and lowering of the open probability of the channel. A caveat to all of the above is that it is quite possible that, as in the heart, FKBP12 and FKBP12.6 expression in smooth muscle may be highly species-dependent – this possibility remains to be explored.

1.4.4.3.4 FKBP mediation of RyR association with proteins of the CRC

There are several reports that the RyR-FKBP relationship influences the RyR association with other regulatory proteins. Perhaps most prominently, RyR1-DHPR functional coupling has been shown to exhibit a dependence on the association of FKBP to RyR (Avila, 2003).

Studies by Eltit (2010, 2011) demonstrated that the dysregulation of RyR function – the classic “leaky” phenotype – consequent to deletion of triadin was in fact caused by the absence of triadin in some way disrupting the RyR1:FKBP12.

1.4.5 FKBP and pathology

Mutations of FKBP are yet to be implicated in disease; however, several mutations of RyR that cause pathologies as reviewed in **1.3.5** are located in putative FKBP-binding pockets in the RyR. Specifically, mutations at Glu161, Arg164, Arg402, and Ile404 in RyR1 are associated with malignant hyperthermia, and mutations at Arg169, Ile417, and Arg418 in RyR2 are associated with catecholaminergic polymorphic ventricular tachycardia. It is therefore possible that for these mutations, pathological symptoms may be consequent to disruption of FKBP-RyR association. Further, as FKBP association has been noted to be affected by non-adjacent RyR domains (Girgenrath,

2013), many other pathogenic RyR mutations may possibly effect a dissociation of FKBP.

While pathogenic FKBP mutations are yet to be identified, both altered expression of FKBP and altered associations between FKBP and RyR are found in many pathologies. In many cases, it is uncertain whether these alterations are merely “side effects”, consequent to the progression of an underlying disease state – for example, hyper-phosphorylation of RyR inducing FKBP dissociation – or are in fact the main driver of the disease state. Moreover, both conditions may be true: a disease which incidentally causes dissociation of FKBP from RyR may then be worsened by the consequences of this dysregulation.

This question of altered FKBP:RyR association in disease states has been explored most thoroughly in cardiac muscle. The “calstabin model” of FKBP regulation of RyR (Marx, 2000) implies that FKBP dissociation is necessarily involved in most cardiac RyR channelopathies, secondary to hyper-phosphorylisation of the RyR. Substantial data exists to demonstrate that altered FKBP-RyR stoichiometries are a feature of heart disease – Yano et al. (2000) showed that FKBP was dissociated from RyR2 in a canine model of heart failure, with 3.6 FKBPs associated per tetramer in healthy tissue but 1.6 per tetramer in the heart failure tissue. Supporting the “calstabin model”, in Ca^{2+} release-based arrhythmias, FKBP bound to RyR2 channels has been found to be depleted in some studies (Wehrens, 2005; Györke & Carnes, 2008), but in other reports FKBP-RyR stoichiometries are unaffected (Xiao, 2007; Zissimopoulos, 2009; Oda, 2015; Salvage, 2019).

Beyond the heart, pathological dysregulation of the FKBP-RyR relationship has been observed in most tissues where both are expressed. In patients already suffering heart failure, FKBP12 has reported to be dissociated from RyR1, leading to skeletal muscle weakness (Reiken, 2003; Rullman, 2013), with RyR1 appearing much like their parallel pathological RyR2 to be excessively phosphorylated, s-nitrosylated, and oxidised – all post-translational modifications which may destabilise the FKBP12-RyR1 relationship (**1.3.4.3**).

In the brain, disruption of FKBP12.6 has been shown to effect dysregulated Ca^{2+} release via RyR in the hippocampus, a phenotype which is characteristic of aged rats (Gant, 2011). This phenotype is also observed in Alzheimer’s disease (Stutzmann,

2007; Bezprozvanny, 2008), implying that impaired FKBP-RyR association may be involved in the pathogenesis of Alzheimer's disease. Kihira et al. (2002, 2005) have further reported that the spinal cord expression of FKBP12 declines in the early stages of motor neuron disease, leading to insufficient FKBP12 bound to RyR, thereby possibly contributing to the progression of the disease. Hoeffer et al. (2008) showed that brain-specific disruption of FKBP12 further affected memory and long-term potentiation. In this paper, the researchers attributed the observed changes in behaviour to altered regulation of the mTOR pathway in the absence of FKBP12, however given the results in Gant (2011) above, it is possible that RyR dysregulation may play a role also. FKBP dissociation from neuronal RyR has further been associated with seizures, cognitive dysfunction, and deficits in learning and memory (Lehnart, 2008; Liu, 2012; Yuan, 2016).

A study by Koide et al. (2011) demonstrated that subsequent to subarachnoid haemorrhage, expression of FKBP12.6 is increased in the cerebral vasculature, while expression of RyR2 is diminished, and these altered patterns of expression are key contributors to post-stroke vasoconstriction events. This novel observation of pathology consequent to an overexpression of FKBP is nevertheless consistent with the observations made in the converse case by Ji et al. (2004), where deletion of the gene encoding FKBP12.6 resulted in a vasodilatory increase in Ca^{2+} spark frequency in smooth muscle.

Given such strong evidence for FKBP-RyR dysregulation being at least a factor in many diverse pathologies, pharmacological interventions aimed at stabilising the FKBP-RyR relationship are therefore of great interest. The drug JTV519 (4-[3-(4-benzylpiperidin-1-yl)propionyl]-7-methoxy-2,3,4,5-tetrahydro-1,4-benzothiazepine monohydrochloride), first synthesised by Kaneko (1994) as K201, was observed to have a potent cardioprotective effect in a myofibrillar over-contraction model of the rat heart. Subsequently Hachida et al. (1999) and Nakaya et al. (2000) confirmed this cardioprotective effect in a rat model of ischemic injury and guinea-pig model of atrial fibrillation respectively. Finally, Yano et al. (2003) found that a primary mechanism of this cardioprotective effect of JTV519 was the reversal of hyperphosphorylation of cardiac RyR2, and the concomitant restoration of normal levels of FKBP12.6 associated with RyR2, in line with the model proposed by Marx et al. (2000). Interestingly, Hunt et al. (2007) demonstrated that JTV519 stabilised spontaneous

Ca^{2+} release even when ventricular myocytes had been pre-treated with FK506 in order to dissociate bound FKBP, and no difference was observed in JTV519 stabilisation of RyR expressed in HEK293 cells either alone or with FKBP12.6. These data would appear to indicate at least some FKBP-independent stabilisation functionality of JTV519.

Another 1,4- benzothiazepine derivative, 2,3,4,5,-tetrahydro-7-methoxy-4-methyl-1,4-benzothiazepine - or S107 – has also attracted significant research interest. S107 has been shown to stabilise the RyR-FKBP complex in a similar manner to JTV519, and to improve muscle function and reduce seizures (Bellinger, 2009; Lehnart, 2008; Mei, 2013; Wehrens, 2004b) – it therefore presents significant potential as a treatment for channelopathies in which FKBP dissociation is implicated (Matecki et al., 2016). This thesis will deal further with S107 stabilisation of FKBP-RyR interactions in Chapter 5.

1.5 Project aims

The uncertainty detailed in **1.4.4** regarding the exact nature of FKBP regulation of RyR underlines the primary aims of this thesis. My central hypothesis, arising from the highly variable observations of FKBP affinity for RyR in different experimental contexts, is that the regulatory behaviour of FKBP upon the RyR is more complex than simple binary inhibition or excitation; that it may be multiphasic, and possibly subject to multiple modes of regulation as the stoichiometry of FKBP associated with RyR changes between 0 and 4 molecules bound to each tetramer. Consequently, it is possible that this change in stoichiometry between FKBP and RyR is not linear in affinity, but rather, each step requires progressively greater FKBP concentrations to cause a binding event – that is, that the binding relationship of FKBP to RyR may be characterised as negatively cooperative.

Experiments have therefore been designed to probe the nature of the relationship between FKBP and RyR: their endogenous stoichiometries, their affinities under certain conditions, and isoform-specific differences in their associations. It is hoped that these data will illuminate further the nature of the FKBP-RyR interaction, and thereby provide clues as to the mode of FKBP's regulation of the RyR.

Chapter 2: Materials and Methods

2.0 Introduction

In this chapter, the experimental techniques used to derive the results in subsequent chapters are presented in detail sufficient for replication. For more complex biophysical techniques, the theory underlying their application will also be briefly presented.

2.1 Reagents and chemicals

Manufacturer details of the reagents and chemicals used are listed below; all were of analytical grade.

α-FKBP12/FKBP12.6 antibody (H5)	Santa Cruz Biotechnology, USA
α-RyR1/RyR2 antibody (34C)	Development Studies Hybridoma Bank, USA
β-mercaptoethanol	Sigma-Aldrich, USA
2-propanol	AnalR Normapur, VWR International, USA
Acetic acid	AnalR Normapur, VWR International, USA
Acrylamide	Bio-Rad Laboratories, USA
Agar	Difco Laboratories, USA
Bovine serum albumin	Sigma-Aldrich, USA
Ammonium persulfate	Sigma-Aldrich, USA
Ampicillin	Sigma-Aldrich, USA
BCA protein assay kit	Thermo Scientific / Pierce, USA
Benzamidine	Sigma-Aldrich, USA
Bolt LDS sample buffer	Life Technologies, USA

Brilliant blue R	Sigma-Aldrich, USA
Bromophenol blue	Sigma-Aldrich, USA
$CaCl_2$	Univar, USA
Calpain inhibitor I	Sigma-Aldrich, USA
Calpain inhibitor II	Sigma-Aldrich, USA
cOmplete Protease Inhibitor Cocktail	Sigma-Aldrich, USA
DC Plus protein assay kit	Bio-Rad Laboratories, USA
Dithiothreitol	Sigma-Aldrich, USA
Ethanol	EMSURE, Merck Millipore, Germany
EGTA	Sigma-Aldrich, USA
EDTA	Sigma-Aldrich, USA
Glycerol	Univar, USA
Glycine	AMRESCO, USA
Goat α-mouse IgG-HRP antibody	Santa Cruz Biotechnology, USA
Goat α-rabbit IgG-HRP antibody	Santa Cruz Biotechnology, USA
Guanidine hydrochloride	AMRESCO, USA
HiSpeed plasmid maxiprep kit	QIAGEN, Netherlands
Imidazole	Sigma-Aldrich, USA
IPTG	Sigma-Aldrich, USA
KCl	Chem-Supply, Australia
Kodak Readymatic dental developer	Carestream Health, USA
Leupeptin	Sigma-Aldrich, USA
Luria broth	JCSMR media, Australia
Methanol	EMSURE, Merck Millipore, Germany

Monolith NT Protein Label BLUE-NHS	NanoTemper, Germany
Monolith NT.115 Capillaries	NanoTemper, Germany
TEMED	Bio-Rad Laboratories, USA
Na_2HPO_4	AnalaR Normapur, VWR International, USA
NaCl	Merck Millipore, Germany
NaH_2PO_4	AnalaR Normapur, VWR International, USA
Pepstatin A	Sigma-Aldrich, USA
4-12% Novex Bolt Bis-Tris gels	Life Technologies, USA
Precision Plus dual colour standard	Bio-Rad Laboratories, USA
EDTA-free complete protease inhibitor	Roche, Switzerland
QIAprep spin miniprep kit	QIAGEN, Netherlands
Silver stain kit	Bio-Rad Laboratories, USA
Skim milk powder	Woolworths, Australia
Sodium dodecyl sulphate	Sigma-Aldrich, USA
Sucrose	Chem-Supply, Australia
SuperSignal West Pico ECL substrate	Thermo Scientific / Pierce, USA
Tris	Sigma-Aldrich, USA
Tris-HCl	Sigma-Aldrich, USA
TWEEN-20	AMRESCO, USA
Urea	Sigma-Aldrich, USA

2.2 Equipment and apparatuses

Manufacturer details for the specific labware and instruments used are listed below.

96-well IWAKI-ELISA assay plate	Asahi Techno Glass Corporation, Japan
An-50 Ti rotor	Beckman Coulter, USA
Blender	Waring, USA
Bolt gel system	Invitrogen, USA
Dounce/teflon glass homogeniser	Edwards Instrument Company
EL8000 Universal Microplate reader	BioTek Instruments, USA
Fuji Super RX medical X-ray film	Fujifilm, Japan
JA-14 rotor	Beckman Coulter, USA
J2-21 centrifuge	Beckman Coulter, USA
L8-70 centrifuge	Beckman Coulter, USA
Monolith NT.155	NanoTemper, Germany
Nanodrop ND-1000 spectrophotometer	Thermo Fisher, USA
RC-5B centrifuge	Sorvall, USA
Sephadex 200 column	Sigma-Aldrich, USA
SLA 3000 rotor	Sorvall, USA
SS-34 rotor	Sorvall, USA
SW28 rotor	Beckman Coulter, USA
Ti-45 rotor	Beckman Coulter, USA
XE-100 ultracentrifuge	Beckman Coulter, USA
XLA-1 analytical ultracentrifuge	Beckman Coulter, USA
Vivaspin-2 concentrator	Sartorius, Germany
Vivaspin-20 concentrator	Sartorius, Germany
Waters 515 HPLC Isocratic pump	Waters, USA

2.3 SR vesicle isolation and RyR purification

The primary source of RyR for the experiments in this thesis were SR vesicles fractionated from muscle homogenate, used either raw or after further purification and solubilisation. As compared to engineered RyRs, RyRs sourced from muscle tissue will be complexed with at least some of their regulatory accessory proteins (such as the FKBP12 observed in Peng, 2016); the disadvantage is that RyR are not analytically pure, necessitating additional purification steps for certain experiments. The majority of SR vesicle isolation that contributed to this thesis was performed by Suzy Pace and Joan Stivala.

2.3.1 Preparation of skeletal muscle SR vesicles

Skeletal muscle SR vesicles were isolated from back and leg muscle tissue from New Zealand white rabbits. SR vesicles were prepared largely according to the method of Saito (1984) with some modifications (Ahern, 1994). Upon removal, skeletal muscle was immediately rinsed in cold PBS + 2 mM EGTA. Fat was removed, the muscle tissue diced, and then snap-frozen in liquid nitrogen and stored at -70 °C.

100 g of tissue was homogenised in a blender for 4 x 15 seconds at high speed in a homogenisation buffer consisting of 5 mM imidazole, 300 mM sucrose, at pH 7.4, with the further addition of protease inhibitors (1 mM benzamadine, 0.5 mM PMSF, 3 µM anti-calpain I, 3 µM anti-calpain II, 2.3 µM leupeptin, and 1.46 µM pepstatin A). The homogenate thus generated was centrifuged at 11000 x g for 20 minutes using a Beckman JA-14 rotor in a Beckman J2-21 centrifuge. The pellet from this centrifugation was recovered and resuspended in homogenisation buffer and homogenised as above once again, and then again centrifuged. The supernatant from this centrifugation was filtered through quadruple-layered cotton gauze and then centrifuged at 110000 x g using a Beckman Ti-45 rotor in a Beckman Coulter Optima XE-100 ultracentrifuge.

The pellet from the last-mentioned centrifugation was recovered and resuspended in 42 mL of homogenisation buffer and homogenised in a Dounce Teflon/glass homogeniser. 8 mL of homogenate was then loaded onto a discontinuous sucrose gradient, composed of the following layers: 4 mL of 45% sucrose; 7 mL of 38%

sucrose; 7 mL of 34% sucrose; 7 mL of 32% sucrose, and finally 4 mL of 27% sucrose. Sucrose solutions were all constituted in a 20 mM imidazole buffer at pH 7.4, with the addition of protease inhibitors as above. The sucrose gradient was centrifuged overnight at 72000 x g and at 4 °C using a Beckman SW28 rotor in a Beckman L8-70 ultracentrifuge. Bands at the 34%-38% (B3) and 38%-45% (B4) interfaces were collected and diluted in at least two volumes of dilution buffer. Finally, diluted fractions were centrifuged at 125000 x g and at 4 °C using a Beckman Ti-45 rotor in a Beckman L8-70 ultracentrifuge. This final pellet was resuspended in 1 mL of homogenisation buffer, divided into 15 µL aliquots, and frozen in liquid nitrogen and stored at -70 °C.

2.3.2 Preparation of cardiac muscle SR vesicles

Cardiac muscle SR vesicles were isolated from sheep heart ventricles, according to the method of Chamberlain & Fleischer (1988) with minor modifications. Upon removal, sheep hearts were immediately submerged into cold PBS + 2 mM EGTA, and rinsed several times to remove blood. Working quickly, fat was trimmed from the ventricles and the auricles removed, and the ventricles cut into small cubes, all while submerged in a homogenisation buffer composed of 0.29 M sucrose, 10 mM imidazole, 0.5 mM DTT, and 3 mM NaN3 at pH 6.9. Diced tissue was then snap-frozen in liquid nitrogen and stored at -70 °C.

Tissue was then homogenised in a blender for 3 x 10 seconds at high speed in the presence of the aforementioned homogenisation buffer. Homogenate was then centrifuged at 9700 x g using a Sorvall SS-34 rotor for 20 minutes. The resulting supernatant was filtered through quadruple-layered cotton gauze and centrifuged again, this time at 104537 x g for 2 hours using a Beckman Ti-45 rotor in a Beckman L8-70 ultracentrifuge. The pellet from this centrifugation was then resuspended in 60 mL of homogenisation buffer to which was further added 0.65 M KCl and the protease inhibitors detailed in **2.1.1**. The suspension was then homogenised in a Potter homogeniser and then iced for 30 minutes and then centrifuged at 4350 x g for 10 minutes using a Beckman JA-20 rotor in a Beckman J2-21 centrifuge. The supernatant was collected and then centrifuged at 257090 x g for 100 minutes using a Beckman Ti-70 rotor in a Beckman L8-70 centrifuge. The resulting pellet was finally suspended

in 15 mL of the homogenisation buffer + 0.65 M KCl + protease inhibitors, divided into 15 µL aliquots, and stored at -70 °C.

2.3.3 Purification and solubilisation of RyR from SR vesicles

Fractions prepared as described in **2.3.1** and **2.3.2** were further purified and rendered soluble according to the technique of Lee (1994) and Laver (1995) with minor modifications. The primary means of fractionation was a continuous sucrose gradient. Sucrose solutions were all composed in a solubilisation buffer consisting of 25mM PIPES, 1 M NaCl, 1 mM DTT, 0.5% CHAPS, 0.25% L-α-phosphatidylcholine, 100 µM EGTA, 92 µM $CaCl_2$, and 500 µM AMP, along with EDTA-free complete protease inhibitor, at pH 7.4. Sucrose gradient layers were in four increasing concentrations – 5%, 10%, 15%, and 20% - in equal 7.5 mL volumes, and were allowed to stabilise into a continuous gradient at 4 °C for at least 4 hours prior to use. Approximately 10 mg of SR vesicles were solubilised on ice for 30 minutes to 1 hours in sufficient solubilisation buffer for a final concentration of 2.5 mg/mL. Insoluble membrane fragments were removed by centrifugation at 163200 x g for 20 minutes using a Beckman TLA 100.3 rotor. The resultant supernatant, approximately 4 mL in volume, was loaded onto the sucrose gradient and centrifuged overnight at 71935 x g using a Beckman SW28 rotor. Fractions were collected and examined vis SDS-PAGE (**2.5.1**) and silver stain (**2.5.2**), and fractions containing large amounts of high-molecular weight protein running at approximately 500 kDa (previously confirmed as being RyR via anti-RyR Western blot) pooled and concentrated via a Vivaspin-2 concentrator approximately 10 fold, and then transferred into 15 µL aliquots and stored at -70 °C. Protein concentration was determined in the first instance via DC Plus protein assay (**2.4.1**). Western blots of purified fractions confirmed no remaining CSQ, junctin, or triadin, and very limited remaining FKBP (see also **Chapter 3** for quantitation of remaining FKBP post-solubilisation). Some fractions contained amounts of a protein appearing at approximately 120 kD, corresponding to SERCA, as can be seen in Figure **2.1**, overleaf.

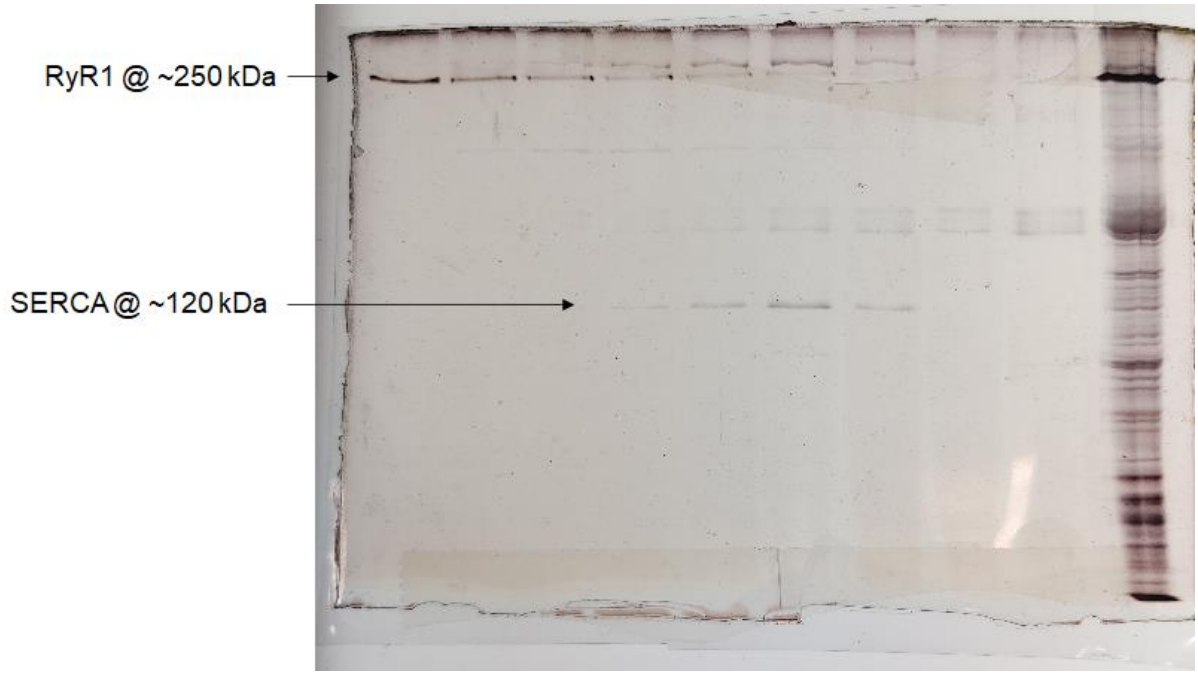

Figure 2.1: Silver stained SDS-PAGE gel of solubilised skeletal muscle SR fractions, showing RyR1 (at ~250 kDa) and SERCA (at ~120 kDa). Fractions containing substantial RyR1 (in this case, fractions 1 through 7) are pooled and aliquoted for future use.

2.4 Protein expression and purification

FKBP12 used throughout this thesis was expressed in bacterial culture and purified to analytical levels. Purified proteins were subsequently assessed via analytical ultracentrifugation and multi-angle laser light scattering (**Chapter 4**) in order to characterise their native oligomeric states and general details of their secondary structures. After expression, protein concentrations were quantified per the techniques described in **2.5**.

First, 25 µL of competent BL21 DE5 cells were transformed with approximately 50 ng of GST-FKBP12 packaged in a PGEX-4T-1 vector via heat shock. Briefly, this involved incubation of cells and DNA at 4 °C for 30 minutes; addition of 125 µL of Luria broth (LB); incubation at 42 °C for 30 seconds; incubation at 4 °C again for 2 minutes; addition of a further 125 µL of Luria broth; and finally, incubation at 37 °C for 1 hour. ~100 µL of transformed cells were then used to inoculate with the 16-streak method the surface of an LB/ampicillin plate (125 µg/mL ampicillin in LB, solidified with 1.5%

Bacto-agar), which was then incubated for 8 hours at 37 °C. A single cell colony was selected and inoculated into ~30 mL of LB/ampicillin solution (125 µg/mL ampicillin in LB) and incubated overnight with rotation at 37 °C. 20 mL of this starter culture was then divided between 4 2L conical flasks containing 400 mL of LB/ampicillin solution. These were then incubated for 4 hours at 37 °C with rotation, until the solution absorbance at 600 nm was approximately 0.8, as measured by a Cary 100 spectrophotometer. Protein expression was then induced by addition to the flasks of 0.1 mM IPTG, and incubation was continued for a further 4 hours. Finally, cells were pelleted at ~4000 x g using a Sorvall SLA 3000 rotor in a Sorvall RC-5B centrifuge for 30 minutes at 4 °C. Supernatant was discarded and cell pellets frozen at -20 °C overnight.

Cell pellets from ~1600 mL of culture were resuspended in 40mL of PBS + complete protease inhibitors. This solution was mixed by vortexing and then sonicated 5 x 30 seconds, with an 80% sonication duty cycle. All sonication took place on ice to minimise heating.

Cell lysate was then clarified from cell membranes and other debris by centrifugation in an SS-34 rotor at ~5000 rpm for 30 minutes at 4 °C. Lysate was pooled and then incubated with ~2mL of a 50:50 slurry of Glutathione Sepharose 4B, previously washed and equilibrated with PBS per manufacturer's instructions. Incubation was overnight at 4 °C, with rotation.

Beads were then washed 3 x with 40 mL PBS, with the lysate and first wash preserved for later analysis. Bound GST-FKBP12 was then eluted from beads by the addition of 3 mL of a 10 mM GSH, 50 mM Tris solution at pH 8. Elution was performed three times and the fractions pooled.

GST-FKBP12 eluate was then either cleaved enzymatically or else the construct preserved intact and going straight to final purification by FPLC. For cleavage, approximately 80 IU of bovine thrombin was incubated with the GST-FKBP12 eluate overnight at room temperature with rotation. Cleaved GST-FKBP12 was then separated into pure FKBP12 via FPLC.

Before FPLC, if sample volume was greater than 5 mL, it was first concentrated to ~5 mL by centrifugation in a Vivaspin 20 spin column with a membrane porosity of 5 kDa. Samples were then separated on a Sephadex 200 size-exclusion column driven by a

Waters pump on a mobile phase of PBS, at a flowrate of 0.5 mL / minute. 35 fractions of 4 mL volume each were collected, and all but the first analysed across two SDS-PAGE gel (**2.6.1**). Together with absorbance measurements (per Figure **2.2**, below), this identified the fractions containing either GST-FKBP12 or pure FKBP12. These fractions were then pooled and concentrated, again using a Vivaspin 20 column, to ~5 mL volume, then quantified as per (**2.5**). Chapter 4 details some further characterisation of the expressed protein via analytical ultracentrifugation.

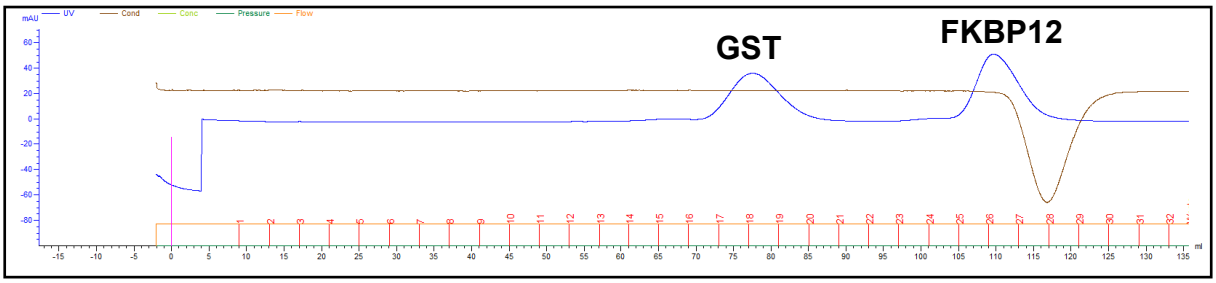

Figure 2.2: Representative FPLC trace of cleaved GST-FKBP12, with peaks corresponding to GST and FKBP12. Blue trace indicates absorbance of fractions at 280 nm; brown trace indicates conductivity of sample, with conductivity dip corresponding to sample buffer desalting. Thrombin and some uncleaved GST-FKBP12 will also be present, but at levels undetectable by spectrophotometry. In this instance, fractions 24 through 28 were pooled to create fractions for concentration, with the fractions and resulting concentrate verified via Coomassie blue stained SDS-PAGE.

2.5 Protein concentration determination

As knowledge of protein concentration was essential, especially for protein characterisation and kinetics experiments, concentrations of expressed proteins and RyR were quantitated by both biochemical and spectrophometric methods, and the results compared for concordance.

2.5.1 Biochemical assays for protein concentration

The primary method of protein concentration determination was the bicinchoninic acid (BCA) assay, supplemented occasionally with the Lowry and Bradford assays. The nature of the proteins being examined and their buffers informed the selection of assay; in general BCA is well-suited to examination of most proteins but reacts poorly to various detergents such as CHAPS in buffers; hence, the Lowry assay was the primary method of quantitation for solubilised RyR (**2.2.3**).

BCA assays were performed with the Pierce BCA protein assay kit according to the manufacturer's instructions. Assays were conducted according to the microplate method, using a 96-well flat bottomed IWAKI-ELISA assay plate (Asahi Techno Glass Corporation, Japan). Working reagent was first prepared by mixing 50 parts BCA reagent A with 1 part BCA reagent B. Protein standards were generated by use of analytically assayed concentrations of BSA diluted into the same buffer as the protein under examination – generally PBS. 20 µL of protein sample to be assayed was dispensed in triplicate into the microplate, along 20 µL volumes of a triplicate protein concentration curve, from 0.025 to 2 mg/mL. 200 µL working reagent was then added to each well and mixed by aspiration, and the plate then shaken for 30 seconds to 1 minute on a microtiter plate shaker (Flow Laboratories, Australia). Plates were then sealed with parafilm (Pechiney, USA) and incubated at 37 °C for 30 minutes. Standard curve and protein samples were then measured for absorbance at 562 nm using an EL8000 Universal Microplate reader (BioTek Instruments, USA), with 750 nm set as the reference spectra. Sample concentrations were then determined by reference against the standard curve via the KCjunior software (BioTek Instruments).

The Lowry assay, in the form of the Bio Rad DC Plus assay with some minor modifications from the manufacturer's instructions, was used supplementary to the BCA assay, and in the first instance when assaying RyR concentrations, as it has greater compatibility with the complex RyR buffer. Assays were conducted in similar fashion to BCA assays, in an IWAKI-ELISA microplate, against a standard curve of BSA dissolved in buffer. Briefly, the supplied reagents S and A were mixed in a 1:50 ratio. 5 µL of samples and standards were pipetted into the wells of the microplate, followed by 25 µL of the S+A reagent mixture. Finally, 200 µL of the supplied reagent B was added to each well. Microplates were mixed for a minute on a microtiter plate

shaker, and then sealed with parafilm and incubated at room temperature for 15 minutes. Standard curve and protein samples were then measured for absorbance at 750 nm using an EL8000 Universal Microplate reader. Sample concentrations were then determined by reference against the standard curve via the KCjunior software.

2.5.2 Spectrophotometric assay for protein concentration

The primary spectrophotometric method of protein concentration determination was measurement of sample absorbance at 280 nm using the Nanodrop ND-1000 spectrophotometer (Thermo Fisher, USA). Samples, approximately 1 µL in volume, were measured for absorbance in excess of that measured in a blank buffer sample, and the generated absorbance value then multiplied by the protein's extinction coefficient, calculated via inputting of the protein's amino acid sequence into the ExPASy ProtParam tool (Gasteiger, 2005). Measurements were repeated in triplicate and the results averaged to exclude sampling anomalies.

2.6 Electrophoresis and Western blotting

Electrophoresis and Western blotting was a primary tool for the visualisation of data generated from co-sedimentation and co-immunoprecipitation experiments (**2.7**). It was also used extensively in diagnostic analysis of RyR fractionation (**2.3**) and protein expression (**2.4**).

2.6.1 SDS-PAGE

Denaturing electrophoretic analysis of proteins and preparation of gels for later Western blotting was performed in the Bolt gel system (Invitrogen), after the method of Laemmli (1970). 4-12% polyacrylamide gradient Bolt gels were used with a MES-based running buffer composed of 50 mM MES, 50 mM Tris base, 1 mM EDTA, and 0.1% SDS (pH 7.3). Occasionally, a MOPS-based running buffer would be substituted for the examination of higher molecular weight proteins, composed of 50 mM MOPS, 50 mM Tris base, 1 mM EDTA, and 0.1% SDS (pH 7.7). Prior to loading on gels, protein samples were mixed 3:1 with a sample buffer containing 250 mM Tris-HCl (pH

6.8), 40% glycerol, 10% SDS, 20% β-mercaptoethanol, and 0.1% bromophenol blue. Occasionally, where reduction was not desired, β-mercaptoethanol was omitted from this buffer. Bolt gel tanks were powered by Bio-Rad 200 or 300 PowerPacs; gels were run at 100 V for 10 minutes to stack protein bands in low-density gel, and then at 150 V for ~50 minutes if using MES buffer and 165 V for ~50 minutes if using MOPS buffer. Bio-Rad Precision Plus Protein Dual Colour Standard was most commonly used as a protein molecular weight marker.

Occasionally, hand-cast gels were used as supplements to Bolt gels, and were cast with the assistance of the Bio-Rad Mini-PROTEAN Tetra system. Here, gels generally followed a discontinuous chemistry, with 4% polyacrylamide in the stacking gel and 12% in the running gel. Stacking gels were formulated with appropriate concentrations of acrylamide-bis, 0.1% SDS, 0.125 M Tris-HCl (pH 6.8), 0.1% APS, and 0.2% TEMED, with MilliQ water making up the remainder of the required volume. Running gels were composed similarly of appropriate acrylamide-bis concentrations, 0.1% SDS, 0.375 M Tris-HCl (pH 8.8), 0.05% APS, and 0.2% TEMED, again with remaining volume made up by MilliQ water. Running buffers for such gels were made with 25 mM Tris, 191 mM glycine, and 0.1% SDS, at pH 8.3. Generally, they were run at 200V continuously for ~60 minutes.

As both FKBP12 and FKBP12.6 could be expected to be present in samples derived from cardiac tissue, it was essential that SDS-PAGE protocols be capable of separating the two proteins, despite their very similar masses. Previous work in our laboratory (Steele, 2013) has addressed this problem and found the MES buffer-based protocol described above capable of sufficiently separating the two proteins (as shown in Figure **2.3**).

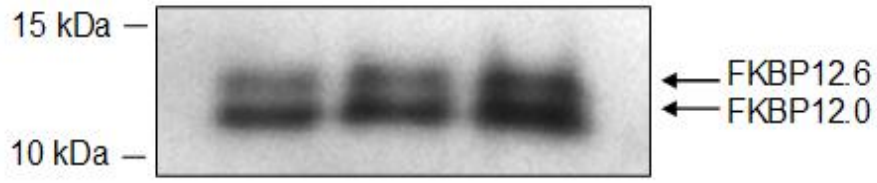

Figure 2.3: Optimisation of FKBP12 and FKBP12.6 separation. Western blot showing, from left to right, increasing concentrations of a cardiac SR vesicle sample, probed with H5 anti-FKBP12 antibody. Samples were run as described above, on the Bolt gel system in conjunction with MES buffer. The low and medium concentrations have the FKBPs sufficiently separated to allow for densitometric analysis (**2.6.5**). Figure adapted from the Honours thesis of Gregory Steele (2013).

2.6.2 Protein staining

Most commonly, protein bands were visualised by staining with Coomassie blue stain, formulated as a solution of 0.1% Coomassie brilliant blue, 40% ethanol, and 10% glacial acetic acid. Gels were allowed to stain for at least 1 hour, and up to overnight, with gentle agitation. Excess background staining was then removed by destaining gels with a solution of 20% ethanol and 5% acetic acid in similar conditions – gentle agitation, and incubation periods of between 1 hour and overnight. Kimtech Science Kimwipes were often added to destain vessels to adsorb liberated Coomassie in order to prevent equilibrium stain diffusion.

For detection of very low concentrations of proteins, silver stain was employed, based on the Bio-Rad Silver Stain Plus kit. Gels were incubated in a fixative enhancer solution composed of 50% methanol, 10% acetic acid, and 10% fixative enhancer concentrate for 20 minutes, with gentle agitation. After fixation, gels were rinsed twice for 10 minutes in MilliQ water, followed by development in stain solution, made of 5% silver complex solution (containing NH_4NO_3 and $AgNO_3$), 5% reduction moderator solution (containing tungstosilicic acid), 5% image development solution, and 2.5% development accelerator reagent (containing Na_2CO_3). Gels were developed in this solution for approximately 15 minutes, or until desired level of staining was achieved; development was stopped by immersion of the gel in 5% acetic acid. Gels were then washed at least twice for 10 minutes in MilliQ water.

2.6.3 Gel preservation

A gel drying apparatus from Invitrogen was used to preserve gels for later reference. Gels were thoroughly washed in MilliQ water, then incubated in a dehydration buffer composed of 2% glycerol and 20% ethanol for at least 20 minutes. Two sheets of cellophane were soaked in this dehydration buffer for 1 minute, and then gels were placed between these two sheets, which were themselves then bound by the drying apparatus frames overnight. Gels were then stored in plastic sleeves in a lab-book, indexed by date.

2.6.4 Western blotting

Western blots were conducted after the method of Towbin (1979). After SDS-PAGE, gels were transferred to a Bio-Rad transfer cassette, overlaid with a 0.45 µm PVDF membrane, and sandwiched between layers of filter paper and fibre pads. Assembly of this transfer cassette was conducted under immersion in transfer buffer, itself composed of 37 mM Tris, 140 mM glycine, and 20% methanol. Prior to assembly, PVDF was equilibrated by brief washes in methanol, then MilliQ water, and finally soaking in transfer buffer. Gels were likewise equilibrated by soaking in transfer buffer. After assembly, cassettes were transferred into a Mini-PROTEAN® Tetra tank along with sufficient transfer buffer for immersion, and then run at 100 V for approximately 1 hour, and then 160 V for approximately 30 minutes. For high concentrations of high molecular weight proteins, this regime would be preceded by 1-2 hours of transfer at 40 V. Power was supplied by a Bio-Rad HC PowerPac. Transfer was conducted at room temperature, but transfer buffer would be pre-chilled to approximately 4 °C and temperature depressed during transfer by addition of a cooling block to the transfer tank.

After protein transfer, membranes were removed from the transfer cassette and briefly immersed in methanol, then washed in PBS. Non-specific binding of antibodies was blocked by incubation of membranes with a 3% solution of either skim milk powder or BSA dissolved in PBS for at least 1 hour, with gentle agitation. If multiple proteins were to be detected, the membrane was cut after blocking according to the expected molecular weights of the proteins, by reference to the protein standard ladder. Cut

membranes were then incubated overnight at 4 °C with rotation in primary antibody diluted to the appropriate concentration in TPBS (0.05% Tween-20 in PBS). Membranes were thoroughly washed (5 x 5 minutes) in TPBS and then incubated for 1-2 hours at room temperature with rotation in HRP-conjugated secondary antibody diluted to 1:6000 in TPBS. Membranes were again washed for 5 x 5 minutes in TPBS, and washed finally in PBS.

After antibody binding, membranes were treated with SuperSignal West Pico ECL substrate as per the manufacturer's instructions: equal parts of the stable peroxide solution and the luminol enhancer solution were mixed together, and the membrane incubated in this mixture for 5 minutes. Membranes were then removed from working solution, excess solution absorbed, and then sealed in plastic wrap. Sealed membranes were then placed in film cassettes and exposed to Fuji Super RX medical X-ray film (Fujifilm, Japan) for between 1 and 5 minutes depending on protein concentrations. Film was developed by submerging first into Kodak Readymatic dental developer (Carestream Health, USA) for between 10 seconds and 1 minute, and then Kodak Readymatic dental fixer for approximately 1 minute; films were then washed in water and allowed to air dry.

The primary antibodies used for probing RyR and FKBP presence were, respectively, 34C and H5. 34C is capable of detecting both RyR1 and RyR2, although binds to RyR2 with a lower affinity than it does to RyR1. H5, similarly, may detect both FKBP12 and FKBP12.6, although is somewhat less sensitive to FKBP12.6. 34C was used diluted 1:6000 in TPBS, while H5 was used diluted 1:1000 in TPBS.

Selection of these antibodies was based on previous work in our laboratory which indicated that although a specific anti-RyR2 antibody (HPA016697, Sigma-Aldrich) offered better binding to RyR2 and hence easier detection of associated proteins in co-immunoprecipiation experiments (**2.7.2**), it also non-specifically bound FKBP12 to some degree, resulting in confounding false positive detection of FKBP12s beyond those which are bound to RyR2 (Figure **2.4**).

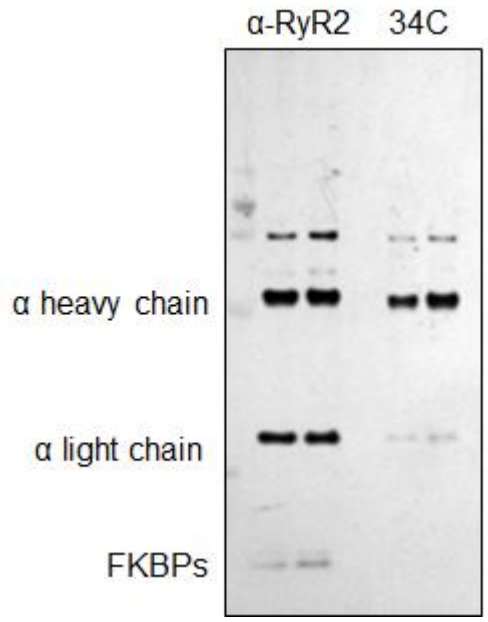

Figure 2.4: Specific anti-RyR2 antibody HPA016697 (labelled as α-RyR2) non-specifically binds to FKBP12, while 34C does not. Western blot of the product of co-immunoprecipitation of FKBP12-rich cardiac SR vesicle supernatant by the indicated anti-RyR antibody; lanes are two different concentrations of supernatant for each antibody. Figure adapted from Honours thesis of Gregory Steele (2013).

2.6.5 Densitometry

Gels or Western films were scanned with a white light transillumination protocol on a Bio-Rad Gel Doc XR, and signals then quantified in the Bio-Rad ImageLab software. Signal areas were manually selected, and signal densities were controlled for background by subtraction of an equal non-signal area. Changes between control and experimental conditions were generally expressed as the change in the ratio between two proteins (e.g., RyR1 and FKBP12) in order to eliminate the necessity for absolute quantitation or loading control.

For densitometry to be a valid means of investigating changes in protein levels, it must be established that any antibodies used for protein detection exhibit linear responsivity across the protein concentrations under examination. That is, as protein concentration is increased, antibody binding should concomitantly increase in a linear fashion. Ideally, the slope of this linear response should also be similar for any proteins that are to be compared in a “set”. Linear response against RyR and FKBP in the normal

range of working concentrations used in experiments was therefore verified for the two primary antibodies used in this thesis, 34C and H5.

2.7 Co-sedimentation and co-immunoprecipitation

Co-sedimentation and co-immunoprecipitation experiments were used primarily to assay the relative levels of FKBP bound to RyR under varying conditions. Co-immunoprecipitation experiments have the advantage of specificity, i.e., discounting non-specific interactions with the precipatory resin, the only proteins that should appear in the co-immunoprecipitation eluate are the targeted protein and its various binding partners. The primary immunoprecipitant antibody used in these experiments, 34C, has been previously found not to non-specifically precipitate FKBP (**2.6.4**).

Co-sedimentation experiments are performed much more quickly, and thus have the advantage of generating statistically robust data in a shorter period of time; however, it is essential to confirm any results obtained with co-sedimentation with co-immunoprecipitation to rule out the possibility of nonspecific co-sedimentation of proteins.

2.7.1 Co-sedimentation

Co-sedimentation was used to observe proteins that remained bound to the membrane-bound RyR found in raw SR vesicles subsequent to thorough washing. Generally, 10 µL of cardiac or skeletal SR vesicle were suspended in a buffer consisting of 20 mM MOPS, 150 mM NaCl, 50 mM sucrose, and EDTA-free complete protease inhibitors. To this, treatment factors were added: FKBP-ablative drugs, for example, in the case of Chapter 3, or exogenous FKBP in Chapter 4. Samples were then incubated for 2 hours at 37 °C. Following incubation, samples were centrifuged at 100000 x g for 30 minutes at 4 °C using a Beckman TLA100.3 rotor. The resulting pellet was washed 3 times with the aforementioned MOPS buffer, with identical centrifugation after each wash. The pellet was then resuspended in 20 µL SDS sample buffer (**2.6.1**) and 20 µL milliQ water, vortexed thoroughly, and then run on SDS-PAGE (**2.6.1**) for subsequent staining (**2.6.2**) or Western blotting (**2.6.4**) as appropriate.

2.7.2 Co-immunoprecipitation

The primary co-immunoprecipitation experiment performed in this thesis involved the immobilisation of RyR1 or RyR2 via the anti-RyR 34C antibody. Optimisation of co-immunoprecipitation conditions was based on Walweel, 2017 and previous work from our laboratory (Steele, 2013).

Reagents were all sourced from the Pierce Co-immunoprecipitation Kit unless otherwise noted. All wash steps involved centrifugation at 1000 x g for 1-2 minutes. First, coupling resin was prepared – 40 µL of a 50% slurry for each reaction – by removal of the storage solution and 2 subsequent washes with 200 µL of PBS. Resin was then resuspended in 200 µL of PBS, and either 2 µL or 4 µL of the 34C anti-RyR antibody added – 2 µL if RyR1 was the precipitation target, 4 µL if RyR2 was the precipitation target. Antibodies were immobilised on the coupling resin by addition of 3 µL of 5M sodium cyanoborohydride, followed by 2 hrs of incubation at room temperature with rotation. Excess antibody was then washed out, and the resin washed as before 2 times with PBS. Remaining active aldehydes on the coupling resin were quenched by addition of 200 µL 1M Tris-HCl along with 3 µL of 5M sodium cyanoborohydride, then incubation for 30 minutes at room temperature with rotation. Coupling resin was again then washed 2 times with PBS, 6 times with a wash solution of 1M NaCl, and then washed/equilibrated 2 times with the final binding buffer of 20mM MOPS, 150mM NaCl, 50 mM sucrose, along with EDTA-free complete protease inhibitors.

Before incubation with the coupling resin, samples were first “pre-cleared” to minimise non-specific interactions with the coupling resin. 100 µL of control (i.e. without activatable aldehydes) resin slurry was centrifuged to remove storage solution and then washed 2 times with 200 µL PBS, then 2 times with the aforementioned binding buffer. SR vesicles, either skeletal or cardiac, containing approximately 400 µg of total protein, were suspended in ~390 µL of binding buffer, along with protease inhibitors). Suspended vesicles were then incubated with the prepared control resin for 30 minutes at room temperature with rotation. Vesicles were then eluted and aliquoted into 4 equal volumes of ~100 µL.

Each of these 100 µL vesicle aliquots were incubated with the prepared anti-RyR coupling resin overnight at 4 °C. Non-immobilsed proteins from the vesicle samples

were removed by low-speed benchtop centrifugation (2000 g approximately) and 3 subsequent washes with the MOPS binding buffer; these wash fractions were saved for analysis. Finally, immunoprecipitated proteins were eluted by the addition of 40 µL of 2 x SDS-PAGE sample buffer (**2.6.1**) and heating at 70 °C for 10 minutes. Samples were then analysed, typically via Western blot (**2.6.4**).

2.8 Analytical ultracentrifugation

Analytical ultracentrifugation (AUC) analyses the mobility of particles in a gravitational field in order to extract information about their homogeneity, mass, or behaviour in associating systems (Svedberg, 1940).

In this experiments described in this thesis, AUC has been used to validate the oligomeric state of expressed proteins, using the sedimentation equilibrium mode of analysis. In sedimentation equilibrium experiments, samples were spun between 3000-12000 x rpm in an AN-50 Ti rotor in the Beckman XLA-1 AUC. These speeds are high enough to force protein toward the bottom of the cell, but not high enough to pellet the sample. The “downwards” force produce a protein concentration gradient across the cell, opposed by particle diffusion. After ~18 hours, a stable balance is reached between sedimentation and diffusion, and the concentration distribution reaches an equilibrium. This equilibrium concentration distribution across the cell is then measured while the sample is spinning, using absorbance measurements at both 280 and 230 nm.

Analysis of data was performed in the Sedphat (Zhao, 2015) software package.

2.9 Microscale thermophoresis

Microscale thermophoresis (MST) exploits the principle of molecular movement along a temperature gradient to ascertain the kinetics of molecular interactions (Jerabek-Willemsen, 2014). Serially-diluted analytes are mixed with a fixed concentration of a fluorescently-tagged binding partner, and then loaded into fine capillary tubes. The MST assay then involves heating a defined region in a capillary tube with a laser, which region is simultaneously monitored for fluorescence. Complexes of

biomolecules, as well as any unbound species, migrate out of the heated region. The migration of the fluorescently-tagged species is measured as a drop in overall fluorescence in the region; this principle is illustrated in Figure **2.5**.

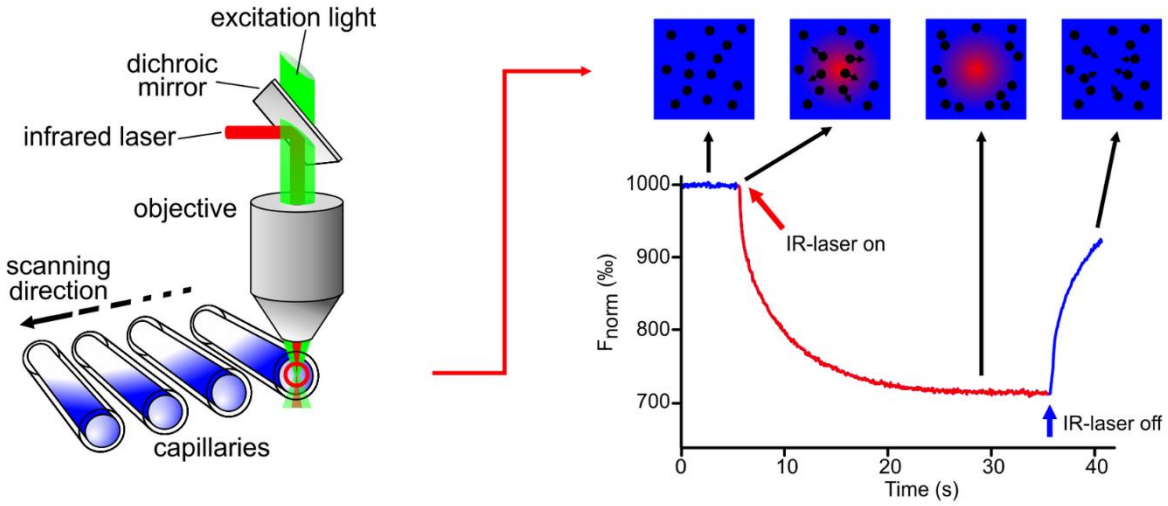

Figure 2.5: Illustration of MST instrument function (from Jerabek-Willemsen, 2014). The left panel shows capillary tubes loaded with mixtures of fluorescently-tagged analytes and binding partners being heated with a laser and monitored for a drop in fluorescence; right panel shows how such a drop in fluorescence is reported by MST software as a decrease in Fnorm (normalised fluorescence) over time, followed by a return to baseline fluorescence as the laser is deactivated.

Preliminary kinetics experiments using MST appear in Chapter 6 of this thesis. For these experiments, FKBP12 cleaved from GST-FKBP12 per **2.4** was incubated with an NHS-ester dye kit from NanoTemper per the manufacturer's instructions. This tagging process resulted in samples of dyed FKBP12 at a concentration of approximately 32 nm, as assayed by spectrophotometry as described in **2.5.2**. Prior to any interaction experiments, a serial dilution of the tagged FKBP12 was prepared and analysed in the Monolith NT.115 MST apparatus to confirm that fluorescence levels fell within the analytical range of the apparatus.

As a binding partner, solubilised RyR1 was prepared in serial dilution, with 14 concentrations generated ranging from approximately 20 µM to 2 nM. RyR1 concentrations were assayed via both Lowry assay. Diluent was solubilisation buffer, as described in **2.3.3**. Additionally, a negative control set of RyR1 dilutions was

prepared, where solubilised RyR1 was pre-incubated with 10 µM FKBP12, separated from excess FKBP12 via FPLC on a Sephadex 200 column, and then serially diluted as above. The concentrations of these pre-incubated RyR1 dilutions similarly ranged from 20 µM to 2 nM. Tagged FKBP12 and RyR1 dilutions were mixed immediately prior to analysis via brief vortexing, and then drawn up into standard NT.155 capillary tubes. MST assays proceeded with standard settings, and the IR laser set to 20% power.

Chapter 3: Differential response of RyR1 and RyR2 to FKBP-dissociating treatments

3.0 Introduction

In this chapter, the efficacy of different agents in dissociating FKBP from RyR1 and RyR2 is compared. Differences in the efficacy of FKBP-dissociation between RyR1 and RyR2 are of intrinsic interest in understanding the relationship between FKBP and the two RyR isoforms – for example, differences in modes of FKBP-dissociation are likely to parallel differences in modes of endogenous association, which inform questions of regulation of RyR by FKBP. These experiments also provide data towards implementing a protocol for FKBP-removal from RyR for later experiments that require RyR to be depleted of as much FKBP as possible.

Two closely-related immunosuppressant drugs have been commonly reported to be effective in removing FKBP from RyR: FK506 and rapamycin (**1.4.3**). These drugs are both generally considered to have nearly-complete efficacy in removing FKBP from RyR. Previous work in this laboratory has indicated that rapamycin is effective in removing ~90% of FKBP12 from RyR1, but removes only ~20% of FKBP12 from RyR2 (Richardson, 2017). In addition to suggesting that FKBP12 could not be completely removed from either isoform by rapamycin, this work revealed significant differences in the degree of rapamycin's effect between RyR1 and RyR2.

This differential response to a FKBP-liberating treatment was seen again in experiments with the FKBP-dissociating CLIC-2 protein (Richardson, 2017). CLIC-2 achieves FKBP-dissociation through a different mechanism to the immunosuppressant drugs: rather than interacting with the FKBP itself, CLIC-2 interacts with the RyR and induces a conformational change that alters the FKBP-binding pocket sufficient to achieve a degree of FKBP-dissociation. CLIC-2 treatment was observed to remove only ~20% of FKBP12 from RyR1 but removed approximately ~50% of RyR2-associated FKBP12 and FKBP12.6 (Richardson, 2017), making it more effective at removing FKBP from RyR2 than rapamycin. Despite their different FKBP-dissociating mechanisms, these CLIC-2 and rapamycin observations together suggest

some potential important differences in the nature of the binding of the FKBPs to RyR1 and RyR2.

Some degree of variability of response between RyR1 and RyR2 to FKBP-dissociation might be expected. It is known that RyR1 and RyR2 interact somewhat differently with their associated FKBP: with respect to the FKBP they share in common, FKBP12, their dissociation constants have been reported by some groups to differ by up to four orders of magnitude: ~100 μM in RyR2 as compared to ~10 nM in RyR1 (**1.4.4**, Lai, 2005). Differences in the sequence of the putative FKBP binding pockets between RyR1 and RyR2 (**1.4.2**) may give rise to further structurally-based variability in their interactions. However, the response of the two isoforms to a wide variety of dissociating treatments has not previously been directly compared.

In addition to immunosuppressant treatment or the action of CLIC-2, a further mechanism has been proposed for FKBP-dissociation from RyR, whereby high ionic strength may “salt off” FKBP from RyR (Galfré, 2012; Qin, 2008). This is an interesting and relatively non-invasive method for FKBP removal, but to date has not been compared alongside the more commonly-used drug treatments.

It is further often assumed in the literature that purification of RyR from vesicles by solubilisation removes associated FKBP12 and FKBP12.6 – but again, this assumption has not been thoroughly tested. The efficacy of RyR vesicle solubilisation as a dissociation mechanism has therefore also been tested here, and compared against the efficacy of FKBP-removing drug treatments.

To summarise, in this chapter the efficacy of the two immunosuppressant drugs, high salt concentration, solubilisation alone and solubilisation in conjunction with drug treatment in dissociating FKBP has been examined and compared, and the results with all three treatments compared with those previously obtained with CLIC-2 (Richardson, 2017). These results reveal further isoform-specific differences not only between the effects of the treatments on RyR1 and RyR2, but also between the effects on FKBP12 and FKBP12.6 as associated with RyR2. In addition, the data provide an assessment of which of these methods is most useful in preparing FKBP-ablated RyR for use in future studies of FKBP:RyR binding.

3.1 Aims

The aims of these experiments are twofold: first, to compare the efficacy of FKBP-dissociating treatments on the RyR isoforms; second, to observe any differences in the response of each isoform to these treatments which may illuminate differences in the nature of their interactions with FKBP.

3.2 Materials and Methods

Rabbit skeletal muscle or sheep cardiac muscle SR vesicles were generated as described in **2.3**, and solubilised RyR was generated as per **2.3.3**. Both co-sedimentation (**2.7.1**) and co-immunoprecipitation (**2.7.2**) were used to assess FKBP binding to RyR in response to treatment conditions: buffers used in both instances were composed of (mM) 20 MOPS, 150 NaCl, 50 sucrose, plus protease inhibitors (cOmplete EDTA-free protease inhibitor tablets, Sigma-Aldrich). To this buffer was added the various treatment factors: either 10 μM FK506, 10 μM rapamycin, or NaCl sufficient for a final concentration of 600 mM. Preparations for co-sedimentation experiments were incubated for 2 hours at 37 ºC, while preparations for co-immunoprecipitation experiments were incubated for 2 hours at room temperature. Co-sedimentation solutes and co-immunoprecipitation eluates were both examined via SDS-PAGE (**2.6.1**) and subsequent Western blot (**2.6.4**), with Western films then analysed by densitometry (**2.6.5**) and data presented as described in detail in the following Results section. Statistical significance of densitometry data was determined by two-tailed Student's t-test.

3.3 Results

Results for the FKBP dissociation experiments are presented as the ratio of the band intensity of the relevant RyR isoform to the band intensity of its associated FKBP(s). All ratios are then divided by the value of the control ratio, giving the control ratio a value of 1. Blots are shown from both co-sedimentation and co-immunoprecipitation experiments, as indicated in figure legends. Data generally achieves significance only for co-sedimentation experiments due to higher n values, but the trends in co-

immunoprecipitation data nonetheless match significant changes in the co-sedimentation data very closely, indicating a negligible amount of membrane-associated FKBP in the SR vesicles which is not bound to RyR. Compare, for example, Figures **3.1** and **3.2**, and Figures **3.3** and **3.4**.

In addition to data from the pellets obtained during co-sedimentation experiments, certain supernatants of the co-sedimentation drug treatment experiments are also presented. Since these supernatants often lack sufficient RyR against which to normalise the FKBP bands, here supernatant FKBP band intensity is compared to that of the FKBP remaining bound to RyR, as seen in the analysis of the pellets. These ratios are also divided by the value of the control experiment ratio, giving the control ratio a value of 1.

3.3.1 Response of RyR1-associated FKBP12 to potential dissociative treatments

Treatment of skeletal SR vesicles with immunosuppressant drugs proved extremely effective in dissociating FKBP12 from RyR1, with 5 of 13 trials reducing FKBP levels to less than visually-detectible levels in a Western blot (although weak signals were still discernible via image analysis) while in the other 8 cases some residual FKBP12 could be clearly observed, as in Figure **3.1**. In general, results of co-sedimentation and co-immunoprecipitation agreed, indicating that the phenomenon observed in co-sedimentation experiments was indeed removal of FKBP directly from RyR. On average, the effects of FK506 and rapamycin were indistinguishable and both drugs reduced RyR1-associated FKBP12 levels by at least 80%; however, it is also apparent, as mentioned above, that neither 10 μM FK506 nor 10 μM rapamycin reliably fully dissociated FKBP12 from rabbit skeletal RyR1. Unexpectedly, the high concentration of NaCl (600 mM) had no discernible effect on FKBP12 associated with RyR1, with average data for this treatment not being significantly different from the average control data. Therefore FKBP12 could not be “salted off” RyR1 in this preparation.

Figure **3.1** shows the results of the co-sedimentation RyR1 dissociation experiments. In panel A, showing an Western blot, RyR1 is quite consistent in signal strength. The

associated FKBP12 signals are roughly equal for the control and high-salt treatments, indicating little effect of high-salt on FKBP12 association with RyR1. Both immunosuppressant drugs appear highly effective, by contrast, with only a faint FKBP12 signal remaining in those lanes. This is reflected in the quantitation of the results in the bar graph in panel B, with significant but not total losses of RyR1-associated FKBP12 subsequent to immunosuppressant treatment: 82±6% loss after FK506 treatment and 81±5% loss after rapamycin treatment. These generally small SEMs reflect the consistency of the results across the 13 trials.

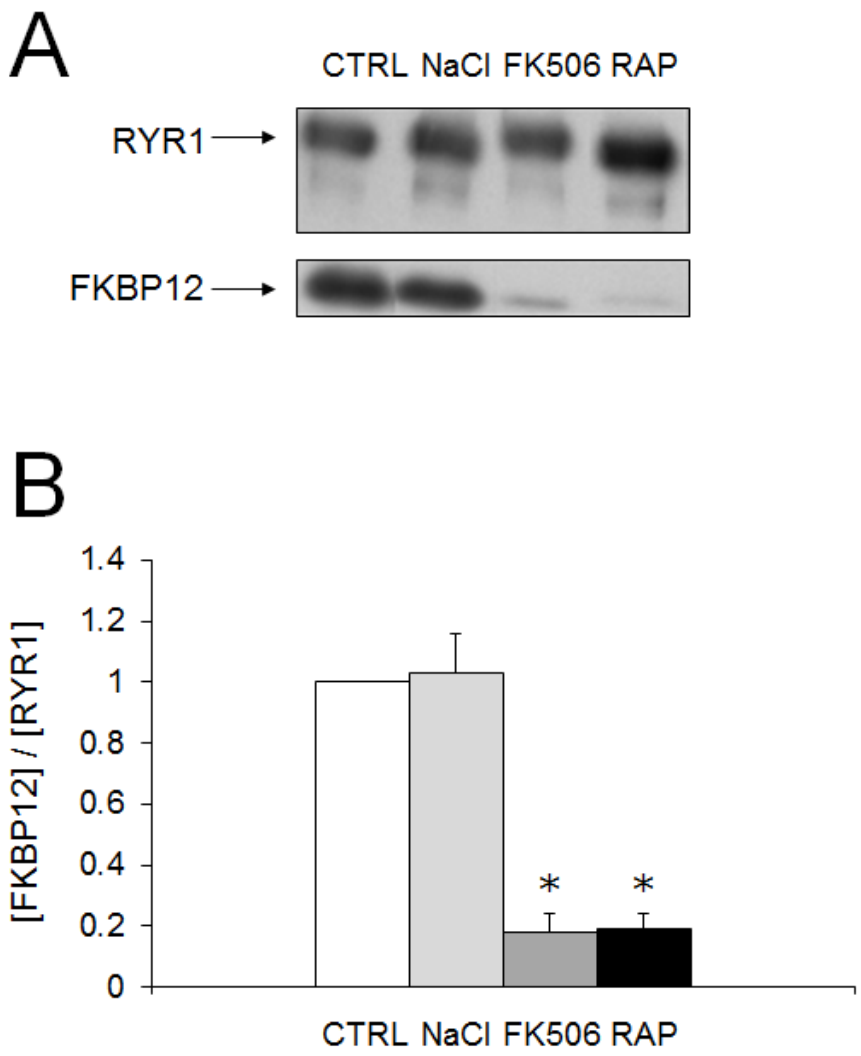

Figure 3.1: **Co-sedimentation shows that RyR1-associated FKBP12 is susceptible to disruption by FK506 and rapamycin, but not by high concentrations of NaCl. A**, Images from a representative post-co-sedimentation Western blot. RyR1 bands are presented above their matching FKBP12 bands. Treatment concentrations from left to right are: control, 600 mM NaCl, 10 μM FK506, 10 μM rapamycin. 10 μL (~150 μg of protein) of skeletal SR vesicle preparation was used in each case; after sedimentation, pellets were resuspended in 40 μL of loading buffer, of which 20 μL was added to each lane. **B**, a graph showing the average data of n=13 co-sedimentation experiments, demonstrating significant reduction of FKBP12 after treatment with 10 μM FK506 or 10 μM rapamycin. Data are presented as the ratio of FKBP12/RyR1 densitometry measurement, normalised to the ratio of the corresponding control FKBP12/RyR1 measurement in each blot. Asterisks indicates significant difference from control for a p value of <0.05.

Figure **3.2** shows the results of the co-immunoprecipitation RyR1 dissociation experiments. These results accord very closely with those shown in Figure **3.1**, confirming the findings of the co-sedimentation experiments. As in Figure **3.1**, panel A shows consistent RyR1 signals, and a dramatic reduction in FKBP12 signals in the lanes treated with immunosuppressant drugs. Indeed, FKBP12 signals here were somewhat fainter on average than were observed in the co-sedimentation experiments: 93±9% of FKBP12 was lost from RyR1 after FK506 treatment, while 97±7% of FKBP12 was lost from RyR1 after rapamycin treatment. Again, these data were consistent across the 6 trials.

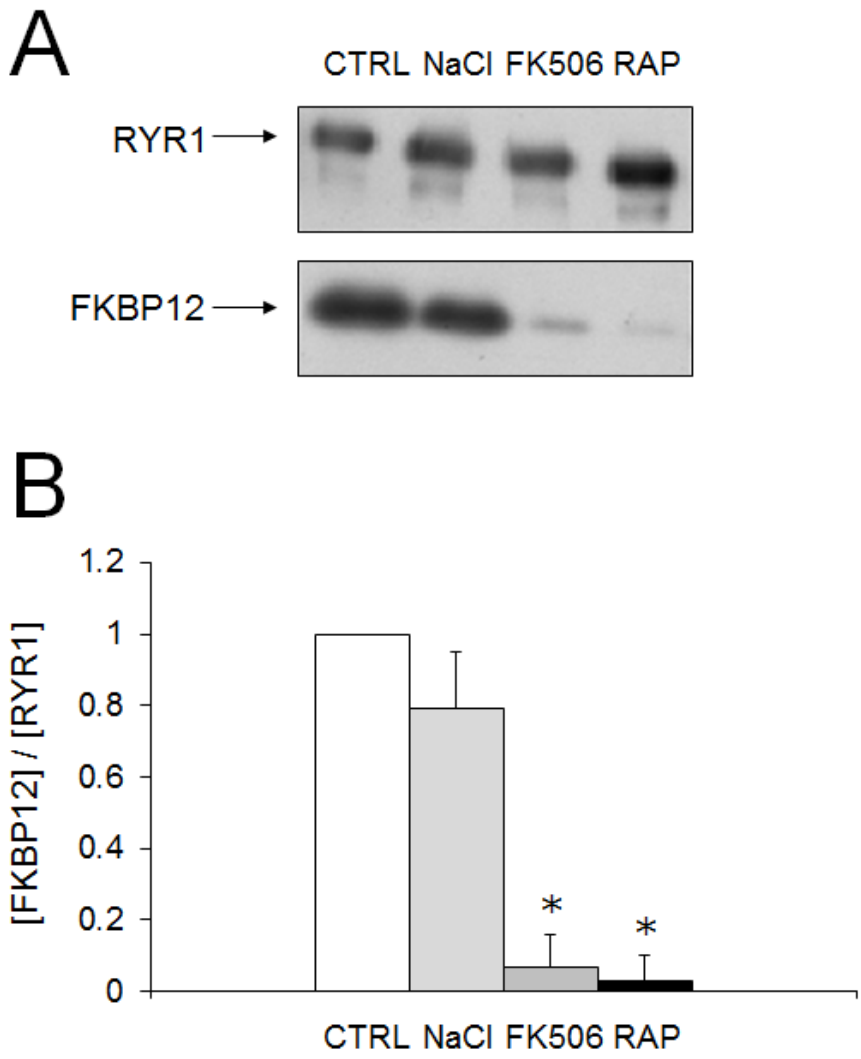

Figure 3.2: Co-immunoprecipitation confirms that RyR1-associated FKBP12 is susceptible to disruption by FK506 and rapamycin, but not by high concentrations of NaCl. A, bands from a representative post-co-immunoprecipitation Western blot. RyR1 bands are presented above their matching FKBP12 bands. Concentrations of potential dissociative factors from left to right are: control, 600 mM NaCl, 10 μM FK506, 10 μM rapamycin. ~400 μg of skeletal SR vesicle protein was added to each sample as indicated; samples were eluted from immobilisation with 70 μL of loading buffer, of which 20 μL was run on SDS-PAGE. **B**, the graph shows the average data of n=6 co-immunoprecipitation experiments, demonstrating a significant reduction in the FKBP12 signal after treatment with 10 μM FK506 or 10 μM rapamycin. Data are presented as the ratio of FKBP12/RyR1 densitometry measurement, normalised to the ratio of the corresponding control FKBP12/RyR1 measurement in each blot. Asterisks indicates significant difference from control for a p value of <0.05.

3.3.2 Response of RyR2-associated FKBP12 to potential dissociative treatments

In contrast to results generated for SR vesicles derived from skeletal muscle, the RyR2:FKBP12 interaction in cardiac SR vesicles proved resistant to all dissociative treatments examined. Compared to the easy liberation of FKBP12 from RyR1 by the immunosuppressant drugs seen in Figures **3.1** and **3.2**, RyR2-associated FKBP12 did not respond to either FK506 or rapamycin treatment (Figures **3.3** and **3.4**), and again, the 600 mM NaCl treatment did not achieve any significant dissociation. Again, both co-sedimentation and co-immunopreciptation experiments generally accord, both sets of experiments failing to detect a reduction in levels of membrane or RyR associated FKBP, indicating that just as with the experiments presented in Figures **3.1** and **3.2**, FKBP was specifically bound to RyR in the co-sedimentation pellets and not simply trapped by some other membranous ligand.

Figure **3.3** shows the results of the co-sedimentation RyR2 dissociation experiments with respect to FKBP12. In panel A, RyR2 varies somewhat in signal strength, but this variation is largely matched by the associated FKBP12 signals. This is reflected in the quantitation of the results in the bar graph in panel B: while all FKBP12/RyR2 signals vary, these variations are not significant, indicating that dissociation was not able to be achieved with any of the treatments.

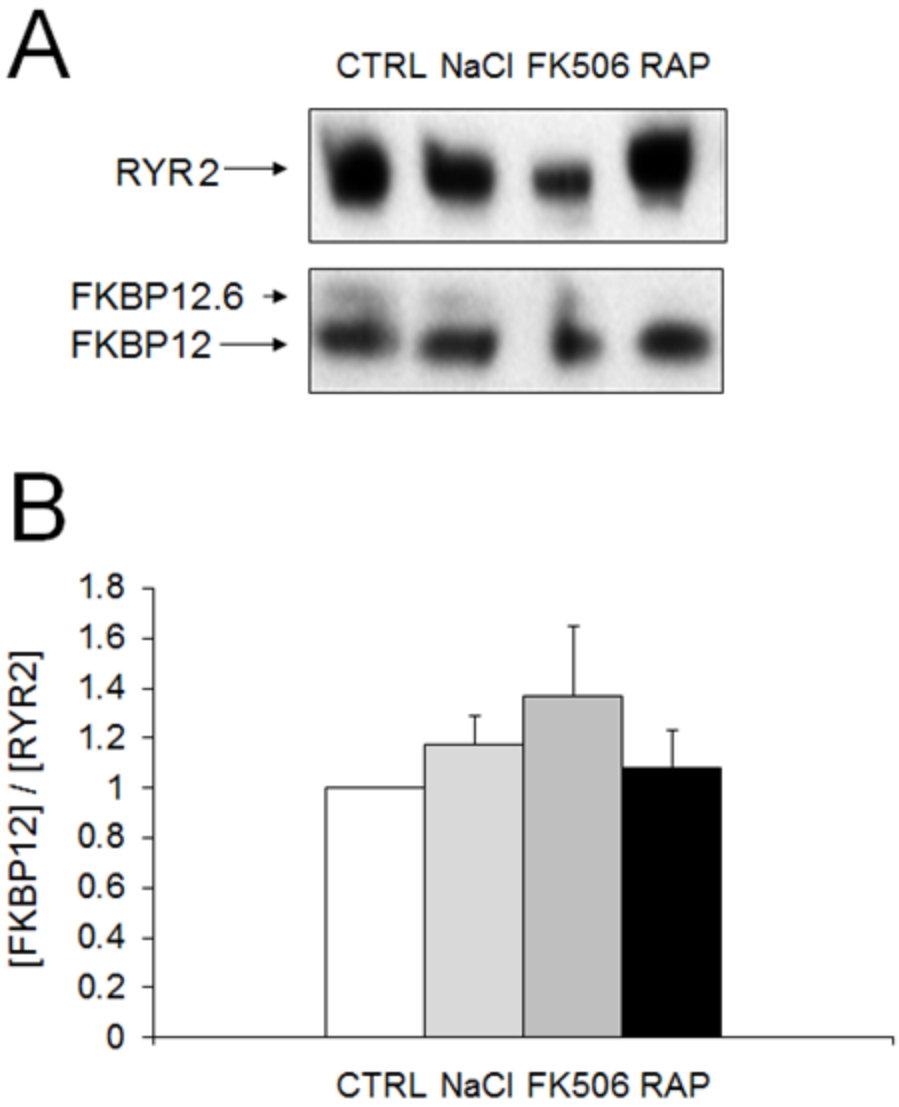

Figure 3.3: **Co-sedimentation shows that RyR2-associated FKBP12 is not susceptible to disruption by FK506, rapamycin, or NaCl. A**, bands from a representative post-co-sedimentation Western blot. RyR2 signals are presented above their matching FKBP12 bands. Concentrations of potential dissociative factors from left to right are: control, 600 mM NaCl, 10 μM FK506, 10 μM rapamycin. 10 μL (~150 μg protein) of skeletal SR vesicles were used to generate each data set; after sedimentation, pellets were resuspended in 40 μL of loading buffer, of which 20 μL was run in each lane. **B**, graph showing the average data of n=6 co-sedimentation experiments, demonstrating that there was no significant effect of any treatment on FKBP12 association with RyR2. Data are presented as the ratio of FKBP12/RyR2 densitometry measurement, normalised to the ratio of the corresponding control FKBP12/RyR2 measurement in each blot.

Figure **3.4** shows the results of the co-immunoprecipitation RyR2 dissociation experiments as regards FKBP12 specifically. In contrast to Figure **3.3**, the RyR2 signals are relatively consistent, as might be expected in co-immunoprecipitation; the associated FKBP12 signals are similarly consistent, although signal quality is somewhat poorer than in the parallel sedimentation experiments. This consistency of signal is reflected in panel B's bar graph, showing that no particular dissociative treatment had any impact on FKBP12 associated with RyR2.

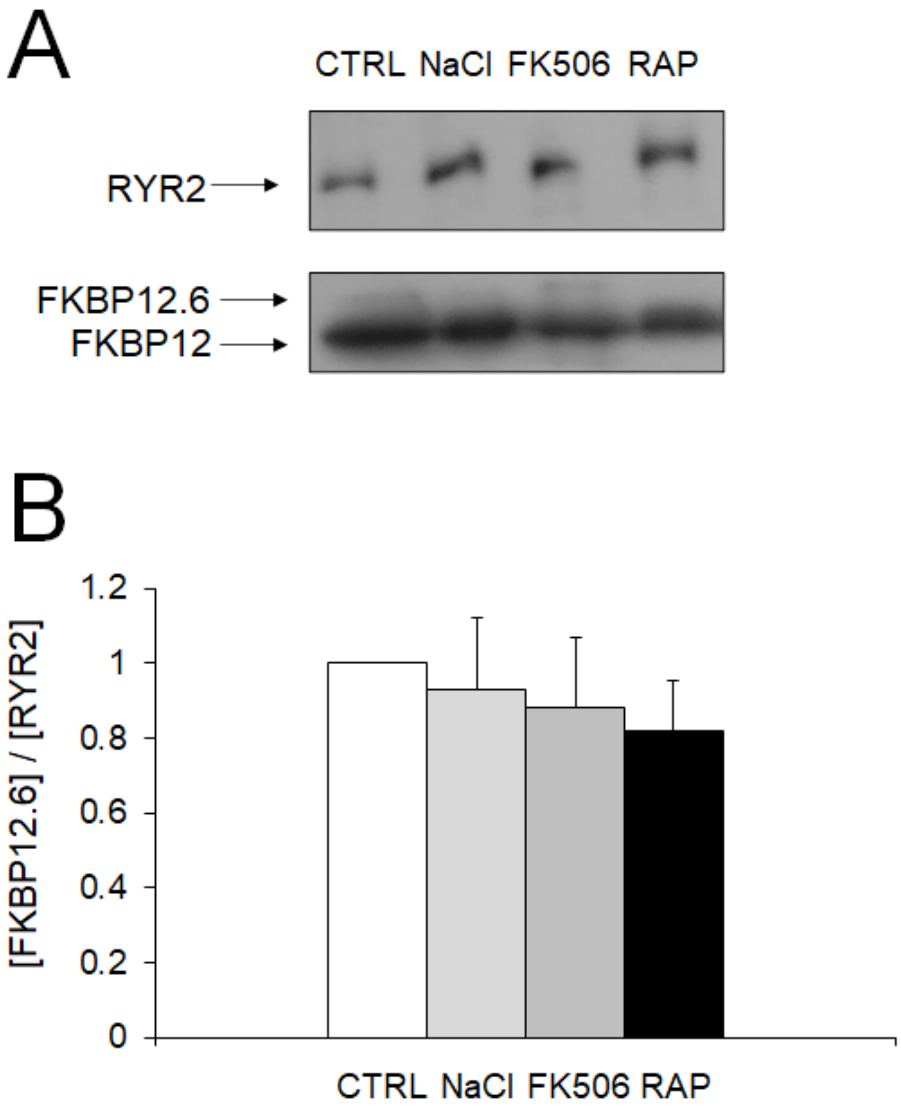

Figure 3.4: **Co-immunoprecipitation confirms that RyR2-associated FKBP12 is not susceptible to disruption by FK506, rapamycin, or high concentrations of NaCl. A**, bands from a representative post-co-immunoprecipitation Western blot. RyR2 signals are presented above their matching FKBP12 signals. Concentrations of potential dissociative factors from left to right are: control, 600 mM NaCl, 10 μM FK506, 10 μM rapamycin. ~400 μg of skeletal SR vesicle protein was used to generate each data set; samples were eluted from immobilisation with 70 μL of loading buffer, of which 20 μL was run in each lane. **B**, graph showing the average data of n=3 co-immunoprecipitation experiments, showing no significant effect of any treatment condition on FKBP12 association. Data are presented as the ratio of FKBP12/RyR2 densitometry measurement, normalised to the ratio of the corresponding control FKBP12/RyR2 measurement in each blot.

3.3.3 Response of RyR2-associated FKBP12.6 to dissociative treatments

While none of the treatments had an effect on FKBP12 association with RyR2, FKBP12.6 associated with RyR2 exhibited some equivocal response to treatment. The co-sedimentation experiments (Figure **3.5**) showed that, while FK506 had little to no effect on liberating FKBP12.6 from RyR2, on average a significant 65±9% moderate dissociation was observed after treatment with 10 μM rapamycin. This result is consistent with previously reported data from our laboratory showing an approximately 80% reduction in FKBP12.6 binding to RyR2 subsequent to treatment with 20 μM rapamycin. It was nevertheless unexpected that an effect should be observed for only one of the two immunosuppressants, considering their structural similarity. Once again, FKBP12.6 binding to RyR2 was not significantly different from control after exposure to the high NaCl concentration. Therefore, neither FKBP isoform was able to be "salted off" under the conditions used in this experiment.

Here, only co-sedimentation experiments were repeated sufficiently (n=6) to render the observation of a moderate reduction in membrane-associated FKBP12.6 significant. Co-immunoprecipitation experiments (Figure **3.6**) showed strong trends in the same direction, with a reduction in RyR-associated FKBP12.6 in 3 of 3 co-immunoprecipitation experiments performed – this, however, was not sufficient trials to establish statistical significance for a p value of <0.05.

Figure **3.5** shows the results of the co-sedimentation RyR2 dissociation experiments as regards FKBP12.6 specifically. Note that the same set of RyR2 and FKBP12/12.6 signals are used in panel A as were in Figure **3.3** for ease of comparison. Thus, as in Figure **3.3**, RyR2 varies somewhat in signal strength in panel A. However, examining the FKBP12.6 signals, they appear entirely absent in the lane treated with rapamycin. Not all experiments demonstrated this apparent abolition of FKBP12.6 binding to RyR2 after treatment with rapamycin: this is reflected in the quantitation of the results in the bar graph in panel B: on average, a significant reduction of 65±9% was observed in FKBP12.6 associated with RyR2, reflecting a combination of several experiments with partial abolition of binding and several experiments with total abolition of binding.

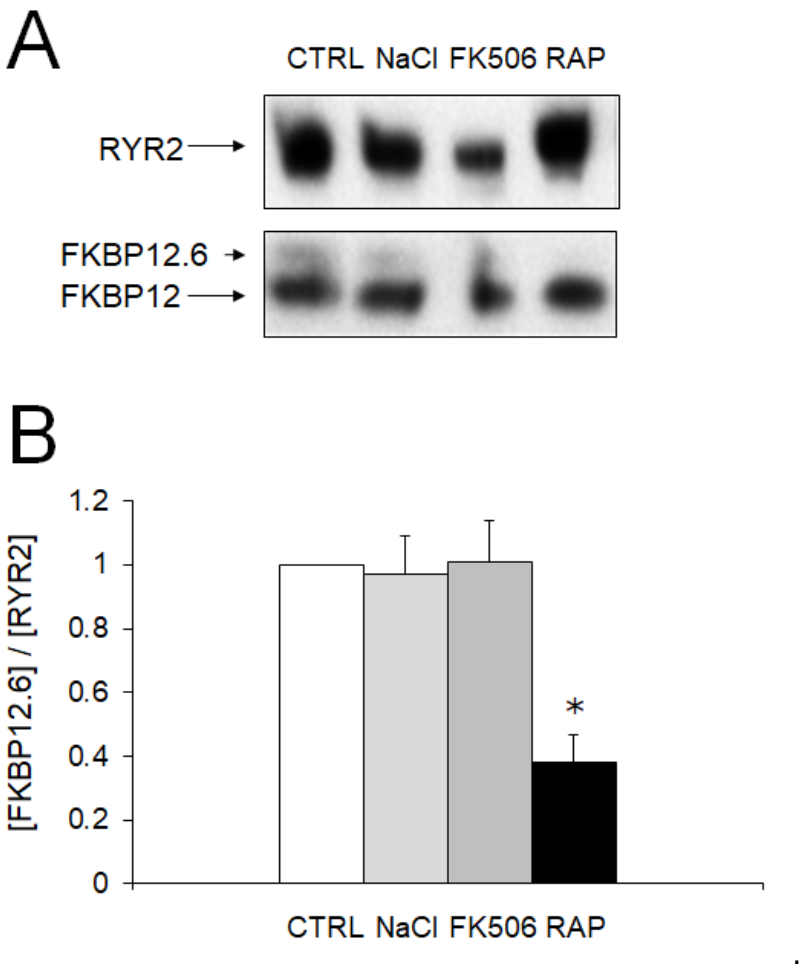

Figure 3.5: **Co-sedimentation shows that RyR2-associated FKBP12.6 is attenuated by rapamycin, but not FK506 or high concentrations of NaCl. A**, bands from a representative post-co-sedimentation Western blot (representative blot is the same as appears in Figure **3.3**., above, for ease of comparison with the average data). RyR2 bands are presented above their matching FKBP12.6 bands. Concentrations of dissociative treatments from left to right are: control, 600 mM NaCl, 10 μM FK506, 10 μM rapamycin. 10 μL (~150 μg of protein) of skeletal SR vesicles were used to generate each set of signals; after sedimentation, pellets were resuspended in 40 μL of loading buffer, of which 20 μL was run in each lane of the gel. **B**, graph showing the average data of n=6 co-sedimentation experiments, demonstrating 65±9% reduction in FKBP12.6 association after rapamycin treatment, but no significant effect of any other treatments. Data are presented as the ratio of FKBP12.6/RyR2 densitometry measurement, normalised to the ratio of the corresponding control FKBP12.6/RyR2 measurement in each blot. Asterisk indicates significant difference from control for a p value of <0.05.

Figure **3.6** shows the results of the co-immunoprecipitation RyR2 dissociation experiments as regards FKBP12.6 specifically. As with Figure **3.5**, the same set of RyR2 and FKBP12/12.6 signals are used in panel A as were in Figure **3.4** for ease of comparison. Similar to Figure **3.5**, panel A shows consistent FKBP12.6 signals (although on average fainter relative to FKBP12 than appeared in the co-sedimentation experiments) with the exception of the rapamycin treatment lane, where FKBP12.6 binding appears abolished. Just as in the co-sedimentation experiments, this was not observed in all trials, with one experiment showing most FKBP12.6 remaining bound. Nevertheless, on average, a trend towards FKBP12.6 was observed, as expressed in panel B, although due to the smaller number of trials this trend did not achieve significance.

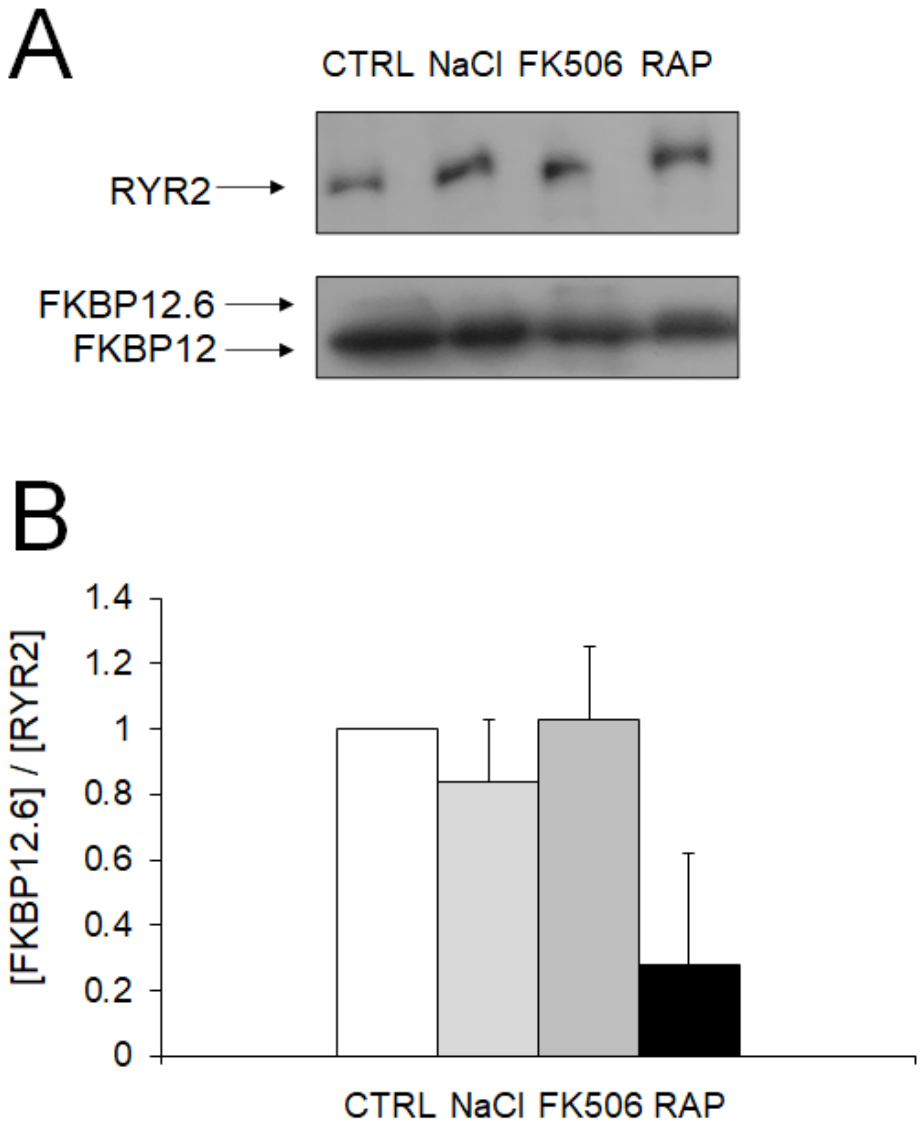

Figure 3.6: **Co-immunoprecipitation indicates a trend towards RyR2-associated FKBP12.6 being attenuated by rapamycin, but not FK506 or high concentrations of NaCl. A**, bands from a representative post-co-immunoprecipitation Western blot. RyR2 bands are presented above their matching FKBP12.6 bands. Concentrations of dissociative treatments from left to right are: control, 600 mM NaCl, 10 μM FK506, 10 μM rapamycin. ~400 μg of skeletal SR vesicle protein was used to generate each set of data; samples were eluted from immobilisation with 70 μL of loading buffer, of which 20 μL was run in each lane of the gel. **B**, graph showing the average data of n=3 co-immunoprecipitation experiments, showing a trend towards reduction in FKBP12.6 signal strength after rapamycin treatment, but no effect of other treatments. Data are presented as the ratio of FKBP12.6/RyR2 densitometry measurement, normalised to the ratio of the corresponding control FKBP12.6/RyR2 measurement in each blot.

3.3.4 RyR1 co-sedimentation FKBP12 supernatant data

Supernatants generated in the co-sedimentation experiments above (Figures **3.1**, **3.3**, **3.5**) were analysed in addition to the pellet data presented in those figures. Analysis of co-sedimentation experiment supernatants is useful for a number of reasons, but primarily because it should produce corollary data to that seen from the pellets. That is, in experiments where FKBP loss is observed from the pellet due to a dissociative treatment, we should expect to see that lost FKBP in the supernatant from the same experiment. But beyond just this corroborative data, analysis of supernatants generated some interesting observations. Here, examining the supernatants from RyR1 co-sedimentation experiments, we see generally a small amount of non-pelleted membranous RyR1 (not shown in Figure **3.7** below) and associated FKBP12, indicating that the skeletal muscle SR pellets are relatively delicate and subject to re-suspension.

Figure **3.7** illustrates FKBP dissociation from RyR1, showing both the signals for FKBP12 still bound to RyR1 after dissociative treatments (in the row marked PELLET) and the signals for FKBP12 not associated with RyR1, washed off in the supernatant after centrifugation (in the row marked SUPERNATANT). As expected from the experiments of Figures **3.1** and **3.2**, far greater quantities of FKBP12 appear in the supernatant for those RyR1 treated with FK506 or rapamycin. Further, generally a small amount of non-pelleted membranous RyR1 (not shown in Figure **3.7** below) and associated FKBP12 appear in all lanes, even in the supernatants of control RyR1. This indicates that the RyR1 in the pellet is subject to resuspension; otherwise, the presence of extra FKBP12 beyond that associated with this “washed-off” RyR1 correlates extremely well with the efficacious FKBP-stripping treatments.

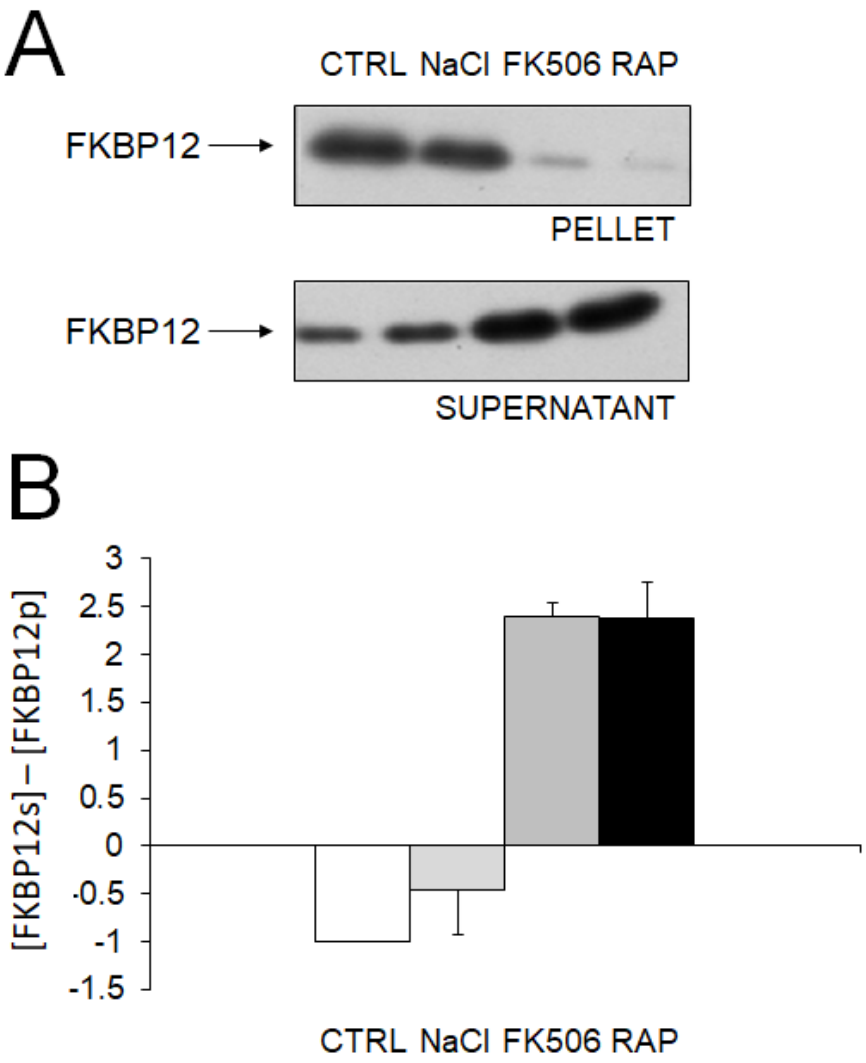

Figure 3.7: **FKBP12 dissociation from RyR1 correlates with the appearance of FKBP12 in treatment supernatants. A**, bands from a representative post-co-sedimentation Western blot. FKBP12 pellet bands are presented above matching FKBP12 bands from the treatment supernatants. Concentrations of dissociative treatments from left to right are: control, 600 mM NaCl, 10 μM FK506, 10 μM rapamycin. 10 μL (~150 μg of protein) of skeletal SR vesicles were used to generate each set of data; after sedimentation, pellets were resuspended in 40 μL of loading buffer, of which 20 μL was run; supernatants were derived from the 50 μL treatment incubation volume, of which 15 μL (+5 μL loading buffer) was run. **B**, graph presenting average data from n=3 experiments showing the net change in FKBP12 signal strength comparing pellets to supernatants, normalised to the change observed in the control. Net change was calculating by subtracting pellet signals from their matching supernatant signals.

3.3.5 RyR2 co-sedimentation FKBP12 supernatant data

Supernatants from the RyR2 co-sedimentation experiments, shown in Figure **3.8**, show a “baseline” level of FKBP12 that appears in each supernatant regardless of treatment, similar to those from RyR1 experiments. Interestingly, however, in RyR2 supernatants this FKBP12 does not appear to be associated with fragments of RyR2-containing cardiac SR pellets making their way to the supernatant, as no RyR2 signals were detected in the Western blot; instead, the FKBP12 that shows up in RyR2-containing cardiac SR supernatants appears to be free. This appearance of roughly similar amounts of FKBP12 in all treatments matches the lack of difference between treatments observed above in Figures **3.3** and **3.4**. Interestingly, however, FKBP12 appears even in the control supernatant, implying that a degree of disassociation of RyR2-associated FKBP12 occurs even under very mild conditions. This observation was one of the first indications encountered in the course of the experiments in this thesis that suggested a non-linear binding relationship between FKBP and RyR, wherein the affinity of FKBP12 for RyR2 appeared to depend on amount of FKBP12 bound to RyR2 – more on this in the discussion below, **3.4**. Finally, FKBP12.6 might be expected to be seen in the supernatant of rapamycin treatments, given that a significant reduction in FKBP12.6 associated with RyR2 was observed post-rapamycin treatment, but unfortunately the supernatant band was generally too diffuse for quantitation.

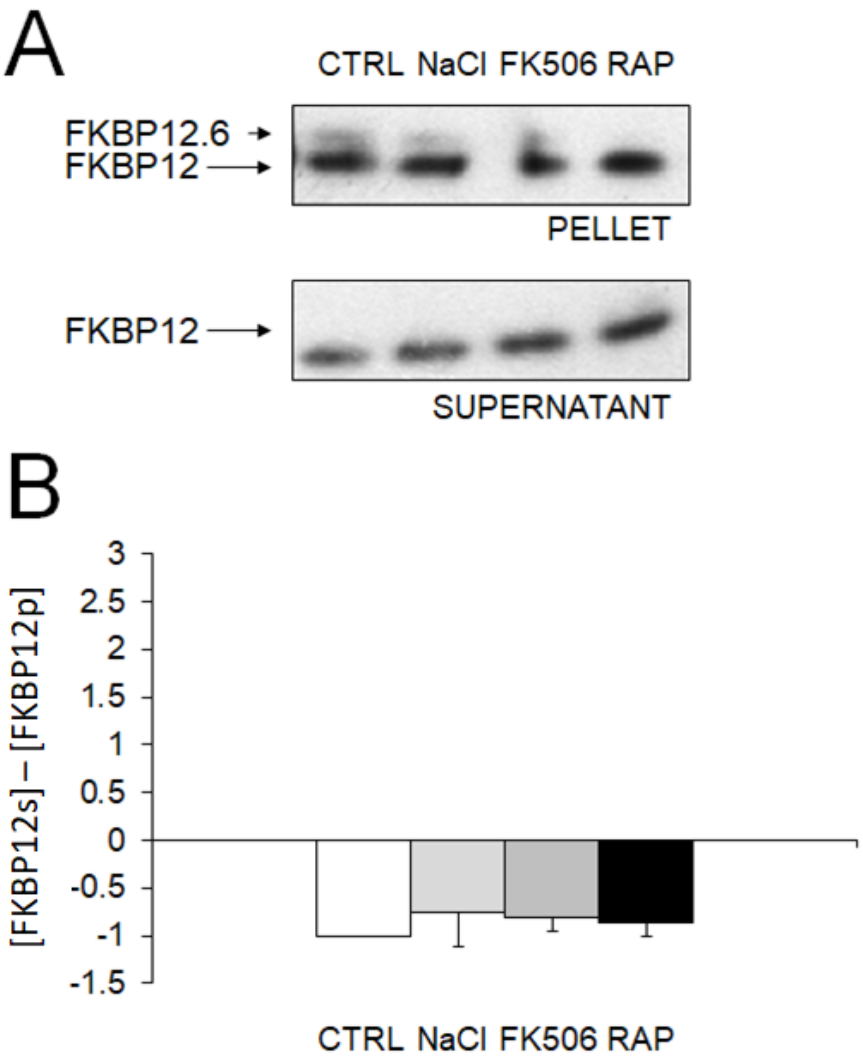

Figure 3.8: FKBP12 dissociation from RyR2 correlates with the presence of FKBP12 in treatment supernatants. A, bands from a representative post-co-sedimentation Western blot. FKBP12 pellet bands are presented above matching FKBP12 bands from the treatment supernatants. Concentrations of dissociative treatments from left to right are: control, 600 mM NaCl, 10 μM FK506, 10 μM rapamycin. 10 μL (~150 μg of protein) of cardiac SR vesicles were used to generate each set of data; after sedimentation, pellets were resuspended in 40 μL of loading buffer, of which 20 μL was run; supernatants were derived from the 50 μL treatment incubation volume, of which 15 μL (+5 μL loading buffer) was run. **B**, graph presenting average data from n=3 experiments showing the net change in FKBP12 signal strength comparing pellets to supernatants, normalised to the change observed in the control. Net change was calculated by subtracting pellet signals from their matching supernatant signals.

3.3.6 Response of RyR1-associated FKBP12 to solubilisation treatment

Solubilisation proved highly effective at removing FKBP12 from RyR1, at the cost of dissociating also most of the other RyR-complex proteins, as well as somewhat reducing total RyR yield from muscle preparations (**1.2**). Figure **3.9** shows that there was a significant decline in FKBP associated with RyR1 after vesicle solubilisation, although regardless of the general efficacy of solubilisation in dissociating FKBP, some remained bound to RyR, providing further evidence that at least a small population of FKBP binds to RyR very tightly.

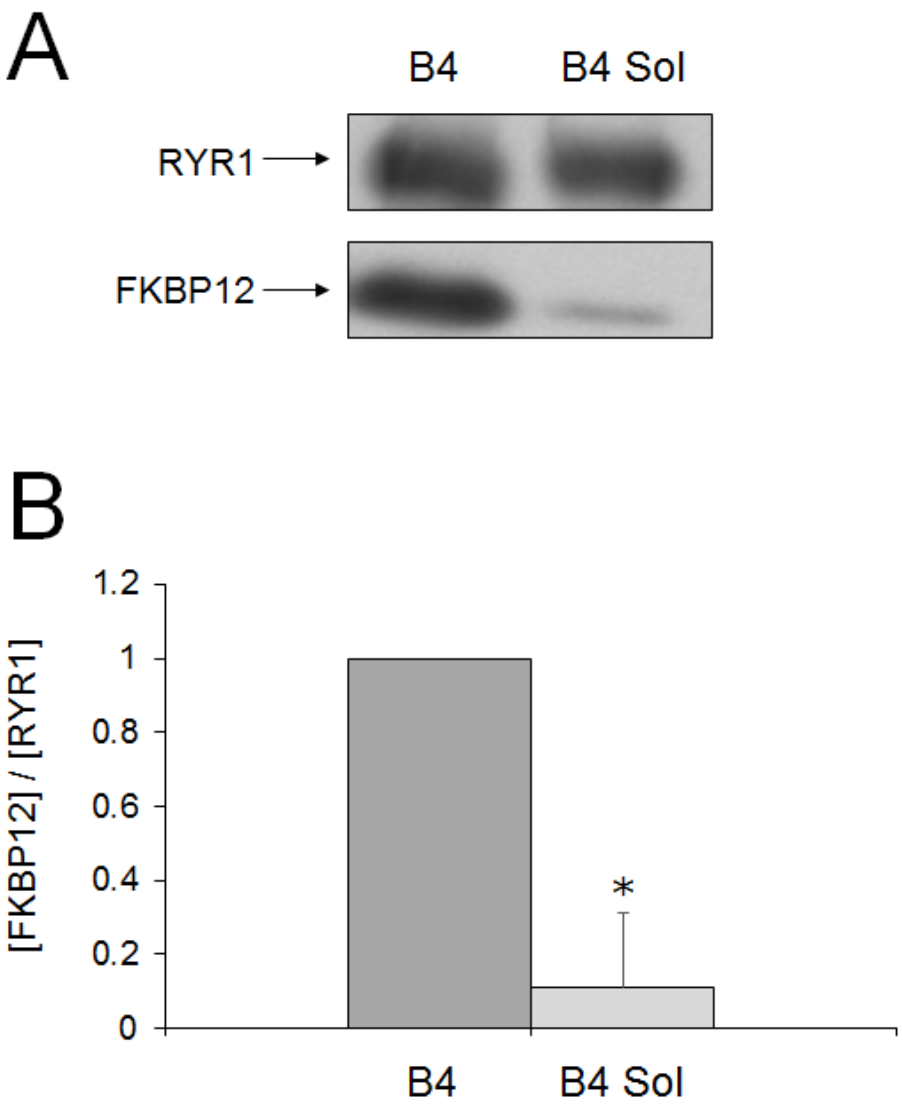

Figure 3.9: Co-immunoprecipitation shows that vesicle solubilisation removes most RyR1-associated FKBP12. A, bands from a representative post-co-immunoprecipitation Western blot. RyR1 signals are presented above their matching FKBP12 signals. Left lane shows B4-stage vesicles, while right lane shows the same vesicles post-solubilisation. Both samples are run with approximately the same total protein content of ~400 µg. Samples were eluted from immobilisation with 70 µL of loading buffer, of which 20 µL was run in each lane. **B**, graph showing the average data of n=5 co-immunoprecipitation experiments, indicating dissociation of ~80% of RyR1-bound FKBP12 post-solubilisation. Data are presented as the ratio of FKBP12/RyR1 densitometry measurement in the solubilisation lane to a normalised FKBP12/RyR1 densitometry ratio of 1 in the untreated lane. Asterisk indicates significant difference from control for a p value of 0.05.

3.3.7 Response of RyR2-associated FKBP12 to solubilisation treatment

Much as for RyR1, FKBP was effectively removed from RyR2 by solubilisation, with a significant decline in RyR2-associated FKBP subsequent to vesicle solubilisation. In several blots, RyR2 were observed apparently wholly free of associated FKBP, although this may be an artefact of the generally lower concentrations of RyR2 as compared to RyR1 observed when using the preparative protocols of Chapter 2, causing levels of RyR2-associated FKBP to fall below detection thresholds. Figure **3.10** summarises these data, with only an extremely faint FKBP12 signal discernible in panel A in the solubilised lane.

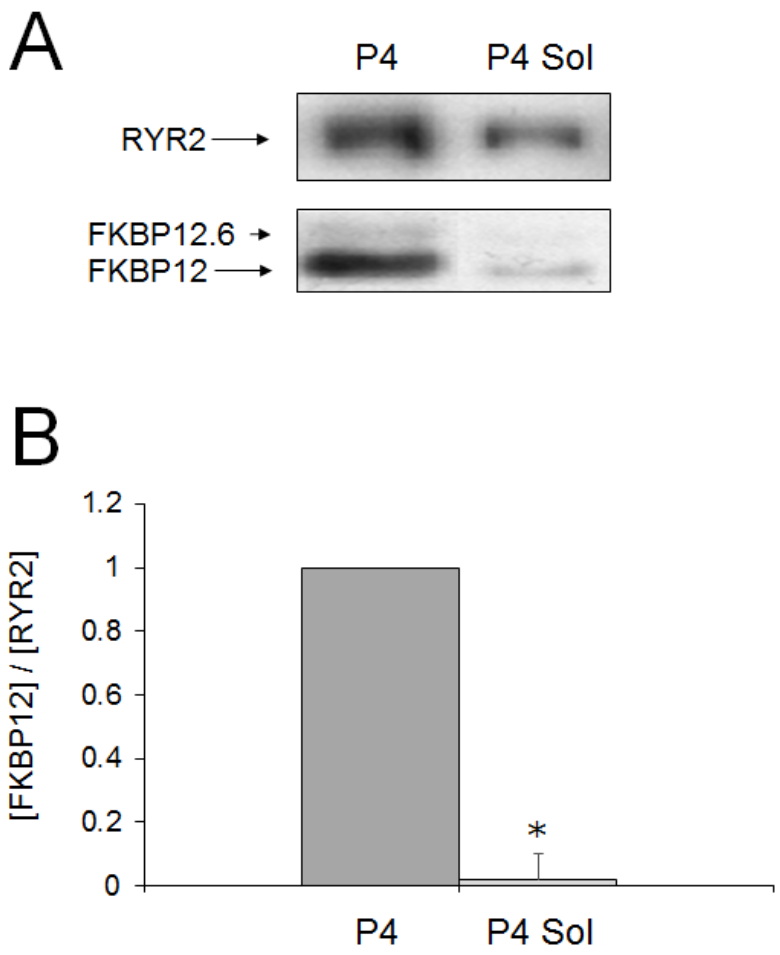

Figure 3.10: Co-immunoprecipitation shows that vesicle solubilisation removes nearly all RyR2-associated FKBP12, and likely nearly all RyR2-associated FKBP12.6. A, bands from a representative post-co-immunoprecipitation Western blot. RyR2 signals are presented above their matching FKBP12 and FKBP12.6 signals. Left lane shows P4-stage vesicles, while right lane shows the same vesicles post-solubilisation. Both samples are run with approximately the same total protein content of ~200 µg. Samples were eluted from immobilisation with 70 µL of loading buffer, of which 20 µL was run in each lane. **B**, graph showing the average data of n=5 co-immunoprecipitation experiments, indicating dissociation of nearly all RyR2-bound FKBP12 post-solubilisation. Data are presented as the ratio of FKBP12/RyR2 densitometry measurement in the solubilisation lane to a normalised FKBP12/RyR2 densitometry ratio of 1 in the untreated lane. FKBP12.6 signals were in general to diffuse to effectively quantify, but showed a similar trend of near complete dissociation upon solubilisation. Asterisk indicates significant difference from control for a p value of 0.05.

3.4 Discussion

Several conclusions can be drawn from the data presented in this chapter. Most apparent is the differential response of RyR1 and RyR2 to drug treatment: while FK506 and rapamycin were both highly effective at dissociating FKBP12 from RyR1, they had little to no effect on FKBP12 associated with RyR2, and only rapamycin showed a moderate effect on FKBP12.6 associated with RyR2. This is important for two reasons: first, it might reasonably be assumed that the dissociative efficacy of FK506 and rapamycin is similar between the two RyR isoforms, i.e., total – contrary to this, the data shown in this chapter indicate that experiments requiring the liberation of FKBP from RyR2 may require further consideration of appropriate dissociation procedures.

Second, it is notable that the FKBP12 bound to either RyR1 or RyR2 responds differently when exposed to the same potential dissociative factors. We observed RyR1 far more easily giving up its bound FKBP12 than RyR2, in spite of previously published work indicating FKBP12 has a higher affinity for RyR1 than RyR2. Potentially this resistance to dissociation may be attributed to differences in the FKBP-binding pocket between RyR1 and RyR2 (Yuchi, 2015) which result in the occlusion of RyR2-associated FKBP or the drug binding sites and consequently a structural impediment to respond to exogenous treatments. Alternatively, the differential response may reflect something other than changes at interaction sites. One potential explanation may be that RyR binds FKBP in a cooperative manner, rather than with an affinity that remains consistent regardless of how many FKBPs are bound to a given RyR tetramer. For a negatively cooperative mode of binding between RyR and FKBP, the first FKBP to bind to a RyR would bind with very high affinity, and then subsequent FKBP would bind to the RyR with decreasing affinity. If the affinity of FKBP for RyR depends on the amount of FKBP already bound to the RYR, and if the RyR isoforms have different “starting” stoichiometries of bound FKBP, then it is possible that some of the differences in the efficacy of dissociative treatments may be explained by e.g. RyR2 having fewer FKBPs on average bound to a tetramer, with these FKBPs therefore relatively more resistant to dissociative treatments. This potential will be further explored in Chapters 4 and 5, below.

Complicating such a negative cooperativity model is the mild degree of removal of RyR2-associated FKBP12.6 by rapamycin, contrasted with the lack of effect of

rapamycin on RyR2-associated FKBP12. This is somewhat paradoxical, given that FKBP12.6 is generally thought to have greater affinity for RyR2 than FKBP12 (Guo, 2010), although see **1.4.4** for more discussion of the inconsistent data regarding FKBP affinities for RyR, and the potentially confounding differences in FKBP isoform expression across species (Zissimopolous, 2012). Potentially, the small sequence differences between the two isoforms may contribute to this differential effect of rapamycin treatment. Related, it is also unexpected that FK506 and rapamycin had differing efficacies on RyR2-associated FKBP12.6. Both drugs are chemically very similar (**1.4.3**), and show very similar efficacy on RyR1-associated FKBP12 – and indeed, a similar lack of efficacy on RyR2-associated FKBP12 – so a difference in their action on FKBP12.6 between the two is not easily explained.

Comparison of the immunosuppressant treatments to CLIC-2's dissociative effect on RyR-associated FKBP reveals further interesting differences between potential dissociative factors. Unlike FK506 and rapamycin, CLIC-2 was able to dissociate FKBP from both RyR1 and RyR2 with roughly equal efficacy, although the degree of dissociation achieved with RyR1 was less than was observed with rapamycin treatment. This difference in dissociative effect can perhaps be best explained by the difference in the mechanism of action between the treatments: while the immunosuppressants bind directly to FKBP and induce a conformational change in the protein which results in their liberation, CLIC-2 binds instead to the RyR, separating (at least in RyR1) domains 9 and 10 into a conformation typical of a channel "open" state in this region and presumably thereby encouraging FKBP dissociation, in which case the phenomena appeared to be closely linked to the conformational state of the RyR (Meng, 2009). Notably, these data together indicate that CLIC-2 treatment may be one of the most effective means of generating RyR2 which are at least partially stripped of associated FKBP. It is possible this dissociative activity of CLIC-2 plays a physiological role, with CLIC-2 usually either membrane-bound or else sequestered by other binding partners, but able to freely move in the cytoplasm under certain conditions, thereby liberating FKBPs from RyRs in order to modulate RyR activity.

Together, the data presented in this chapter further suggest that even in preparation of FKBP-stripped RyR1, treatment with immunosuppressants might likely not result in complete loss of all FKBP, as in the majority of RyR1 drug-treatment experiment reported here, even when strong ablation was observed it was not complete, with

perhaps 20% of the native FKBP12 retained. Notably, the proportion of this “retained fraction” correlates well with a negative cooperativity model of FKBP12 binding to RyR1, where approximately a quarter of the FKBP12 bound to a fully saturated RyR1 would be expected to bind with extremely high affinity. Such a potential model is explored in depth in Chapter 6. These data also accord with observations made previously in this laboratory with a higher concentration of 20 μM rapamycin (Honours thesis of Gregory Steele, 2013), where approximately 10% of native FKBP12 was retained, as well as with observations from mass spectrometry performed upon vesicles similarly treated with 20 μM rapamycin (Galfré, 2012). The degree of saturation of FKBP binding sites on RyR is difficult to ascertain from these experiments. While complete dissociation proves difficult, these ratios of FKBP12 retained post-treatment indicate that even if RyR1 in vesicles is assumed to be fully saturated with the maximal stoichiometry of 4 FKBPs per RyR1, then immunosuppressant treatment may result in at least a fractional population of RyR1 stripped of FKBP, which may be sufficient for many qualitative analyses.

While the immunosuppressant drugs indicated at least some ability to dissociate FKBP from both RyR isoforms, supraphysiological ionic strength proved to have no dissociative capacity beyond the control incubations at roughly physiological ionic strength. A possible additional approach to this protocol is to examine the ability of a different salt, such as KCl, to test the hypothesis that the dissociative mechanism of action observed by some groups (as in Galfré, 2012) is dependent upon the ionic species interacting with RyR rather than simply a high ionic strength.

Examination of the co-sedimentation supernatants reveals a further interesting nuance to FKBP’s binding to the RyR: FKBP12 was apparent to some level in the supernatants of all treatment factors, including mild control incubations. In experiments with skeletal SR vesicles there also appeared some RyR1 in the supernatants, and hence, the FKBP12 observed in these supernatants cannot be necessarily assumed to be unbound. However, in the cardiac SR vesicle experiments no such RyR2 was apparent, indicating that the FKBP12 appearing in these treatment supernatants was free. This implies a degree of dissociation of FKBP12, at least in RyR2, in response simply to dilution/incubation in physiological buffer. In other words, RyR2 remained resistant to the “strong” potential dissociative conditions that were used, but gave up a fraction of their bound FKBP12 in response to mild buffer incubations. This result

suggests that within the RyR2-bound FKBP there may be a population of FKBP bound with a lower affinity, able to be easily washed off by buffer alone, while a remainder binds with a high enough affinity to withstand dissociation by drug treatment. Two hypotheses may explain this. First, the two populations are distinct “populations” of FKBP binding to different sites on the RyR2 with different affinities; this is unlikely, given the cryo-EM structures of RyR2 saturated with FKBP12 show binding only at the canonical binding sites (Peng, 2016, and **1.3.2**). Second, the FKBP bound to the RyR2 at the canonical site exhibits a degree of negative cooperativity, resisting both total dissociation from the RyR2 but also total occupation of the RyR2. Such a relationship may pertain for RyR1 also, though likely with less steep differences in affinity. The potentially complex nature of this binding relationship will be further explored in Chapter 6 of this thesis.

The high efficacy of solubilisation treatments in dissociating FKBP from RyR was somewhat unexpected. While solubilisation treatments would be expected to disrupt the RyR complex and associated integral membrane proteins such as junctin or triadin, the FKBP isoforms bind with high affinity only to the cytoplasmic surface of the RyR, and so disruption of the SR membrane would not be expected to significantly impact FKBP associated with RyR. Also interestingly, solubilisation appears to be the only dissociative treatment with equal efficacy in removing FKBP from both RyR isoforms. The most likely agent responsible for inducing FKBP dissociation from RyR in the solubilisation process is the zwitterionic surfactant CHAPS, which is present in high concentrations during most stages of solubilisation. CHAPS is generally acknowledged as a non-denaturing detergent, yet it is possible that the disruptive effect of CHAPS on the SR membrane into which RyR are incorporated itself causes a conformational change in RyR which results in dissociation of bound FKBP. That is, while CHAPS likely does not directly induce a denaturation conformational change in RyR as might SDS, simply by liberating the RyR from its stabilising SR membrane a conformational change may nevertheless result.

Finally, the ease with which a certain amount of FKBP dissociated from RyR simply in response to incubation in a mild buffer also raises the question of whether our examined population of isolated RyR binds a physiologically-accurate stoichiometry of FKBP, or whether perhaps some dissociates during the fractionation of muscle homogenate into SR vesicles, which takes place in considerably harsher chemical and

mechanical conditions than those considered in these experiments (**2.3**) – this question is addressed further in Chapters 4 and 5.

3.5 Conclusions

FK506 and rapamycin are both effective at removing FKBP12 from RyR1, but seldom removed the entirety of FKBP12.

Neither immunosuppressant had any efficacy in removing FKBP12 from RyR2.

Rapamycin alone was able to remove ~65% of the FKBP12.6 associated with RyR2.

High concentrations of NaCl were no more effective than control incubations at physiological ionic strength in dissociating FKBP from RyR.

RyR2 and RyR1 both exhibited a degree of “passive” FKBP12 dissociation even after treatment by only control incubations, indicating that at least a proportion of FKBP12 is bound to RyR with a relatively low affinity, contrasting with the resistance to total dissociation observed in parallel experiments.

Solubilisation has similar efficacy to drug treatments in removing FKBP12 from RyR1, but unlike drug treatments, was of nearly equal efficacy in removing FKBP12 from RyR2. This suggests solubilisation as the most effective current technique for generating RyR stripped of endogenously-associated FKBP, although such stripped RyR may lack not just FKBP but other endogenously-associated EC coupling proteins as well, potentially confounding experiments in which the regulatory environment of RyR is intended to be as physiological as possible.

Chapter 4: Occupation of RyR1 and RyR2 in SR vesicles by FKBP

4.0 Introduction

In this chapter I examine the ability of RyR in isolated SR vesicles to bind additional exogenous FKBP, building on the observation from Chapter 3 that a population of FKBP quite readily dissociated from SR vesicle RyR, suggesting that SR vesicle RyR may have a different FKBP:RyR stoichiometry than the generally assumed maximal stoichiometry of 4 FKBPs per RyR. The functional implications of submaximal occupation of RyR FKBP-binding sites are currently unknown; however, a substantial body of evidence shows that FKBP acts to regulate or stabilise the function of the RyR to which they are associated, at least in the case of RyR1 (Timerman, 1993; Ahern, 1994 & 1997; Brillantes, 1994; McCall, 1996; Ondrias, 1998; Marx, 1998 & 2001; Avila, 2003). Concomitantly, submaximal or disrupted occupation of RyR1 or RyR2 by FKBP has been considered characteristic of a pathological phenotype (Marx, 2000; Reiken, 2003), with FKBP dissociation resulting in dysregulated opening of RyR, which thereby leak Ca^{2+} into the cytoplasm under resting conditions in the absence of DHPR activation. Depending on the tissue affected and the severity of the Ca^{2+} leak, this dysregulated opening is reported to have consequences ranging from simple muscle weakness to potentially fatal cardiac arrhythmia. Consequently, knowledge about the endogenous occupancy of RyR by FKBP is critical in order to fully understand and assess the impact of pathological FKBP dissociation. It is possible that the submaximal occupancy of RyR by FKBP observed in Chapter 3 is specifically characteristic of SR vesicle RyR; that is, loss of FKBP occurs during SR vesicle processing, resulting in submaximally occupied RyR. This would be a significant finding: SR vesicles are frequently used in functional and biochemical study of the RyR, and so it is important to accurately know the occupancy of their RyR by FKBP, as this directly affects conclusions drawn about RyR function from such studies. The question of whether incomplete RyR occupancy represents physiological reality or is a consequence of SR vesicle processing will be explored further in the following chapter: this present chapter

is centrally concerned with establishing the degree of submaximal occupancy in SR vesicles, if any.

The central hypothesis of this chapter is therefore that RyR in isolated SR vesicles are not fully occupied by FKBP: as mentioned above, this hypothesis is based on several observations. As reported in Chapter 3 (see particularly figures **3.7** and **3.8**), a considerable amount of FKBP is dissociated from RyR in both skeletal and cardiac SR vesicles under even very mild control conditions, that is, simple incubation in physiological-temperature buffered saline. This raises the possibility that there might also be some earlier loss of FKBP12 during the initial homogenisation and processing of SR vesicles, which may present harsher challenges to the RyR complex than do the control experiments described in Chapter 3. A further indication of possible incomplete occupancy of RyR by FKBP in SR vesicles is the behaviour of the channels when they are incorporated into planar lipid bilayers. We and others have previously shown (Ahern, 1997; Richardson, 2017) that both RyR1 and RyR2 in SR vesicles may exhibit “substate” gating behaviour after incorporation into lipid bilayers – that is, they will open sufficiently to allow to the passage of ions, but in a submaximal fashion, not attaining the ionic flux that might be expected from the full opening of the pore, that is, the maximum single channel conductance. If these substate gating events are particularly long, and occur independent of stimulus, this behaviour would most likely seem to represent a degree of pathology. In the live cell, such a leak of Ca^{2+} from the SR, uncoordinated by any DHPR action, would have various non-optimal downstream consequences. Further, we (but not all groups – see Chapter **1.4.4.2** in particular) have found in work yet to be published that addition of exogenous FKBP12 to the cytoplasmic side of incorporated channels subsequently stabilises their gating, reducing the frequency and duration of these substate opening, implying then that these substate openings are at least partially consequent to insufficient – and very likely non-endogenous – levels of FKBP bound to the RyR of these SR vesicles.

The major question addressed in this chapter is therefore the occupancy of RyR by FKBP in both cardiac and skeletal SR vesicle preparations. I address this question by determining the amount of additional FKBP12 that can bind to the RyR, and comparing this observed “fully saturated” state with the degree of FKBP:RyR binding observed in untreated control SR vesicles. To that end, vesicles were incubated with exogenous GST-FKBP12 fusion protein, with the GST component of the fusion protein serving to

distinguish the exogenous FKBP12 associated with the RyR from that found endogenously, on the basis of MW. Broadly, if the incubated RyR have additional FKBP-binding capacity, this shows that prior to incubation, they were submaximally occupied by FKBP. Of note, a possibility exists that the GST-FKBP12 fusion protein used in these experiments may exist in solution primarily as a dimer or even a more complex multimer, since GSTs are known to exist as dimers, and FKBP12 are also known to dimerise under certain conditions (Schories, 2007). This dimerisation/multimerisation would affect any densitometric determinations of the amount of exogenous FKBP12 present bound to SR vesicle RyR, as at least two FKBP molecules would be associated with any particular RyR binding site, rather than the single one that might otherwise be expected. Therefore, the polymeric states of both GST-FKBP12 and purified FKBP12 following cleavage of the GST tag were also investigated and reported in this chapter, and this data used to establish densitometric calculations in the subsequent co-immunoprecipitation experiments.

A secondary question I address in this chapter is whether endogenously-bound FKBP may be displaced in their association with RyR by exogenous FKBP. As was observed in Chapter 3, RyR1 and RyR2 exhibited quite different responses to FKBP-dissociating treatments, and the response of the RyR to exogenous FKBP offers a new angle from which to examine differences or similarities in response between RyR1 and RyR2. Furthermore, should endogenous FKBP prove displaceable by exogenous FKBP, the degree to which this occurs provides insight into the speculated negatively cooperative binding relationship between RyR and FKBP, as already mentioned in Chapter 3, and elaborated upon further in the following chapter. The capacity for FKBP12 constructs to displace native FKBP12 has been indicated previously by the binding of fluorescently tagged FKBP12 in a myocyte-based system (Guo, 2010). In this experiment, provision of fluorescently tagged FKBP12 to the cytoplasm of permeabilised myocytes resulted in a gradual replacement of endogenous FKBP bound to RyR with the fusion protein. However, such a replacement has not previously been demonstrated with co-precipitation methods in isolated channels, as in this chapter. The ability of exogenous FKBP to displace endogenous FKBP is therefore further interesting in that can provide evidence about the nature of possible FKBP turnover in the live cell; that is, whether the RyR-bound and cytoplasmic FKBP

populations exchange with one another, and whether this exchange may have a physiological function.

4.1 Aims

The central aim in this chapter is to establish whether the RyR in both skeletal and cardiac SR vesicles are saturated by FKBP, by determining whether they have the capacity to bind exogenous GST-FKBP12 additional to their endogenously-bound FKBP. If additional FKBP12 binds it will demonstrate that the RyR in these SR vesicles are submaximally occupied by FKBP.

A second aim is to determine whether exogenous GST-FKBP12 is able to displace endogenous FKBP12.

The tertiary aim was to characterise the polymeric state of both GST-FKBP12 and purified FKBP12 in solution at a range of different concentrations, both for the purposes of densitometric analysis here and other analyses in subsequent chapters.

4.2 Methods

Rabbit skeletal muscle or sheep cardiac muscle SR vesicles were generated as described in chapter **2.1**. GST-FKBP12 was expressed in *E.coli* with the pGEX2TK vector and purified via glutathione-agarose affinity chromatography, and protein concentration determined via BCA assay (**2.8**).

The polymeric state of the GST-FKBP12 construct, as well as FKBP12 subsequent to being cleaved from its GST tag, was assessed by analytical ultracentrifugation (AUC) (**2.10**)**.** As outlined in the protocol of Chapter 2, AUC experimental cells were set up as seven sequential serial dilutions, beginning with a GST-FKBP12 or FKBP12 concentration of 320 μM, and diluting by half for each subsequent dilution. Experiments were run as sedimentation equilibrium assays, with equilibrium reached after ~14 hours, and absorbance readings thereafter measured in triplicate at both 230 and 280 nm.

SR vesicle saturation experiments were conducted with 10 µL of SR vesicles suspended in 90 uL of buffer containing 150 mM NaCl and 20 mM MOPS, at pH 7.4. GST-FKBP12 was introduced at a concentration of approximately 10 µM, twice the highest reported minimum concentration required to stabilise RyR in bilayer experiments, and at least an order of magnitude greater than any reported kD values for a RyR:FKBP interaction (Blayney, 2010; Guo, 2010). Vesicles from either skeletal or cardiac muscle both with and without additional GST-FKBP12 were incubated for one hour at 37 °C, and then subjected to anti-RyR co-immunoprecipitation (**2.5**). Co-sedimentation solutes and co-immunoprecipitation eluates were both examined via SDS-PAGE (**2.3**) and subsequent Western blot (**2.4**), with relative levels of GST-FKBP12 and FKBP12 bound to the RyR visualised on Western films and then quantitated via densitometry (**2.6**). Statistical significance of densitometry data was established by two-tailed Student's t-test.

4.3 Results

Results from analysis of the dimerisation capability of GST-FKBP12 and FKBP12 are presented first, as they are necessary for accurate interpretation of the results of the subsequent co-immunoprecipitation experiments. Next, the capacity of RyR1 and RyR2 to bind GST-FKBP12 and FKBP12 is investigated. Finally, I examine the degree to which GST-FKBP12 was able to displace endogenously-bound FKBP in both RyR1 and RyR2, and characterise some of the differences in the response of the RyR to exogenous FKBP12.

4.3.1 Dimerisation of expressed FKBP12

It has previously been reported that FKBP12 overexpressed in mammalian cells exists primarily as a dimer (Schories, 2007), and certain fungal isoforms of FKBP12 have been crystallised as dimers once extracted from the cell (Tonthat, 2016). This dimerisation has not been reported for human FKBP12 either *in vivo* or *in vitro*; however, it is nevertheless important to investigate. Only one FKBP per dimer may bind to a RyR subunit, as the span between binding sites on adjacent subunits is far greater than the diameter of the FKBP molecule (Zalk, 2015, among many others).

Possibly, a dimeric bond may occlude FKBP binding determinants and hence interfere with its ability to bind to RyR. Even if binding is unaffected, the presence of an “extra” FKBP associated with each RyR subunit would give falsely high values for estimates of levels of FKBP bound to RyR after any immunodetection methods. This is a particularly important consideration, as later experiments in this chapter attempt to work backwards from a saturation state in order to estimate endogenous levels of RyR occupancy by FKBP. A potential determinant of FKBP dimerisation is the cysteine residue at position 23 (Schories, 2007); hence, experiments were carried out in neutral redox environments matching those of the later saturation experiments. The possibility also exists that dimerisation occurs in a concentration-dependant fashion, so assays were conducted across a range of concentrations.

Seven analytical cells were loaded with a serial dilution of FKBP12, as described in the methods in **4.2**, above, and spun at 100000 x g until equilibrium distribution was reached – approximately 14 hours. Readings were then taken in triplicate at both 230 and 280 nm. For analysis, however, only 230 nm signals were used, as these were consistently detectible in even the lowest analysed FKBP12 concentrations, while 280 nm readings proved somewhat unreliable at concentrations less than 20 µM.

Figure **4.1** presents a representative trace of the AUC experiments conducted to establish the polymerisation capacity of FKBP12. Each “dot” in the figure represents a scanning pass through the analytical cell; their slope and associated parameters are calculated by the Sedphat software package (Zhao, 2015). At approximately 6.75 cm and 6.80 cm, two outlier points are discernable, representing the spectrophotometer detecting the meniscus of the sample of the analytical cell. Red vertical lines indicate the area analysed in Sedphat to determine the mass of the sedimented FKBP12.

As predicted, the vast majority of FKBP12 existed as a roughly 12 kDa monomer with most concentrations. Interestingly, at 160 µM and 320 µM, the average mass of FKBP12 species was approximately 23 kDa, indicating the majority of FKBP12 had dimerised. While somewhat unexpected, this finding is nonetheless consonant with the previously reported findings in Schories et al (2007), among others, that FKBP12 has the capacity to dimerise at higher than physiological concentrations, likely due to concentration-dependent disulphide formation at cysteine 23.

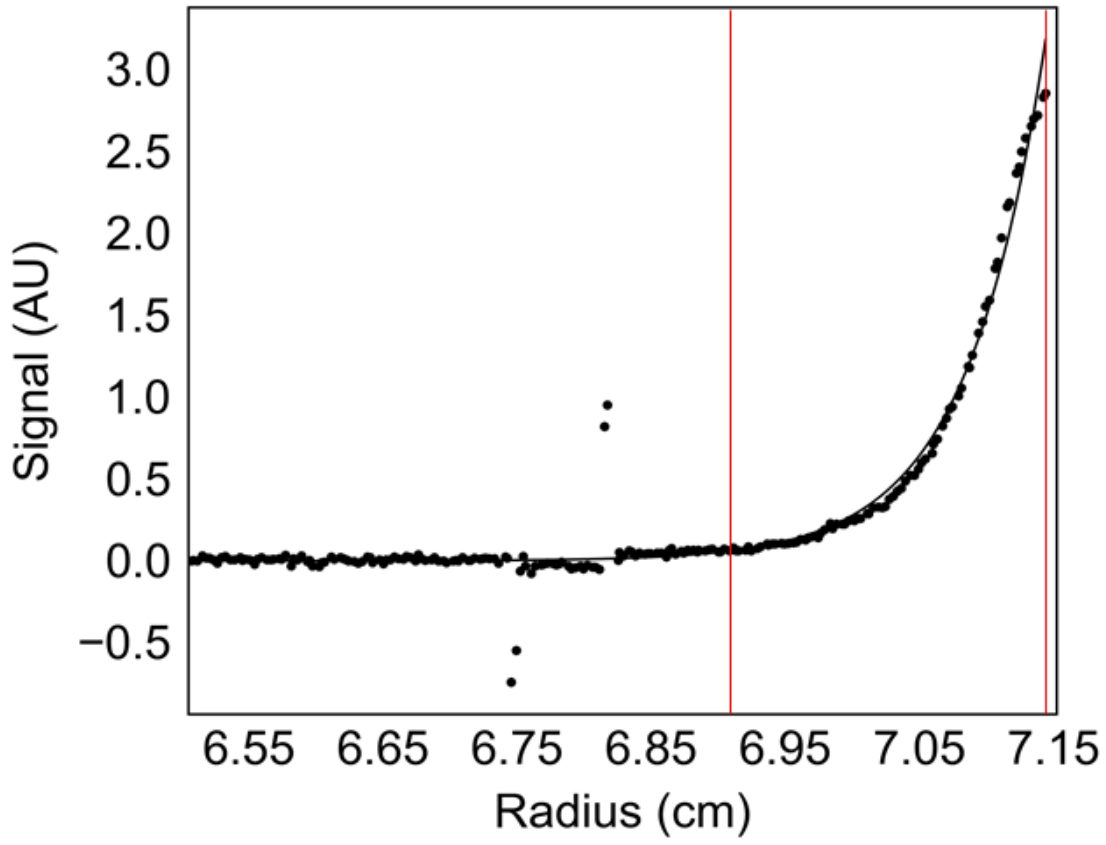

Figure 4.1: Absolute mass determination of FKBP12 by analytical ultracentrifugation. A sample sedimentation equilibrium curve is shown here, demonstrating the sedimentation profile of FKBP12 at a concentration of 10 μM and under 100000 x g, with absorbance read at 230 nm. As radius, i.e. distance from the axis of centrifugation, increases, FKBP12 sediments against the bottom of the analytical cell (at approximately 7.15 cm). Analysis of exponential curve of sedimentation (between the red vertical lines in the figure above) gives an average mass value for FKBP12 of 12.8 kDa, very close to the actual mass of FKBP12, approximately 12.1 kDa. The slight difference from the expected FKBP12 value is likely accounted for by either a very small percentage of FKBP12 existing as a dimer at 10 μm, or by FKBP12 inherently deviating somewhat from the “standard” protein buoyancy constant used in calculations.

4.3.2 Dimerisation of expressed GST-FKBP12

The GSTs are well-characterised as dimers in both the cytosol and mitochondria, and GST-fusion proteins may also exist as dimers, so long as the fused protein does not interfere with the GST dimerisation domain. For the same reasons as given in **4.3.1**, it is therefore important to characterise GST-FKBP12 to determine whether it exists as a dimer, and whether this dimerisation capacity is in some way concentration dependent. While GST itself has been reported to interact with the RyR (Dulhunty, 2011), the possibility can also be experimentally assessed by comparison of RyR binding capacities for exogenous FKBP12 and GST-FKBP12, with any significantly greater amount of GST-FKBP12 binding perhaps attributable to GST-specific interactions with the RyR.

This experiment has further significance, as GST-FKBP12 is often used as an intact fusion protein in studies of FKBP12 interaction with RyR (e.g. Masumiya, 2003; Jones, 2005), so that information about its dimeric state is important in the determination of the concentration dependence of any observed effects. The unlikely possibility also exists that if the FKBP12 component of the GST-FKBP12 is also able to dimerise, then proteins could form large polymers, which would render them unsuitable for use in analysis of FKBP12 function, and also unsuitable in examinations of RyR:FKBP stoichiometry, giving as they would vastly inflated values for levels of FKBP associated with RyR.

Seven analytical cells were loaded with a serial dilution of FKBP12, as described above in **4.2**, and spun at 100000 x g until equilibrium distribution was reached – approximately 14 hours. Readings were then taken in triplicate at both 230 and 280 nm. As expected, the vast majority of GST-FKBP12 appeared as a dimer in solution, with the two highest concentrations (160 and 320 µM) showing evidence of further aggregation at greater than physiological concentrations, speculatively due to the formation of FKBP12-FKBP12 bonds as was observed in **4.3.1**, above. Nominally, the average size of these aggregates appeared to be approximately 300 kDa, indicating that the most likely species of GST-FKBP12 at these concentrations are octomers.

Figure **4.2** presents a representative trace of the AUC experiments conducted to establish the polymerisation capacity of GST-FKBP12. Each “dot” in the figure represents a scanning pass through the analytical cell; their slope and associated

parameters are calculated by the Sedphat software package (Zhao, 2015). At approximately 6.75 cm and 6.85 cm, two outlier points are discernable, representing the spectrophotometer detecting the meniscus of the sample of the analytical cell. Red vertical lines indicate the area analysed in Sedphat to determine the mass of the sedimented FKBP12.

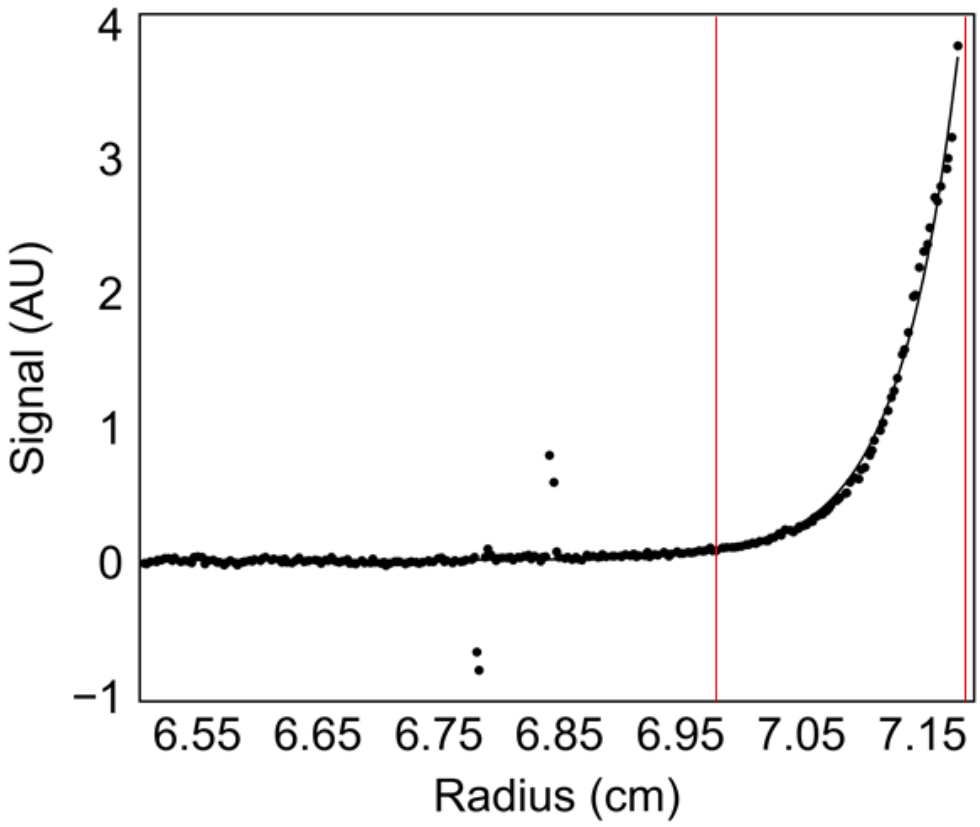

Figure 4.2: Absolute mass determination of GST-FKBP12 by analytical ultracentrifugation. A sample sedimentation equilibrium curve is shown here, demonstrating the sedimentation profile of GST-FKBP12 at a concentration of 10 μM and under 100000 x g, with absorbance read at 230 nm. As radius, i.e. distance from the axis of centrifugation, increases, FKBP12 sediments against the bottom of the analytical cell (at approximately 7.15 cm). Analysis of exponential curve of sedimentation (between the red vertical lines in the figure above) gives an average mass value for GST-FKBP12 of 72.4 kDa, only somewhat less than the predicted mass of a GST-FKBP12 dimer, 76 kDa. This is likely due to small population of GST-FKBP12 remaining as a monomer.

4.3.3 Saturation of RyR1 in SR vesicles by exogenous FKBP12

In order to determine the occupancy by FKBP12 of RyR1 in rabbit skeletal muscle SR vesicles, GST-FKBP12 was added to RyR1 at a concentration of 10 μM, an approximately 10-fold excess of physiological FKBP12 levels (Guo, 2010), and the resulting treated RyR1 examined in co-immunoprecipitation experiments. GST-FKBP12 was initially used un-cleaved in order to distinguish exogenous FKBP12 from endogenous FKBP12 on the basis of molecular weight. Later experiments used FKBP12 cleaved from its GST tag, to ensure that the tag was not causing any off-target interactions with the RyR1, either increasing or decreasing the affinity of the FKBP12 for RyR1. The difference in size between the GST-FKBP12 fusion protein and endogenous FKBP12 further allowed assessment of the degree to which exogenous FKBP12 was able to displace endogenously-bound FKBP12, providing further information about the nature of binding between FKBP12 and RyR1. A crucial assumption underlying these experiments is that the GST-FKBP12 remains a dimer when bound to RyR1, such that the visible intensity of the GST-FKBP12 band must be divided by 2 in order to generate an accurate estimate of occupancy. This assumption finds validation in the experiments with FKBP12 cleaved from its GST tag (Figures 4.4 and 4.6), the results of which accord with those found in the experiments using GST-FKBP12.

The RyR1 from these co-immunoprecipitation experiments was analysed via Western blot and its levels of bound FKBP12 compared with control untreated RyR1. Densitometry measurements obtained for GST-FKBP12 signals were divided by a factor of 2, reflecting that at the range of concentrations used in these co-immunoprecipitation experiments GST-FKBP12 exists almost wholly as a dimer (see **4.3.2**).

Figure **4.3** illustrates the results from these experiments. RyR1 signals are consistent between the control and treatment lanes, indicating roughly similar quantities of RyR1 present in both samples. GST-FKBP12 is strongly visible in the treatment lane, with none appearing in the control lane, as expected, since none had been added. The level of endogenous FKBP12 diminishes from the control lane to the treatment lane, indicating that the exogenous GST-FKBP12 has a dissociative effect on endogenous FKBP12, most likely by replacing it as the species bound to RyR1. Finally, the

quantitation of these observations in the bar graph shows that RyR1 from skeletal SR vesicles was able to bind on average 75±18% further exogenous GST-FKBP12 than it had bound endogenous FKBP12; that is, the sum of the bound GST-FKBP12 and the fraction of endogenous FKBP12 not displaced by GST-FKBP12 was ~75% greater than the pre-saturation endogenous FKBP12 signal, a significant increase in total bound FKBP12. This indicates that in SR vesicles the stoichiometry of endogenous FKBP12 was ~2.3 FKBPs per RyR1 tetramer. This number was determined by assuming that the saturated state represented 4 FKBPs bound per RyR tetramer, and then 4 * (100 / 175) gives 2.3±0.25 FKBPs per tetramer for the unsaturated vesicles. It is uncertain whether this deviation from the putative maximal 4:1 stoichiometry of FKBP12:RyR1 reflects an endogenous stoichiometry within the muscle cell or FKBP12 loss at some point during tissue homogenisation and vesicle isolation: more on these two possibilities later in this chapter's discussion, as well as in the following chapter.

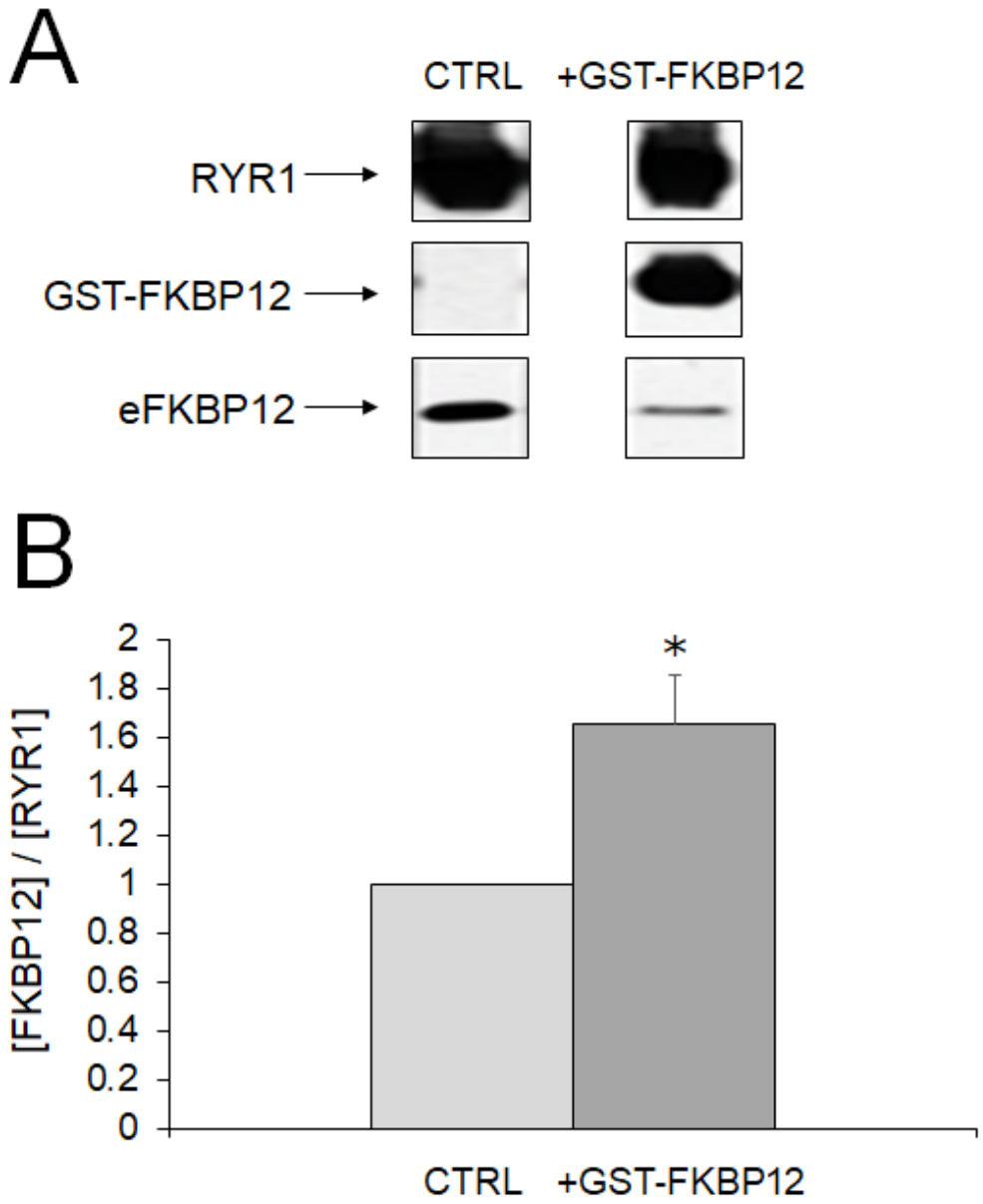

Figure 4.3: Co-immunoprecipitation of RyR1 saturated with exogenous GST-FKBP12 shows that SR vesicle RyR1 can bind additional FKBP12. A, images from a representative post-co-immunoprecipitation Western blot. RyR1 bands are presented above bands showing GST-FKBP12, in turn above bands showing the endogenous FKBP12 signal. Saturating concentrations of 10 µM GST-FKBP12 were added to the treatment lane. **B**, a graph showing the average data of n=4 co-immunoprecipitation experiments, demonstrating binding of 75±18% extra GST-FKBP12 in SR vesicle RyR1. Binding % has been normalised to reflect the fraction of GST-FKBP12 measured to exist as a dimer (Figure **4.1**, above). Asterisk indicates significant difference from control for a p value of <0.05.

Figure **4.4** illustrates the results from experiments where exogenous FKBP12, cleaved from its GST tag, was used instead of the full GST-FKBP12 fusion protein. As with the previous set of experiments, RyR1 signals are strongly similar between control and treatment lanes, indicating consistent RyR1 loading between conditions. Distinct from the previous set, however, exogenous and endogenous FKBP12 signals are indistinguishable, resulting in the treatment "FKBP12" signal being considerably stronger than the control FKBP12 signal. In this set of experiments it is impossible to determine the degree to which exogenous FKBP12 displaced endogenous FKBP12 as a binding partner for RyR1, but nevertheless, the total % of extra binding can be calculated. Importantly, these experiments with cleaved FKBP12 demonstrate that the GST tag has minimal impact on the binding of the GST-FKBP12 fusion protein to RyR1. The total increase in total bound FKBP12 in this set of experiments trended slightly higher than was observed in the GST-FKBP12 experiments (approximately 80±13% extra binding of cleaved FKBP12 vs 75±18% for GST-FKBP12), which possibly indicates a mild inhibitory effect of the GST tag on FKBP12:RyR1 binding, but even if genuine, this effect is marginal.

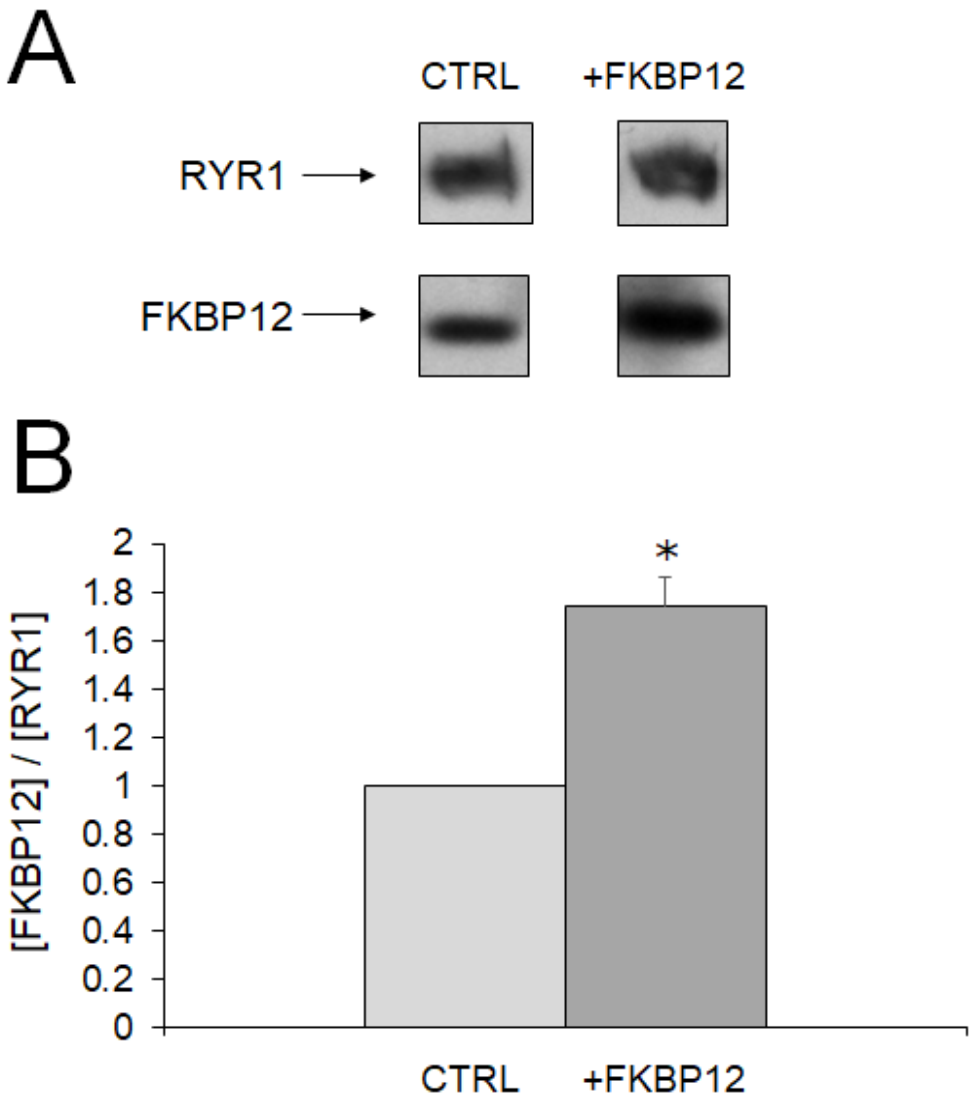

Figure 4.4: Co-immunoprecipitation of RyR1 saturated with exogenous FKBP12 cleaved from GST tag confirms that SR vesicle RyR1 can bind additional FKBP12, and that FKBP12 binding is not enhanced by GST tag. A, images from a representative post-co-immunoprecipitation Western blot. RyR1 bands are presented above band showing FKBP12; note that in the +FKBP12 lane the endogenous and exogenous FKBP12s are indistinguishable. Saturating concentrations of 10 µM FKBP12 were added to the treatment lane. **B**, a graph showing the average data of n=3 co-immunoprecipitation experiments, demonstrating binding of 80%±13% extra FKBP12 in SR vesicle RyR1. As shown in Figure **4.2**, above, extremely minimal FKBP12 exists as a dimer at 10 µM, and hence no normalisation has been applied in constructing the graph. Asterisk indicates significant difference from control for a p value of <0.05.

4.3.4 Saturation of RyR2 in SR vesicles by exogenous FKBP12

As for RyR1 in rabbit skeletal muscle SR vesicles, RyR2 in sheep cardiac muscle SR vesicles were exposed to saturating concentrations of both GST-FKBP12 and cleaved FKBP12 in order to determine the stoichiometry of FKBP to RyR2 present in the vesicles.

The RyR2 from these co-immunoprecipitation experiments was then examined via Western blot and its levels of bound FKBP12 and FKBP12.6 compared with control untreated RyR2. GST-FKBP12 signal strength was divided by a factor of 2 in densitometry calculations, reflecting the measurement that at range of concentrations used in these co-immunoprecipitation experiments almost all GST-FKBP12 is present as a dimer (see **4.3.2**).

Figure **4.5** shows the results of the GST-FKBP12:RyR2 saturation co-immunoprecipitation experiments. The RyR2 signals in both treatment and control lanes are of roughly equal strength, indicating similar loading concentrations. GST-FKBP12, as expected, appears only in the treatment lane. FKBP12 and FKBP12.6 signals appear distinct from one another in the control lane, and while still somewhat separate, appear to merge together in the treatment lane. Alternatively, FKBP12.6 is totally replaced by GST-FKBP12, such that none appears in the treatment lane. Most notable is the significant drop in FKBP12 and FKBP12.6 overall strength in the treatment lane, presumably consequent to their displacement by GST-FKBP12. Interestingly, despite different reported affinities for RyR2, both FKBP12 and FKBP12.6 signals appear to be equally diminished in strength. Finally, the bar graph illustrates that RyR2 from cardiac SR vesicles was able to bind on average 150±39% more exogenous GST-FKBP12 than it had bound endogenous FKBP12 – approximately double the amount of additional FKBP binding than was observed in RyR1. This degree of additional binding indicates that the stoichiometry of endogenous FKBP bound to SR vesicle RyR2 was ~1.6 FKBPs per RyR2. This calculation was arrived at by again assuming that the saturated state represented 4 FKBPs bound per RyR tetramer (whether FKBP12 or FKBP12.6), and then 4 * (100 / 250) gives 1.6±0.3 FKBPs per tetramer for the unsaturated vesicles. This significantly lower level of endogenous FKBP:RyR2 stoichiometry as compared to that observed in RyR1 interestingly parallels the differences in the capacity of immunosuppressant

drugs to remove FKBP12 from the two isoforms (see Chapter 3) – the implications of this difference between the isoforms will be discussed further at the end of this chapter.

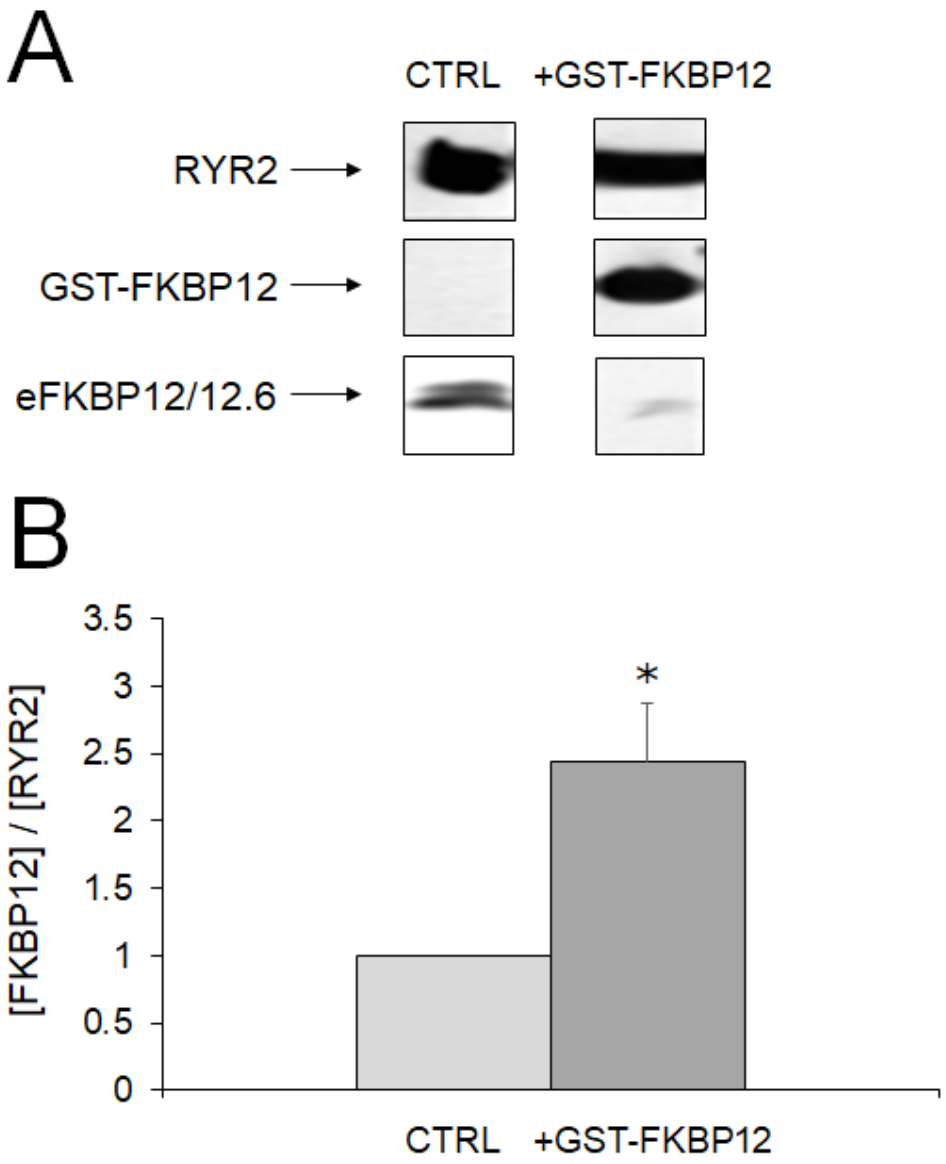

Figure 4.5 Co-immunoprecipitation of RyR2 saturated with exogenous GST-FKBP12 shows that SR vesicle RyR2 can bind additional FKBP12. A, images from a representative post-co-immunoprecipitation Western blot. RyR2 bands are presented above bands showing GST-FKBP12, in turn above bands showing the endogenous FKBP12 and FKBP12.6 signals. Notably, GST-FKBP12 has almost entirely displaced endogenous FKBP in the treatment lane. Saturating concentrations of 10 µM GST-FKBP12 were added to the treatment lane. **B**, a graph showing the average data of n=4 co-immunoprecipitation experiments, demonstrating binding of approximately 150±39% extra GST-FKBP12 in SR vesicle RyR1. Binding % has been normalised to reflect the fraction of GST-FKBP12 existing as a dimer (Figure **4.1**, above). Asterisk indicates significant difference from control for a p value of <0.05.

Figure **4.6**, following on from Figure **4.5**, shows the results of the co-immunoprecipitation experiments wherein RyR2 was saturated with FKBP12 cleaved from its GST tag. Similarly to the GST-FKBP12 experiment, additional FKBP12 was bound by RyR2, indicating incomplete occupancy of the RyR2. Interestingly, however, cleaved FKBP12 appeared to be bound by RyR2 in SR vesicles somewhat less readily than was GST-FKBP12. This is in sharp contrast to the RyR1 saturation experiments, where similar amounts of additional GST-FKBP12 and FKBP12 were able to bind to RyR2 This difference may indicate that the GST tag promotes FKBP12 binding to RyR2, but not RyR1; one hypothesis might be that GST is capable of binding to RyR2 independent of FKBP12 (as demonstrated in Dulhunty, 2011) with these “off-target” binding events contributing to a higher-than-expected signal in the GST-FKBP12 saturation experiments.

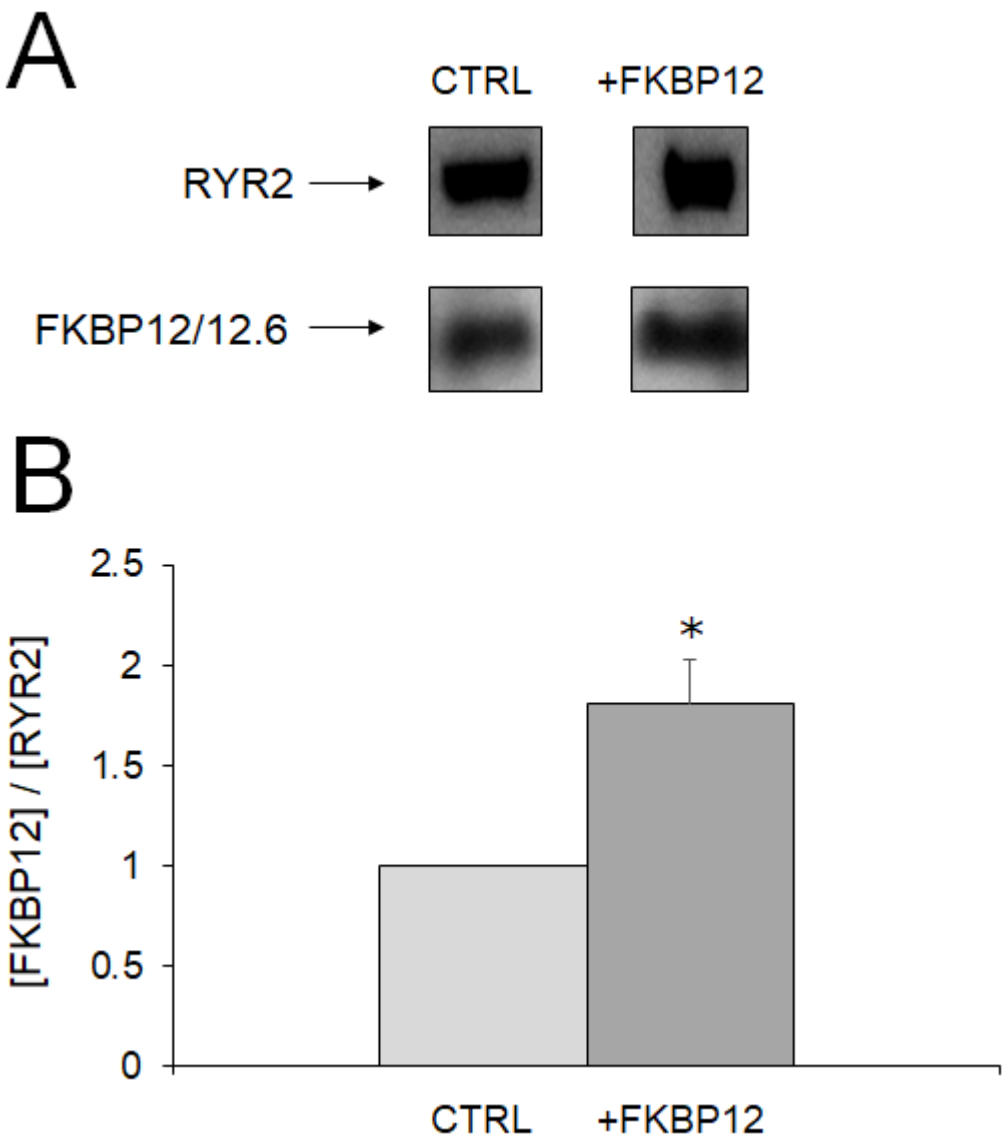

Figure 4.6: Co-immunoprecipitation of RyR2 saturated with exogenous FKBP12. **A**, images from a representative post-co-immunoprecipitation Western blot. RyR2 bands are presented above band showing FKBP12; note that in the +FKBP12 lane the endogenous and exogenous FKBP12s (and any FKBP12.6 present) are indistinguishable. Saturating concentrations of 10 µM FKBP12 were added to the treatment lane. **B**, a graph showing the average data of n=3 co-immunoprecipitation experiments, demonstrating binding of 80±22% extra FKBP12 in SR vesicle RyR2. Per Figure **4.2**, above, extremely minimal FKBP12 exists as a dimer at 10 µM, and hence no normalisation of the FKBP12 blot signal has been applied in constructing the graph. Asterisk indicates significant difference from control for a p value of <0.05.

4.3.5 Displacement of endogenous FKBP12 by exogenous GST-FKBP12 seen in experimental supernatants

As observed during the saturation experiments in this chapter (**4.3.3**, **4.3.4**), exogenous GST-FKBP12 was able to displace endogenous FKBP12 as a binding partner for both RyR1 and RyR2. Displacement of FKBP12.6 may also have occurred but is difficult to quantify due to low endogenous concentrations. Exogenous cleaved FKBP12 was likely also able to displace endogenous FKBP12, but the effect was not able to be seen on Western blots due to the two proteins' identical molecular weights.

Supernatants from these co-immunoprecipitation experiments were therefore also examined via Western blot, with the hypothesis that dissociated endogenous FKBP12 should appear in the supernatants roughly in proportion with the amount which was observed to be displaced by exogenous GST- FKBP12. 15 uL of the first wash following GST-FKBP12 saturation was therefore collected and analysed alongside the eventual eluates of the co-immunoprecipitation experiments.

Figures **4.7** and **4.8** illustrate the results of this analysis. In both RyR1 and RyR2 control experiments, where no exogenous GST-FKBP12 was introduced, a low level of FKBP dissociation was nevertheless observed, paralleling the observations from Chapter 3 that a certain population of RyR-bound FKBP appears extremely amenable to dissociation. This "baseline" level of FKBP dissociation can be seen in the CTRL boxes in the figures below. When the RyR were treated with GST-FKBP12, however, a significantly greater degree of FKBP dissociation was observed: the bar graphs in Figures **4.7** and **4.8** express this increase in dissociation relative to the "baseline" level of dissociation. For RyR1, approximately three times more FKBP12 appeared in the supernatants of vesicles treated with GST-FKBP12, while for RyR2, approximately four times more FKBP12 and FKBP12.6 together appeared than in the untreated supernatants: a statistically significant difference. This suggests a somewhat greater capacity for GST-FKBP12 to replace FKBP12 or FKBP12.6 in RyR2 than FKBP12 in RyR1. Interestingly, this data is independent of the observation from the above saturation experiments that SR vesicle RyR2 appears less occupied by FKBP than SR vesicle RyR1. Indeed, if RyR2 had less FKBP associated before GST-FKBP12 saturation than did RyR1, then a negatively cooperative model of binding, as proposed in Chapter 3, would predict that this smaller population of bound FKBP would be more

resistant to displacement by GST-FKBP12. Alternatively, a negatively cooperative model of binding might still obtain, with the differences between RyR1 and RyR2 affinity for FKBP being different enough that a small but significant difference in starting stoichiometry – 2.3 FKBPs per RyR1 vs 1.6 FKBPs per RyR2 – is not sufficient to overcome this difference in affinity.

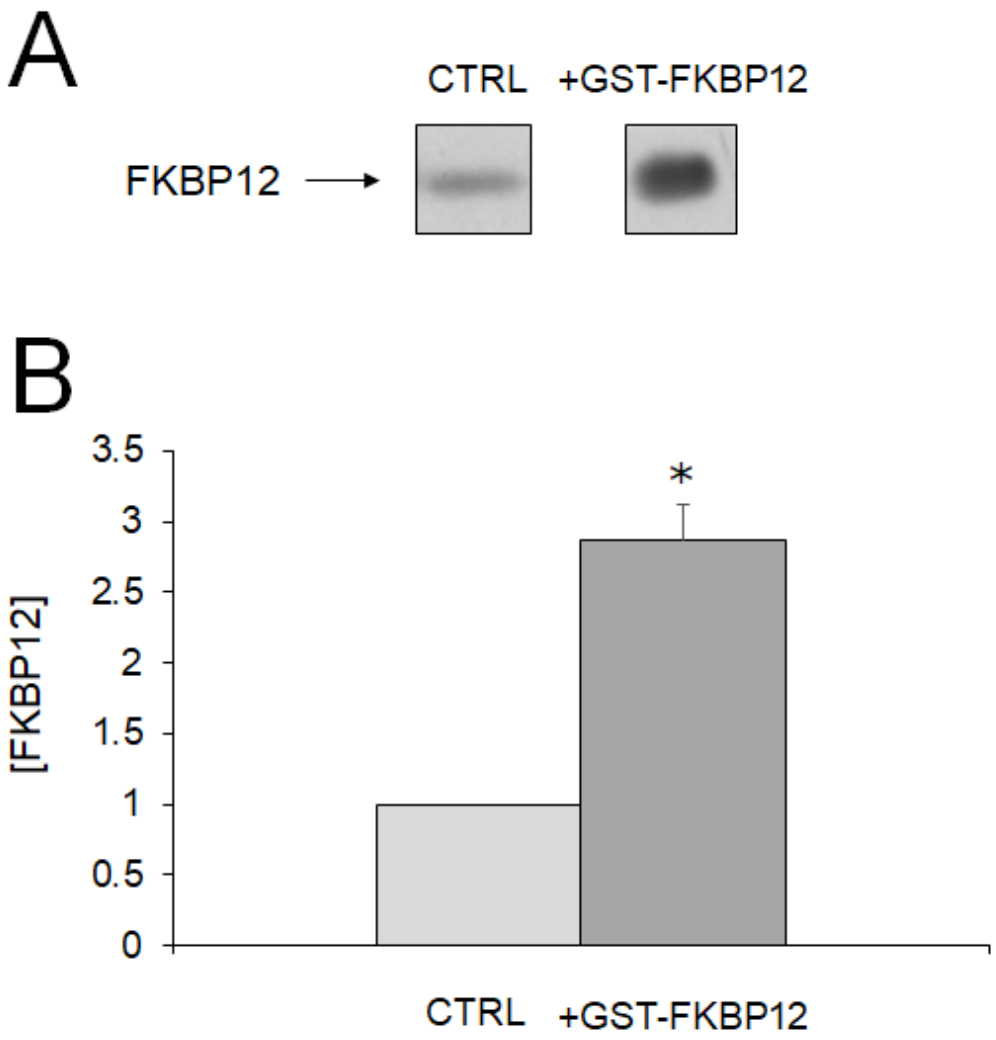

Figure 4.7: Comparison of supernatant FKBP12 signals from RyR1 GST-FKBP12 saturation experiments. **A**, images from a representative post-co-immunoprecipitation Western blot of experimental supernatants, showing endogenous FKBP12 dissociated after RyR1 SR vesicles were incubated with either a control buffer or 10 µM GST-FKBP12. **B**, a graph expressing the increase in FKBP12 dissociation from RyR1 following treatment with GST-FKBP12. As these data are drawn solely from the experiments using GST-FKBP12 as the exogenous additive, rather than cleaved FKBP12, all present FKBP12 signals are endogenous. Excess unbound GST-FKBP12 did appear in the +GST-FKBP12 supernatant lane, and not in the control lane, but is not presented in the figure above for the sake of clarity. Asterisk indicates significant difference from control for a p value of <0.05.

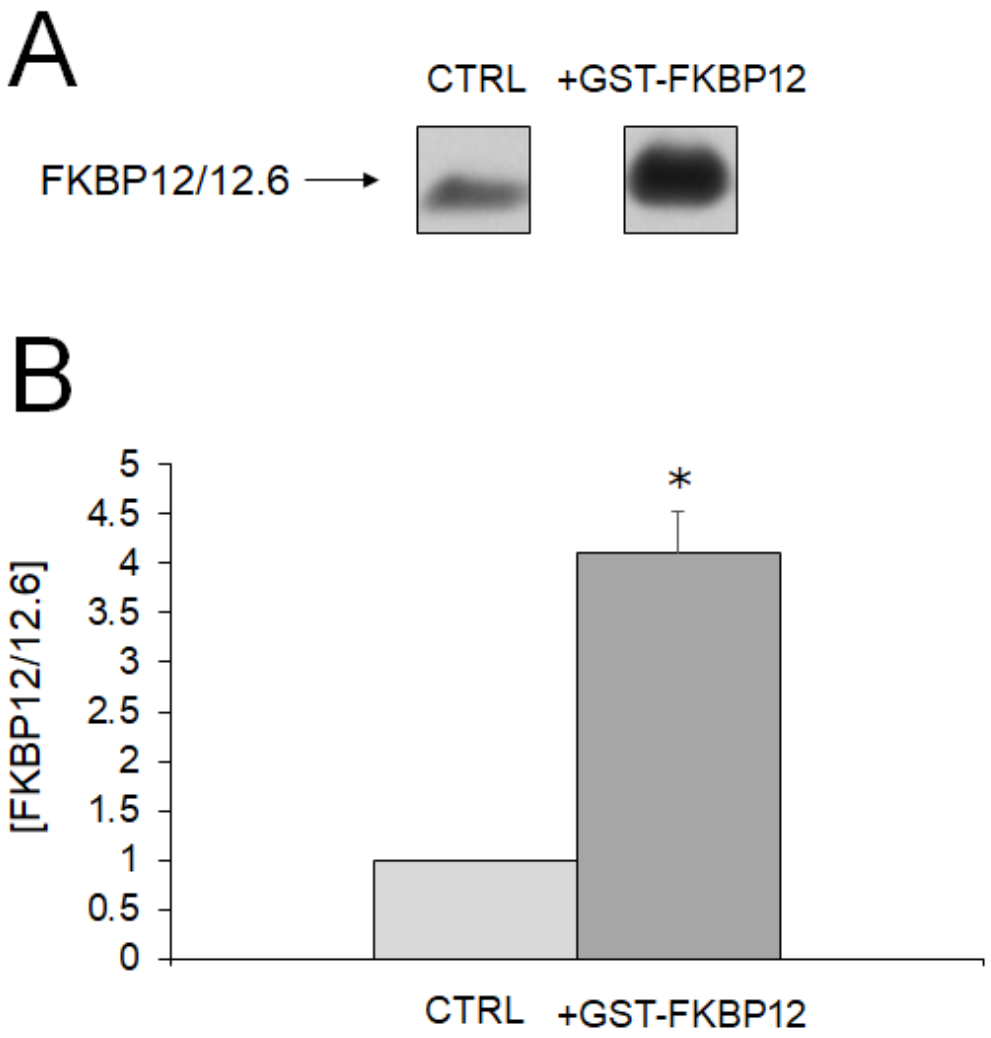

Figure 4.8: Comparison of supernatant FKBP12/12.6 signals from RyR2 GST-FKBP12 saturation experiments. A, images from a representative post-co-immunoprecipitation Western blot of experimental supernatants, showing endogenous FKBP12 and FKBP12.6 dissociated after RyR2 SR vesicles were incubated with either a control buffer or 10 µM GST-FKBP12. Notably, here the FKBP12 and FKBP12.6 signals are not sufficiently separated to be distinguishable, and are hence considered together. **B**, a graph expressing the increase in FKBP12/12.6 dissociation from RyR2 following treatment with GST-FKBP12. As these data are drawn solely from the experiments using GST-FKBP12 as the exogenous additive, rather than cleaved FKBP12, all present FKBP12/12.6 signals are endogenous. Excess unbound GST-FKBP12 did appear in the +GST-FKBP12 supernatant lane, and not in the control lane, but is not presented in the figure above for the sake of clarity. Asterisk indicates significant difference from control for a p value of <0.05.

4.4 Discussion

The results in this chapter confirm the hypothesis that SR vesicle RyR exhibit submaximal FKBP occupancy, with RyR2 somewhat less occupied on average than RyR1. This has significant consequences for physiological examination of SR vesicle RyR: with the assumption that “normal” RyR occupancy by FKBP is maximal, and further that submaximal occupation drives “pathological” RyR behaviour, then SR vesicle RyR represent a non-ideal baseline in this respect for drawing conclusions about physiological RyR function. Possible interventions to address this deficit might include either actively protecting RyR-associated FKBP from dissociation during the SR vesicle fractionation process, possibly with exogenous small molecules with capability to stabilise the RyR:FKBP relationship, such as S107 (**1.4.5**; Bellinger, 2009; Lehnart, 2008; Mei, 2013; Wehrens, 2004b). More on this possible intervention in the following chapter. Alternatively, it might be useful to try to replicate in experimental solutions the normal cytoplasmic FKBP12 concentration (~1 μM, Guo, 2010), based on the assumption that this will replicate the endogenous binding state.

It is important to note that the conclusions drawn above rely on the assumption that “normal” RyR occupancy by FKBP is maximal: that is, four FKBPs per RyR tetramer. This assumption has not been rigourously tested: while high-resolution cryo-EM has shown RyR fully occupied with FKBP, these RyR have generally been exposed to saturating concentrations of FKBP12 or FKBP12.6 (e.g. to elute them from an affinity column) at some point during their purification, and so it is not possible from this to conclude that such a binding relationship would obtain in normal physiology. The question of whether the submaximal occupancy by FKBP observed in RyR1 and RyR2 in the present chapter might be a normal stoichiometry, or whether it is in fact consequent to processing-induced dissociation will be further explored in the following chapter. A further assumption is that saturating concentrations of exogenous FKBP12 are indeed sufficient to achieve maximal occupancy of RyRs: as was observed in Chapter 3, a certain amount of FKBPs passively dissociated from both RyR1 and RyR2. Should even the saturating concentrations of FKBP12 used in the experiments of this chapter not be sufficient to reliably achieve a maximal stoichiometry of 4 FKBPs per RyR, this does not call into question the general finding of sub-maximal occupancy, nor the comparison of relative RyR1 and RyR2 SR vesicle FKBP

stoichiometries, but may render problematic the calculations of the “actual” stoichiometries for both species (i.e. ~2.3 and ~1.6 respectively).

The observation that RyR2 is less-occupied than RyR1 by FKBP interestingly parallels data from the previous chapter, where it was observed that while a population of RyR1-associated FKBP readily dissociated upon exposure to rapamycin or FK506, RyR2-associated FKBP remained largely bound. In RyR1, despite the ready dissociation of the majority of RyR1-associated FKBP12, a certain population remained firmly bound, and difficult to dissociate. In the discussion of the previous chapter, it was hypothesised this may be consequent to a negatively cooperative relationship between RyR and FKBP. If that is the case, then the data in the present chapter, showing that RyR2 have on average fewer FKBPs associated with them, might go some way towards explaining the differences in RyR response to FKBP-dissociative drug treatments: while RyR1 had capacity to shed the 2nd or 3rd FKBP associated with them, many RyR2 would on average have only a single associated FKBP, which single associated FKBP would be, using the logic of negative cooperativity, the most difficult to dissociate. The differences in FKBP stoichiometry between RyR isoforms observed in this chapter does not precisely map to the differences observed in their response to FKBP-dissociative drugs, however: the differences in drug response are greater than would be accounted for by ~1 FKBP worth of difference in stoichiometry, so it is likely further factors are involved.

Addressing the second aim of this chapter, exogenous GST-FKBP12 proved highly capable of displacing endogenously-bound FKBP from the RyR, with RyR2-associated FKBP more vulnerable to displacement than RyR1-associated FKBP. This provides an additional interesting contrast to data from Chapter 3, in which RyR2-associated FKBP proved more resistant to dissociation than did RyR1-associated FKBP. In both RyR1 and RyR2, a population of FKBP12 proved resistant to displacement by high concentrations of exogenous GST-FKBP12, again providing evidence for the hypothesis that a certain population of FKBP12 binds with a greater than normal affinity to the RyR, suggesting a negatively cooperative relationship between RyR and FKBP.

Finally, assessment of the polymeric state of both GST-FKBP12 and FKBP12 confirms that as predicted, over the normal range of concentrations that might be expected in

either normal physiology or physiological experimental conditions (i.e., from nanomolar to low micromolar), the overwhelming majority of GST-FKBP12 is present as a dimer in solution, while the overwhelming majority of cleaved FKBP12 is a present as a monomer. Interestingly, FKBP12 does begin to dimerise at ~150 µM, and so in the case of GST-FKBP12, with both halves of the fusion protein capable of independent dimerisation, large polymeric aggregates quickly form. This finding is particularly relevant to researchers expressing their own GST-FKBP12, where this concentration threshold may well be reached during the process of concentrating purified protein for the preparation of aliquots or the like.

4.5 Conclusions

Both RyR1 and RyR2 in SR vesicles are submaximally occupied by FKBP, with RyR2 somewhat less occupied than RyR1.

Exogenous GST-FKBP12 proved capable of displacing a large proportion of the endogenously bound FKBP in both RyR1 and RyR2, with significantly more endogenously bound FKBP being displaced in RyR2.

The vast majority of GST-FKBP12 exists as a dimer under normal physiological and experimental conditions, while the vast majority of FKBP12 exists as a monomer. At >100 µM, FKBP12 begins to dimerise, and so GST-FKBP12 fusion proteins begin to polymerise at this concentration.

Chapter 5: Processing loss of FKBP from RyR, and S107 stabilisation of RyR:FKBP interaction

5.0 Introduction

In this chapter, I examine the loss of FKBPs from their associated RyRs, and one potential method for redressing this loss: treatment with the FKBP:RyR stabilising agent S107. This Chapter therefore builds on the findings in Chapter 4, in which I demonstrated that RyR in SR vesicles from both rabbit skeletal and sheep cardiac muscle tissue are capable of taking up significant amounts of exogenous FKBP12, pointing towards a degree of FKBP dissociation occurring during vesicle processing.

The findings of Chapter 4 present significant issues for the interpretation of data from studies of such RyR, as it has been generally assumed that SR vesicle RyR retain their endogenously bound complement of FKBP through processing. However, as the RyR/FKBP ratio is probably altered due to the loss of FKBP during processing – as observed in Chapter 4 - such a disruption of a key RyR-regulatory protein likely has a significant impact on experimentally-observed RyR behaviour. Non-physiological RyR behaviour consequent to experimental treatment of native RyR has been observed previously, where CSQ depletion from RyR due to alterations in buffer Ca^{2+} content resulted in an increased sensitivity of RyR to luminal Ca^{2+} concentration (Beard, 2005).

By contrast, the non-physiological RyR behaviour most likely attributable to FKBP loss is “subconductance” gating, where RyR are observed to open submaximally, sometimes very frequently, with each opening less than the normally-observed amplitude. Substate activity is quite commonly observed in native RyR which have been incorporated into bilayers via SR vesicles (Ahern, 1997; Richardson, 2017). The association of substate activity with FKBP depletion is fortified by observations that addition of exogenous FKBP to RyR channels may recover a more stable gating phenotype, which is presumably nearer to physiological reality (Richardson, 2017, and further work from our group, yet to be published). A caveat, however, is that other

groups have found the addition of exogenous FKBP to have little effect on channel gating – see particularly **1.4.4.2** for more details. Regardless, to usefully interpret such observed subconductance activity in terms of the number of occupied FKBP binding sites, on the assumption that the amount of bound FKBP has a direct relationship to the gating phenotype of their parent RyR, it is necessary to estimate the actual amount of FKBP dissociated during processing, relative to the amount that would be endogenously bound in a living cell.

Pilot experiments on processing loss of FKBP provided strong circumstantial evidence that the endogenous stoichiometry of RyR might not be the assumed maximal 4 FKBPs per 1 RyR tetramer, as the data from Chapter 4 showed that SR vesicle RyR1 and RyR2 were able to bind exogenous FKBP12 in greater quantities than could be accounted for by recouping of the processing-induced loss observed between initial homogenate phases of processing and the final SR vesicles. A starting point for examination of the true cellular stoichiometry of RyR:FKBP is analysis of raw muscle homogenate, which we assume are the samples most likely to contain a RyR:FKBP relationship most closely matching that found in the living cell. Saturation studies similar to those that were conducted in Chapter 4 are able to determine the fraction of RyR in muscle homogenate occupied by FKBP, although such studies are much more difficult to conduct due to the complex, membranous nature of raw homogenates.

As mentioned above, the effect of FKBP association on RyR channel behaviour has been studied by reintroducing exogenous FKBP to purified RyR and observing changes in channel activity, and this suggests a simple method for restoring normal channel behaviour after FKBP have been stripped by processing. However, should RyR not be endogenously saturated with FKBP, as Chapter 4 suggests, then calculation of the necessary amount of FKBP to reintroduce will be very difficult, and require an estimate of both the initial RyR:FKBP stoichiometry, and the stoichiometry arrived at after processing-induced FKBP dissociation. An assessment of these stoichiometries will be attempted in this chapter in order to inform such FKBP reintroduction protocols, although full validation of reintroduction protocols is beyond the scope of this thesis.

In addition to FKBP reintroduction protocols, it is useful to explore methods of generating SR vesicle RyR with preserved physiological RyR:FKBP ratios, which

avoid both the necessity of a source of exogenous FKBP and potential off-target interactions of FKBP with other experimental compounds. To examine the endogenous association between FKBP and RyR, the RyR:FKBP complex could be stabilised in muscle homogenates prior to any processing apart from tissue homogenisation, with the goal of preserving this endogenous stoichiometry through the subsequent processing steps. Several methods may be effective here. Chemically cross-linking RyR with FKBP might seem to be a simple way to preserve the binding relationship through processing. However, this may prove extremely difficult to achieve before any processing-induced loss has occurred, as cross-linking would need to take place within the extremely complex environment of the total muscle homogenate, which both complicates the execution of a crosslinking protocol and introduces the strong possibility of non-specific crosslinking. Further, cross-linking would likely disrupt RyR function, with mobility of the channel inhibited by association with other compounds. Besides this, the process of homogenisation itself introduces muscle tissue to a non-physiological buffer and exposes the contents of many intracellular compartments to the general cytoplasm, complicating further the “result” of any crosslinking protocols. Finally, irreversibly cross-linking FKBPs to their parent RyRs will defeat any potential regulatory dynamism in the the RyR:FKBP association.

As an attractive alternative, drugs exist which specifically stabilise the RyR:FKBP interaction and can be easily introduced to muscle homogenate, or even applied systemically prior to animal sacrifice or tissue homogenisation. While the stabilisation achieved by these compounds may not be as absolute as that found with cross-linking protocols, as they generally act indirectly upon the RyR:FKBP complex by stabilising a particular conformational state rather than covalently bonding proteins, the specificity of their effect enables treatment from very early in processing. In this chapter the efficacy of one of the better-characterised of such compounds, S107, will be examined in generating SR vesicles with closer-to-endogenous RyR:FKBP stoichiometries.

S107 – 2,3,4,5,-tetrahydro-7-methoxy-4-methyl-1,4-benzothiazepine – is a drug that has been demonstrated to stabilise the RyR-FKBP complex in a similar fashion to a previously characterised analogous drug, JTV519 (Yano, 2003). Consequently, the drug improves pathological cardiac and skeletal muscle function in animal models, and also reduces the incidence of certain neurological RyR:FKBP related seizures in animal models (Bellinger, 2009; Lehnart, 2008; Mei, 2013; Wehrens, 2004b). S107 is

thus considered to present significant potential as a treatment for channelopathies in which FKBP dissociation is implicated (Matecki, 2016); indeed, a drug of the same class as S107, S48168/ARM210 is currently in phase II clinical trials as a treatment RyR1-related myopathies (Armgo, 2019). S107 stabilisation of the FKBP-RyR relationship has further been observed in vesicle-based systems (Mei, 2013) with application of exogenous FKBP. It is therefore reasonable to assume that S107 may also stabilise the binding of endogenous FKBP to RyR, and thereby prevent their loss during processing.

A consideration in assessing the efficacy of S107 stabilising FKBP binding to RyR is the possibility of creating an unphysiological association between the two proteins. This may occur if the endogenous association between FKBP and RyR is less than saturated because of on/off exchange between RyR-bound FKBP and free FKBP in the cytoplasm. This appears likely, given the easy exchange between bound FKBP and added GST-FKBP as seen in results in Chapter 4. In this situation, especially if there is a significant excess of free FKBP, S107 treatment could result in supra-physiological levels of FKBP bound to RyR, thus distorting the “snapshot” of the physiological RyR:FKBP stoichiometry that early intervention with S107 is intended to capture. This possibility will be potentially assessed by conducting the homogenate saturation experiments in the presence or absence of S107. If the experiments conducted with S107 exhibit increased binding of FKBP to RyR, it would suggest excess binding due to the presence of S107.

A further question of interest is whether S107 stabilises the interactions of RyR1 and RyR2-associated FKBP equally. Previous work (Lehnart, 2008) has shown that S107 has efficacy in stabilising the relationship of FKBP12.6 to CPVT mutant RyR2, but as yet no direct comparison has been made of the efficacy of S107 across the RyR isoforms. Since S107 appears to bind to multiple low-affinity sites on the RyR in addition to a “canonical” binding site proximate the RyR:FKBP interface (Mei, 2013), some isoform-specificity in the action of S107 might be possible, on the assumption that the non-specific binding of S107 indirectly contributes to its stabilisation activity, and that RyR isoform differences will naturally impact this non-specific consequent activity.

5.1 Aims

The central aim in this chapter was to establish the degree to which SR vesicle processing is responsible for the submaximal occupancy of RyR by FKBP observed in Chapter 4, and further, at what point in SR vesicle processing significant losses of FKBP from RyR occur.

The second aim was assess whether S107, a drug with demonstrated efficacy in stabilising the RyR:FKBP relationship, is able to usefully correct any loss of FKBP from RyR during SR vesicle processing, and if so, to what degree.

A tertiary aim was to establish the occupancy of RyR by FKBP in raw muscle homogenates, on the assumption that this particular stoichiometry best recapitulates their endogenous state. Combining the findings from this and the first aim, I will attempt to suggest a protocol for reintroduction of FKBP to RyR in experiments making use of SR vesicles for analysis of RyR.

5.2 Methods

Rabbit skeletal muscle or sheep cardiac muscle SR vesicles were generated as described in **2.1**; however, each preparation was split into two parallel preparations, with one containing from the beginning of the tissue homogenisation process 20 μM of S107. During the preparation process, samples were taken at the homogenate, “P2” intermediate (approximately the midpoint of vesicle processing and fractionation), and “P4/B4” final purified SR vesicle phases.

GST-FKBP12 was expressed in *E.coli* with the pGEX2TK vector and purified via glutathione-agarose affinity chromatography, and protein concentration determined via BCA assay (**2.8**).

Analysis of RyR:FKBP associations in all phases of processing were conducted with 10 μL of sample suspended in 90 μL of buffer containing 150 mM NaCl and 20 mM MOPS, at pH 7.4. These samples were subjected to anti-RyR co-immunoprecipitation (**2.5**). Co-immunoprecipitation eluates were both examined via SDS-PAGE (**2.3**) and subsequent Western blot (**2.4**), with levels of FKBP12 bound to the RyR visualised on Western films and then quantitated via densitometry (**2.6**). Statistical significance of

densitometry data was established by two-tailed Student's t-test with $p < 0.05$ as the threshold for significance.

FKBP saturation experiments in raw muscle homogenates were conducted in a similar manner to that described in Chapter 4, with FKBP12 introduced at a concentration of approximately 10 μM, twice the highest reported minimum concentration required to stabilise RyR in bilayer experiments, and at least an order of magnitude greater than any reported kD values for a RyR:FKBP interaction (Blayney, 2010; Guo, 2010). Samples were incubated for one hour at 37 °C, before being subject to anti-RyR co-immunoprecipitation as per **2.5**.

5.3 Results

As detailed in **5.2**, all SR vesicle processing experiments consisted of comparisons of two different time points in SR vesicle processing. Due to limited space on SDS-PAGE gels, a full comparison of homogenates, intermediate phases, and final SR vesicles was not possible within a single experiment: **5.3.1** therefore presents a comparative analysis of homogenates and final SR vesicles, and then **5.3.2** presents the same analysis across the intermediate phase and the final SR vesicle stage. A theoretical concatenation of these experiments is then presented in the discussion section, **5.4**.

As in several previous experiments, the separation of FKBP12 and FKBP12.6 species in analysis of RyR2-associated FKBP was not always sufficient to distinguish one from another; consequently, results for RyR2-associated FKBP are presented as the sum of both species of FKBP, although as seen in previous Chapters, FKBP12 would be expected to generally be the predominant species observed.

5.3.1 FKBP loss from homogenate to processed vesicles, and S107 stabilisation

In order to assess the degree of loss of FKBP from RyR in SR vesicles, and the potential protective effects of S107 on this loss, samples were taken from SR preparations at the initial homogenate phase of processing and at the final B4/P4 phase of processing. Two such SR vesicle preparations were conducted in parallel,

with one including a constant concentration 20 μM of S107 at every phase of processing and the other lacking S107. These samples were examined via Western blot to establish the ratios of FKBP to RyR at each time point. Figures **5.1** and **5.2** illustrate the results of these experiments for cardiac and skeletal muscle SR vesicle preparations, respectively.

Figure **5.1** illustrates results from experiments comparing the association of FKBP12 and FKBP12.6 together with RyR2 at both the initial homogenate and final “P4” stage of vesicle processing. Results from parallel experiments conducted in the presence of S107 are presented alongside. FKBP12/12.6 signals associated with untreated P4 vesicle RyR2s appear significantly weaker, with a 72±4% loss observed over the course of n=5 experiments. FKBP12/12.6 signals appear somewhat reduced even in P4 vesicles prepared in the presence of S107, but this trend towards increased dissociation did not achieve significance in comparison with any of the homogenates. Put another way, S107 treatment appears to ameliorate significant loss of FKBPs from RyR2 during vesicle processing. Additionally, compared to untreated P4 vesicles, a significantly increased amount of FKBPs appear bound to P4 vesicles prepared in the presence of S107.

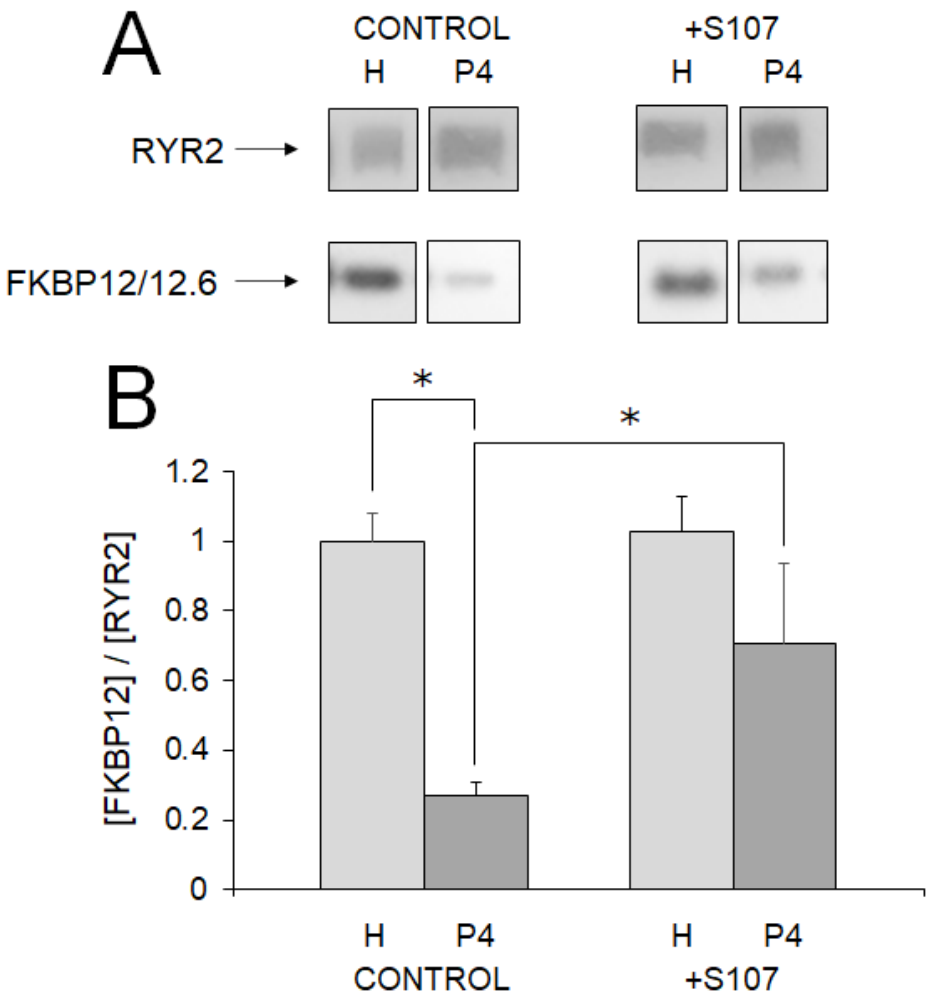

Figure 5.1: Co-immunoprecipitation confirms that S107 stabilises the RyR2:FKBP interaction through vesicle processing. A, bands from a representative post-co-immunoprecipitation blot. RyR2 bands are presented above their matching FKBP12/12.6 bands. From left to right, lanes are: untreated muscle homogenates, untreated P4 vesicles, S107-treated muscle homogenates, and S107 treated P4 vesicles. **B**, the graph shows the average data of n=5 co-immunoprecipitation experiments, demonstrating significant retention of RyR2-associated FKBPs in the S107-treated species, as well as significant loss of RyR2-associated FKBPs between the homogenate and P4 phases in untreated species. Data are presented as the ratio of FKBP12/12.6 / RyR2 densitometry measurements, normalised to the ratio in the untreated homogenate. While observed FKBP loss between homogenate and P4 stages in the S107-treated species did not meet significance thresholds, a strong trend is nevertheless apparent; that is, S107

stabilisation appears to be incomplete. Asterisk indicates significant differences with a p value of <0.05.

Figure **5.2** illustrates results from experiments comparing the association of FKBP12 to skeletal muscle RyR1 at both the initial homogenate and final “B4” stage of vesicle processing. Results from parallel experiments conducted in the presence of S107 are presented alongside. FKBP12 signals associated with untreated B4 vesicle RyR1s appear significantly weaker, with a 52±13% loss observed over the course of n=6 experiments. FKBP12 signals otherwise appear consistent with levels observed in untreated homogenate. Notably, this indicates that S107 treatment appears to largely rescue any loss of FKBP12 associated with the processing of RyR1-containing skeletal muscle vesicles.

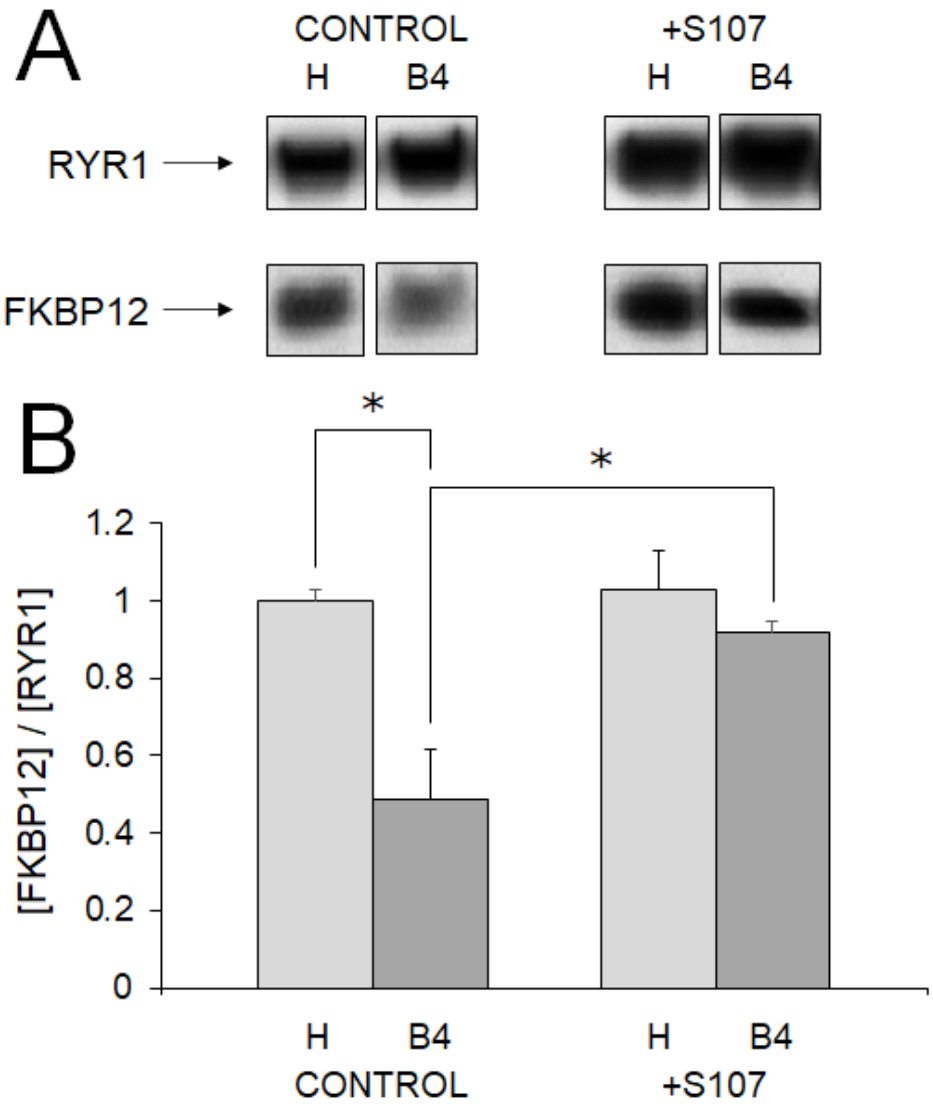

Figure 5.2: Co-immunoprecipitation confirms that 20 μM S107 stabilises the RyR1:FKBP interaction through vesicle processing. A, bands from a representative post-co-immunoprecipitation blot. RyR1 bands are presented above their matching FKBP12 bands. From left to right, lanes are: untreated muscle homogenates, untreated B4 vesicles, S107-treated muscle homogenates, and S107 treated B4 vesicles. **B**, the graph shows the average data of n=6 co-immunoprecipitation experiments, demonstrating significant retention of RyR1-associated FKBPs in the S107-treated species, as well as significant loss of RyR1-associated FKBPs between the homogenate and B4 processing phases. Data are presented as the ratio of FKBP12 / RyR1 densitometry measurements, normalised to the ratio in the untreated homogenate. Asterisks indicates significant differences between columns, for a p value of <0.05.

Figures **5.1** and **5.2** demonstrate that significant amounts of FKBP are lost from both RyR1 and RyR2 during vesicle processing: 72±4% of FKBP bound to RyR2 in muscle homogenates is lost in the processing to the P4 phase, while 52±13% of FKBP bound to RyR1 in muscle homogenates is lost in the processing to the B4 phase. A constant concentration of 20 μM S107 during homogenisation and processing rescues some of this FKBP loss from both RyR1 and RyR2, reducing FKBP processing loss from RyR2 to 30±23%, and rendering processing loss of FKBP from both RyR1 and RyR2 not statistically significant.

S107 treatment therefore appears to offer an effective means by which to stabilise the RyR:FKBP relationship during the generation of both cardiac and skeletal muscle vesicles, particularly so in the case of RyR1. Further, in the absence of S107 treatment, the degree of FKBP loss observed from both RyR isoforms may be substantial enough to effect RyR physiology.

5.3.2 FKBP loss from intermediate-phase vesicles to processed vesicles, and S107 stabilisation

While the experiments in **5.3.1** established both that significant quantities of FKBPs are lost from both RyR1 and RyR2 during vesicle processing, and that S107 treatment largely rescues this loss, those experiments only examined the “start” and “end” states of vesicle processing. Examining an “intermediate” phase offers both a more finely grained picture of this observed loss, and may suggest alternative means to remediate FKBP-loss: if FKBP loss occurs only at the final phases of processing, then an alternative to S107 treatment may be to simply work with somewhat cruder vesicle fractions, or else to adjust processing protocols such that the methods most responsible for FKBP loss are minimised. Finally, any differences in the mechanisms of FKBP loss between RyR1 and RyR2 may offer interesting insight into the different relationship of the RyR isoforms to their associated FKBP species.

Figure **5.3**, illustrates results from experiments comparing the association of FKBP12 and FKBP12.6 to cardiac muscle RyR2 at both the intermediate “P2” and final “P4” stage of vesicle processing. Results from parallel experiments conducted in the presence of S107 are presented alongside. FKBP signals associated with untreated

P4 vesicle RyR2s appear significantly weaker than in other lanes, with a 70±4% loss observed over the course of n=6 experiments: very close to the degree of loss observed in Figure 5.1. From these two figures, it follows that the majority of FKBP loss from RyR2 during vesicle processing occurs between the P2 and P4 processing stages. FKBP12 signals otherwise appear consistent with levels observed in the untreated P2, indicating a relatively good effect of S107 treatment on stabilising FKBP association to RyR2 during vesicle processing.

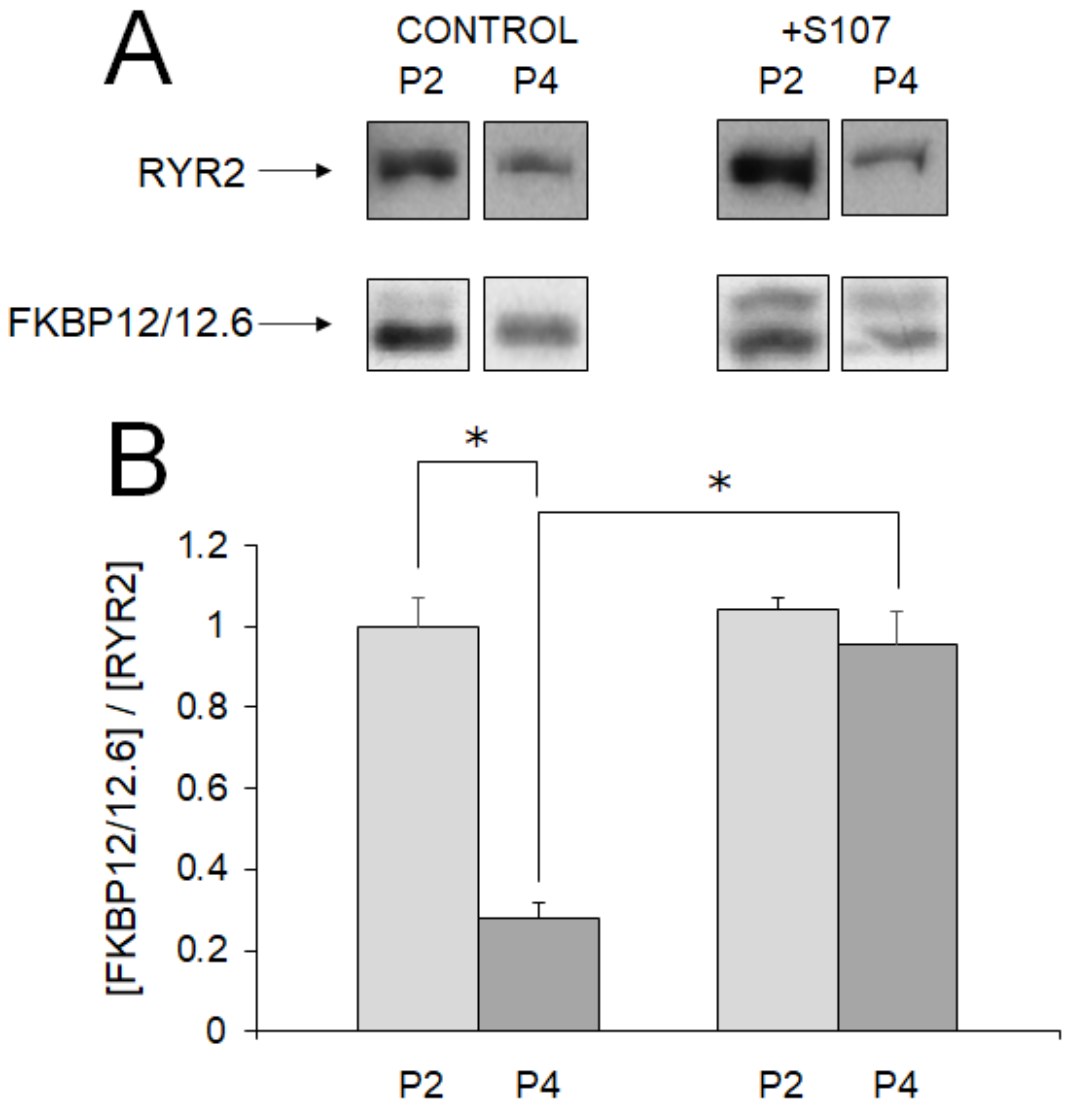

Figure 5.3: **Co-immunoprecipitation confirms that 20 μM S107 stabilises the RyR2:FKBP interaction through intermediate phase to final SR vesicle processing. A**, bands from a representative post-co-immunoprecipitation blot. RyR2 bands are presented above their matching FKBP12/12.6 bands. From left to right, lanes are: untreated P2 vesicles, untreated P4 vesicles, S107-treated P2 vesicles, and S107 treated P4 vesicles. **B**, the graph shows the average data of n=6 co-immunoprecipitation experiments, demonstrating significant retention of RyR2-associated FKBPs in the S107-treated species and significant loss of RyR2-associated FKBPs between the P2 and P4 processing stages in non-treated species. Data are presented as the ratio of FKBP12/12.6 / RyR2 densitometry measurements, normalised to the ratio in Sthe untreated P2. Asterisks indicates significant differences between columns, for a p value of <0.05.

Figure **5.4** illustrates results from experiments comparing the association of FKBP12 to skeletal muscle RyR1 at both the intermediate “P2” and final “B4” stage of vesicle processing. Results from parallel experiments conducted in the presence of S107 are presented alongside. All FKBP12 signals are relatively consistent with one another, indicating both little loss of FKBP12 from the P2 to B4 processing stages and little effect of S107 upon FKBP12 association at these processing stages. Comparing with Figure **5.2**, this would appear to indicate that the majority of FKBP12 loss from RyR1 occurs between the homogenate and P2 stages of vesicles processing, i.e. earlier than appears in this figure.

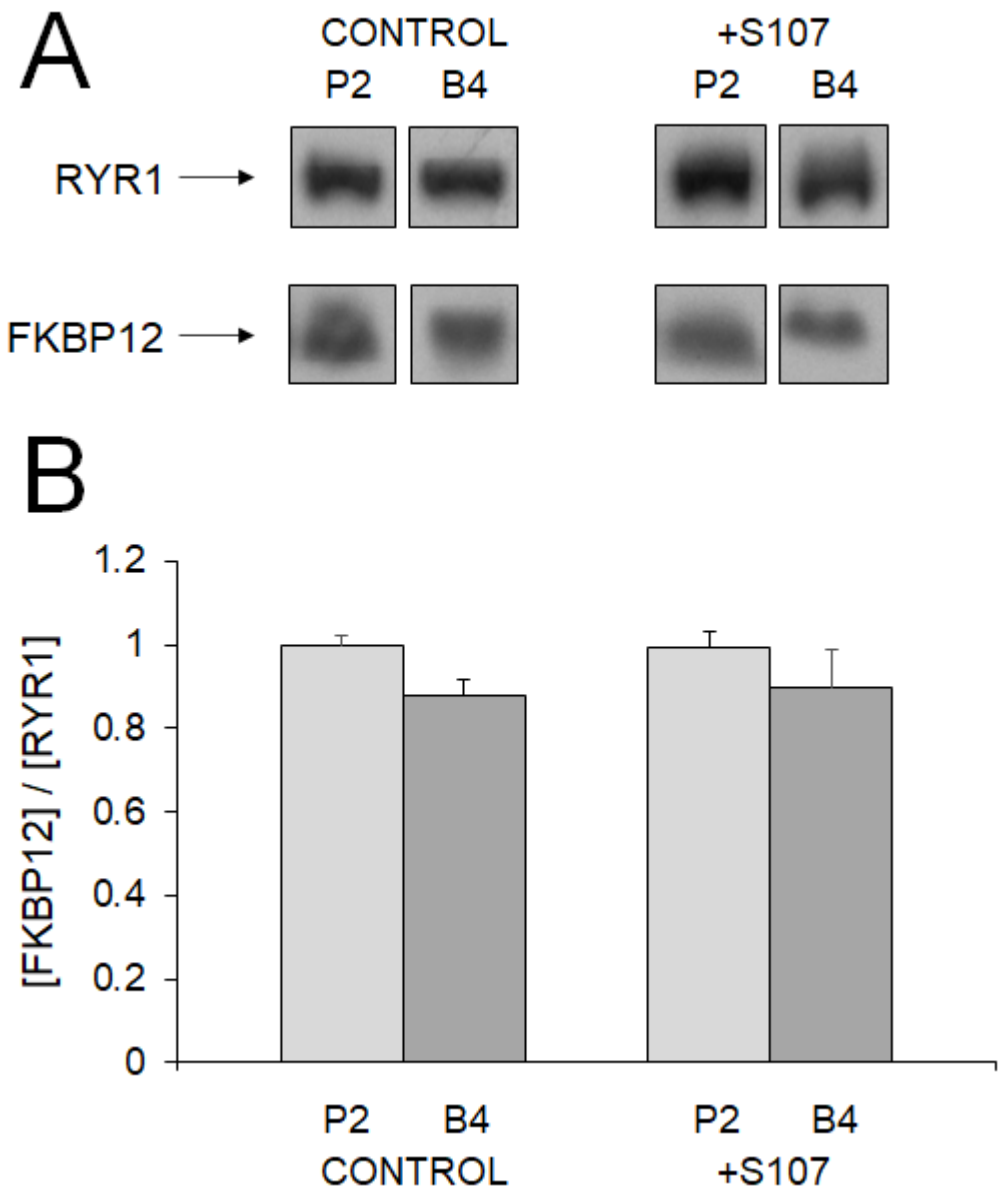

Figure 5.4: **Co-immunoprecipitation demonstrates that little FKBP is lost from RyR1 between the P2 and B4 processing phases, and that S107 therefore has little effect between these phases of processing**. **A**, bands from a representative post-co-immunoprecipitation blot. RyR1 bands are presented above their matching FKBP12 bands. From left to right, lanes are: untreated P2 vesicles, untreated B4 vesicles, S107-treated P2 vesicles, and S107 treated B4 vesicles. **B**, the graph shows the average data of n=6 co-immunoprecipitation experiments, demonstrating retention of RyR1-associated FKBPs in the S107-treated species. Data are presented as the ratio of FKBP12 / RyR1 densitometry measurements, normalised to the ratio in the untreated P2.

Figures **5.3** and **5.4** demonstrate that FKBP loss from RyR1 and RyR2 occurs at different phases in processing. For RyR2, massive, significant loss is observed between the P2 and P4 processing phases, indicating that almost all of the observed loss in Figure **5.1** occurs during the latter half of vesicle processing. By contrast, the level of FKBP associated with RyR1 remains relatively consistent between the P2 and B4 processing phases, indicating that the majority of processing loss occurs in the first half of vesicle processing. As expected, the observed degree of S107 remediation of FKBP loss in RyR1 approximately accords with the degree of S107 remediation observed in **5.3.1**, above.

While it may therefore be difficult to alter RyR1 vesicle processing protocols to remediate FKBP loss, since the first phases of vesicle processing to fractionate out homogenate material are all but essential to effective analysis of RyR1, it is possible that alteration to RyR2 vesicle protocols, or even ceasing processing at the P2 phase, may offer a means to study RyR2 with relatively endogenous levels of associated FKBP, absent the need for any drug treatment protocols. An important caveat to this observation, however, is that there may be differences in FKBP12 and FKBP12.6 association with RyR2 between the homogenate and P2 phases that are occluded by the condensation of the FKBP species in this study.

5.3.3 Homogenate saturation

As mentioned in the introduction to this Chapter, analysis of the capacity of muscle homogenates to take up additional exogenous FKBPs is interesting for a few reasons. First, excepting *in vivo* study, analysis of muscle homogenates offers the closest representation of the “endogenous” state of RyR, at least in regard to its associated regulatory FKBPs. Consequently, by conducing similar saturation experiments to those in Chapter 4, it should be possible to assess with reasonable confidence the endogenous stoichiometry of RyR:FKBP – most particularly, whether this endogenous stoichiometry is maximal, i.e. 4 FKBPs per RyR tetramer. Should homogenate RyR be capable of taking up additional exogenous FKBP, it is also then possible to “work backwards” and estimate the endogenous stoichiometry. This estimate of endogenous stoichiometries “completes the picture” for many of the analyses presented in this thesis, offering a starting point from which the processing loss experiments in **5.3.1**

and **5.3.2** may be benchmarked. That is, assuming the stoichiometry determined for RyR:FKBP in muscle homogenate reflects the endogenous stoichiometry, the RyR:FKBP stoichiometry after processing loss can be estimated. Further, by conducting the homogenate saturation experiments +/- the presence of S107, the potential issue of prevention of normal on/off associations, may be examined. That is: is it possible that S107 treatment may encourage supra-physiological binding of FKBP to RyR? This has potential significance in particular for any experiments that might use a combination of S107 and exogenous FKBPs, whether as an axis of comparison or simply as treatments prior to experimentation in order to recapitulate a physiological RyR:FKBP association.

Figures **5.5** and **5.6** summarise the results of these experiments. Figure **5.5** illustrates results from experiments comparing the amount of FKBP12 and FKBP12.6 associated with RyR2 in both raw muscle homogenates and those same homogenates after treatment with exogenous FKBP12. Parallel experiments were also conducted in the presence of S107. In both untreated and S107-treated homogenates, FKBP12/12.6 signals are significantly stronger after exposure to exogenous FKBP12. Interestingly, FKBP12 signals appear somewhat weaker in S107-treated experiments (compare the FKBP12 signals in panel A of particularly Figure **5.6**) indicating less uptake of exogenous FKBP12; the trend does not achieve significance, however.

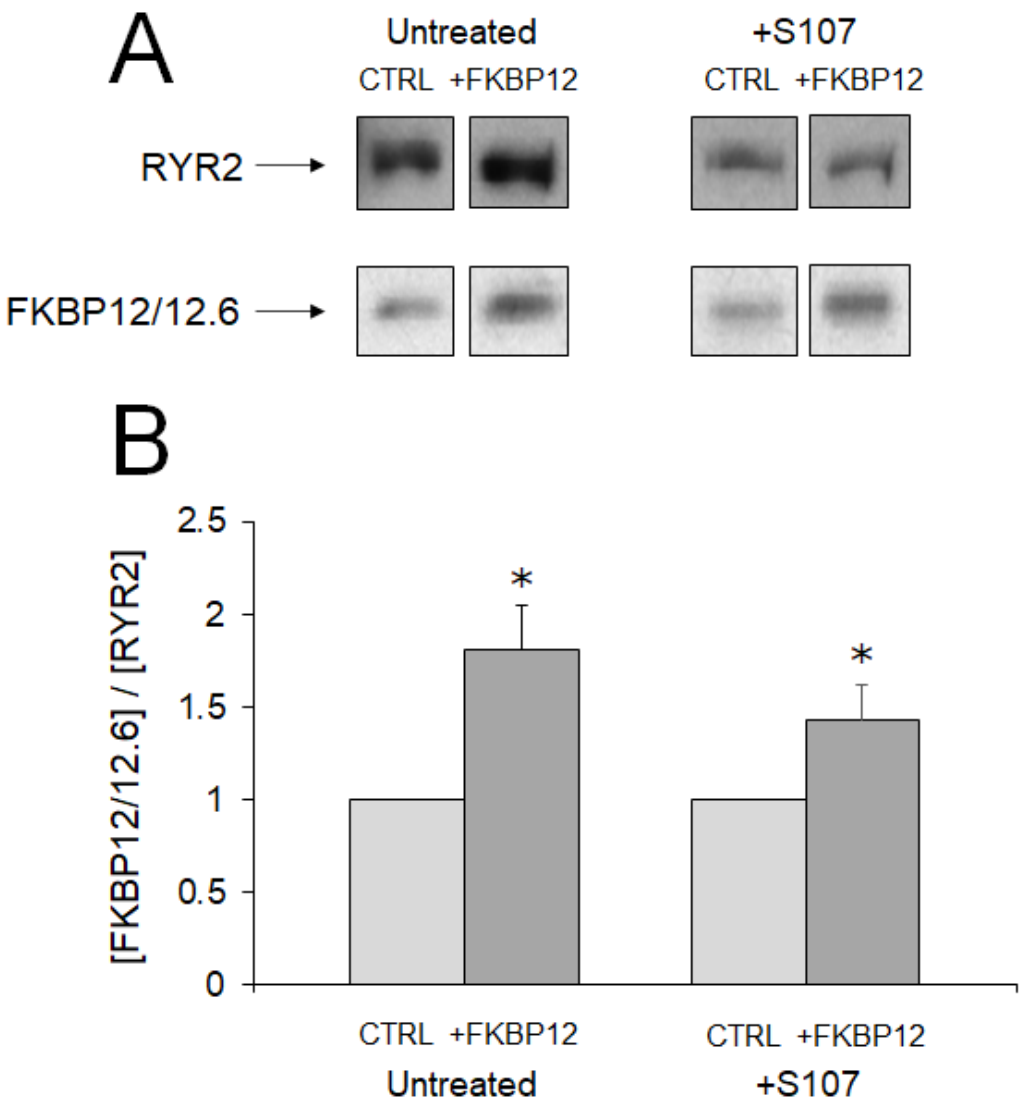

Figure 5.5: Co-immunoprecipitation demonstrates that RyR2 in muscle homogenate are able to take up significant amounts of exogenous FKBP12, indicating a likely submaximal stoichiometry between RyR2 and FKBPs *in vivo*. **A**, bands from a representative post-co-immunoprecipitation blot. RyR2 bands are presented above their matching FKBP12/12.6 bands. From left to right, lanes are: unsaturated homogenate, saturated homogenate, unsaturated S107-treated homogenate, and saturated S107-treated homogenate. **B**, the graph shows the average data of n=5 co-immunoprecipitation experiments, demonstrating uptake of exogenous FKBP12 in both the S107-treated and non-treated homogenates. Data are presented as the ratio of FKBP12/12.6 / RyR2 densitometry measurements, normalised to the ratio in the untreated homogenate. Asterisk indicates significant differences between columns, for a p value of <0.05.

Figure **5.6** illustrates results from experiments comparing the amount of FKBP12 associated with RyR1 in both raw muscle homogenates and those same homogenates after treatment with exogenous FKBP12. Parallel experiments were also conducted in the presence of S107. Only in untreated homogenates were FKBP12 signals significantly stronger after exposure to exogenous FKBP12. That is, as with the RyR2 of Figure **5.5**, S107 treatment appeared to inhibit uptake of exogenous FKBP12, this time such that any uptake was non-significant.

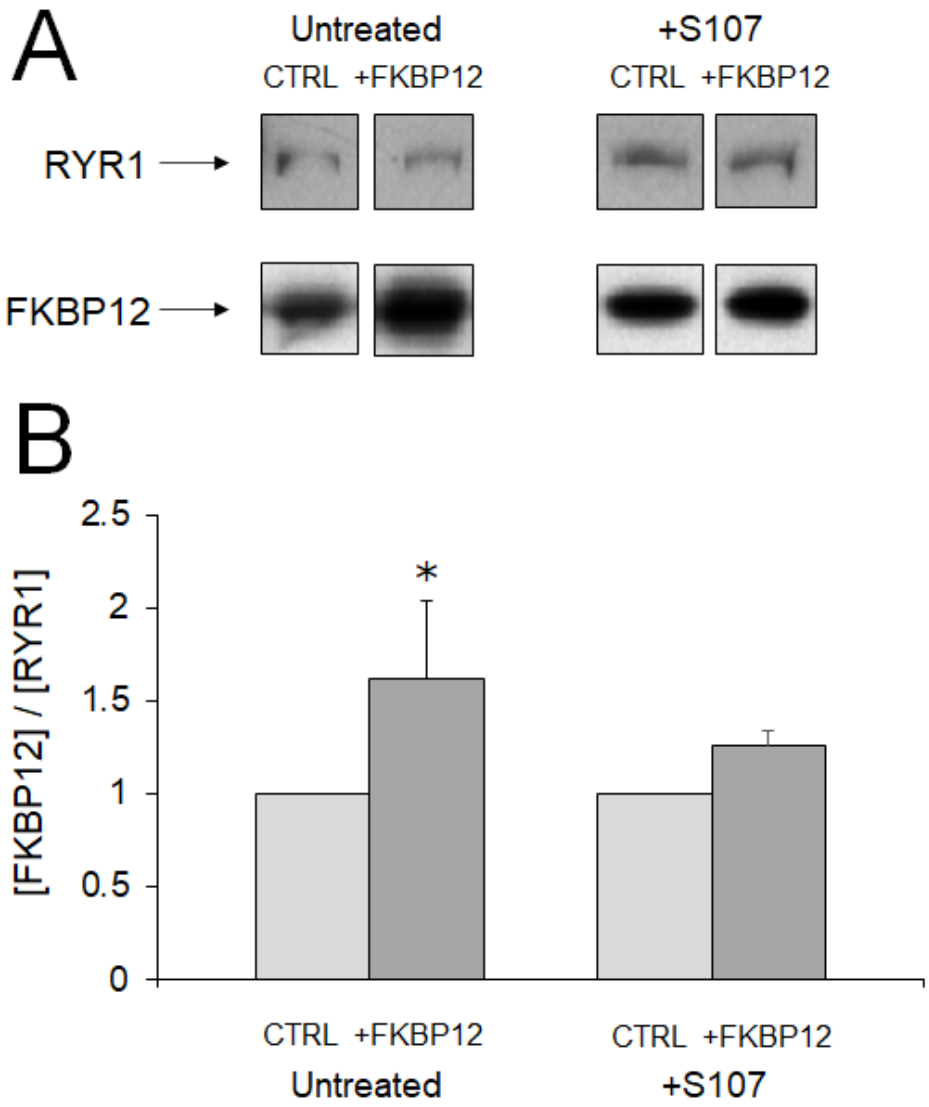

Figure 5.6: Co-immunoprecipitation demonstrates that RyR1 in muscle homogenate are able to take up significant amounts of exogenous FKBP12, indicating a likely submaximal stoichiometry between RyR1 and FKBP12 *in vivo*. **A**, bands from a representative post-co-immunoprecipitation blot. RyR1 bands are presented above their matching FKBP12 bands. From left to right, lanes are: unsaturated homogenate, saturated homogenate, unsaturated S107-treated homogenate, and saturated S107-treated homogenate. **B**, the graph shows the average data of n=5 co-immunoprecipitation experiments, demonstrating uptake of exogenous FKBP12 in both the S107-treated and non-treated homogenates. Data are presented as the ratio of FKBP12 / RyR1 densitometry measurements, normalised to the ratio in the untreated homogenate. Asterisk indicates significant differences between columns, for a p value of <0.05.

From Figures **5.5** and **5.6**, it is apparent RyR in both skeletal and cardiac homogenates were able to take up significant additional exogenous FKBP12, indicating that for both, the endogenous RyR:FKBP stoichiometry is submaximal. Specifically, it appears that the endogenous occupancy of RyR2 by FKBPs is on average ~2.2 FKBPs per RyR2 tetramer, while the endogenous occupancy of RyR1 by FKBPs is on average ~2.6 FKBPs per RyR1 tetramer. Put another way, any given RyR molecule seems likely to have bound to either 2 or 3 FKBPs, with RyR1 trending towards being more likely to have 3 FKBPs bound, and RyR2 trending towards being more likely to have 2 FKBPs bound.

Adding these data to the observations of processing loss in **5.3.1** and **5.3.2**, above, we can approximate the RyR:FKBP stoichiometry in final B4/P4 phase vesicles. RyR2 appears to bind 0.55 FKBPs per RyR in P4 vesicles, while RyR1 appears to bind 1.2 FKBPs per RyR in B4 vesicles. That is, “on average”, RyR in end phase processed vesicles will have only a single FKBP bound, with RyR2 almost as likely to have no FKBP bound at all. Given the regulatory function of FKBP, it is highly likely that such unoccupied RyR2 will then exhibit “pathological” function when examined.

Interestingly, contrary to what might have been expected, S107 treatment somewhat inhibited the uptake of exogenous FKBP12 for both RyR1 and RyR2. A possible explanation might be that when bound to certain sites in the absence of FKBPs, particularly those proximate to e.g. the SPRY2 interface that binds FKBPs, S107 acts to inhibit the binding of additional FKBPs. Alternatively, treatment with S107 may increase saturation of RyRs by endogenous FKBPs, leaving less capacity for exogenous uptake.

5.4 Discussion

The following graphs summarise the results presented in **5.3.1** and **5.3.2**. Note that this represents a concatenation of the data from two independent “sets” of experiments: the homogenate to final vesicle analysis of **5.3.1**, and the intermediate phase to final vesicle analysis of **5.3.2**. As the “common” element in both these sets of experiments are the P4 / B4 phases, the homogenate and intermediate phase data have been presented relative to an artificial “single” P4 / B4 data point, on the

assumption that the P4 / B4 results should be similar across both sets of experiments, as preparations in each case were obtained from tissues from the same sheep or rabbit.

In Figure **5.7**, the results of Figures **5.1** and **5.3** are summarised together. The average FKBP12/12.6 occupancy of RyR2 (relative to occupancy levels in the homogenate) is shown at each vesicle processing point that was examined: homogenate, P2, and P4. Results from experiments conducted in parallel in the presence of 20 μM S107 (solid line) are presented in the same figure as untreated experiments (broken line), such that the effects of S107 treatment, if any, at each stage is illustrated.

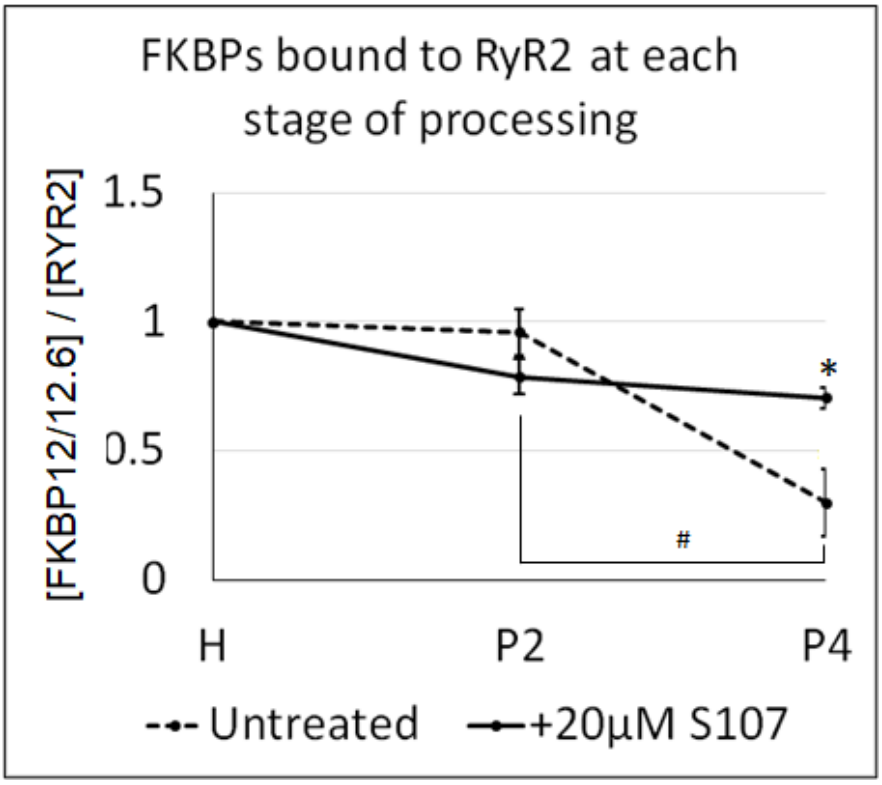

Figure 5.7: Approximately three quarters of bound FKBPs are lost from RyR2 during processing from homogenate to P4 vesicles; S107 treatment significantly, but not fully, preserves the endogenous RyR2:FKBP stoichiometry. An asterisk above a pair of processing points indicate a significant difference in FKBP association between the untreated and S107 treated preparations at that time point, while a hash in between two treatment points indicates a significant difference in FKBP association between the two processing points indicated. All p values were <0.05.

In Figure **5.8**, similarly to Figure **5.7**, the results of Figures **5.2** and **5.4** are summarised together. The average FKBP12 occupancy of RyR1 (relative to occupancy levels in the homogenate) is shown at each vesicle processing point that was examined: homogenate, P2, and B4. Results from experiments conducted in parallel in the presence of 20 μM S107 (solid line) are presented in the same figure as untreated experiments (broken line), such that the effects of S107 treatment, if any, at each stage is illustrated.

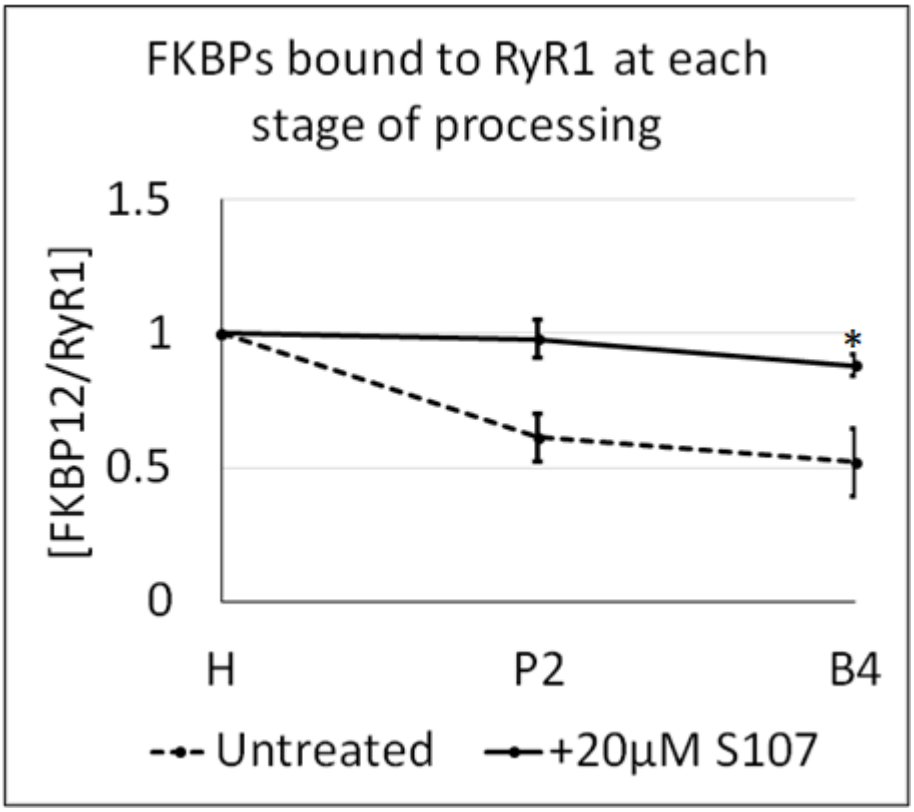

Figure 5.8: Approximately half of bound FKBPs are lost from RyR1 during processing from homogenate to B4 vesicles; S107 treatment significantly and almost fully preserves the endogenous RyR1:FKBP stoichiometry. An asterisk above a pair of processing points indicate a significant difference in FKBP association between the untreated and S107 treated preparations at that stage of preparation, for a p value of <0.05.

From Figures **5.7** and **5.8**, S107 treatment appears to be most useful in the context of RyR1 studies, where treatment from the homogenate phase should ensure B4 vesicles with essentially endogenous levels of RyR1:FKBP stoichiometry. While not

as effective in terms of treating FKBP loss from RyR2, treatment with S107 does ensure that the average occupancy of RyR2 by FKBP remains greater than one FKBP per RyR2 tetramer; that is, there should be few, if any, wholly unoccupied RyR2 in S107-treated P4 vesicles. On the assumption that wholly unoccupied RyR2 exhibit more gravely pathological behaviour than partially occupied RyR2, S107 treatment may therefore still be of use.

The finding that RyR1 and RyR2 lose associated FKBPs at different phases of vesicle processing is intriguing, although no immediate mechanism to explain this difference is apparent. Vesicle processing protocols differ slightly between RyR1 and RyR2, with RyR1 vesicles from skeletal muscle being additionally fractionated via ultracentrifugation along a sucrose density gradient (see Chapter 2). This fractionation occurs subsequent to the early phases in which most FKBP is lost from RyR1, however, so is unlikely to be a contributing factor to observed loss. The initial RyR:FKBP stoichiometries for both RyR isoforms, as determined by the homogenate saturation experiments in this Chapter, are broadly similar: 2.6 FKBPs per RyR1 tetramer as compared to 2.2 FKBPs per RyR2. Were RyR1 more fully occupied in muscle homogenates, then potentially a negative cooperativity model of RyR:FKBP binding would explain this difference in when FKBP loss occurs, with RyR1 shedding FKBPs bound with lower affinity early in processing. Given the relatively similar initial RyR:FKBP stoichiometries for both species, however, while negative cooperativity may explain some of the difference in when FKBP loss occurs, it cannot account for the degree of observed difference. Finally, a potential contributing factor to this difference in phases where FKBP loss occurs may be a difference in affinity for RyR2 for FKBP12 and FKBP12.6. As separation of these two species was not always achieved via SDS-PAGE, it is possible that a difference in when they dissociate from RyR2 has been obscured. FKBP12.6 is thought to bind RyR2 with a higher affinity than FKBP12, so loss of FKBP12.6 at later stages of processing may be logical. While FKBP12.6 has not been observed in this thesis to constitute more than approximately a third of RyR2-associated FKBPs, notably, the observations on FKBP12.6 association to RyR2 have generally been made on RyR2 from P4, that is, end-phase vesicles. As it is known (Zissimopolous, 2012) that different species may present extremely different patterns of FKBP12/12.6 association to RyR2, the potential exists that sheep RyR2 in the cytoplasm may endogenously bind primarily FKBP12.6, such

that the loss of FKBP observed in later phases of vesicle processing may be attributable at least in part to FKBP12.6 dissociation. More finely-grained analysis of RyR2-associated FKBPs in muscle homogenates may better inform an answer to this question.

The finding that the average occupancy of RyR2s by FKBPs subsequent to vesicle processing treatments is ~0.55 FKBPs per RyR2, indicating at least a sub-population of RyR2 might be completely unoccupied by FKBP, stands somewhat in opposition to the data from Chapter 3 that indicated that while complete dissociation of FKBPs from RyR1 was relatively easy to achieve, complete dissociation of FKBPs from RyR2 was not possible via drug treatment. Specifically, the calculated figure for RyR2 occupancy in P4 vesicles indicates the possibility that a subpopulation of RyR2 may be completely unoccupied by FKBP subsequent to vesicle processing. A few explanations may account for this. First, the difference between the population of RyR2 that retain a single FKBP bound and the population of RyR2 that are wholly unoccupied may be a functionally significant one. That is, there may be a physiological reason for a certain percentage of the RyR2 population to be unoccupied by FKBP, which a study like that in Chapter 3, concerned only with relative differences in occupancies, would not detect. Second, if the hypothesis developed throughout this thesis that the binding of FKBP to RyR is negatively cooperative, and the RyR2 vesicles under examination in Chapter 3 were as sparsely occupied as the results from this Chapter suggest, then it makes sense that dissociative treatments would have much less efficacy than in a more fully occupied species.

Finally, contra to the expectation that S107 treatment of muscle homogenates may result in “overstabilisation” of the RyR:FKBP relationship, there appears to be a notable trend towards S107 treatment reducing the binding capacity of muscle homogenate RyR for exogenous FKBP. A possible explanation for this may be that S107 binding to RyR when FKBP are already bound stabilises this relationship by obstructing FKBP dissociation, but if S107 binds proximate to an unoccupied FKBP binding site, then it similarly obstructs association of free FKBP. Alternatively, S107 treatment may increase the saturation of RyR by endogenous FKBPs, leaving less capacity for binding exogenous FKBP12. Should either of these reasons pertain, it would appear to be inappropriate to use S107-treated samples to assess the endogenous occupancy of RyR by FKBPs via saturation methods such as were

employed in Chapter 4, particularly as the finding of S107 reducing FKBP12 binding capacity is seen even in the homogenate preparations of **5.3.3**.

5.5 Conclusions

Vesicle processing is responsible for a proportion of the submaximal occupancy of RyR by FKBP observed in Chapter 4. Specifically, between homogenate and final vesicle processing phases, RyR1 loses 52±13% of its associated FKBP, while RyR2 loses approximately 72±4% of its associated FKBP. Interestingly, this loss occurs at different stages for each isoform, with the majority of loss from RyR1 occurring in early vesicle processing, while the majority of loss from RyR2 occurs in the final stages of vesicle processing.

S107 has a stabilising effect on this observed loss, ameliorating a significant degree of FKBP dissociation for both RyR isoforms, although with much more efficacy in RyR1, where S107 treatment almost entirely rescued the loss associated with vesicle processing.

Homogenate saturation experiments provide an estimate for the endogenous occupancy of both RyR1 and RyR2 by FKBP:RyR1 in muscle homogenate has ~2.6 FKBPs per RyR1 tetramer, while RyR2 in muscle homogenate has ~2.2 FKBPs per RyR2 tetramer. This calculation enables further elucidation of the impact of vesicle processing on RyR. From these starting stoichiometries, by the final stage of vesicle processing, RyR1 binds ~1.2 FKBPs per RyR1 tetramer, while RyR2 binds ~0.55 FKBPs per RyR2 tetramer. This low occupancy, with the RyR2 data in particular indicating that a substantial fraction of processed RyR2 is wholly unoccupied by FKBP, has considerable significance for physiological studies of RyR that rely upon processed vesicles. Curiously, S107 treatment appeared to reduce the amount of exogenous FKBP that homogenate RyR was able to take up, rather than cause any kind of “overstabilisation” phenomena.

Chapter 6: Discussion

The experiments comprising this thesis were intended to explore the association between FKBP and RyR in isolated preparations and to address some of the controversy attending the regulation of RyR by FKBP; in this attempt, a number of interesting aspects of the RyR:FKBP relationship have been uncovered. These aspects will be explored in the following discussion, with the overall aim of better understanding the RyR:FKBP relationship, as well as providing support for future investigations of the nature of the RyR:FKBP relationship.

First, the findings in the three results chapters will be summarised, and the key implications and recommendations arising from these findings laid out. Adjunct to this summary, the experiments from those chapters will be critically examined for any limitations which might be addressed in future work. Next, and most importantly, a particularly intriguing observation arising from the experimental chapters will be explored in greater depth: that is, the possibility of a negatively cooperative model of binding between RyR and FKBP. This exploration will encompass some additional data not included in the three experimental chapters which, although preliminary, provides intriguing support for the negative cooperativity model. Finally, some future directions for study of the RyR:FKBP interaction will be proposed, drawing on both the present state of the field as summarised in the introductory chapter and the findings of the results chapters.

In each of the three results chapters a specific aspect of the RyR:FKBP relationship has been examined. In Chapter 3, the effect of various methods of dissociating FKBP from RyR was examined; in Chapter 4, the effects of introducing supraphysiological concentrations of FKBP to RyR-rich SR vesicles was studied; and in Chapter 5, the focus was on the loss of FKBP from RyR during vesicle processing, and the potential for ameliorating this loss with the FKBP-stabilising drug S107.

6.1 Effects of FKBP-dissociating treatments on FKBP dissociation from RyR

In the investigation of the effects of different FKBP-dissociating treatments on FKBP dissociation from RyR reported in Chapter 3, some intriguing differences in the nature of the association between FKBP with the RyR1 and RyR2 isoforms was observed.

6.1.1 Treatment with immunosuppressive drugs

Most surprisingly, treatment with the immunosuppressant drugs FK506 and rapamycin, which have extremely high affinity for the FKBP12 and FKBP12.6, appeared highly effective at dissociating FKBP12 from RyR1, but had no significant effect at all upon FKBP12 associated with RyR2. This result indicates an interesting difference in the nature of the association between FKBP12 to RyR1 and RyR2. A number of explanations might account for this difference: perhaps most obviously, a structural difference in the binding pocket for FKBP12 between RyR1 and RyR2 would make sense. That is, the conformation of FKBP12 bound to RyR2 being such that its binding regions are unable to be accessed by the immunosuppressant drugs. Such an absolute mechanism would appear to be contradicted by other data from results reported in the chapter: in particular, the observation that a proportion of FKBP12 readily dissociates from RyR2 without the need for any specific dissociating treatment. If the RyR2 FKBP binding pocket is indeed somewhat occluded such that immunosuppressants are unable to access the FKBP and force it into a non-binding conformation, it seems possible that this occlusion would also block free dissociation of FKBPs from RyR2. Other possible explanations might be that the immunosuppressant drugs are somehow sequestered in the RyR2 experiments: perhaps there exists for the drugs a coincidental affinity to some motif on the RyR2 surface, in binding to which the drugs are unable to act upon FKBP12. Again, however, this would appear not to be a satisfactory explanation, as an effect of at least rapamycin was observed on FKBP12.6, although not FKBP12, which would not be expected were the drugs to be bound elsewhere. An explanation might perhaps lie in the *nature* of the binding of FKBP12 to RyR2: that for whatever reason, the population of FKBP12 amenable to removal by immunosuppressant drugs in RyR1 is, in RyR2, bound with considerably greater affinity. While the literature on the affinity of FKBP12

to RyR1 and RyR2 would appear to indicate a similar affinity for both isoforms (see chapter **1.4.4**), the possibility of a complex mode of affinity, such as a negatively cooperative relationship between RyR and FKBP12, might account for the observed difference. For this hypothesis to hold, it would have to be assumed that the population of RyR2 under examination had less FKBP12 initially bound than did the population of RyR1, such that the remaining population of FKBP12 bound to RyR2 was commensurately more resistant to dissociation. Interestingly, the experiments of Chapter 4, summarised below, seem to indicate that this may in the fact be the case.

Several further aspects of the drug treatment experiments are notable. While the immunosuppressant drugs were highly effective at stripping FKBP12 from RyR1, in no experiments was the removal completely effective – that is, a small portion of FKBP12 remained bound to RyR1 regardless of treatment. This was the first data indicating that perhaps a small population of FKBP bound to RyR1 with a higher affinity than the bulk of the bound FKBP, and so, the first data indicating that the affinity of FKBP association to RyR might have a more complex mode. Further data supporting this possibility arose from the examination of the supernatants of these experiments – that is, the discarded non RyR-containing proportion of the various incubations. Even in the control experiments, where RyR were simply incubated with buffer, a degree of non drug-induced FKBP dissociation was observed. In other words, a population of FKBP appeared to bind only very loosely to RyR, such that gentle agitation in the presence of buffer was sufficient to induce dissociation. These dissociation experiments, therefore, appeared to indicate at least three “populations” of FKBP were bound to RyR, with varying affinities: a population which readily dissociated, a population which dissociated (at least from RyR1) upon exposure to immunosuppressant drugs, and a population which resisted dissociation even after drug treatment. The implications of these varying populations will be explored later in the chapter, in the discussion of a negative cooperativity model for FKBP binding to RyR.

The drug treatment experiments revealed an additional notable difference between the FKBP isoforms under examination. As alluded to above, rapamycin treatment appeared to effectively dissociate more than half the associated FKBP12.6 from RyR2, while not having any particular effect on the FKBP12 associated with RyR2. This is puzzling for a number of reasons. For one, FK506 (as opposed to rapamycin)

treatment appeared to have no effect on FKBP12.6 associated with RyR2, where it would be supposed that the two immunosuppressant drugs would have identical impacts on bound FKBPs, having both highly analogous structures and highly similar affinities for FKBPs. Another puzzle emerging from this finding is that FKBP12.6 has been widely reported as having a greater affinity for RyR2 than FKBP12 – in some reports, such as Guo (2010), at least two orders of magnitude greater – such that it might be expected that if any FKBP species were to be dissociated from RyR2, it would be FKBP12; in Guo (2010), this is justified by a hypothesis that intracellular [FKBP12.6] is likely extremely low in the rat myocytes examined, explaining the very low occupancy of RyR2 by FKBP12.6 that was observed. It is difficult to account for this data except by assuming that FKBP12.6 and rapamycin share an unusually high affinity, greater than the affinity of FKBP12 for rapamycin, and greater than the affinity of FKBP12.6 for FK506. Additionally, the caveat remains that different species appear to bind different ratios of FKBP12 and FKBP12.6 to RyR2 (Zissimopolous, 2012), presumably consequent to either different affinities for FKBP12 and FKBP12.6 for the RyR2, different levels of expression of FKBP12 and FKBP12.6 in the heart, or a combination of both factors. Consequently, affinity experiments conducted in rat or mouse myocytes, such as those of Guo (2010), may not be generalised to RyR2:FKBP12/12.6 systems as present in the sheep myocytes used in this thesis. Notably, in the experiments of Chapter 3, the removal of FKBP12.6 was not observed to be complete, with only approximately 2/3rds of the population of bound FKBP12.6 being dissociated by rapamycin. This would agree with a hypothesis that the special affinity of FKBP12.6 for rapamycin is only incrementally greater than FKBP12.6's affinity for FK506, perhaps only sufficient to overcome the affinity of FKBP12.6 for RyR2 in a subset of the populations under examination. In other words, while FKBP12.6 might have a higher affinity for rapamycin than for FK506, it is unlikely to be orders of magnitude greater. Nevertheless, this unusual and counterintuitive difference in behaviour between FKBP isoforms warrants further investigation.

6.1.2 Effects of high ionic strength on FKBP association with RyR

Aside from the immunosuppressant drugs, high concentrations of NaCl were also examined for efficacy in dissociating FKBP from RyR, as some reports (e.g. Galfré,

2012) have indicated this as a useful means for achieving “stripped” RyR. However, no dissociation was observed here, at least at the concentrations examined. A further experiment was performed, which, although not repeated sufficiently to achieve statistical significance, indicated that KCl – more commonly used in the preparation of SR vesicles than NaCl – had no more efficacy than NaCl in achieving stripped RyR.

In some respects, these findings that high ionic strength have little to no efficacy in dissociating FKBP from RyR may come as a relief, as many protocols for the preparation of RyR-rich SR vesicles include relatively high salt concentrations relatively early in vesicle processing. If high ionic strength did indeed induce FKBP dissociation from RyR, the vast majority of such vesicles might be expected to be stripped, thereby abstracting the RyR in such vesicles further from physiological reality, at least in terms of their regulation by FKBP.

6.1.3 Effects of solubilisation of SR vesicles on FKBP association with RyR

Finally, another common protocol for treating RyR-rich SR vesicles was examined for efficacy as a FKBP-stripping protocol: solubilisation. As vesicles are inherently hydrophobic and resist easy dispersal into solutions, solubilisation protocols employing some combination of mechanical force and detergent treatment are commonly used when solution-mobility of RyR is required for a given experiment. Somewhat surprisingly, solubilisation appeared highly effective at dissociating FKBPs from both RyR1 and RyR2, with both isoforms appearing largely free of bound FKBPs after treatment, although as in previous dissociation experiments, a small population of FKBP12 remained bound to both RyR isoforms post-solubilisation. This finding is something of a double-edged sword. While this solubilisation protocol is useful for experiments requiring specifically FKBP-stripped soluble RyR, for experiments just requiring soluble RyR with no particular concern as to whether or not FKBP is bound, it is important to note that the solubilised RyR are not being regulated by FKBP association as they might in normal physiology.

6.2 Re-introduction of exogenous FKBP to RyR in SR vesicles

In Chapter 4, the RyR:FKBP relationship in the specific context of SR vesicles was further explored via the reintroduction of exogenous FKBP12 to the SR vesicles. This followed from the observations made in Chapter 3, particularly the observation that FKBP were passively lost from RyR under even mild control conditions. This raised the possibility that the behaviour of RyR in SR vesicles might be non-physiological in terms of FKBP regulation.

6.2.1 RyR saturation with exogenous FKBP

Experiments were therefore designed to probe the occupancy of RyR in SR vesicles by FKBP, with saturating concentrations of FKBP12 incubated with both RyR1 and RyR2-containing SR vesicles. The initial goal of these experiments was to determine whether “normal” FKBP occupancy might be restored by such an incubation; the question of whether full FKBP occupancy in fact represents the “normal” level of FKBP occupancy will be further explored later in this chapter.

The saturation experiments confirmed that indeed, both RyR1 and RyR2 as present in SR vesicles are not fully occupied by FKBPs, with RyR2 somewhat less occupied than RyR1. This finding reinforces the hypothesis, above, that RyR2’s resistance to the FKBP12-dissociating treatments of Chapter 3 may be consequent to the large part of remaining FKBP12 bound to RyR2 being bound at the highest affinity “state” of a negatively cooperative binding system. Regardless, it is important to note that this observation of incomplete occupancy of SR vesicle RyR is not necessarily evidence of FKBP being “lost” from RyR: it is unknown whether RyR are physiologically fully occupied by FKBP, or whether perhaps the partial occupancy of RyR might in fact perform some useful regulatory function, such that partially occupied SR vesicles represent a “snapshot” of RyR occupancy at some particular point in the on/off association of FKBP to RyR. This point of ambiguity led directly to the experiments of Chapter 5, which are discussed further below.

6.2.2 Distinguishing exogenous and endogenous FKBP via GST-FKBP12

In order to distinguish endogenous from exogenous FKBP in the experiments of Chapter 4, the exogenous FKBP were in this case expressed with a GST tag. This is a very common technique in studies of FKBPs, with many papers both in the field of muscle physiology and elsewhere (e.g. Bultynck, 2002; Cheung, 2020) using FKBP thus tagged. It was useful, therefore, to devote some time to examining the properties of this recombinant molecule.

The key finding of these investigations was that indeed, the vast majority of GST-FKBP12 exists as a dimer at experimental concentrations. This is a significant factor if binding to another protein is to be assessed by immunodetection of FKBP12, because any such detections will return roughly double the expected signal, due to bound GST-FKBP12s necessarily carrying with them an extra, “free” FKBP12. This is not particularly surprising, given that GST naturally exists as a dimer.

FKBP12 itself, cleaved from the GST tag, was also assessed for dimerisation, which had been reported previously in the literature under certain conditions (Schories, 2007), but is not commonly observed. It was found that FKBP12 dimerisation occurred only at concentrations greater than 100 µM, which are unlikely to be found in most experiments. Nevertheless, this has significant ramifications for experiments such as those which monitor reaction energies based on a titration of FKBP12, such as isothermal titration calorimetry experiments: if titration curves extend to concentrations of 100 µM and above, it is very likely that observed reaction energies will be half of what might otherwise be expected. In conjunction with this finding of dimerisation of FKBP12 at high concentrations, it was observed that GST-FKBP12 begins to unpredictably polymerise at unphysiological concentrations above 100 µM, consequent to both halves of the fusion protein independently dimerising, with octomers being the most common polymer observed. This obviously constitutes a strong recommendation against using high concentrations of GST-FKBP12 in experiments.

6.2.3 Displacement of endogenous FKBP12 by exogenous FKBP12

As mentioned above, exogenous GST-tagged FKBP12 was easily distinguished from endogenous FKBP12, being considerably more massive. This enabled an assessment of the degree to which exogenous FKBP12 might displace endogenous FKBP, offering an interesting insight in the physiological dynamism of the RyR:FKBP relationship.

Both RyR1 and RyR2-associated endogenous FKBPs were substantially displaced by exogenous GST-FKBP12, with RyR2-associated FKBPs somewhat more easily replaced by GST-FKBP12. This stands in interesting contrast to the dissociation experiments of Chapter 3, wherein RyR2-associated FKBP was largely resistant to dissociation, while RyR1-associated FKBP readily dissociated upon exposure to the immunosuppressant treatments. Again, however, a certain portion of endogenous FKBP remained resistant to displacement, further supporting the notion that a population of FKBP remains bound to the RyR with very high affinity, resisting both drug-induced dissociation and displacement by exogenous FKBP species.

Nevertheless, the relative ease with which FKBP endogenously bound to RyR2 was displaced suggests another possible mechanism for achieving “stripped” RyR2 channels, largely free of associated FKBP. RyR2 would need to be incubated with tagged FKBP12, as in the experiments of Chapter 4, such that the majority of endogenously bound FKBP are replaced by exogenous tagged FKBP12. Once replaced, the tagged FKBP12 could then be more easily removed by exploiting the affinity of the FKBP12 tag for glutathione in the case of a GST tag, or imidazole in the case of a polyHis tag.

6.3 Effects of vesicle processing on FKBP occupancy

Finally, in Chapter 5, the question raised in Chapter 4 of whether the incomplete occupancy of SR vesicle RyR was an artifact of vesicle processing was further explored. This possibility of processing-induced loss was also plausible in light of the non drug-induced dissociation of FKBP from RyR described in Chapter 3, as the conditions in SR vesicle processing in terms of buffer composition, agitation, and centrifugation etc. in Chapter 5 were identical to the control conditions of Chapter 3.

6.3.1 Vesicle processing induced dissociation of FKBP

Vesicle processing was observed to indeed account for some – although not all – of the submaximal FKBP occupancy of RyR described in Chapter 4. Between the raw muscle homogenate and final vesicle processing phases, RyR1 lost approximately 50% of its associated FKBP12, while RyR2 lost approximately 75% of its associated FKBPs. This loss occurred at different stages for each isoform, with most of the loss from RyR1 occurring very soon after vesicle processing began, while the majority of the loss from RyR2 occurred in the final stages of vesicle processing. A conclusion arising from this is that where “intermediate”, or “P2” stage, cardiac SR vesicles (see Chapter 2) are useable for experiments, these are likely to have a considerably more preserved FKBP-regulatory environment than the equivalent final stage, or P4 vesicles. Naturally, the P2 vesicles are considerably less “pure”, in terms of containing assorted other non-SR microsomal vesicles and additional proteins, and so will not be appropriate for all experiments, although arguably this complexity of proteome might represent a closer picture of the physiological environment of the RyR2.

6.3.2 S107 stabilisation of FKBP loss from RyR during vesicle processing

S107 was observed to stabilize this processing loss of FKBP somewhat from both RyR isoforms. The efficacy of this stabilisation was much greater in RyR1, where S107 treatment almost entirely rescued processing loss of FKBP12. This raises the possibility of S107 incubation as a useful adjunct in the generation of skeletal muscle SR vesicles. Such incubation would be of most use in investigations of RyR1 function that do not involve manipulation of the bound FKBP12, as it is likely that the stabilising S107 molecules will interfere with any dynamic association or dissociation of FKBP12. While a “wash-out” protocol may have some efficacy in removing S107, it is unknown whether the removal of S107 would result in further dissociation of FKBP12 from RyR1: this question will be explored further below, in the discussion about future experimental directions.

6.3.3 Saturation of muscle homogenates with exogenous FKBP

The observation that loss from vesicle processing did not fully account for the degree of submaximal FKBP occupancy seen from the experiments of Chapter 4 raised the possibility that perhaps RyR were endogenously submaximally occupied by FKBP. To investigate this possibility, saturation experiments, similar to those of Chapter 4, were conducted on the raw muscle homogenates of both the cardiac and skeletal muscle tissues from which vesicles were generated.

Working backwards from the fully saturated state of these homogenates, it was found that RyR1 in muscle homogenate has ~2.6 FKBPs per RyR1 tetramer, while RyR2 in muscle homogenate has ~2.2 FKBPs per RyR2 tetramer, although this difference between the two isoforms was not statistically significant. Combining these calculations with the data from the processing loss experiments, it was found by the final stage of vesicle processing, RyR1 binds ~1.2 FKBPs per RyR1 tetramer, while RyR2 binds ~0.55 FKBPs per RyR2 tetramer. This low occupancy, with the RyR2 data in particular indicating that a substantial fraction of processed RyR2 are wholly unoccupied by FKBP, has considerable significance for physiological studies of RyR that rely upon processed vesicles. Interestingly, this low occupancy for RyR2 provides some support for the hypothesis first outlined in Chapter 3, that the resistance of RyR2-associated FKBP to drug-induced dissociation might be consequent to a negative cooperativity. This model would hold that the final FKBP bound to a RyR would adhere with the highest affinity. For the RyR1 populations, the data would indicate that at least a certain number of RyR were occupied by two or more FKBPs when drug treatments were applied, with the FKBPs in these “second” or “third” occupancies therefore amenable to removal. This hypothesis will be discussed further below.

6.3.4 Saturation of muscle homogenates with exogenous FKBP and additional S107

The homogenate saturation experiments were also carried out in the presence of S107, on the assumption that perhaps the drug could increase uptake of FKBP12 and ensure maximal saturation of the RyRs. Curiously, however, S107 treatment appeared to reduce the amount of exogenous FKBP that homogenate RyRs were able to take

up. This is something of a confounding observation: one possible explanation might be that binding S107 before exogenous FKBPs are introduced actually obstructs somewhat the binding surface on the RyR. That is, S107 acts something like a “deadbolt”, securing already bound FKBPs, while preventing the binding of additional FKBPs.

An assumption made throughout this discussion of endogenous occupancy based on the occupancy state of raw muscle homogenates is that the homogenates represent an accurate picture of the endogenous state of the RyRs, having been only minimally processed from the source muscle tissue. While this assumption is fair to make, based on the minimal treatment steps between harvesting of muscle tissue and preparation of muscle homogenates, only in-cell experiments are capable of answering the question of endogenous occupancy states definitively. Several such potential experiments will be explored below, in the discussion about future experimental directions.

6.3.5 Limitations of Chapter 5 experiments

Finally, it is worth noting an unfortunate limitation of the experiments described in Chapter 5: distinction between FKBP12 and FKBP12.6 in cardiac preps was not always possible, in contrast to experiments described in Chapter 3. Relatively often in the experiments of Chapter 5, only a single band appeared in analysis of FKBPs associated with RyR2, possibly due to FKBP12 and FKBP12.6 migrating on SDS-PAGE closely together, and therefore being unable to be distinguished from one another. It is unclear why this was particularly the case for the experiments of Chapter 5, although a hypothesis might be that residual membranous material from muscle lysates slightly inhibited electrophoretic migration of the FKBP, enough that they were unable to be clearly separated; the experiments of Chapter 3, by contrast, were conducted entirely with fully processed vesicles, such that contamination of samples by membranous material was considerably less likely. Indeed, at least a proportion of the RyR2 examined in Chapter 5 showed a clear distinction between associated FKBP12 and FKBP12.6, and as SDS-PAGE running conditions and gel composition were identical between experiments, it is unusual that the proteins may have migrated differently from experiment to experiment. Another possibility is simply that certain of

the RyR2-rich SR vesicles under examination had very low levels of FKBP12.6 associated, such that the amount of associated FKBP12.6 fell below Western blot detection thresholds. As the samples in both Chapters 3 and 5 were drawn from a number of different animals, it is possible that a significant degree of intra-species variability in FKBP12.6 expression exists, just as does inter-species variability (Zissimopolous, 2012). In either case, results in Chapter 5 were therefore expressed in terms of "total FKBP" rather than in terms of each FKBP species individually. This may possibly have occluded some interesting data regarding the comparative rates of loss of FKBP12 and FKBP12.6 from RyR2 during vesicle processing: this gap in analysis therefore represents a limitation that may be improved upon in future studies.

6.4 Negative cooperation between RyRs and FKBPs

"Cooperativity" in the context of biomolecule association refers to the phenomena where 1) a first species of molecule may bind multiple of a second species of molecule, and 2) where an initial binding event alters the affinity of the first species for the second species in some way. If the affinity is altered such that an initial binding event makes further binding more likely, the relationship between the two species is considered "positively cooperative", as in the classic experiments of Bohr which characterised the first known cooperative relationship, that of haemoglobin for oxygen (Bohr, 1904). If, however, the affinity is altered such that an initial binding event makes further binding less likely, then the relationship between the two species is considered "negatively cooperative". Negative cooperativity is somewhat rarer than positive cooperativity, and is most commonly found in enzymes with multiple substrate-binding surfaces.

This section of the Discussion describes a potential negatively cooperative relationship between the RyRs and the FKBPs. First, cooperation in human ion channels is briefly reviewed. Next, evidence from the previous Results chapters which points towards a negatively cooperative relationship between the RyRs and FKBPs is summarised. Data presented in the Results chapters as well as preliminary microscale thermophoresis experiments which provide support for negative cooperation are then discussed. Following presentation of the microscale thermophoresis experiments and a summary of the data from the Results chapters, a potential model for RyR:FKBP cooperativity is presented, along with some discussion of how such models are

generated. Finally, this proposed model of RyR:FKBP negative cooperativity will be considered in the context of evidence from other papers which would appear contradictory.

6.4.1 Cooperativity in ion channels

Cooperative binding is a well-characterised phenomena in ion channels, particularly those with homomeric “lobe” structures. As early as 1967, before any structural detail was known, it was suggested that nicotinic acetylcholine receptors might bind their endogenous ligand acetylcholine cooperatively (Karlin, 1967). Purification and characterisation of the protein complex revealed a pentameric “lobed” structure with likely acetylcholine binding sites in the clefts between these lobes (Changeux, 1970). This model was eventually confirmed when the structure of the nicotinic acetylcholine receptor was solved (Brejc, 2001). The case of nicotinic acetylcholine receptors demonstrates that a tentative characterisation of cooperativity in ion channels may proceed from relatively little information, even in the absence of structural data.

Turning to an example more directly relevant to the ryanodine receptors, inositol 1,4,5-trisphosphate receptors (IP3R) have been characterised as binding their endogenous ligand in a cooperative fashion. The IP3R are a family of ion channels with significant structural and functional similarities to the RyRs – see part **1.3** of the Introduction. Briefly, both IP3R and RyR control intracellular Ca^{2+} release, with RyR highly concentrated in muscle and neurons and IP3R expressed ubiquitously, including in muscle tissue, where they may act synergistically with RyR. Notably, IP3R and RyR are both homotetramers, although IP3R heterotetramers comprising subunits from multiple IP3R types have been observed to form spontaneously in complex lysates, and may even be present endogenously (Chandrasekhar, 2016). The most striking difference between the two families of ion channels is that RyR present a massive cytoplasmic surface which is capable of binding multiple regulatory proteins, such as calmodulin or FKBP, while the IP3R cytoplasmic surface is comparatively modest.

As well as Ca^{2+}, IP3R are agonised by IP3: that is, inositol 1,4,5-trisphosphate. The binding of IP3 to IP3R was first hypothesised as highly cooperative in 1988 by Meyer et al., where it was also found that at least three IP3 molecules needed to bind the

IP3R tetramer before it was able to open and release Ca^{2+}. Notably though, it was recognised in the field that since IP3 agonism caused an efflux of Ca^{2+}, itself an agonist of IP3R, it was difficult to distinguish IP3-associated positive cooperativity from the Ca^{2+} agonism that IP3 binding induced. Later experiments examining the response of the IP3R to IP3 in the absence of Ca^{2+} appeared to confirm a positively cooperative relationship between the channel and its ligand, as well as indicating that in the absence of Ca^{2+}, the IP3R channels took a considerable amount of time (~35ms) to open, even in the presence of supersaturating concentrations of IP3 (Marchant & Taylor, 1997). This led to the development of a model wherein Ca^{2+} agonism acts to hasten IP3-induced channel opening, with each IP3 binding event exposing a Ca^{2+} binding site which enhances the speed of the conformational change required to efflux stored Ca^{2+}.

Given the similarity in physiological role between the IP3R and RyR it is plausible that they might have similar capacities for cooperative modes of regulation. Notably, however, what is proposed for the RyRs is a mechanism of control and stabilisation for an inherently unstable and “leaky” channel, whereas for IP3R, IP3 binding acts to stimulate and open an inherently very “stable” channel which seldom spontaneously opens in the absence of agonists. That is, a negative cooperativity model of FKBP association stabilising and coordinating the RyR subunit actions would be essentially the inverse of the observed relationship between IP3R and IP3. Such a model of the FKBPs as “free” ligands which spontaneously associate and dissociate from the RyR as a regulatory mechanism is supported somewhat by the observations that the total cytoplasmic concentration of FKBP12 (together with FKBP12.6 in the relevant tissues) is somewhat higher than is required to fully saturate all available RyR binding sites (Guo, 2010). In the absence of a negatively cooperative binding mechanism between FKBPs and RyRs, it would be expected that RyRs would always be saturated with FKBPs, which the homogenate saturation experiments of Chapter 5 argue against (see **5.5**).

6.4.2 Evidence for negative cooperativity from the Results chapters

In each Results chapter so far there have been data which support a negatively cooperative model of binding between RyRs and FKBPs.

In Chapter 3, the effects of various FKBP-dissociative treatments were examined. Both RyR1 and RyR2 exhibited a degree of “passive” FKBP12 dissociation even in the absence of any experimental dissociative treatments, however, as was apparent from examining the supernatants of experiments conducted as controls for the dissociation procedures. This would appear to indicate a population of FKBP12 bound to the RyRs with a relatively low affinity, such that they dissociated spontaneously during incubation in a neutral buffer. Conversely, while certain dissociative treatments had strong efficacy in removing FKBPs from RyRs (for example, both rapamycin and FK506 were highly effective at removing FKBP12 from RyR1) in no experiments was complete dissociation of FKBPs achieved, indicating another population of FKBPs bound to the RyRs with an unusually high affinity. From Chapter 3, then, there appeared to be three populations of RyR-binding FKBP12/12.6s: a population which bound with low affinity, able to be “washed” off; a population which bound securely, but was able to be displaced by e.g. rapamycin; and a population which resisted dissociative treatments. Given that there is only one recognised binding site for FKBPs per RyR monomer (see **1.4.3**), a parsimonious explanation for these three different populations would be a negatively cooperative relationship between the RyRs and FKBPs.

In Chapter 4 the effect of saturating SR vesicle RyRs with exogenous FKBP12 was explored. These experiments provided something of a corollary to the evidence for negative cooperativity from Chapter 3. Retaining the GST tag on expressed FKBP12 made it possible to distinguish from endogenous FKBPs, and therefore to assess the degree to which exogenous FKBP12 was able to displace bound endogenous FKBPs. Here, similarly to the drug treatment experiments, exogenous GST-FKBP12 proved able to displace most, but not all, of the endogenous FKBPs bound to both RyR1 and RyR2. Once again, a small population of endogenous FKBP12 proved resistant to displacement, even in the presence of super-saturating quantities of exogenous GST-FKBP12. This reinforces the idea that a small population of FKBPs bind to the RyRs with a greater affinity than the majority of bound FKBP.

Finally, in Chapter 5 the loss of FKBPs from RyRs during vesicle processing as well as remediation thereof with S107 treatment was addressed. Also investigated was the capacity of RyRs in raw muscle homogenates to uptake exogenous FKBP12, with the goal of determining whether RyRs were physiologically fully-occupied by FKBP.

Evidence for negative cooperativity in this Chapter is mainly drawn from the complementary observations that 1) RyR1 possesses a higher initial stoichiometry of bound FKBP, with ~3 FKBP bound on average to each tetramer, as compared to ~2 FKBP bound to RyR2 and 2) that RyR1 loses a greater proportion of its associated FKBP earlier in processing than does RyR2. In the context of a negative cooperativity model, it is logical that the more occupied species of RyR would exhibit an easier dissociation of at least a population of its bound FKBPs. Given a starting stoichiometry of 3 FKBP12 per RyR1, it would be expected that between 1/3 and 2/3 of the bound FKBP12 would "easily" dissociate from RyR1, and that is indeed what was observed, with the average occupancy of RyR1 dropping rapidly from ~3 to ~1 FKBP per tetramer. Note however that the data for FKBP association to RyR2 is a little more confounding. Here, a significant drop in FKBP association is observed only in the final stages of processing, and the drop reducing the average occupancy of RyR2 by FKBP to less than 1. That is, at least a population of RyR2 appears to be wholly unoccupied by FKBP subsequent to vesicle processing. While it might be expected that the final bound FKBP to a RyR2 would be highly resistant to dissociation, this is not to say that complete dissociation of FKBP is impossible: given harsh enough conditions, a population of completely stripped RyR is plausible. Indeed, given the well-characterised differences in affinity for the FKBPs between the RyR isoforms (see **1.4.3**), it is possible that the "strength" of any cooperative RyR:FKBP relationship might similarly differ between RyR isoforms. That is, a greater degree of negative cooperativity might be present in RyR1 as compared to RyR2, where both complete dissociation of FKBPs from RyR1 and association of a "fourth" FKBP to RyR1 are energetically disfavoured as compared to RyR2.

The remainder of this section of the Discussion will reinforce these observations from the Results chapters with some preliminary experimental evidence, as well as attempting to reconcile the idea of negative cooperativity with previous work in the field related to the characterisation of the binding relationship of RyRs to FKBPs.

6.4.3 Evidence for negative cooperativity from microscale thermophoresis

While incomplete due to time limitations, preliminary experiments employing microscale thermophoresis (MST) assays were conducted which appeared to indicate a negatively cooperative relationship between specifically FKBP12 and RyR1. For details about MST protocols, see Chapter **2.5**. Briefly, MST examines the movement of biomolecules along a thermal gradient, the rate of which movement is proportional to the mass of the biomolecules. Serially-diluted analytes are mixed with a fixed concentration of a fluorescently-tagged binding partner and loaded into fine capillary tubes. The MST assay then involves heating a defined region in the capillary tubes with a laser, which region is simultaneously monitored for fluorescence. Complexes of biomolecules, as well as any unbound species, then migrate out of the heated region. The migration of the fluorescently-tagged species is measured as a drop in overall fluorescence in the region: for example, in Figure 6.2, this migration, measured as a decrease in fluorescence, is taking place between ~5 seconds and ~35 seconds. The higher the concentration of untagged analytes, the more fluorescently-tagged species are complexed, and as these complexed species migrate more slowly along the thermal gradient, the drop in overall fluorescence is less in those capillary tubes with the highest concentrations of analytes.

Where a serial dilution of analytes generates a highly linear relationship between change in fluorescence and concentration of analyte, an affinity between the analyte and the fluorescently-tagged species can be easily determined. In the case of the pilot experiment conducted in this thesis, however, the relationship between stripped RyR1 and fluorescently-tagged FKBP12 exhibited three “levels” of association, with two “inflection points”, representing a sizeable quantum difference in affinity, between each. This is largely what might be expected to be seen in a negatively cooperative relationship, and so offers further intriguing evidence supporting this model. One puzzle is that the negatively-cooperative relationship between RyR1 and FKBP12 would be expected to have four “levels” of association, representing each potential FKBP12 occupancy state – one, two, three, or four FKBP12s bound to the RyR1 tetramer – with three “inflection points” describing the shift in affinity between each occupancy state. A possible explanation might be that the first two occupancy states,

both presumably with extremely high RyR:FKBP12 affinities, have been somewhat concatenated, such that Figure **6.2** is presenting only the shifts in affinity between 2, 3, or 4 FKBPs occupying the RyR1, with the shift between the 1 and 2 occupancy states unobserved due to insufficient granularity and the difficulty of preparing highly accurate dilutions of very low concentrations of RyR1. Notably, the first three traces, where RyR1 concentration is the lowest (the lowest three traces on panel A of Figure 6.2, and the first three datapoints on panel B), exhibit somewhat steeper a slope in panel B of Figure 6.2 than do the remaining traces: possibly a higher-resolution examination of this concentration range would reveal a similar set of two “levels” of association with an affinity “inflection point” somewhere between the two. Figure 6.3 is presented by way of contrast, acting as something of a negative control to Figure 6.2: here, all RyR1 was pre-incubated with saturating concentrations of non-tagged FKBP12 before being mixed with fluorescently-tagged FKBP12. While it might have been expected that some of the fluorescently-tagged FKBP12 would displace some of the non-tagged FKBP12, just as the GST-tagged FKBP12 displaced endogenous FKBP12 in the experiments of Chapter 4, such displacement appears not to have occurred. One reason may be the relatively short time course of the mixing process in this experiment, compared to the incubations of Chapter 4 – approximately a minute at room temperature, against an hour at 37 °C. Further, due to the indiscriminate binding of the NHS-ester chemistry of the FKBP12 dye, for a proportion of FKBPs, interaction surfaces may have been sufficiently disrupted such that the aggregate affinity between the fluorescently-tagged FKBPs and RyR1 decreased, making replacement events overall less likely to occur.

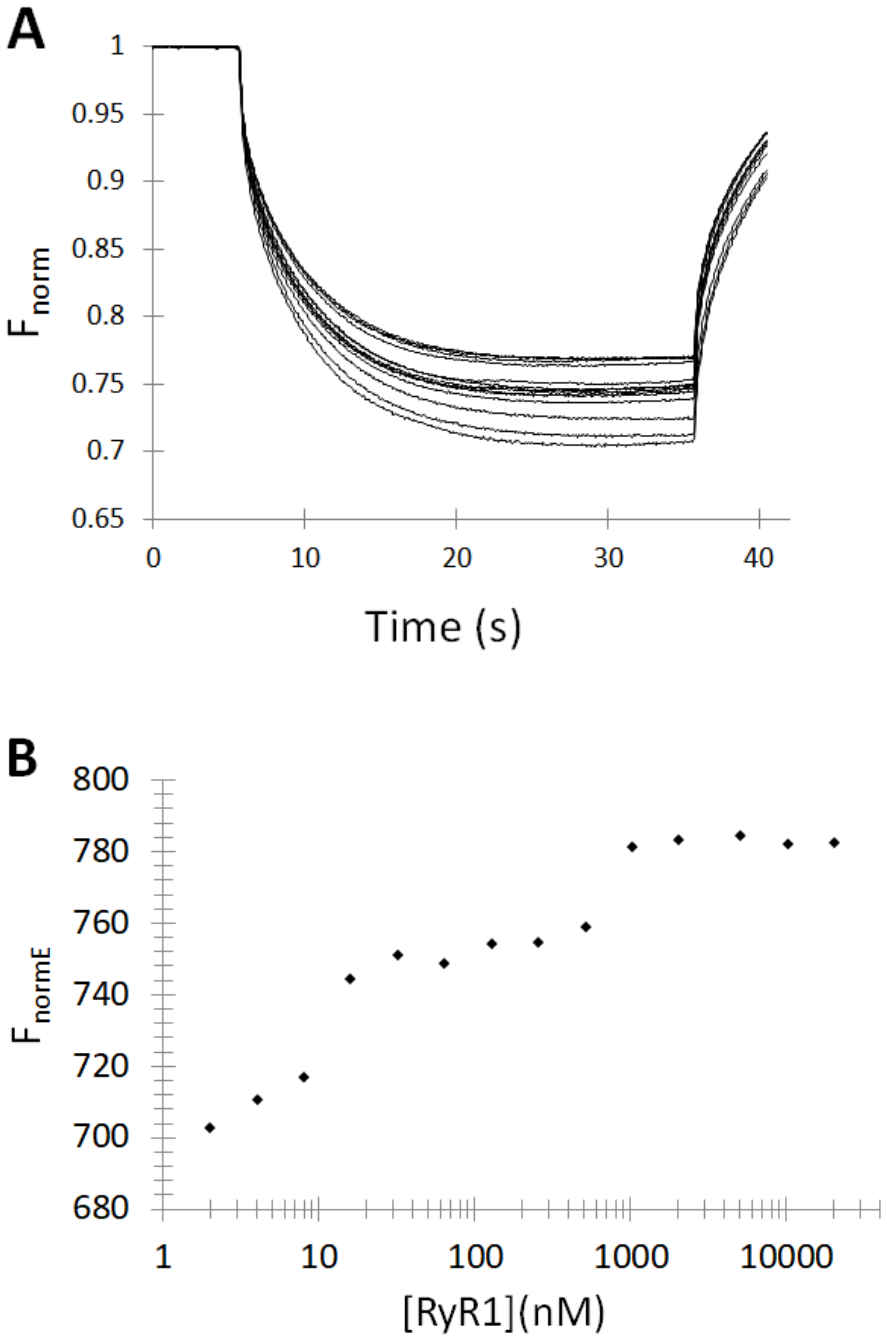

Figure 6.1: MST suggests at least three levels of affinity between RyR1 and FKBP. A serial dilution of 14 concentrations of RyR1 (ranging from ~20 µM to ~2 nM) was titrated against 32 nM of fluorescently-tagged FKBP12. **A**, the change in normalised fluorescence for each dilution over the 40 second assay period. **B**, the normalised fluorescence at maximal thermophoresis against RyR1 titrant concentration. Two "inflection points" appear in the association of RyR1 to FKBP12, at about 10 nM [RyR1] and at about 1 µM, indicating a change in affinity at these ratios of [RyR1]:[FKBP12].

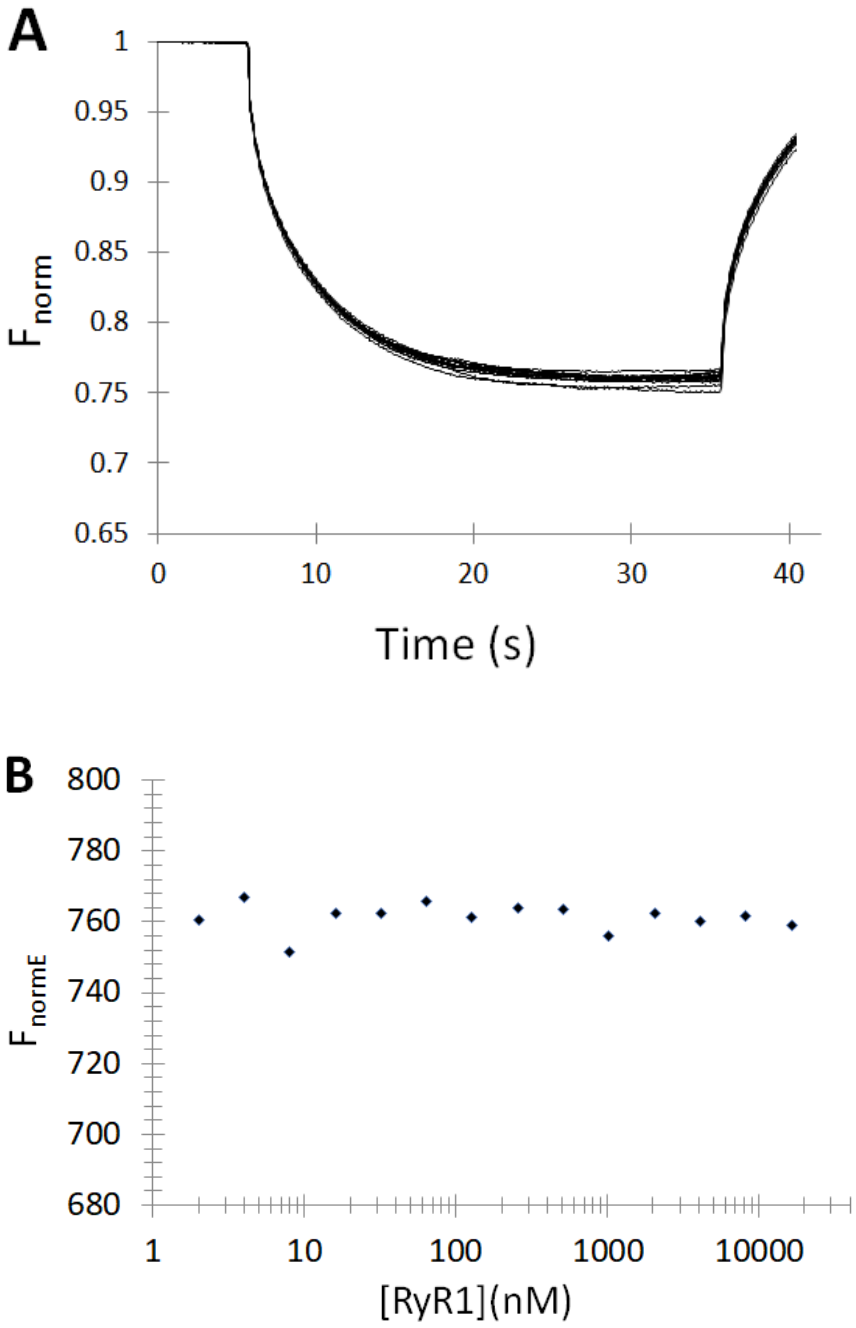

Figure 6.2: Pre-saturated RyR1 exhibits no further FKBP12 binding. A serial dilution of 14 concentrations of RyR1 (ranging from ~20 µM to ~2 nM) was pre-incubated with 10 µM FKBP12, separated from excess FKBP12, and then titrated against 32 nM of fluorescently-tagged FKBP12. **A**, the change in normalised fluorescence for each dilution over the 40 second assay period. **B**, the normalised fluorescence at maximal thermophoresis against RyR1 titrant concentration. A lack of change in normalised fluorescence signal between samples indicates little to no additional binding of fluorescently-tagged FKBP12 by saturated RyR1.

6.4.4 Reconciling a negative cooperativity model with previous work on the RyR:FKBP relationship

As summarised in the Introduction to this thesis, most particularly in section **1.4.3**, a significant amount of work has gone into characterising the affinity of FKBP for RyR, although the results of these characterisations differ considerably. Notably, none of these previous reports appear to have indicated a negatively cooperative relationship between FKBP and RyR, although to be fair, none have been specifically designed to address the potential existence of cooperativity. Nevertheless, a model for negative cooperativity is generally reconcilable with this previous biophysical work: presented below are two case studies of such a reconciliation.

As a general observation, the fact that a remarkably wide range of affinities for FKBP to RyR have been reported provides some support for the negative cooperativity hypothesis. Certain papers start with RyRs which still endogenously bind FKBPs, while others start with RyRs that have been stripped of all associated FKBPs. Should a negative cooperativity hypothesis hold, it would be expected that papers beginning with stripped RyRs would report much higher affinities. Indeed, this is the case for the first two papers discussed below.

One of the first papers which attempted an in-cell characterisation of the affinity of both FKBP12 and FKBP12.6 for RyR2 was by Guo et al. (2010). In this paper, isolated cardiac myocytes were permeabilised and fluorescently-tagged exogenous FKBP12 or FKBP12.6 was introduced to the myocytes at differing concentrations, whereupon the rate of its binding to RyR2 was assayed. Complementary experiments photobleached sections of the myocytes, such that the migration of “new” tagged FKBPs to replace bound bleached FKBPs could also be followed. Notably, a maximum binding quantity of approximately 1 µmol FKBPs was determined, with binding sites highly localised to the myocyte Z-line. Given the assayed concentration of RyR2 tetramers in myocytes is approximately 250 nmol (Bers, 1993), this would imply that the RyR2s were fully occupied by the fluorescent exogenous FKBPs, and therefore that each “step” of negative cooperativity should have been observed in the experiment; however, the reported affinities are “flat”. A few factors may account for this. First, not all FKBP may have been bound to RyR, despite the seemingly strong localisation of both species to the myocyte Z-line: FKBP12, at least, is known to

participate in many cytoplasmic processes beyond its interactions with RyRs, with both enzymatic functionality and as a signalling molecule in the mTOR pathway (**1.4.1**). While permeabilization may have removed many cytoplasmic interaction partners for FKBP12, some would be expected to remain, as well as any non-RyR2 membranous interaction partners. If such interactions sequestered even a half of the exogenous FKBPs, with their fluorescence spread relatively evenly over the cytoplasm such that the Z-line localisation of the remaining FKBPs still presented a vivid contrast, then it is possible that only the replacement of the “second” and “third” RyR-associated FKBPs was observed, where any difference in affinities may only be slight.

Perhaps the most comprehensive work on surface plasmon resonance (SPR)-based characterisation of the RyR:FKBP relationship is Blayney et al. (2010), mentioned briefly in section **1.4.3** of the Introduction. This paper examined the effect of PKA phosphorylation on the affinity of both FKBP12 and FKBP12.6 for RyR1 and RyR2, and the remediation of phosphorylation-induced FKBP dissociation with the drug JTV-519 / K201, an analogous drug to S107. SPR experiments generally are sensitive enough to changes in affinity consequent to a cooperative relationship that a useful Hill curve can be constructed based on the data they generate. For the experiments of this particular paper, however, it was the FKBP species which were immobilised on the detection surface, with RyRs comprising the mobile phase which was flowed over the immobilised FKBPs. Such an experimental set-up is entirely logical for SPR work: the much greater mass of the RyRs significantly enhances the sensitivity and precision of plasmonic-based detection. Restricting RyRs to the mobile phase also means there is much less chance of time-based degradation and disorganisation of the large, membrane-bound molecule. Further, immobilising the RyRs is difficult to achieve without significant inefficiencies. To ensure that the majority of RyRs are oriented such that they present their cytoplasmic “face” to the mobile phase, an antibody specific to luminal residues would be needed, the validation of which would likely comprise a further paper’s worth of work. Notwithstanding these considerations, the fact that FKBP was immobilised as a “capture” ligand means that only one binding event per RyR would ever be detected: once bound by an immobilised FKBP, no further FKBPs could bind to the RyR, since the spacing of the immobilised FKBPs on the sensor surface is extremely highly unlikely to “align” with even two separate FKBP-binding sites on a RyR, let alone three or four. Further, as the RyRs reported in this paper

were stripped of endogenous FKBP prior to SPR experiments, this binding event would be the “first” i.e. most kinetically favoured binding event, which perhaps accounts for the extremely high affinities determined for FKBP binding to the RyR: approaching picomolar Kds for the association of FKBP12.6 for “closed state” RyR2. It may be possible to set up a similar experiment which is able to determine negative cooperativity, even using immobilised FKBP. Stripped RyRs would need to be incubated with a standard curve of different FKBP concentrations, ranging from picomolar through to super-saturating, and then flowed over the FKBP detection surface. If any differences in affinities for the differentially-occupied RyRs are detected, this would be strong evidence for a cooperative relationship between the two molecules; if the differences are quite distinct, it would also allow for estimation of the different “steps” of negatively-cooperative affinity, based on the FKBP incubation concentrations proximate to each “step”.

6.5 Conclusions

In **1.5**, Project Aims, I stated that in this thesis I hoped to clarify somewhat the nature of FKBP regulation of RyR, specifically by addressing a hypothesis that FKBP binding to RyR may be negatively cooperative, which in turn might indicate a potential dynamic relationship between the two species in normal physiology.

In each results chapter, observations supported the negative cooperativity hypothesis. In Chapter 3, a population of FKBP was observed to be readily dissociated from both RyR isoforms even in control treatments. Conversely, a population of FKBP remained resistant to dissociation, even after exposure to highly effective dissociative treatments, such as FK506 or rapamycin acting on RyR1. This seemed to indicate multiple populations of FKBP bound to RyR with differing affinities. In Chapter 4, this observation was reinforced, when GST-FKBP12 was observed to dissociate large quantities of endogenously bound FKBP from RyR – but not all FKBP, with a population remaining bound despite the saturating excess of exogenous GST-FKBP12, again pointing towards a population of FKBP bound to RyR with very high affinity. Then in Chapter 5, particularly for RyR1, it was observed that processing loss of FKBP altered the stoichiometry of FKBP:RyR1 from ~3:1 to ~1:1, much as would

be expected from a negatively cooperative relationship between the two species, with the final FKBP bound to RyR1 highly resistant to dissociation.

Further, while unfortunately biophysical experiments directly probing the RyR and FKBP relationship could not be completed due to time limitations, preliminary MST studies offer intriguing support for the negative cooperativity hypothesis, showing at least three “levels” of affinity of FKBP12 for RyR1. This offers the most obvious suggestion for future work on this topic: whether via MST or other biophysical techniques such as surface plasmon resonance or isothermal titration calorimetry, experiments designed specifically to interrogate a hypothesis of negative cooperativity should be capable of definitively accepting or rejecting the hypothesis. Nevertheless, taken together, the biophysical observations of this chapter and the findings of the results chapters are highly suggestive of a negatively cooperative relationship between RyR and FKBP.

Finally, beyond interrogation of the negative cooperativity hypothesis, each of the results chapters have generated interesting and useful findings regarding the relationship between RyR and FKBP. A few of the most intriguing results follow. RyR as present in SR vesicles, commonly used in experiments probing RyR function, have a sub-physiological level of FKBP occupancy, possibly giving rise to non-physiological RyR activity. This sub-physiological occupancy is consequent to vesicle processing methods, and can be somewhat rescued by treatment with S107. While both FK506 and rapamycin are highly effective at dissociating FKBP12 from RyR1, they have little to no impact on FKBP12 associated with RyR2, and strangely, only rapamycin has a moderate effect on FKBP12.6 associate d with RyR2. Solubilisation or displacement with GST-FKBP12 proved a far more effective means of dissociating FKBP from RyR2: for experiments requiring stripped RyR2, these methods are therefore recommended, with GST-FKBP12 removed after treatment via saturation with glutathione. Finally, it appears likely that RyR physiologically are not fully occupied by FKBP, given that RyR as present in muscle homogenate appear able to uptake additional exogenous FKBP12. Hopefully, these findings will assist in future work probing the relationship between RyR and FKBP.

References

Aghdasi, B., Ye, K., Resnick, A., Huang, A., Ha, H. C., Guo, X., Dawson, T. M., Dawson, V. L., & Snyder, S. H. (2001). FKBP12, the 12-kDa FK506-binding protein, is a physiologic regulator of the cell cycle. *Proceedings of the National Academy of Sciences of the United States of America*, 98(5), 2425–2430. https://doi.org/10.1073/pnas.041614198

Ahern, C. A., Bhattacharya, D., Mortenson, L., & Coronado, R. (2001). A component of excitation-contraction coupling triggered in the absence of the T671-L690 and L720-Q765 regions of the II-III loop of the dihydropyridine receptor alpha(1s) pore subunit. *Biophysical journal*, 81(6), 3294–3307. https://doi.org/10.1016/S0006-3495(01)75963-2

Ahern, G. P., Junankar, P. R., & Dulhunty, A. F. (1994). Single channel activity of the ryanodine receptor calcium release channel is modulated by FK-506. *FEBS letters*, 352(3), 369–374. https://doi.org/10.1016/0014-5793(94)01001-3

Ahern, G. P., Junankar, P. R., & Dulhunty, A. F. (1997). Subconductance states in single-channel activity of skeletal muscle ryanodine receptors after removal of FKBP12. *Biophysical journal*, 72(1), 146–162. https://doi.org/10.1016/S0006-3495(97)78654-5

Ai, X., Curran, J. W., Shannon, T. R., Bers, D. M., & Pogwizd, S. M. (2005). Ca2+/calmodulin-dependent protein kinase modulates cardiac ryanodine receptor phosphorylation and sarcoplasmic reticulum Ca2+ leak in heart failure. *Circulation research*, 97(12), 1314–1322. https://doi.org/10.1161/01.RES.0000194329.41863.89

Avila, G., Lee, E. H., Perez, C. F., Allen, P. D., & Dirksen, R. T. (2003). FKBP12 binding to RyR1 modulates excitation-contraction coupling in mouse skeletal myotubes. *The Journal of biological chemistry*, 278(25), 22600–22608. https://doi.org/10.1074/jbc.M205866200

Balog, E. M., Fruen, B. R., Shomer, N. H., & Louis, C. F. (2001). Divergent effects of the malignant hyperthermia-susceptible Arg(615)-->Cys mutation on the

Ca(2+) and Mg(2+) dependence of the RyR1. *Biophysical journal*, 81(4), 2050–2058. https://doi.org/10.1016/S0006-3495(01)75854-7

Balshaw, D. M., Xu, L., Yamaguchi, N., Pasek, D. A., & Meissner, G. (2001). Calmodulin binding and inhibition of cardiac muscle calcium release channel (ryanodine receptor). *The Journal of biological chemistry*, 276(23), 20144–20153. https://doi.org/10.1074/jbc.M010771200

Balshaw, D., Gao, L., & Meissner, G. (1999). Luminal loop of the ryanodine receptor: a pore-forming segment?. *Proceedings of the National Academy of Sciences of the United States of America*, 96(7), 3345–3347. https://doi.org/10.1073/pnas.96.7.3345

Bannister, M. L., Thomas, N. L., Sikkel, M. B., Mukherjee, S., Maxwell, C., MacLeod, K. T., George, C. H., & Williams, A. J. (2015). The mechanism of flecainide action in CPVT does not involve a direct effect on RyR2. Circulation research, 116(8), 1324–1335. https://doi.org/10.1161/CIRCRESAHA.116.305347

Barg, S., Copello, J. A., & Fleischer, S. (1997). Different interactions of cardiac and skeletal muscle ryanodine receptors with FK-506 binding protein isoforms. *The American journal of physiology*, 272(5 Pt 1), C1726–C1733. https://doi.org/10.1152/ajpcell.1997.272.5.C1726

Batiste, S. M., Blackwell, D. J., Kim, K., Kryshtal, D. O., Gomez-Hurtado, N., Rebbeck, R. T., Cornea, R. L., Johnston, J. N., & Knollmann, B. C. (2019). Unnatural verticilide enantiomer inhibits type 2 ryanodine receptor-mediated calcium leak and is antiarrhythmic. *Proceedings of the National Academy of Sciences of the United States of America*, 116(11), 4810–4815. https://doi.org/10.1073/pnas.1816685116

Baumann, C. W., Rogers, R. G., Gahlot, N., & Ingalls, C. P. (2014). Eccentric contractions disrupt FKBP12 content in mouse skeletal muscle. *Physiological reports*, 2(7), e12081. https://doi.org/10.14814/phy2.12081

Beam, K. G., & Bannister, R. A. (2010). Looking for answers to EC coupling's persistent questions. *The Journal of general physiology*, 136(1), 7–12. https://doi.org/10.1085/jgp.201010461

Beard, N. A., & Dulhunty, A. F. (2015). C-terminal residues of skeletal muscle calsequestrin are essential for calcium binding and for skeletal ryanodine receptor inhibition. *Skeletal muscle*, 5, 6. https://doi.org/10.1186/s13395-015-0029-7

Bellinger, A. M., Reiken, S., Carlson, C., Mongillo, M., Liu, X., Rothman, L., Matecki, S., Lacampagne, A., & Marks, A. R. (2009). Hypernitrosylated ryanodine receptor calcium release channels are leaky in dystrophic muscle. *Nature medicine*, 15(3), 325–330. https://doi.org/10.1038/nm.1916

Beltrán, M., Bull, R., Donoso, P., & Hidalgo, C. (1996). Ca(2+)- and pH-dependent halothane stimulation of Ca2+ release in sarcoplasmic reticulum from frog muscle. *The American journal of physiology*, 271(2 Pt 1), C540–C546. https://doi.org/10.1152/ajpcell.1996.271.2.C540

Benkusky, N. A., Weber, C. S., Scherman, J. A., Farrell, E. F., Hacker, T. A., John, M. C., Powers, P. A., & Valdivia, H. H. (2007). Intact beta-adrenergic response and unmodified progression toward heart failure in mice with genetic ablation of a major protein kinase A phosphorylation site in the cardiac ryanodine receptor. *Circulation research*, 101(8), 819–829. https://doi.org/10.1161/CIRCRESAHA.107.153007

Berridge, M. J., Lipp, P., & Bootman, M. D. (2000). The versatility and universality of calcium signalling. *Nature reviews. Molecular cell biology*, 1(1), 11–21. https://doi.org/10.1038/35036035

Bers D. M. (2002). Cardiac excitation-contraction coupling. *Nature*, 415(6868), 198–205. https://doi.org/10.1038/415198a

Bezprozvanny, I., & Mattson, M. P. (2008). Neuronal calcium mishandling and the pathogenesis of Alzheimer's disease. *Trends in neurosciences*, 31(9), 454–463. https://doi.org/10.1016/j.tins.2008.06.005

Bezprozvanny, I., Watras, J., & Ehrlich, B. E. (1991). Bell-shaped calcium-response curves of Ins(1,4,5)P3- and calcium-gated channels from endoplasmic reticulum of cerebellum. *Nature*, 351(6329), 751–754. https://doi.org/10.1038/351751a0

Bielefeldt, K., Sharma, R. V., Whiteis, C., Yedidag, E., & Abboud, F. M. (1997). Tacrolimus (FK506) modulates calcium release and contractility of intestinal smooth muscle. *Cell calcium*, 22(6), 507–514. https://doi.org/10.1016/s0143-4160(97)90078-6

Biernacka, E. K., & Hoffman, P. (2011). Efficacy of flecainide in a patient with catecholaminergic polymorphic ventricular tachycardia. *Europace : European pacing, arrhythmias, and cardiac electrophysiology : journal of the working groups on cardiac pacing, arrhythmias, and cardiac cellular electrophysiology of the European Society of Cardiology*, 13(1), 129–130. https://doi.org/10.1093/europace/euq279

Blayney, L. M., Jones, J. L., Griffiths, J., & Lai, F. A. (2010). A mechanism of ryanodine receptor modulation by FKBP12/12.6, protein kinase A, and K201. *Cardiovascular research*, 85(1), 68–78. https://doi.org/10.1093/cvr/cvp273

Brejc, K., van Dijk, W. J., Klaassen, R. V., Schuurmans, M., van Der Oost, J., Smit, A. B., & Sixma, T. K. (2001). Crystal structure of an ACh-binding protein reveals the ligand-binding domain of nicotinic receptors. *Nature*, 411(6835), 269–276. https://doi.org/10.1038/35077011

Brillantes, A. B., Ondrias, K., Scott, A., Kobrinsky, E., Ondriasová, E., Moschella, M. C., Jayaraman, T., Landers, M., Ehrlich, B. E., & Marks, A. R. (1994). Stabilization of calcium release channel (ryanodine receptor) function by FK506-binding protein. *Cell*, 77(4), 513–523. https://doi.org/10.1016/0092-8674(94)90214-3

Brown, E. J., Beal, P. A., Keith, C. T., Chen, J., Shin, T. B., & Schreiber, S. L. (1995). Control of p70 s6 kinase by kinase activity of FRAP in vivo. *Nature*, 377(6548), 441–446. https://doi.org/10.1038/377441a0

Bull, R., & Marengo, J. J. (1994). Calcium-dependent halothane activation of sarcoplasmic reticulum calcium channels from frog skeletal muscle. *The American journal of physiology*, 266(2 Pt 1), C391–C396. https://doi.org/10.1152/ajpcell.1994.266.2.C391

Bultynck, G., De Smedt, H., Parys, J. B., Callewaert, G., & Missiaen, L. (2002). Washing out of lipophilic compounds induces a transient increase in the

passive Ca(2+) leak in permeabilized A7r5 cells. *Cell calcium*, 31(5), 229–233. https://doi.org/10.1016/S0143-4160(02)00051-9

Bultynck, G., De Smet, P., Rossi, D., Callewaert, G., Missiaen, L., Sorrentino, V., De Smedt, H., & Parys, J. B. (2001a). Characterization and mapping of the 12 kDa FK506-binding protein (FKBP12)-binding site on different isoforms of the ryanodine receptor and of the inositol 1,4,5-trisphosphate receptor. *The Biochemical journal*, 354(Pt 2), 413–422. https://doi.org/10.1042/0264-6021:3540413

Bultynck, G., Rossi, D., Callewaert, G., Missiaen, L., Sorrentino, V., Parys, J. B., & De Smedt, H. (2001). The conserved sites for the FK506-binding proteins in ryanodine receptors and inositol 1,4,5-trisphosphate receptors are structurally and functionally different. *The Journal of biological chemistry*, 276(50), 47715–47724. https://doi.org/10.1074/jbc.M106573200

Callewaert, G., Cleemann, L., & Morad, M. (1988). Epinephrine enhances Ca2+ current-regulated Ca2+ release and Ca2+ reuptake in rat ventricular myocytes. *Proceedings of the National Academy of Sciences of the United States of America*, 85(6), 2009–2013. https://doi.org/10.1073/pnas.85.6.2009

Camors, E., & Valdivia, H. H. (2014). CaMKII regulation of cardiac ryanodine receptors and inositol triphosphate receptors. *Frontiers in pharmacology*, 5, 101. https://doi.org/10.3389/fphar.2014.00101

Campbell, K. P., MacLennan, D. H., Jorgensen, A. O., & Mintzer, M. C. (1983). Purification and characterization of calsequestrin from canine cardiac sarcoplasmic reticulum and identification of the 53,000 dalton glycoprotein. *The Journal of biological chemistry*, 258(2), 1197–1204.

Campiglio, M., & Flucher, B. E. (2017). STAC3 stably interacts through its C1 domain with CaV1.1 in skeletal muscle triads. *Scientific reports*, 7, 41003. https://doi.org/10.1038/srep41003

Campiglio, M., Kaplan, M. M., & Flucher, B. E. (2018). STAC3 incorporation into skeletal muscle triads occurs independent of the dihydropyridine receptor. *Journal of cellular physiology*, 233(12), 9045–9051. https://doi.org/10.1002/jcp.26767

Capacchione, J. F., Sambuughin, N., Bina, S., Mulligan, L. P., Lawson, T. D., & Muldoon, S. M. (2010). Exertional rhabdomyolysis and malignant hyperthermia in a patient with ryanodine receptor type 1 gene, L-type calcium channel alpha-1 subunit gene, and calsequestrin-1 gene polymorphisms. *Anesthesiology*, 112(1), 239–244. https://doi.org/10.1097/ALN.0b013e3181c29504

Carmody, M., Mackrill, J. J., Sorrentino, V., & O'Neill, C. (2001). FKBP12 associates tightly with the skeletal muscle type 1 ryanodine receptor, but not with other intracellular calcium release channels. *FEBS letters*, 505(1), 97–102. https://doi.org/10.1016/s0014-5793(01)02787-9

Casarotto, M. G., Cui, Y., Karunasekara, Y., Harvey, P. J., Norris, N., Board, P. G., & Dulhunty, A. F. (2006). Structural and functional characterization of interactions between the dihydropyridine receptor II-III loop and the ryanodine receptor. *Clinical and experimental pharmacology & physiology*, 33(11), 1114–1117. https://doi.org/10.1111/j.1440-1681.2006.04501.x

Chamberlain, B. K., & Fleischer, S. (1988). Isolation of canine cardiac sarcoplasmic reticulum. *Methods in enzymology*, 157, 91–99. https://doi.org/10.1016/0076-6879(88)57071-4

Chandrasekhar, R., Alzayady, K. J., Wagner, L. E., 2nd, & Yule, D. I. (2016). Unique Regulatory Properties of Heterotetrameric Inositol 1,4,5-Trisphosphate Receptors Revealed by Studying Concatenated Receptor Constructs. The *Journal of biological chemistry*, 291(10), 4846–4860. https://doi.org/10.1074/jbc.M115.705301

Changeux, J. P., Kasai, M., & Lee, C. Y. (1970). Use of a snake venom toxin to characterize the cholinergic receptor protein. *Proceedings of the National Academy of Sciences of the United States of America*, 67(3), 1241–1247. https://doi.org/10.1073/pnas.67.3.1241

Chelu, M. G., Danila, C. I., Gilman, C. P., & Hamilton, S. L. (2004). Regulation of ryanodine receptors by FK506 binding proteins. *Trends in cardiovascular medicine*, 14(6), 227–234. https://doi.org/10.1016/j.tcm.2004.06.003

Cheng, W., Altafaj, X., Ronjat, M., & Coronado, R. (2005). Interaction between the dihydropyridine receptor Ca2+ channel beta-subunit and ryanodine receptor type 1 strengthens excitation-contraction coupling. *Proceedings of the National Academy of Sciences of the United States of America*, 102(52), 19225–19230. https://doi.org/10.1073/pnas.0504334102

Cheung, M. Y., Auyeung, W. K., Li, K. P., & Lam, H. M. (2020). A Rice Immunophilin Homolog, OsFKBP12, Is a Negative Regulator of Both Biotic and Abiotic Stress Responses. *International journal of molecular sciences*, 21(22), 8791. https://doi.org/10.3390/ijms21228791

Collins J. H. (1991). Sequence analysis of the ryanodine receptor: possible association with a 12K, FK506-binding immunophilin/protein kinase C inhibitor. *Biochemical and biophysical research communications*, 178(3), 1288–1290. https://doi.org/10.1016/0006-291x(91)91033-9

Connelly, T. J., & Coronado, R. (1994). Activation of the Ca2+ release channel of cardiac sarcoplasmic reticulum by volatile anesthetics. *Anesthesiology*, 81(2), 459–469. https://doi.org/10.1097/00000542-199408000-00025

Cornea, R. L., Nitu, F., Gruber, S., Kohler, K., Satzer, M., Thomas, D. D., & Fruen, B. R. (2009). FRET-based mapping of calmodulin bound to the RyR1 Ca2+ release channel. *Proceedings of the National Academy of Sciences of the United States of America*, 106(15), 6128–6133. https://doi.org/10.1073/pnas.0813010106

Corona, B. T., Rouviere, C., Hamilton, S. L., & Ingalls, C. P. (2008). FKBP12 deficiency reduces strength deficits after eccentric contraction-induced muscle injury. *Journal of applied physiology (Bethesda, Md. : 1985)*, 105(2), 527–537. https://doi.org/10.1152/japplphysiol.01145.2007

Corrado, D., Basso, C., & Thiene, G. (2000). Arrhythmogenic right ventricular cardiomyopathy: diagnosis, prognosis, and treatment. *Heart (British Cardiac Society)*, 83(5), 588–595. https://doi.org/10.1136/heart.83.5.588

Court, F. (2008). Court Lab Gallery, accessed 4 November 2021, <http://courtlab.cl/site/gallery>

Coussin, F., Macrez, N., Morel, J. L., & Mironneau, J. (2000). Requirement of ryanodine receptor subtypes 1 and 2 for Ca(2+)-induced Ca(2+) release in vascular myocytes. *The Journal of biological chemistry*, 275(13), 9596–9603. https://doi.org/10.1074/jbc.275.13.9596

Cui, Y., Tae, H. S., Norris, N. C., Karunasekara, Y., Pouliquin, P., Board, P. G., Dulhunty, A. F., & Casarotto, M. G. (2009). A dihydropyridine receptor alpha1s loop region critical for skeletal muscle contraction is intrinsically unstructured and binds to a SPRY domain of the type 1 ryanodine receptor. *The international journal of biochemistry & cell biology*, 41(3), 677–686. https://doi.org/10.1016/j.biocel.2008.08.004

Dalla Volta, S., Battaglia, G., & Zerbini, E. (1961). "Auricularization' of right ventricular pressure curve. *American heart journal*, 61, 25–33. https://doi.org/10.1016/0002-8703(61)90513-0

Deivanayagam, C. C., Carson, M., Thotakura, A., Narayana, S. V., & Chodavarapu, R. S. (2000). Structure of FKBP12.6 in complex with rapamycin. *Acta crystallographica. Section D, Biological crystallography*, 56(Pt 3), 266–271. https://doi.org/10.1107/s0907444999016571

Denniss, A., Dulhunty, A. F., & Beard, N. A. (2018). Ryanodine receptor Ca2+ release channel post-translational modification: Central player in cardiac and skeletal muscle disease. *The international journal of biochemistry & cell biology*, 101, 49–53. https://doi.org/10.1016/j.biocel.2018.05.004

des Georges, A., Clarke, O. B., Zalk, R., Yuan, Q., Condon, K. J., Grassucci, R. A., Hendrickson, W. A., Marks, A. R., & Frank, J. (2016). Structural Basis for Gating and Activation of RyR1. *Cell*, 167(1), 145–157.e17. https://doi.org/10.1016/j.cell.2016.08.075

Dhindwal, S., Lobo, J., Cabra, V., Santiago, D. J., Nayak, A. R., Dryden, K., & Samsó, M. (2017). A cryo-EM-based model of phosphorylation- and FKBP12.6-mediated allosterism of the cardiac ryanodine receptor. *Science signaling*, 10(480), eaai8842. https://doi.org/10.1126/scisignal.aai8842

Diaz-Sylvester, P. L., Porta, M., & Copello, J. A. (2008). Halothane modulation of skeletal muscle ryanodine receptors: dependence on Ca2+, Mg2+, and ATP

. American journal of physiology. *Cell physiology*, 294(4), C1103–C1112. https://doi.org/10.1152/ajpcell.90642.2007

Dirksen, R. T., & Avila, G. (2002). Altered ryanodine receptor function in central core disease: leaky or uncoupled Ca(2+) release channels?. *Trends in cardiovascular medicine*, 12(5), 189–197. https://doi.org/10.1016/s1050-1738(02)00163-9

Domeier, T. L., Zima, A. V., Maxwell, J. T., Huke, S., Mignery, G. A., & Blatter, L. A. (2008). IP3 receptor-dependent Ca2+ release modulates excitation-contraction coupling in rabbit ventricular myocytes. *American journal of physiology. Heart and circulatory physiology*, 294(2), H596–H604. https://doi.org/10.1152/ajpheart.01155.2007

Du, G. G., Khanna, V. K., & MacLennan, D. H. (2000). Mutation of divergent region 1 alters caffeine and Ca(2+) sensitivity of the skeletal muscle Ca(2+) release channel (ryanodine receptor). *The Journal of biological chemistry*, 275(16), 11778–11783. https://doi.org/10.1074/jbc.275.16.11778

Dulhunty A. F. (1984). Heterogeneity of T-tubule geometry in vertebrate skeletal muscle fibres. *Journal of muscle research and cell motility*, 5(3), 333–347. https://doi.org/10.1007/BF00713111

Dulhunty, A. F., Haarmann, C. S., Green, D., Laver, D. R., Board, P. G., & Casarotto, M. G. (2002). Interactions between dihydropyridine receptors and ryanodine receptors in striated muscle. *Progress in biophysics and molecular biology*, 79(1-3), 45–75. https://doi.org/10.1016/s0079-6107(02)00013-5

Dulhunty, A. F., Hewawasam, R., Liu, D., Casarotto, M. G., & Board, P. G. (2011). Regulation of the cardiac muscle ryanodine receptor by glutathione transferases. *Drug metabolism reviews*, 43(2), 236–252. https://doi.org/10.3109/03602532.2010.549134

Dulhunty, A. F., Junankar, P. R., Eager, K. R., Ahern, G. P., & Laver, D. R. (1996). Ion channels in the sarcoplasmic reticulum of striated muscle. *Acta physiologica Scandinavica*, 156(3), 375–385. https://doi.org/10.1046/j.1365-201X.1996.193000.x

Dulhunty, A. F., Laver, D. R., Gallant, E. M., Casarotto, M. G., Pace, S. M., & Curtis, S. (1999). Activation and inhibition of skeletal RyR channels by a part of the skeletal DHPR II-III loop: effects of DHPR Ser687 and FKBP12. *Biophysical journal*, 77(1), 189–203. https://doi.org/10.1016/S0006-3495(99)76881-5

Dulhunty, A. F., Laver, D., Curtis, S. M., Pace, S., Haarmann, C., & Gallant, E. M. (2001). Characteristics of irreversible ATP activation suggest that native skeletal ryanodine receptors can be phosphorylated via an endogenous CaMKII. *Biophysical journal*, 81(6), 3240–3252. https://doi.org/10.1016/S0006-3495(01)75959-0

Dutka, T. L., & Lamb, G. D. (2004). Effect of low cytoplasmic [ATP] on excitation-contraction coupling in fast-twitch muscle fibres of the rat. *The Journal of physiology*, 560, 451–468. https://doi.org/10.1113/jphysiol.2004.069112

Eager, K. R., & Dulhunty, A. F. (1998). Activation of the cardiac ryanodine receptor by sulfhydryl oxidation is modified by Mg2+ and ATP. *The Journal of membrane biology*, 163(1), 9–18. https://doi.org/10.1007/s002329900365

Ebbinghaus-Kintscher, U., Luemmen, P., Lobitz, N., Schulte, T., Funke, C., Fischer, R., Masaki, T., Yasokawa, N., & Tohnishi, M. (2006). Phthalic acid diamides activate ryanodine-sensitive Ca2+ release channels in insects. *Cell calcium*, 39(1), 21–33. https://doi.org/10.1016/j.ceca.2005.09.002

Efremov, R. G., Leitner, A., Aebersold, R., & Raunser, S. (2015). Architecture and conformational switch mechanism of the ryanodine receptor. *Nature*, 517(7532), 39–43. https://doi.org/10.1038/nature13916

Eltit, J. M., Feng, W., Lopez, J. R., Padilla, I. T., Pessah, I. N., Molinski, T. F., Fruen, B. R., Allen, P. D., & Perez, C. F. (2010). Ablation of skeletal muscle triadin impairs FKBP12/RyR1 channel interactions essential for maintaining resting cytoplasmic Ca2+. *The Journal of biological chemistry*, 285(49), 38453–38462. https://doi.org/10.1074/jbc.M110.164525

Eltit, J. M., Szpyt, J., Li, H., Allen, P. D., & Perez, C. F. (2011). Reduced gain of excitation-contraction coupling in triadin-null myotubes is mediated by the disruption of FKBP12/RyR1 interaction. *Cell calcium*, 49(2), 128–135. https://doi.org/10.1016/j.ceca.2011.01.005

Endo M. (1977). Calcium release from the sarcoplasmic reticulum. *Physiological reviews*, 57(1), 71–108. https://doi.org/10.1152/physrev.1977.57.1.71

Ferreiro, A., Monnier, N., Romero, N. B., Leroy, J. P., Bönnemann, C., Haenggeli, C. A., Straub, V., Voss, W. D., Nivoche, Y., Jungbluth, H., Lemainque, A., Voit, T., Lunardi, J., Fardeau, M., & Guicheney, P. (2002). A recessive form of central core disease, transiently presenting as multi-minicore disease, is associated with a homozygous mutation in the ryanodine receptor type 1 gene. *Annals of neurology*, 51(6), 750–759. https://doi.org/10.1002/ana.10231

Fill, M., & Copello, J. A. (2002). Ryanodine receptor calcium release channels. *Physiological reviews*, 82(4), 893–922. https://doi.org/10.1152/physrev.00013.2002

Fleischer, S., Ogunbunmi, E. M., Dixon, M. C., & Fleer, E. A. (1985). Localization of Ca2+ release channels with ryanodine in junctional terminal cisternae of sarcoplasmic reticulum of fast skeletal muscle. *Proceedings of the National Academy of Sciences of the United States of America*, 82(21), 7256–7259. https://doi.org/10.1073/pnas.82.21.7256

Fontaine, G., Frank, R., Guiraudon, G., Pavie, A., Tereau, Y., Chomette, G., & Grosgogeat, Y. (1984). Signification des troubles de conduction intraventriculaires observés dans la dysplasie ventriculaire droite arythmogène [Significance of intraventricular conduction disorders observed in arrhythmogenic right ventricular dysplasia]. *Archives des maladies du coeur et des vaisseaux*, 77(8), 872–879.

Fontaine, G., Gallais, Y., Fornes, P., Hébert, J. L., & Frank, R. (2001). Arrhythmogenic right ventricular dysplasia/cardiomyopathy. *Anesthesiology*, 95(1), 250–254. https://doi.org/10.1097/00000542-200107000-00035

Foskett, J. K., White, C., Cheung, K. H., & Mak, D. O. (2007). Inositol trisphosphate receptor Ca2+ release channels. *Physiological reviews*, 87(2), 593–658. https://doi.org/10.1152/physrev.00035.2006

Fozzard H. A. (1992). Afterdepolarizations and triggered activity. *Basic research in cardiology*, 87 Suppl 2, 105–113. https://doi.org/10.1007/978-3-642-72477-0_10

Franzini-Armstrong C. (1970). Studies of The Triad: I. Structure of the Junction in Frog Twitch Fibers. *The Journal of cell biology*, 47(2), 488–499. https://doi.org/10.1083/jcb.47.2.488

Franzini-Armstrong C. (1972). Studies of the triad. 3. Structure of the junction in fast twitch fibers. *Tissue & cell*, 4(3), 469–478. https://doi.org/10.1016/s0040-8166(72)80023-5

Franzini-Armstrong, C., & Porter, K. R. (1964). Sarcolemmal invaginations constituting the T system in fish muscle fibers. *The Journal of cell biology*, 22(3), 675–696. https://doi.org/10.1083/jcb.22.3.675

Franzini-Armstrong, C., Kenney, L. J., & Varriano-Marston, E. (1987). The structure of calsequestrin in triads of vertebrate skeletal muscle: a deep-etch study. *The Journal of cell biology*, 105(1), 49–56. https://doi.org/10.1083/jcb.105.1.49

Franzini-Armstrong, C., Landmesser, L., & Pilar, G. (1975). Size and shape of transverse tubule openings in frog twitch muscle fibers. *The Journal of cell biology*, 64(2), 493–497. https://doi.org/10.1083/jcb.64.2.493

Franzini-Armstrong, C., Protasi, F., & Ramesh, V. (1998). Comparative ultrastructure of Ca2+ release units in skeletal and cardiac muscle. *Annals of the New York Academy of Sciences*, 853, 20–30. https://doi.org/10.1111/j.1749-6632.1998.tb08253.x

Franzini-Armstrong, C., Protasi, F., & Ramesh, V. (1999). Shape, size, and distribution of Ca(2+) release units and couplons in skeletal and cardiac muscles. *Biophysical journal*, 77(3), 1528–1539. https://doi.org/10.1016/S0006-3495(99)77000-1

Franzini-Armstrong, C., Protasi, F., & Tijskens, P. (2005). The assembly of calcium release units in cardiac muscle. *Annals of the New York Academy of Sciences*, 1047, 76–85. https://doi.org/10.1196/annals.1341.007

Frazer, M. J., & Lynch, C., 3rd (1992). Halothane and isoflurane effects on Ca2+ fluxes of isolated myocardial sarcoplasmic reticulum. *Anesthesiology*, 77(2), 316–323. https://doi.org/10.1097/00000542-199208000-00015

Fritz, N., Morel, J. L., Jeyakumar, L. H., Fleischer, S., Allen, P. D., Mironneau, J., & Macrez, N. (2007). RyR1-specific requirement for depolarization-induced Ca2+ sparks in urinary bladder smooth muscle. *Journal of cell science*, 120(Pt 21), 3784–3791. https://doi.org/10.1242/jcs.009415

Fruen, B. R., Bardy, J. M., Byrem, T. M., Strasburg, G. M., & Louis, C. F. (2000). Differential Ca(2+) sensitivity of skeletal and cardiac muscle ryanodine receptors in the presence of calmodulin. *American journal of physiology*. Cell physiology, 279(3), C724–C733. https://doi.org/10.1152/ajpcell.2000.279.3.C724

Fruman, D. A., Klee, C. B., Bierer, B. E., & Burakoff, S. J. (1992). Calcineurin phosphatase activity in T lymphocytes is inhibited by FK 506 and cyclosporin A. *Proceedings of the National Academy of Sciences of the United States of America*, 89(9), 3686–3690. https://doi.org/10.1073/pnas.89.9.3686

Fulton, K. F., Jackson, S. E., & Buckle, A. M. (2003). Energetic and structural analysis of the role of tryptophan 59 in FKBP12. *Biochemistry*, 42(8), 2364–2372. https://doi.org/10.1021/bi020564a

Furuichi, T., Furutama, D., Hakamata, Y., Nakai, J., Takeshima, H., & Mikoshiba, K. (1994). Multiple types of ryanodine receptor/Ca2+ release channels are differentially expressed in rabbit brain. *The Journal of neuroscience: the official journal of the Society for Neuroscience*, 14(8), 4794–4805. https://doi.org/10.1523/JNEUROSCI.14-08-04794.1994

Gaburjakova, M., Gaburjakova, J., Reiken, S., Huang, F., Marx, S. O., Rosemblit, N., & Marks, A. R. (2001). FKBP12 binding modulates ryanodine receptor channel gating. *The Journal of biological chemistry*, 276(20), 16931–16935. https://doi.org/10.1074/jbc.M100856200

Gaburjakova, M., Gaburjakova, J., Reiken, S., Huang, F., Marx, S. O., Rosemblit, N., & Marks, A. R. (2001). FKBP12 binding modulates ryanodine receptor channel gating. *The Journal of biological chemistry*, 276(20), 16931–16935. https://doi.org/10.1074/jbc.M100856200

Galfré, E., Pitt, S. J., Venturi, E., Sitsapesan, M., Zaccai, N. R., Tsaneva-Atanasova, K., O'Neill, S., & Sitsapesan, R. (2012). FKBP12 activates the cardiac

ryanodine receptor Ca2+-release channel and is antagonised by FKBP12.6. *PloS one*, 7(2), e31956. https://doi.org/10.1371/journal.pone.0031956

Gant, J. C., Chen, K. C., Norris, C. M., Kadish, I., Thibault, O., Blalock, E. M., Porter, N. M., & Landfield, P. W. (2011). Disrupting function of FK506-binding protein 1b/12.6 induces the Ca^{2}+-dysregulation aging phenotype in hippocampal neurons. *The Journal of neuroscience: the official journal of the Society for Neuroscience*, 31(5), 1693–1703. https://doi.org/10.1523/JNEUROSCI.4805-10.2011

Gao, L., Balshaw, D., Xu, L., Tripathy, A., Xin, C., & Meissner, G. (2000). Evidence for a role of the lumenal M3-M4 loop in skeletal muscle Ca(2+) release channel (ryanodine receptor) activity and conductance. *Biophysical journal*, 79(2), 828–840. https://doi.org/10.1016/S0006-3495(00)76339-9

Gasteiger E., Hoogland C., Gattiker A., Duvaud S., Wilkins M. R., Appel R. D., and Bairoch A.. 2005. *Protein Identification and Analysis Tools on the ExPASy Server*. In J. M. Walker (Ed.), The Proteomics Protocols Handbook, (pp. 571-607). Humana Press.

Gergs, U., Berndt, T., Buskase, J., Jones, L. R., Kirchhefer, U., Müller, F. U., Schlüter, K. D., Schmitz, W., & Neumann, J. (2007). On the role of junctin in cardiac Ca2+ handling, contractility, and heart failure. *American journal of physiology. Heart and circulatory physiology*, 293(1), H728–H734. https://doi.org/10.1152/ajpheart.01187.2006

Giannini, G., Conti, A., Mammarella, S., Scrobogna, M., & Sorrentino, V. (1995). The ryanodine receptor/calcium channel genes are widely and differentially expressed in murine brain and peripheral tissues. *The Journal of cell biology*, 128(5), 893–904. https://doi.org/10.1083/jcb.128.5.893

Girgenrath, T., Mahalingam, M., Svensson, B., Nitu, F. R., Cornea, R. L., & Fessenden, J. D. (2013). N-terminal and central segments of the type 1 ryanodine receptor mediate its interaction with FK506-binding proteins. *The Journal of biological chemistry*, 288(22), 16073–16084. https://doi.org/10.1074/jbc.M113.463299

Goonasekera, S. A., Beard, N. A., Groom, L., Kimura, T., Lyfenko, A. D., Rosenfeld, A., Marty, I., Dulhunty, A. F., & Dirksen, R. T. (2007). Triadin binding to the C-terminal luminal loop of the ryanodine receptor is important for skeletal muscle excitation contraction coupling. *The Journal of general physiology*, 130(4), 365–378. https://doi.org/10.1085/jgp.200709790

Gordienko, D. V., & Bolton, T. B. (2002). Crosstalk between ryanodine receptors and IP(3) receptors as a factor shaping spontaneous Ca(2+)-release events in rabbit portal vein myocytes. *The Journal of physiology*, 542(Pt 3), 743–762. https://doi.org/10.1113/jphysiol.2001.015966

Grabner, M., Dirksen, R. T., Suda, N., & Beam, K. G. (1999). The II-III loop of the skeletal muscle dihydropyridine receptor is responsible for the Bi-directional coupling with the ryanodine receptor. *The Journal of biological chemistry*, 274(31), 21913–21919. https://doi.org/10.1074/jbc.274.31.21913

Guo, T., Cornea, R. L., Huke, S., Camors, E., Yang, Y., Picht, E., Fruen, B. R., & Bers, D. M. (2010). Kinetics of FKBP12.6 binding to ryanodine receptors in permeabilized cardiac myocytes and effects on Ca sparks. *Circulation research*, 106(11), 1743–1752. https://doi.org/10.1161/CIRCRESAHA.110.219816

Guo, W., & Campbell, K. P. (1995). Association of triadin with the ryanodine receptor and calsequestrin in the lumen of the sarcoplasmic reticulum. *The Journal of biological chemistry*, 270(16), 9027–9030. https://doi.org/10.1074/jbc.270.16.9027

Guo, W., Jorgensen, A. O., Jones, L. R., & Campbell, K. P. (1996). Biochemical characterization and molecular cloning of cardiac triadin. *The Journal of biological chemistry*, 271(1), 458–465. https://doi.org/10.1074/jbc.271.1.458

Gutteridge, S. (2003). *Ryanodine receptor polypeptides* (U.S. Patent No. 7.498,408) U.S. Patent and Trademark Office.

Györke, I., Hester, N., Jones, L. R., & Györke, S. (2004). The role of calsequestrin, triadin, and junctin in conferring cardiac ryanodine receptor responsiveness to luminal calcium. *Biophysical journal*, 86(4), 2121–2128. https://doi.org/10.1016/S0006-3495(04)74271-X

Györke, S., & Carnes, C. (2008). Dysregulated sarcoplasmic reticulum calcium release: potential pharmacological target in cardiac disease. *Pharmacology & therapeutics*, 119(3), 340–354. https://doi.org/10.1016/j.pharmthera.2008.06.002

Hachida, M., Kihara, S., Nonoyama, M., & Koyanagi, H. (1999). Protective effect of JTV519, a new 1,4-benzothiazepine derivative, on prolonged myocardial preservation. *Journal of cardiac surgery*, 14(3), 187–193. https://doi.org/10.1111/j.1540-8191.1999.tb00977.x

Hakamata, Y., Nakai, J., Takeshima, H., & Imoto, K. (1992). Primary structure and distribution of a novel ryanodine receptor/calcium release channel from rabbit brain. *FEBS letters*, 312(2-3), 229–235. https://doi.org/10.1016/0014-5793(92)80941-9

Hamilton, S. L., & Serysheva, I. I. (2009). Ryanodine receptor structure: progress and challenges. *The Journal of biological chemistry*, 284(7), 4047–4051. https://doi.org/10.1074/jbc.R800054200

Hanna, A. D., Lam, A., Thekkedam, C., Willemse, H., Dulhunty, A. F., & Beard, N. A. (2017). The Anthracycline Metabolite Doxorubicinol Abolishes RyR2 Sensitivity to Physiological Changes in Luminal Ca2+ through an Interaction with Calsequestrin. *Molecular pharmacology*, 92(5), 576–587. https://doi.org/10.1124/mol.117.108183

Harrison G. G. (1975). Control of the malignant hyperpyrexic syndrome in MHS swine by dantrolene sodium. *British journal of anaesthesia*, 47(1), 62–65. https://doi.org/10.1093/bja/47.1.62

Hayek, S. M., Zhao, J., Bhat, M., Xu, X., Nagaraj, R., Pan, Z., Takeshima, H., & Ma, J. (1999). A negatively charged region of the skeletal muscle ryanodine receptor is involved in Ca(2+)-dependent regulation of the Ca(2+) release channel. *FEBS letters*, 461(3), 157–164. https://doi.org/10.1016/s0014-5793(99)01464-7

Heitman, J., Movva, N. R., & Hall, M. N. (1991). Targets for cell cycle arrest by the immunosuppressant rapamycin in yeast. *Science (New York, N.Y.)*, 253(5022), 905–909. https://doi.org/10.1126/science.1715094

Hilliard, F. A., Steele, D. S., Laver, D., Yang, Z., Le Marchand, S. J., Chopra, N., Piston, D. W., Huke, S., & Knollmann, B. C. (2010). Flecainide inhibits arrhythmogenic Ca2+ waves by open state block of ryanodine receptor Ca2+ release channels and reduction of Ca2+ spark mass. *Journal of molecular and cellular cardiology*, 48(2), 293–301. https://doi.org/10.1016/j.yjmcc.2009.10.005

Hoeffer, C. A., Tang, W., Wong, H., Santillan, A., Patterson, R. J., Martinez, L. A., Tejada-Simon, M. V., Paylor, R., Hamilton, S. L., & Klann, E. (2008). Removal of FKBP12 enhances mTOR-Raptor interactions, LTP, memory, and perseverative/repetitive behavior. *Neuron*, 60(5), 832–845. https://doi.org/10.1016/j.neuron.2008.09.037

Holmes, B., & Heel, R. C. (1985). Flecainide. A preliminary review of its pharmacodynamic properties and therapeutic efficacy. *Drugs*, 29(1), 1–33. https://doi.org/10.2165/00003495-198529010-00001

Hong, C. S., Ji, J. H., Kim, J. P., Jung, D. H., & Kim, D. H. (2001). Molecular cloning and characterization of mouse cardiac triadin isoforms. *Gene*, 278(1-2), 193–199. https://doi.org/10.1016/s0378-1119(01)00718-1

Hong, T., & Shaw, R. M. (2017). Cardiac T-Tubule Microanatomy and Function. *Physiological reviews*, 97(1), 227–252. https://doi.org/10.1152/physrev.00037.2015

Horstick, E. J., Linsley, J. W., Dowling, J. J., Hauser, M. A., McDonald, K. K., Ashley-Koch, A., Saint-Amant, L., Satish, A., Cui, W. W., Zhou, W., Sprague, S. M., Stamm, D. S., Powell, C. M., Speer, M. C., Franzini-Armstrong, C., Hirata, H., & Kuwada, J. Y. (2013). Stac3 is a component of the excitation-contraction coupling machinery and mutated in Native American myopathy. *Nature communications*, 4, 1952. https://doi.org/10.1038/ncomms2952

Huai, Q., Kim, H. Y., Liu, Y., Zhao, Y., Mondragon, A., Liu, J. O., & Ke, H. (2002). Crystal structure of calcineurin-cyclophilin-cyclosporin shows common but distinct recognition of immunophilin-drug complexes. *Proceedings of the National Academy of Sciences of the United States of America*, 99(19), 12037–12042. https://doi.org/10.1073/pnas.192206699

Hudak, J. M., Banitt, E. H., & Schmid, J. R. (1984). Discovery and development of flecainide. *The American journal of cardiology*, 53(5), 17B–20B. https://doi.org/10.1016/0002-9149(84)90495-8

Huke, S., & Bers, D. M. (2008). Ryanodine receptor phosphorylation at Serine 2030, 2808 and 2814 in rat cardiomyocytes. *Biochemical and biophysical research communications*, 376(1), 80–85. https://doi.org/10.1016/j.bbrc.2008.08.084

Hunt, D. J., Jones, P. P., Wang, R., Chen, W., Bolstad, J., Chen, K., Shimoni, Y., & Chen, S. R. (2007). K201 (JTV519) suppresses spontaneous Ca2+ release and [3H]ryanodine binding to RyR2 irrespective of FKBP12.6 association. *The Biochemical journal*, 404(3), 431–438. https://doi.org/10.1042/BJ20070135

Hwang, H. S., Baldo, M. P., Rodriguez, J. P., Faggioni, M., & Knollmann, B. C. (2019). Efficacy of Flecainide in Catecholaminergic Polymorphic Ventricular Tachycardia Is Mutation-Independent but Reduced by Calcium Overload. *Frontiers in physiology*, 10, 992. https://doi.org/10.3389/fphys.2019.00992

Hymel, L., Inui, M., Fleischer, S., & Schindler, H. (1988). Purified ryanodine receptor of skeletal muscle sarcoplasmic reticulum forms Ca2+-activated oligomeric Ca2+ channels in planar bilayers. *Proceedings of the National Academy of Sciences of the United States of America*, 85(2), 441–445. https://doi.org/10.1073/pnas.85.2.441

Ikemoto, N., Bhatnagar, G. M., Nagy, B., & Gergely, J. (1972). Interaction of divalent cations with the 55,000-dalton protein component of the sarcoplasmic reticulum. Studies of fluorescence and circular dichroism. *The Journal of biological chemistry*, 247(23), 7835–7837.

Ikemoto, T., Takeshima, H., Iino, M., & Endo, M. (1998). Effect of calmodulin on Ca2+-induced Ca2+ release of skeletal muscle from mutant mice expressing either ryanodine receptor type 1 or type 3. *European journal of physiology*, 437(1), 43–48. https://doi.org/10.1007/s004240050744

Inui, M., Saito, A., & Fleischer, S. (1987). Isolation of the ryanodine receptor from cardiac sarcoplasmic reticulum and identity with the feet structures. The *Journal of biological chemistry*, 262(32), 15637–15642.

Ishikawa, Y., Holden, P., & Bächinger, H. P. (2017). Heat shock protein 47 and 65-kDa FK506-binding protein weakly but synergistically interact during collagen folding in the endoplasmic reticulum. *The Journal of biological chemistry*, 292(42), 17216–17224. https://doi.org/10.1074/jbc.M117.802298

Jayaraman, T., Brillantes, A. M., Timerman, A. P., Fleischer, S., Erdjument-Bromage, H., Tempst, P., & Marks, A. R. (1992). FK506 binding protein associated with the calcium release channel (ryanodine receptor). *The Journal of biological chemistry*, 267(14), 9474–9477.

Jerabek-Willemsen, M., Wienken, C. J., Braun, D., Baaske, P., & Duhr, S. (2011). Molecular interaction studies using microscale thermophoresis. *Assay and drug development technologies*, 9(4), 342–353. https://doi.org/10.1089/adt.2011.0380

Jeyakumar, L. H., Gleaves, L. A., Ridley, B. D., Chang, P., Atkinson, J., Barnett, J. V., & Fleischer, S. (2002). The skeletal muscle ryanodine receptor isoform 1 is found at the intercalated discs in human and mouse hearts. *Journal of muscle research and cell motility*, 23(4), 285–292. https://doi.org/10.1023/a:1022091931677

Ji, G., Feldman, M. E., Greene, K. S., Sorrentino, V., Xin, H. B., & Kotlikoff, M. I. (2004). RYR2 proteins contribute to the formation of Ca(2+) sparks in smooth muscle. *The Journal of general physiology*, 123(4), 377–386. https://doi.org/10.1085/jgp.200308999

Jiang, D., Wang, R., Xiao, B., Kong, H., Hunt, D. J., Choi, P., Zhang, L., & Chen, S. R. (2005). Enhanced store overload-induced Ca2+ release and channel sensitivity to luminal Ca2+ activation are common defects of RyR2 mutations linked to ventricular tachycardia and sudden death. *Circulation research*, 97(11), 1173–1181. https://doi.org/10.1161/01.RES.0000192146.85173.4b

Jiang, D., Xiao, B., Yang, D., Wang, R., Choi, P., Zhang, L., Cheng, H., & Chen, S. R. (2004). RyR2 mutations linked to ventricular tachycardia and sudden death reduce the threshold for store-overload-induced Ca2+ release (SOICR). *Proceedings of the National Academy of Sciences of the United States of America*, 101(35), 13062–13067. https://doi.org/10.1073/pnas.0402388101

Johnson, J., Corbisier, R., Stensgard, B., & Toft, D. (1996). The involvement of p23, hsp90, and immunophilins in the assembly of progesterone receptor complexes. *The Journal of steroid biochemistry and molecular biology*, 56(1-6 Spec No), 31–37. https://doi.org/10.1016/0960-0760(95)00221-9

Jones, L. R., Suzuki, Y. J., Wang, W., Kobayashi, Y. M., Ramesh, V., Franzini-Armstrong, C., Cleemann, L., & Morad, M. (1998). Regulation of Ca2+ signaling in transgenic mouse cardiac myocytes overexpressing calsequestrin. *The Journal of clinical investigation*, 101(7), 1385–1393. https://doi.org/10.1172/JCI1362

Jones, L. R., Zhang, L., Sanborn, K., Jorgensen, A. O., & Kelley, J. (1995). Purification, primary structure, and immunological characterization of the 26-kDa calsequestrin binding protein (junctin) from cardiac junctional sarcoplasmic reticulum. *The Journal of biological chemistry*, 270(51), 30787–30796. https://doi.org/10.1074/jbc.270.51.30787

Jungbluth H. (2007). Multi-minicore Disease. *Orphanet journal of rare diseases*, 2, 31. https://doi.org/10.1186/1750-1172-2-31

Jungbluth, H., Sewry, C. A., & Muntoni, F. (2003). What's new in neuromuscular disorders? The congenital myopathies. *European journal of paediatric neurology: EJPN: official journal of the European Paediatric Neurology Society*, 7(1), 23–30. https://doi.org/10.1016/s1090-3798(02)00136-8

Kaftan, E., Marks, A. R., & Ehrlich, B. E. (1996). Effects of rapamycin on ryanodine receptor/Ca(2+)-release channels from cardiac muscle. *Circulation research*, 78(6), 990–997. https://doi.org/10.1161/01.res.78.6.990

Kandel, E. R., Schwartz, J. H., Jessell, T. M., Siegelbaum, S. A., Hudspeth, A. J., & Mack, S. (2013). *Principles of neural science* (Fifth edition.). New York, N.Y.: McGraw-Hill Education LLC.

Kaneko, N. (1994). New 1,4-benzothiazepine derivative, K201, demonstrates cardioprotective effects against sudden cardiac cell death and intracellular calcium blocking action. *Drug Development Research*, 33(4), 429–438. https://doi.org/10.1002/ddr.430330406

Karlin A. (1967). On the application of "a plausible model" of allosteric proteins to the receptor for acetylcholine. *Journal of theoretical biology*, 16(2), 306–320. https://doi.org/10.1016/0022-5193(67)90011-2

Kay, J. E., Kromwel, L., Doe, S. E., & Denyer, M. (1991). Inhibition of T and B lymphocyte proliferation by rapamycin. *Immunology*, 72(4), 544–549.

Ke, H., & Huai, Q. (2003). Structures of calcineurin and its complexes with immunophilins-immunosuppressants. *Biochemical and biophysical research communications*, 311(4), 1095–1102. https://doi.org/10.1016/s0006-291x(03)01537-7

Kermode, H., Williams, A. J., & Sitsapesan, R. (1998). The interactions of ATP, ADP, and inorganic phosphate with the sheep cardiac ryanodine receptor. *Biophysical journal*, 74(3), 1296–1304. https://doi.org/10.1016/S0006-3495(98)77843-9

Kihira, T., Hironishi, M., Utunomiya, H., & Kondo, T. (2002). FKBP12 immunoreactivity in the human spinal cord of motor neuron disease patients. *Neuropathology: official journal of the Japanese Society of Neuropathology*, 22(4), 269–274. https://doi.org/10.1046/j.1440-1789.2002.00452.x

Kihira, T., Utunomiya, H., & Kondo, T. (2005). Expression of FKBP12 and ryanodine receptors (RyRs) in the spinal cord of MND patients. *Amyotrophic lateral sclerosis and other motor neuron disorders: official publication of the World Federation of Neurology, Research Group on Motor Neuron Diseases*, 6(2), 94–99. https://doi.org/10.1080/14660820510034442

Kim, K. C., Caswell, A. H., Talvenheimo, J. A., & Brandt, N. R. (1990). Isolation of a terminal cisterna protein which may link the dihydropyridine receptor to the junctional foot protein in skeletal muscle. *Biochemistry*, 29(39), 9281–9289. https://doi.org/10.1021/bi00491a025

Kobayashi, Y. M., & Jones, L. R. (1999). Identification of triadin 1 as the predominant triadin isoform expressed in mammalian myocardium. *The Journal of biological chemistry*, 274(40), 28660–28668. https://doi.org/10.1074/jbc.274.40.28660

Kohn, T. A., Burroughs, R., Hartman, M. J., & Noakes, T. D. (2011). Fiber type and metabolic characteristics of lion (Panthera leo), caracal (Caracal caracal) and human skeletal muscle. *Comparative biochemistry and physiology. Part A, Molecular & integrative physiology*, 159(2), 125–133. https://doi.org/10.1016/j.cbpa.2011.02.006

Koide, M., Nystoriak, M. A., Krishnamoorthy, G., O'Connor, K. P., Bonev, A. D., Nelson, M. T., & Wellman, G. C. (2011). Reduced Ca2+ spark activity after subarachnoid hemorrhage disables BK channel control of cerebral artery tone. *Journal of cerebral blood flow and metabolism: official journal of the International Society of Cerebral Blood Flow and Metabolism*, 31(1), 3–16. https://doi.org/10.1038/jcbfm.2010.143

Kugler, G., Weiss, R. G., Flucher, B. E., & Grabner, M. (2004). Structural requirements of the dihydropyridine receptor alpha1S II-III loop for skeletal-type excitation-contraction coupling. *The Journal of biological chemistry*, 279(6), 4721–4728. https://doi.org/10.1074/jbc.M307538200

Kuwajima, G., Futatsugi, A., Niinobe, M., Nakanishi, S., & Mikoshiba, K. (1992). Two types of ryanodine receptors in mouse brain: skeletal muscle type exclusively in Purkinje cells and cardiac muscle type in various neurons. *Neuron*, 9(6), 1133–1142. https://doi.org/10.1016/0896-6273(92)90071-k

Laemmli U. K. (1970). Cleavage of structural proteins during the assembly of the head of bacteriophage T4. *Nature*, 227(5259), 680–685. https://doi.org/10.1038/227680a0

Lahat, H., Pras, E., & Eldar, M. (2004). A missense mutation in CASQ2 is associated with autosomal recessive catecholamine-induced polymorphic ventricular tachycardia in Bedouin families from Israel. *Annals of medicine*, 36 Suppl 1, 87–91. https://doi.org/10.1080/17431380410032517

Lahm, G. P., Stevenson, T. M., Selby, T. P., Freudenberger, J. H., Cordova, D., Flexner, L., Bellin, C. A., Dubas, C. M., Smith, B. K., Hughes, K. A., Hollingshaus, J. G., Clark, C. E., & Benner, E. A. (2007). Rynaxypyr: a new insecticidal anthranilic diamide that acts as a potent and selective ryanodine

receptor activator. *Bioorganic & medicinal chemistry letters*, 17(22), 6274–6279. https://doi.org/10.1016/j.bmcl.2007.09.012

Lai, F. A., Dent, M., Wickenden, C., Xu, L., Kumari, G., Misra, M., Lee, H. B., Sar, M., & Meissner, G. (1992). Expression of a cardiac Ca(2+)-release channel isoform in mammalian brain. *The Biochemical journal*, 288, 553–564. https://doi.org/10.1042/bj2880553

Lai, F. A., Misra, M., Xu, L., Smith, H. A., & Meissner, G. (1989). The ryanodine receptor-Ca2+ release channel complex of skeletal muscle sarcoplasmic reticulum. Evidence for a cooperatively coupled, negatively charged homotetramer. *The Journal of biological chemistry*, 264(28), 16776–16785.

Laitinen, P. J., Swan, H., & Kontula, K. (2003). Molecular genetics of exercise-induced polymorphic ventricular tachycardia: identification of three novel cardiac ryanodine receptor mutations and two common calsequestrin 2 amino-acid polymorphisms. *European journal of human genetics: EJHG*, 11(11), 888–891. https://doi.org/10.1038/sj.ejhg.5201061

Lam, E., Martin, M. M., Timerman, A. P., Sabers, C., Fleischer, S., Lukas, T., Abraham, R. T., O'Keefe, S. J., O'Neill, E. A., & Wiederrecht, G. J. (1995). A novel FK506 binding protein can mediate the immunosuppressive effects of FK506 and is associated with the cardiac ryanodine receptor. *The Journal of biological chemistry*, 270(44), 26511–26522. https://doi.org/10.1074/jbc.270.44.26511

Lamb, G. D., & Stephenson, D. G. (1991). Effect of Mg2+ on the control of Ca2+ release in skeletal muscle fibres of the toad. *The Journal of physiology*, 434, 507–528. https://doi.org/10.1113/jphysiol.1991.sp018483

Lamb, G. D., & Stephenson, D. G. (1994). Effects of intracellular pH and [Mg2+] on excitation-contraction coupling in skeletal muscle fibres of the rat. *The Journal of physiology*, 478, 331–339. https://doi.org/10.1113/jphysiol.1994.sp020253

Lanner, J. T., Georgiou, D. K., Joshi, A. D., & Hamilton, S. L. (2010). Ryanodine receptors: structure, expression, molecular details, and function in calcium

release. *Cold Spring Harbor perspectives in biology*, 2(11), a003996. https://doi.org/10.1101/cshperspect.a003996

Larsen, S., Nielsen, J., Hansen, C. N., Nielsen, L. B., Wibrand, F., Stride, N., Schroder, H. D., Boushel, R., Helge, J. W., Dela, F., & Hey-Mogensen, M. (2012). Biomarkers of mitochondrial content in skeletal muscle of healthy young human subjects. *The Journal of physiology*, 590(14), 3349–3360. https://doi.org/10.1113/jphysiol.2012.230185

Laver D. R. (2007). Ca2+ stores regulate ryanodine receptor Ca2+ release channels via luminal and cytosolic Ca2+ sites. *Biophysical journal*, 92(10), 3541–3555. https://doi.org/10.1529/biophysj.106.099028

Laver D. R. (2010). Regulation of RyR Channel Gating by Ca(2+), Mg(2+) and ATP. *Current topics in membranes*, 66, 69–89. https://doi.org/10.1016/S1063-5823(10)66004-8

Laver D. R. (2018). Regulation of the RyR channel gating by Ca2+ and Mg2. *Biophysical reviews*, 10(4), 1087–1095. https://doi.org/10.1007/s12551-018-0433-4

Laver, D. R., & Honen, B. N. (2008). Luminal Mg2+, a key factor controlling RYR2-mediated Ca2+ release: cytoplasmic and luminal regulation modeled in a tetrameric channel. *The Journal of general physiology*, 132(4), 429–446. https://doi.org/10.1085/jgp.200810001

Laver, D. R., Baynes, T. M., & Dulhunty, A. F. (1997). Magnesium inhibition of ryanodine-receptor calcium channels: evidence for two independent mechanisms. *The Journal of membrane biology*, 156(3), 213–229. https://doi.org/10.1007/s002329900202

Laver, D. R., Lenz, G. K., & Lamb, G. D. (2001). Regulation of the calcium release channel from rabbit skeletal muscle by the nucleotides ATP, AMP, IMP and adenosine. *The Journal of physiology*, 537(Pt 3), 763–778. https://doi.org/10.1111/j.1469-7793.2001.00763.x

Laver, D. R., O'Neill, E. R., & Lamb, G. D. (2004). Luminal Ca2+-regulated Mg2+ inhibition of skeletal RyRs reconstituted as isolated channels or coupled

clusters. *The Journal of general physiology*, 124(6), 741–758. https://doi.org/10.1085/jgp.200409092

Laver, D. R., Roden, L. D., Ahern, G. P., Eager, K. R., Junankar, P. R., & Dulhunty, A. F. (1995). Cytoplasmic Ca2+ inhibits the ryanodine receptor from cardiac muscle. *The Journal of membrane biology*, 147(1), 7–22. https://doi.org/10.1007/BF00235394

Law B. K. (2005). Rapamycin: an anti-cancer immunosuppressant?. *Critical reviews in oncology/hematology*, 56(1), 47–60. https://doi.org/10.1016/j.critrevonc.2004.09.009

Lawal, T. A., Wires, E. S., Terry, N. L., Dowling, J. J., & Todd, J. J. (2020). Preclinical model systems of ryanodine receptor 1-related myopathies and malignant hyperthermia: a comprehensive scoping review of works published 1990-2019. *Orphanet journal of rare diseases*, 15(1), 113. https://doi.org/10.1186/s13023-020-01384-x

Lawrence, J. C., Lin, T. A., McMahon, L. P., & Choi, K. M. (2004). Modulation of the protein kinase activity of mTOR. *Current topics in microbiology and immunology*, 279, 199–213. https://doi.org/10.1007/978-3-642-18930-2_12

Lee, B. S., Sessanna, S., Laychock, S. G., & Rubin, R. P. (2002). Expression and cellular localization of a modified type 1 ryanodine receptor and L-type channel proteins in non-muscle cells. *The Journal of membrane biology*, 189(3), 181–190. https://doi.org/10.1007/s00232-002-1012-x

Lee, C. S., Georgiou, D. K., Dagnino-Acosta, A., Xu, J., Ismailov, I. I., Knoblauch, M., Monroe, T. O., Ji, R., Hanna, A. D., Joshi, A. D., Long, C., Oakes, J., Tran, T., Corona, B. T., Lorca, S., Ingalls, C. P., Narkar, V. A., Lanner, J. T., Bayle, J. H., Durham, W. J., … Hamilton, S. L. (2014). Ligands for FKBP12 increase Ca2+ influx and protein synthesis to improve skeletal muscle function. *The Journal of biological chemistry*, 289(37), 25556–25570. https://doi.org/10.1074/jbc.M114.586289

Lee, H. B., Xu, L., & Meissner, G. (1994). Reconstitution of the skeletal muscle ryanodine receptor-Ca2+ release channel protein complex into proteoliposomes. *The Journal of biological chemistry*, 269(18), 13305–13312.

Lee, J. M., Rho, S. H., Shin, D. W., Cho, C., Park, W. J., Eom, S. H., Ma, J., & Kim, D. H. (2004). Negatively charged amino acids within the intraluminal loop of ryanodine receptor are involved in the interaction with triadin. *The Journal of biological chemistry*, 279(8), 6994–7000. https://doi.org/10.1074/jbc.M312446200

Lehnart, S. E., Mongillo, M., Bellinger, A., Lindegger, N., Chen, B. X., Hsueh, W., Reiken, S., Wronska, A., Drew, L. J., Ward, C. W., Lederer, W. J., Kass, R. S., Morley, G., & Marks, A. R. (2008). Leaky Ca2+ release channel/ryanodine receptor 2 causes seizures and sudden cardiac death in mice. *The Journal of clinical investigation*, 118(6), 2230–2245. https://doi.org/10.1172/JCI35346

Li, L., Mirza, S., Richardson, S. J., Gallant, E. M., Thekkedam, C., Pace, S. M., Zorzato, F., Liu, D., Beard, N. A., & Dulhunty, A. F. (2015). A new cytoplasmic interaction between junctin and ryanodine receptor Ca2+ release channels. *Journal of cell science*, 128(5), 951–963. https://doi.org/10.1242/jcs.160689

Liao, B., Zheng, Y. M., Yadav, V. R., Korde, A. S., & Wang, Y. X. (2011). Hypoxia induces intracellular Ca2+ release by causing reactive oxygen species-mediated dissociation of FK506-binding protein 12.6 from ryanodine receptor 2 in pulmonary artery myocytes. *Antioxidants & redox signaling*, 14(1), 37–47. https://doi.org/10.1089/ars.2009.3047

Lim, K. Y., Hong, C. S., & Kim, D. H. (2000). cDNA cloning and characterization of human cardiac junctin. *Gene*, 255(1), 35–42. https://doi.org/10.1016/s0378-1119(00)00299-7

Lindsay, A. R., Manning, S. D., & Williams, A. J. (1991). Monovalent cation conductance in the ryanodine receptor-channel of sheep cardiac muscle sarcoplasmic reticulum. *The Journal of physiology*, 439, 463–480. https://doi.org/10.1113/jphysiol.1991.sp018676

Liu, J., Farmer, J. D., Jr, Lane, W. S., Friedman, J., Weissman, I., & Schreiber, S. L. (1991). Calcineurin is a common target of cyclophilin-cyclosporin A and FKBP-FK506 complexes. *Cell*, 66(4), 807–815. https://doi.org/10.1016/0092-8674(91)90124-h

Liu, X., Betzenhauser, M. J., Reiken, S., Meli, A. C., Xie, W., Chen, B. X., Arancio, O., & Marks, A. R. (2012). Role of leaky neuronal ryanodine receptors in stress-induced cognitive dysfunction. *Cell*, 150(5), 1055–1067. https://doi.org/10.1016/j.cell.2012.06.052

Lopez, R. J., Byrne, S., Vukcevic, M., Sekulic-Jablanovic, M., Xu, L., Brink, M., Alamelu, J., Voermans, N., Snoeck, M., Clement, E., Muntoni, F., Zhou, H., Radunovic, A., Mohammed, S., Wraige, E., Zorzato, F., Treves, S., & Jungbluth, H. (2016). An RYR1 mutation associated with malignant hyperthermia is also associated with bleeding abnormalities. *Science signaling*, 9(435), ra68. https://doi.org/10.1126/scisignal.aad9813

Loughrey, C. M., Seidler, T., Miller, S. L., Prestle, J., MacEachern, K. E., Reynolds, D. F., Hasenfuss, G., & Smith, G. L. (2004). Over-expression of FK506-binding protein FKBP12.6 alters excitation-contraction coupling in adult rabbit cardiomyocytes. *The Journal of physiology*, 556(Pt 3), 919–934. https://doi.org/10.1113/jphysiol.2003.057166

MacLennan, D. H., Duff, C., Zorzato, F., Fujii, J., Phillips, M., Korneluk, R. G., Frodis, W., Britt, B. A., & Worton, R. G. (1990). Ryanodine receptor gene is a candidate for predisposition to malignant hyperthermia. *Nature*, 343(6258), 559–561. https://doi.org/10.1038/343559a0

MacMillan, D., Currie, S., & McCarron, J. G. (2008). FK506-binding protein (FKBP12) regulates ryanodine receptor-evoked Ca2+ release in colonic but not aortic smooth muscle. *Cell calcium*, 43(6), 539–549. https://doi.org/10.1016/j.ceca.2007.09.002

MacMillan, D., Currie, S., Bradley, K. N., Muir, T. C., & McCarron, J. G. (2005). In smooth muscle, FK506-binding protein modulates IP3 receptor-evoked Ca2+ release by mTOR and calcineurin. *Journal of cell science*, 118(Pt 23), 5443–5451. https://doi.org/10.1242/jcs.02657

Mahalingam, M., Perez, C. F., & Fessenden, J. D. (2016). Fluorescence Resonance Energy Transfer-based Structural Analysis of the Dihydropyridine Receptor α1S Subunit Reveals Conformational Differences Induced by Binding of the

β1a Subunit. *The Journal of biological chemistry*, 291(26), 13762–13770. https://doi.org/10.1074/jbc.M115.704049

Maier, L. S., & Bers, D. M. (2002). Calcium, calmodulin, and calcium-calmodulin kinase II: heartbeat to heartbeat and beyond. *Journal of molecular and cellular cardiology*, 34(8), 919–939. https://doi.org/10.1006/jmcc.2002.2038

Marchant, J. S., & Taylor, C. W. (1997). Cooperative activation of IP3 receptors by sequential binding of IP3 and Ca2+ safeguards against spontaneous activity. *Current biology: CB*, 7(7), 510–518. https://doi.org/10.1016/s0960-9822(06)00222-3

Marengo, J. J., Hidalgo, C., & Bull, R. (1998). Sulfhydryl oxidation modifies the calcium dependence of ryanodine-sensitive calcium channels of excitable cells. *Biophysical journal*, 74(3), 1263–1277. https://doi.org/10.1016/S0006-3495(98)77840-3

Marks A. R. (2002). Clinical implications of cardiac ryanodine receptor/calcium release channel mutations linked to sudden cardiac death. *Circulation*, 106(1), 8–10. https://doi.org/10.1161/01.cir.0000021746.82888.83

Marks, A. R., Tempst, P., Hwang, K. S., Taubman, M. B., Inui, M., Chadwick, C., Fleischer, S., & Nadal-Ginard, B. (1989). Molecular cloning and characterization of the ryanodine receptor/junctional channel complex cDNA from skeletal muscle sarcoplasmic reticulum. *Proceedings of the National Academy of Sciences of the United States of America*, 86(22), 8683–8687. https://doi.org/10.1073/pnas.86.22.8683

Marty, I., Thevenon, D., Scotto, C., Groh, S., Sainnier, S., Robert, M., Grunwald, D., & Villaz, M. (2000). Cloning and characterization of a new isoform of skeletal muscle triadin. *The Journal of biological chemistry*, 275(11), 8206–8212. https://doi.org/10.1074/jbc.275.11.8206

Maruyama, M., Li, B. Y., Chen, H., Xu, X., Song, L. S., Guatimosim, S., Zhu, W., Yong, W., Zhang, W., Bu, G., Lin, S. F., Fishbein, M. C., Lederer, W. J., Schild, J. H., Field, L. J., Rubart, M., Chen, P. S., & Shou, W. (2011). FKBP12 is a critical regulator of the heart rhythm and the cardiac voltage-gated sodium

current in mice. *Circulation research*, 108(9), 1042–1052. https://doi.org/10.1161/CIRCRESAHA.110.237867

Marx, S. O., Gaburjakova, J., Gaburjakova, M., Henrikson, C., Ondrias, K., & Marks, A. R. (2001). Coupled gating between cardiac calcium release channels (ryanodine receptors). *Circulation research*, 88(11), 1151–1158. https://doi.org/10.1161/hh1101.091268

Marx, S. O., Ondrias, K., & Marks, A. R. (1998). Coupled gating between individual skeletal muscle Ca2+ release channels (ryanodine receptors). *Science (New York, N.Y.)*, 281(5378), 818–821. https://doi.org/10.1126/science.281.5378.818

Marx, S. O., Reiken, S., Hisamatsu, Y., Jayaraman, T., Burkhoff, D., Rosemblit, N., & Marks, A. R. (2000). PKA phosphorylation dissociates FKBP12.6 from the calcium release channel (ryanodine receptor): defective regulation in failing hearts. *Cell*, 101(4), 365–376. https://doi.org/10.1016/s0092-8674(00)80847-8

Maryon, E. B., Coronado, R., & Anderson, P. (1996). unc-68 encodes a ryanodine receptor involved in regulating C. elegans body-wall muscle contraction. *The Journal of cell biology*, 134(4), 885–893. https://doi.org/10.1083/jcb.134.4.885

Masumiya, H., Wang, R., Zhang, J., Xiao, B., & Chen, S. R. (2003). Localization of the 12.6-kDa FK506-binding protein (FKBP12.6) binding site to the NH2-terminal domain of the cardiac Ca2+ release channel (ryanodine receptor). *The Journal of biological chemistry*, 278(6), 3786–3792. https://doi.org/10.1074/jbc.M210962200

Matecki, S., Dridi, H., Jung, B., Saint, N., Reiken, S. R., Scheuermann, V., Mrozek, S., Santulli, G., Umanskaya, A., Petrof, B. J., Jaber, S., Marks, A. R., & Lacampagne, A. (2016). Leaky ryanodine receptors contribute to diaphragmatic weakness during mechanical ventilation. *Proceedings of the National Academy of Sciences of the United States of America*, 113(32), 9069–9074. https://doi.org/10.1073/pnas.1609707113

Mattei, M. G., Giannini, G., Moscatelli, F., & Sorrentino, V. (1994). Chromosomal localization of murine ryanodine receptor genes RYR1, RYR2, and RYR3 by

in situ hybridization. *Genomics*, 22(1), 202–204. https://doi.org/10.1006/geno.1994.1362

Matthews, E., Neuwirth, C., Jaffer, F., Scalco, R. S., Fialho, D., Parton, M., Raja Rayan, D., Suetterlin, K., Sud, R., Spiegel, R., Mein, R., Houlden, H., Schaefer, A., Healy, E., Palace, J., Quinlivan, R., Treves, S., Holton, J. L., Jungbluth, H., & Hanna, M. G. (2018). Atypical periodic paralysis and myalgia: A novel RYR1 phenotype. *Neurology*, 90(5), e412–e418. https://doi.org/10.1212/WNL.0000000000004894

Mayrleitner, M., Timerman, A. P., Wiederrecht, G., & Fleischer, S. (1994). The calcium release channel of sarcoplasmic reticulum is modulated by FK-506 binding protein: effect of FKBP-12 on single channel activity of the skeletal muscle ryanodine receptor. *Cell calcium*, 15(2), 99–108. https://doi.org/10.1016/0143-4160(94)90048-5

McCall, E., Li, L., Satoh, H., Shannon, T. R., Blatter, L. A., & Bers, D. M. (1996). Effects of FK-506 on contraction and Ca2+ transients in rat cardiac myocytes. *Circulation research*, 79(6), 1110–1121. https://doi.org/10.1161/01.res.79.6.1110

Mei, Y., Xu, L., Kramer, H. F., Tomberlin, G. H., Townsend, C., & Meissner, G. (2013). Stabilization of the skeletal muscle ryanodine receptor ion channel-FKBP12 complex by the 1,4-benzothiazepine derivative S107. *PloS one*, 8(1), e54208. https://doi.org/10.1371/journal.pone.0054208

Meissner G. (1973). ATP and Ca2+ binding by the Ca2+ pump protein of sarcoplasmic reticulum. *Biochimica et biophysica acta*, 298(4), 906–926. https://doi.org/10.1016/0005-2736(73)90395-7

Meissner G. (1984). Adenine nucleotide stimulation of Ca2+-induced Ca2+ release in sarcoplasmic reticulum. *The Journal of biological chemistry*, 259(4), 2365–2374.

Meissner G. (1986). Ryanodine activation and inhibition of the Ca2+ release channel of sarcoplasmic reticulum. *The Journal of biological chemistry*, 261(14), 6300–6306.

Meissner G. (1994). Ryanodine receptor/Ca2+ release channels and their regulation by endogenous effectors. *Annual review of physiology*, 56, 485–508. https://doi.org/10.1146/annurev.ph.56.030194.002413

Meng, X., Wang, G., Viero, C., Wang, Q., Mi, W., Su, X. D., Wagenknecht, T., Williams, A. J., Liu, Z., & Yin, C. C. (2009). CLIC2-RyR1 interaction and structural characterization by cryo-electron microscopy. *Journal of molecular biology*, 387(2), 320–334. https://doi.org/10.1016/j.jmb.2009.01.059

Mickelson, J. R., & Louis, C. F. (1996). Malignant hyperthermia: excitation-contraction coupling, Ca2+ release channel, and cell Ca2+ regulation defects. *Physiological reviews*, 76(2), 537–592. https://doi.org/10.1152/physrev.1996.76.2.537

Mitchell, R. D., Simmerman, H. K., & Jones, L. R. (1988). Ca2+ binding effects on protein conformation and protein interactions of canine cardiac calsequestrin. *The Journal of biological chemistry*, 263(3), 1376–1381.

Monnier, N., Romero, N. B., Lerale, J., Nivoche, Y., Qi, D., MacLennan, D. H., Fardeau, M., & Lunardi, J. (2000). An autosomal dominant congenital myopathy with cores and rods is associated with a neomutation in the RYR1 gene encoding the skeletal muscle ryanodine receptor. *Human molecular genetics*, 9(18), 2599–2608. https://doi.org/10.1093/hmg/9.18.2599

Moore, C. P., Rodney, G., Zhang, J. Z., Santacruz-Toloza, L., Strasburg, G., & Hamilton, S. L. (1999). Apocalmodulin and Ca2+ calmodulin bind to the same region on the skeletal muscle Ca2+ release channel. *Biochemistry*, 38(26), 8532–8537. https://doi.org/10.1021/bi9907431

Nakai, J., Imagawa, T., Hakamat, Y., Shigekawa, M., Takeshima, H., & Numa, S. (1990). Primary structure and functional expression from cDNA of the cardiac ryanodine receptor/calcium release channel. *FEBS letters*, 271(1-2), 169–177. https://doi.org/10.1016/0014-5793(90)80399-4

Nakai, J., Tanabe, T., Konno, T., Adams, B., & Beam, K. G. (1998). Localization in the II-III loop of the dihydropyridine receptor of a sequence critical for excitation-contraction coupling. *The Journal of biological chemistry*, 273(39), 24983–24986. https://doi.org/10.1074/jbc.273.39.24983

Nakanishi, S., Kuwajima, G., & Mikoshiba, K. (1992). Immunohistochemical localization of ryanodine receptors in mouse central nervous system. *Neuroscience research*, 15(1-2), 130–142. https://doi.org/10.1016/0168-0102(92)90026-9

Nakaya, H., Furusawa, Y., Ogura, T., Tamagawa, M., & Uemura, H. (2000). Inhibitory effects of JTV-519, a novel cardioprotective drug, on potassium currents and experimental atrial fibrillation in guinea-pig hearts. *British journal of pharmacology*, 131(7), 1363–1372. https://doi.org/10.1038/sj.bjp.0703713

Narita, A., Yasunaga, T., Ishikawa, T., Mayanagi, K., & Wakabayashi, T. (2001). Ca(2+)-induced switching of troponin and tropomyosin on actin filaments as revealed by electron cryo-microscopy. *Journal of molecular biology*, 308(2), 241–261. https://doi.org/10.1006/jmbi.2001.4598

Neef, S., Dybkova, N., Sossalla, S., Ort, K. R., Fluschnik, N., Neumann, K., Seipelt, R., Schöndube, F. A., Hasenfuss, G., & Maier, L. S. (2010). CaMKII-dependent diastolic SR Ca2+ leak and elevated diastolic Ca2+ levels in right atrial myocardium of patients with atrial fibrillation. *Circulation research*, 106(6), 1134–1144. https://doi.org/10.1161/CIRCRESAHA.109.203836

Nelson, B. R., Wu, F., Liu, Y., Anderson, D. M., McAnally, J., Lin, W., Cannon, S. C., Bassel-Duby, R., & Olson, E. N. (2013). Skeletal muscle-specific T-tubule protein STAC3 mediates voltage-induced Ca2+ release and contractility. *Proceedings of the National Academy of Sciences of the United States of America*, 110(29), 11881–11886. https://doi.org/10.1073/pnas.1310571110

Nelson, T. E., Lin, M., Zapata-Sudo, G., & Sudo, R. T. (1996). Dantrolene sodium can increase or attenuate activity of skeletal muscle ryanodine receptor calcium release channel. Clinical implications. *Anesthesiology*, 84(6), 1368–1379. https://doi.org/10.1097/00000542-199606000-00013

Neylon, C. B., Richards, S. M., Larsen, M. A., Agrotis, A., & Bobik, A. (1995). Multiple types of ryanodine receptor/Ca2+ release channels are expressed in vascular smooth muscle. *Biochemical and biophysical research communications*, 215(3), 814–821. https://doi.org/10.1006/bbrc.1995.2536

Niu, J., Dick, I. E., Yang, W., Bamgboye, M. A., Yue, D. T., Tomaselli, G., Inoue, T., & Ben-Johny, M. (2018b). Allosteric regulators selectively prevent Ca2+-feedback of CaV and NaV channels. *eLife*, 7, e35222. https://doi.org/10.7554/eLife.35222

Niu, J., Yang, W., Yue, D. T., Inoue, T., & Ben-Johny, M. (2018a). Duplex signaling by CaM and Stac3 enhances CaV1.1 function and provides insights into congenital myopathy. *The Journal of general physiology*, 150(8), 1145–1161. https://doi.org/10.1085/jgp.201812005

Nomikos, M., Thanassoulas, A., Beck, K., Vassilakopoulou, V., Hu, H., Calver, B. L., Theodoridou, M., Kashir, J., Blayney, L., Livaniou, E., Rizkallah, P., Nounesis, G., & Lai, F. A. (2014). Altered RyR2 regulation by the calmodulin F90L mutation associated with idiopathic ventricular fibrillation and early sudden cardiac death. *FEBS letters*, 588(17), 2898–2902. https://doi.org/10.1016/j.febslet.2014.07.007

Nyegaard, M., Overgaard, M. T., Søndergaard, M. T., Vranas, M., Behr, E. R., Hildebrandt, L. L., Lund, J., Hedley, P. L., Camm, A. J., Wettrell, G., Fosdal, I., Christiansen, M., & Børglum, A. D. (2012). Mutations in calmodulin cause ventricular tachycardia and sudden cardiac death. *American journal of human genetics*, 91(4), 703–712. https://doi.org/10.1016/j.ajhg.2012.08.015

Oda, T., Yang, Y., Uchinoumi, H., Thomas, D. D., Chen-Izu, Y., Kato, T., Yamamoto, T., Yano, M., Cornea, R. L., & Bers, D. M. (2015). Oxidation of ryanodine receptor (RyR) and calmodulin enhance Ca release and pathologically alter, RyR structure and calmodulin affinity. *Journal of molecular and cellular cardiology*, 85, 240–248. https://doi.org/10.1016/j.yjmcc.2015.06.009

Olubando, D., Hopton, C., Eden, J., Caswell, R., Lowri Thomas, N., Roberts, S. A., Morris-Rosendahl, D., Venetucci, L., & Newman, W. G. (2020). Classification and correlation of RYR2 missense variants in individuals with catecholaminergic polymorphic ventricular tachycardia reveals phenotypic relationships. *Journal of human genetics*, 65(6), 531–539. https://doi.org/10.1038/s10038-020-0738-6

Ondrias, K., Marx, S. O., Gaburjakova, M., & Marks, A. R. (1998). FKBP12 modulates gating of the ryanodine receptor/calcium release channel. *Annals of the New York Academy of Sciences*, 853, 149–156. https://doi.org/10.1111/j.1749-6632.1998.tb08263.x

Oo, Y. W., Gomez-Hurtado, N., Walweel, K., van Helden, D. F., Imtiaz, M. S., Knollmann, B. C., & Laver, D. R. (2015). Essential Role of Calmodulin in RyR Inhibition by Dantrolene. *Molecular pharmacology*, 88(1), 57–63. https://doi.org/10.1124/mol.115.097691

Otsu, K., Willard, H. F., Khanna, V. K., Zorzato, F., Green, N. M., & MacLennan, D. H. (1990). Molecular cloning of cDNA encoding the Ca2+ release channel (ryanodine receptor) of rabbit cardiac muscle sarcoplasmic reticulum. *The Journal of biological chemistry*, 265(23), 13472–13483.

Ottini, L., Marziali, G., Conti, A., Charlesworth, A., & Sorrentino, V. (1996). Alpha and beta isoforms of ryanodine receptor from chicken skeletal muscle are the homologues of mammalian RyR1 and RyR3. *The Biochemical journal*, 315, 207–216. https://doi.org/10.1042/bj3150207

Oyamada, H., Murayama, T., Takagi, T., Iino, M., Iwabe, N., Miyata, T., Ogawa, Y., & Endo, M. (1994). Primary structure and distribution of ryanodine-binding protein isoforms of the bullfrog skeletal muscle. *The Journal of biological chemistry*, 269(25), 17206–17214.

Page, E., & Surdyk-Droske, M. (1979). Distribution, surface density, and membrane area of diadic junctional contacts between plasma membrane and terminal cisterns in mammalian ventricle. *Circulation research*, 45(2), 260–267. https://doi.org/10.1161/01.res.45.2.260

Page, E., McCallister, L. P., & Power, B. (1971). Sterological measurements of cardiac ultrastructures implicated in excitation-contraction coupling. *Proceedings of the National Academy of Sciences of the United States of America*, 68(7), 1465–1466. https://doi.org/10.1073/pnas.68.7.1465

Panwalkar, A., Verstovsek, S., & Giles, F. J. (2004). Mammalian target of rapamycin inhibition as therapy for hematologic malignancies. *Cancer*, 100(4), 657–666. https://doi.org/10.1002/cncr.20026

Paolini, C., Protasi, F., & Franzini-Armstrong, C. (2004). The relative position of RyR feet and DHPR tetrads in skeletal muscle. *Journal of molecular biology*, 342(1), 145–153. https://doi.org/10.1016/j.jmb.2004.07.035

Peachey, L & Eisenberg, B. (1978). Helicoids in the T system and striations of frog skeletal muscle fibers seen by high voltage electron microscopy. *Biophysical journal*. 22. 145-54. 10.1016/S0006-3495(78)85480-0

Peng, M., Fan, H., Kirley, T. L., Caswell, A. H., & Schwartz, A. (1994). Structural diversity of triadin in skeletal muscle and evidence of its existence in heart. *FEBS letters*, 348(1), 17–20. https://doi.org/10.1016/0014-5793(94)00556-7

Peng, W., Shen, H., Wu, J., Guo, W., Pan, X., Wang, R., Chen, S. R., & Yan, N. (2016). Structural basis for the gating mechanism of the type 2 ryanodine receptor RyR2. *Science (New York, N.Y.)*, 354(6310), aah5324. https://doi.org/10.1126/science.aah5324

Perez, C. F., Mukherjee, S., & Allen, P. D. (2003). Amino acids 1-1,680 of ryanodine receptor type 1 hold critical determinants of skeletal type for excitation-contraction coupling. Role of divergence domain D2. *The Journal of biological chemistry*, 278(41), 39644–39652. https://doi.org/10.1074/jbc.M305160200

Perez, P. J., Ramos-Franco, J., Fill, M., & Mignery, G. A. (1997). Identification and functional reconstitution of the type 2 inositol 1,4,5-trisphosphate receptor from ventricular cardiac myocytes. *The Journal of biological chemistry*, 272(38), 23961–23969. https://doi.org/10.1074/jbc.272.38.23961

Pessah, I. N., & Zimanyi, I. (1991). Characterization of multiple [3H]ryanodine binding sites on the Ca2+ release channel of sarcoplasmic reticulum from skeletal and cardiac muscle: evidence for a sequential mechanism in ryanodine action. *Molecular pharmacology*, 39(5), 679–689.

Peterson, R. T., Beal, P. A., Comb, M. J., & Schreiber, S. L. (2000). FKBP12-rapamycin-associated protein (FRAP) autophosphorylates at serine 2481 under translationally repressive conditions. *The Journal of biological chemistry*, 275(10), 7416–7423. https://doi.org/10.1074/jbc.275.10.7416

Phillips, M. S., Khanna, V. K., De Leon, S., Frodis, W., Britt, B. A., & MacLennan, D. H. (1994). The substitution of Arg for Gly2433 in the human skeletal muscle ryanodine receptor is associated with malignant hyperthermia. *Human molecular genetics*, 3(12), 2181–2186. https://doi.org/10.1093/hmg/3.12.2181

Ponting, C., Schultz, J., & Bork, P. (1997). SPRY domains in ryanodine receptors (Ca(2+)-release channels). *Trends in biochemical sciences*, 22(6), 193–194. https://doi.org/10.1016/s0968-0004(97)01049-9

Postma, A. V., Denjoy, I., Hoorntje, T. M., Lupoglazoff, J. M., Da Costa, A., Sebillon, P., Mannens, M. M., Wilde, A. A., & Guicheney, P. (2002). Absence of calsequestrin 2 causes severe forms of catecholaminergic polymorphic ventricular tachycardia. *Circulation research*, 91(8), e21–e26. https://doi.org/10.1161/01.res.0000038886.18992.6b

Pott, C., Dechering, D. G., Reinke, F., Muszynski, A., Zellerhoff, S., Bittner, A., Köbe, J., Wasmer, K., Schulze-Bahr, E., Mönnig, G., Kotthoff, S., & Eckardt, L. (2011). Successful treatment of catecholaminergic polymorphic ventricular tachycardia with flecainide: a case report and review of the current literature. *Europace : European pacing, arrhythmias, and cardiac electrophysiology : journal of the working groups on cardiac pacing, arrhythmias, and cardiac cellular electrophysiology of the European Society of Cardiology*, 13(6), 897–901. https://doi.org/10.1093/europace/euq517

Prakash, A., Shin, J., Rajan, S., & Yoon, H. S. (2016). Structural basis of nucleic acid recognition by FK506-binding protein 25 (FKBP25), a nuclear immunophilin. *Nucleic acids research*, 44(6), 2909–2925. https://doi.org/10.1093/nar/gkw001

Proenza, C., O'Brien, J., Nakai, J., Mukherjee, S., Allen, P. D., & Beam, K. G. (2002). Identification of a region of RyR1 that participates in allosteric coupling with the alpha(1S) (Ca(V)1.1) II-III loop. *The Journal of biological chemistry*, 277(8), 6530–6535. https://doi.org/10.1074/jbc.M106471200

Prosser, B. L., Wright, N. T., Hernãndez-Ochoa, E. O., Varney, K. M., Liu, Y., Olojo, R. O., Zimmer, D. B., Weber, D. J., & Schneider, M. F. (2008). S100A1 binds to the calmodulin-binding site of ryanodine receptor and modulates skeletal

muscle excitation-contraction coupling. *The Journal of biological chemistry*, 283(8), 5046–5057. https://doi.org/10.1074/jbc.M709231200

Protasi, F., Paolini, C., & Dainese, M. (2009). Calsequestrin-1: a new candidate gene for malignant hyperthermia and exertional/environmental heat stroke. *The Journal of physiology*, 587(Pt 13), 3095–3100. https://doi.org/10.1113/jphysiol.2009.171967

Qi, Y., Ogunbunmi, E. M., Freund, E. A., Timerman, A. P., & Fleischer, S. (1998). FK-binding protein is associated with the ryanodine receptor of skeletal muscle in vertebrate animals. *The Journal of biological chemistry*, 273(52), 34813–34819. https://doi.org/10.1074/jbc.273.52.34813

Qin, J., Valle, G., Nani, A., Chen, H., Ramos-Franco, J., Nori, A., Volpe, P., & Fill, M. (2009). Ryanodine receptor luminal Ca2+ regulation: swapping calsequestrin and channel isoforms. *Biophysical journal*, 97(7), 1961–1970. https://doi.org/10.1016/j.bpj.2009.07.030

Quane, K. A., Keating, K. E., Manning, B. M., Healy, J. M., Monsieurs, K., Heffron, J. J., Lehane, M., Heytens, L., Krivosic-Horber, R., & Adnet, P. (1994). Detection of a novel common mutation in the ryanodine receptor gene in malignant hyperthermia: implications for diagnosis and heterogeneity studies. *Human molecular genetics*, 3(3), 471–476. https://doi.org/10.1093/hmg/3.3.471

Quinn, K. E., Castellani, L., Ondrias, K., & Ehrlich, B. E. (1998). Characterization of the ryanodine receptor/channel of invertebrate muscle. *The American journal of physiology*, 274(2), R494–R502. https://doi.org/10.1152/ajpregu.1998.274.2.R494

Rebbeck, R. T., Karunasekara, Y., Board, P. G., Beard, N. A., Casarotto, M. G., & Dulhunty, A. F. (2014). Skeletal muscle excitation-contraction coupling: who are the dancing partners?. *The international journal of biochemistry & cell biology*, 48, 28–38. https://doi.org/10.1016/j.biocel.2013.12.001

Rebbeck, R. T., Karunasekara, Y., Gallant, E. M., Board, P. G., Beard, N. A., Casarotto, M. G., & Dulhunty, A. F. (2011). The β(1a) subunit of the skeletal DHPR binds to skeletal RyR1 and activates the channel via its 35-residue C-

terminal tail. *Biophysical journal*, 100(4), 922–930. https://doi.org/10.1016/j.bpj.2011.01.022

Rebbeck, R. T., Nitu, F. R., Rohde, D., Most, P., Bers, D. M., Thomas, D. D., & Cornea, R. L. (2016). S100A1 Protein Does Not Compete with Calmodulin for Ryanodine Receptor Binding but Structurally Alters the Ryanodine Receptor·Calmodulin Complex. *The Journal of biological chemistry*, 291(30), 15896–15907. https://doi.org/10.1074/jbc.M115.713107

Reiken, S., Lacampagne, A., Zhou, H., Kherani, A., Lehnart, S. E., Ward, C., Huang, F., Gaburjakova, M., Gaburjakova, J., Rosemblit, N., Warren, M. S., He, K. L., Yi, G. H., Wang, J., Burkhoff, D., Vassort, G., & Marks, A. R. (2003). PKA phosphorylation activates the calcium release channel (ryanodine receptor) in skeletal muscle: defective regulation in heart failure. *The Journal of cell biology*, 160(6), 919–928. https://doi.org/10.1083/jcb.200211012

Respress, J. L., van Oort, R. J., Li, N., Rolim, N., Dixit, S. S., deAlmeida, A., Voigt, N., Lawrence, W. S., Skapura, D. G., Skårdal, K., Wisløff, U., Wieland, T., Ai, X., Pogwizd, S. M., Dobrev, D., & Wehrens, X. H. (2012). Role of RyR2 phosphorylation at S2814 during heart failure progression. *Circulation research*, 110(11), 1474–1483. https://doi.org/10.1161/CIRCRESAHA.112.268094

Rezgui, S. S., Vassilopoulos, S., Brocard, J., Platel, J. C., Bouron, A., Arnoult, C., Oddoux, S., Garcia, L., De Waard, M., & Marty, I. (2005). Triadin (Trisk 95) overexpression blocks excitation-contraction coupling in rat skeletal myotubes. *The Journal of biological chemistry*, 280(47), 39302–39308. https://doi.org/10.1074/jbc.M506566200

Rhodes, D. A., de Bono, B., & Trowsdale, J. (2005). Relationship between SPRY and B30.2 protein domains. Evolution of a component of immune defence?. *Immunology*, 116(4), 411–417. https://doi.org/10.1111/j.1365-2567.2005.02248.x

Richardson, S. J., Steele, G. A., Gallant, E. M., Lam, A., Schwartz, C. E., Board, P. G., Casarotto, M. G., Beard, N. A., & Dulhunty, A. F. (2017). Association of FK506 binding proteins with RyR channels - effect of CLIC2 binding on sub-

conductance opening and FKBP binding. *Journal of cell science*, 130(20), 3588–3600. https://doi.org/10.1242/jcs.204461

Rios, E., & Brum, G. (1987). Involvement of dihydropyridine receptors in excitation-contraction coupling in skeletal muscle. *Nature*, 325(6106), 717–720. https://doi.org/10.1038/325717a0

Rodriguez, P., Bhogal, M. S., & Colyer, J. (2003). Stoichiometric phosphorylation of cardiac ryanodine receptor on serine 2809 by calmodulin-dependent kinase II and protein kinase A. *The Journal of biological chemistry*, 278(40), 38593–38600. https://doi.org/10.1074/jbc.C301180200

Rosenberg, H., Davis, M., James, D., Pollock, N., & Stowell, K. (2007). Malignant hyperthermia. *Orphanet journal of rare diseases*, 2, 21. https://doi.org/10.1186/1750-1172-2-21

Rousseau, E., Ladine, J., Liu, Q. Y., & Meissner, G. (1988). Activation of the Ca2+ release channel of skeletal muscle sarcoplasmic reticulum by caffeine and related compounds. *Archives of biochemistry and biophysics*, 267(1), 75–86. https://doi.org/10.1016/0003-9861(88)90010-0

Rullman, E., Andersson, D. C., Melin, M., Reiken, S., Mancini, D. M., Marks, A. R., Lund, L. H., & Gustafsson, T. (2013). Modifications of skeletal muscle ryanodine receptor type 1 and exercise intolerance in heart failure. *The Journal of heart and lung transplantation : the official publication of the International Society for Heart Transplantation*, 32(9), 925–929. https://doi.org/10.1016/j.healun.2013.06.026

Rulten, S. L., Kinloch, R. A., Tateossian, H., Robinson, C., Gettins, L., & Kay, J. E. (2006). The human FK506-binding proteins: characterization of human FKBP19. *Mammalian genome: official journal of the International Mammalian Genome Society*, 17(4), 322–331. https://doi.org/10.1007/s00335-005-0127-7

Ryan, J. F., & Tedeschi, L. G. (1997). Sudden unexplained death in a patient with a family history of malignant hyperthermia. *Journal of clinical anesthesia*, 9(1), 66–68. https://doi.org/10.1016/S0952-8180(96)00207-3

Sabatini, D. M., Erdjument-Bromage, H., Lui, M., Tempst, P., & Snyder, S. H. (1994). RAFT1: a mammalian protein that binds to FKBP12 in a rapamycin-dependent fashion and is homologous to yeast TORs. *Cell*, 78(1), 35–43. https://doi.org/10.1016/0092-8674(94)90570-3

Saito, A., Seiler, S., Chu, A., & Fleischer, S. (1984). Preparation and morphology of sarcoplasmic reticulum terminal cisternae from rabbit skeletal muscle. *The Journal of cell biology*, 99(3), 875–885. https://doi.org/10.1083/jcb.99.3.875

Salvage, S. C., Gallant, E. M., Beard, N. A., Ahmad, S., Valli, H., Fraser, J. A., Huang, C. L., & Dulhunty, A. F. (2019). Ion channel gating in cardiac ryanodine receptors from the arrhythmic RyR2-P2328S mouse. *Journal of cell science*, 132(10), jcs229039. https://doi.org/10.1242/jcs.229039

Samsó M. (2017). A guide to the 3D structure of the ryanodine receptor type 1 by cryoEM. *Protein science: a publication of the Protein Society*, 26(1), 52–68. https://doi.org/10.1002/pro.3052

Samsó, M., Feng, W., Pessah, I. N., & Allen, P. D. (2009). Coordinated movement of cytoplasmic and transmembrane domains of RyR1 upon gating. *PLoS biology*, 7(4), e85. https://doi.org/10.1371/journal.pbio.1000085

Samsó, M., Shen, X., & Allen, P. D. (2006). Structural characterization of the RyR1-FKBP12 interaction. *Journal of molecular biology*, 356(4), 917–927. https://doi.org/10.1016/j.jmb.2005.12.023

Samsó, M., Wagenknecht, T., & Allen, P. D. (2005). Internal structure and visualization of transmembrane domains of the RyR1 calcium release channel by cryo-EM. *Nature structural & molecular biology*, 12(6), 539–544. https://doi.org/10.1038/nsmb938

Sandow A. (1952). Excitation-contraction coupling in muscular response. *The Yale journal of biology and medicine*, 25(3), 176–201.

Sato, Y., Ferguson, D. G., Sako, H., Dorn, G. W., 2nd, Kadambi, V. J., Yatani, A., Hoit, B. D., Walsh, R. A., & Kranias, E. G. (1998). Cardiac-specific overexpression of mouse cardiac calsequestrin is associated with depressed cardiovascular function and hypertrophy in transgenic mice. *The Journal of*

biological chemistry, 273(43), 28470–28477. https://doi.org/10.1074/jbc.273.43.28470

Sattelle, D. B., Cordova, D., & Cheek, T. R. (2008). Insect ryanodine receptors: molecular targets for novel pest control chemicals. *Invertebrate neuroscience*, 8(3), 107–119. https://doi.org/10.1007/s10158-008-0076-4

Savio-Galimberti, E., & Knollmann, B. C. (2015). Channel Activity of Cardiac Ryanodine Receptors (RyR2) Determines Potency and Efficacy of Flecainide and R-Propafenone against Arrhythmogenic Calcium Waves in Ventricular Cardiomyocytes. *PloS one*, 10(6), e0131179. https://doi.org/10.1371/journal.pone.0131179

Savio-Galimberti, E., Frank, J., Inoue, M., Goldhaber, J. I., Cannell, M. B., Bridge, J. H., & Sachse, F. B. (2008). Novel features of the rabbit transverse tubular system revealed by quantitative analysis of three-dimensional reconstructions from confocal images. *Biophysical journal*, 95(4), 2053–2062. https://doi.org/10.1529/biophysj.108.130617

Scacheri, P. C., Hoffman, E. P., Fratkin, J. D., Semino-Mora, C., Senchak, A., Davis, M. R., Laing, N. G., Vedanarayanan, V., & Subramony, S. H. (2000). A novel ryanodine receptor gene mutation causing both cores and rods in congenital myopathy. *Neurology*, 55(11), 1689–1696. https://doi.org/10.1212/wnl.55.11.1689

Schneider, M. F., & Chandler, W. K. (1973). Voltage dependent charge movement of skeletal muscle: a possible step in excitation-contraction coupling. *Nature*, 242(5395), 244–246. https://doi.org/10.1038/242244a0

Schories, B., Nelson, T. E., & Sane, D. C. (2007). Multimer formation by FKBP-12: roles for cysteine 23 and phenylalanine 36. *Journal of peptide science: an official publication of the European Peptide Society*, 13(7), 475–480. https://doi.org/10.1002/psc.871

Schredelseker, J., Di Biase, V., Obermair, G. J., Felder, E. T., Flucher, B. E., Franzini-Armstrong, C., & Grabner, M. (2005). The beta 1a subunit is essential for the assembly of dihydropyridine-receptor arrays in skeletal muscle. *Proceedings of the National Academy of Sciences of the United*

States of America, 102(47), 17219–17224. https://doi.org/10.1073/pnas.0508710102

Seidler, T., Loughrey, C. M., Zibrova, D., Kettlewell, S., Teucher, N., Kögler, H., Hasenfuss, G., & Smith, G. L. (2007). Overexpression of FK-506 binding protein 12.0 modulates excitation contraction coupling in adult rabbit ventricular cardiomyocytes. *Circulation research*, 101(10), 1020–1029. https://doi.org/10.1161/CIRCRESAHA.107.154609

Seidman, R. J. (2021). 'Muscle Biopsy and Clinical and Laboratory Features of Neuromuscular Disease'. *Medscape Clinical Procedures*, accessed 4 November 2021, <https://emedicine.medscape.com/article/1847877-overview>

Sewell, T. J., Lam, E., Martin, M. M., Leszyk, J., Weidner, J., Calaycay, J., Griffin, P., Williams, H., Hung, S., & Cryan, J. (1994). Inhibition of calcineurin by a novel FK-506-binding protein. *The Journal of biological chemistry*, 269(33), 21094–21102.

Shan, J., Betzenhauser, M. J., Kushnir, A., Reiken, S., Meli, A. C., Wronska, A., Dura, M., Chen, B. X., & Marks, A. R. (2010). Role of chronic ryanodine receptor phosphorylation in heart failure and β-adrenergic receptor blockade in mice. *The Journal of clinical investigation*, 120(12), 4375–4387. https://doi.org/10.1172/JCI37649

Shan, J., Xie, W., Betzenhauser, M., Reiken, S., Chen, B. X., Wronska, A., & Marks, A. R. (2012). Calcium leak through ryanodine receptors leads to atrial fibrillation in 3 mouse models of catecholaminergic polymorphic ventricular tachycardia. *Circulation research*, 111(6), 708–717. https://doi.org/10.1161/CIRCRESAHA.112.273342

Sharma, M. C., Gulati, S., Sarkar, C., Jain, D., Kalra, V., & Suri, V. (2007). Multi-minicore disease: a rare form of myopathy. *Neurology India*, 55(1), 50–53. https://doi.org/10.4103/0028-3886.30427

Sharma, V. K., Li, B., Khanna, A., Sehajpal, P. K., & Suthanthiran, M. (1994). Which way for drug-mediated immunosuppression?. *Current opinion in immunology*, 6(5), 784–790. https://doi.org/10.1016/0952-7915(94)90085-x

Shen, X., Franzini-Armstrong, C., Lopez, J. R., Jones, L. R., Kobayashi, Y. M., Wang, Y., Kerrick, W. G., Caswell, A. H., Potter, J. D., Miller, T., Allen, P. D., & Perez, C. F. (2007). Triadins modulate intracellular Ca(2+) homeostasis but are not essential for excitation-contraction coupling in skeletal muscle. *The Journal of biological chemistry*, 282(52), 37864–37874. https://doi.org/10.1074/jbc.M705702200

Shin, D. W., Ma, J., & Kim, D. H. (2000). The asp-rich region at the carboxyl-terminus of calsequestrin binds to Ca(2+) and interacts with triadin. *FEBS letters*, 486(2), 178–182. https://doi.org/10.1016/s0014-5793(00)02246-8

Shou, W., Aghdasi, B., Armstrong, D. L., Guo, Q., Bao, S., Charng, M. J., Mathews, L. M., Schneider, M. D., Hamilton, S. L., & Matzuk, M. M. (1998). Cardiac defects and altered ryanodine receptor function in mice lacking FKBP12. *Nature*, 391(6666), 489–492. https://doi.org/10.1038/35146

Shuaib, A., Paasuke, R. T., & Brownell, K. W. (1987). Central core disease. Clinical features in 13 patients. *Medicine*, 66(5), 389–396.

Sikkel, M. B., Collins, T. P., Rowlands, C., Shah, M., O'Gara, P., Williams, A. J., Harding, S. E., Lyon, A. R., & MacLeod, K. T. (2013). Flecainide reduces Ca(2+) spark and wave frequency via inhibition of the sarcolemmal sodium current. *Cardiovascular research*, 98(2), 286–296. https://doi.org/10.1093/cvr/cvt012

Sitsapesan, R., & Williams, A. J. (1990). Mechanisms of caffeine activation of single calcium-release channels of sheep cardiac sarcoplasmic reticulum. *The Journal of physiology*, 423, 425–439. https://doi.org/10.1113/jphysiol.1990.sp018031

Sitsapesan, R., & Williams, A. J. (1994). Regulation of the gating of the sheep cardiac sarcoplasmic reticulum Ca(2+)-release channel by luminal Ca2+. *The Journal of membrane biology*, 137(3), 215–226. https://doi.org/10.1007/BF00232590

Smith, J. S., Coronado, R., & Meissner, G. (1985). Sarcoplasmic reticulum contains adenine nucleotide-activated calcium channels. *Nature*, 316(6027), 446–449. https://doi.org/10.1038/316446a0

Smith, J. S., Coronado, R., & Meissner, G. (1986). Single channel measurements of the calcium release channel from skeletal muscle sarcoplasmic reticulum. Activation by Ca2+ and ATP and modulation by Mg2+. *The Journal of general physiology*, 88(5), 573–588. https://doi.org/10.1085/jgp.88.5.573

Smith, T. F., Waterman, M. S., & Fitch, W. M. (1981). Comparative biosequence metrics. *Journal of molecular evolution*, 18(1), 38–46. https://doi.org/10.1007/BF01733210

Søndergaard, M. T., Sorensen, A. B., Skov, L. L., Kjaer-Sorensen, K., Bauer, M. C., Nyegaard, M., Linse, S., Oxvig, C., & Overgaard, M. T. (2015). Calmodulin mutations causing catecholaminergic polymorphic ventricular tachycardia confer opposing functional and biophysical molecular changes. *The FEBS journal*, 282(4), 803–816. https://doi.org/10.1111/febs.13184

Søndergaard, M. T., Liu, Y., Larsen, K. T., Nani, A., Tian, X., Holt, C., Wang, R., Wimmer, R., Van Petegem, F., Fill, M., Chen, S. R., & Overgaard, M. T. (2017). The Arrhythmogenic Calmodulin p.Phe142Leu Mutation Impairs C-domain Ca2+ Binding but Not Calmodulin-dependent Inhibition of the Cardiac Ryanodine Receptor. *The Journal of biological chemistry*, 292(4), 1385–1395. https://doi.org/10.1074/jbc.M116.766253

Søndergaard, M. T., Liu, Y., Larsen, K. T., Nani, A., Tian, X., Holt, C., Wang, R., Wimmer, R., Van Petegem, F., Fill, M., Chen, S. R., & Overgaard, M. T. (2017). The Arrhythmogenic Calmodulin p.Phe142Leu Mutation Impairs C-domain Ca2+ Binding but Not Calmodulin-dependent Inhibition of the Cardiac Ryanodine Receptor. *The Journal of biological chemistry*, 292(4), 1385–1395. https://doi.org/10.1074/jbc.M116.766253

Sonnleitner, A., Fleischer, S., & Schindler, H. (1997). Gating of the skeletal calcium release channel by ATP is inhibited by protein phosphatase 1 but not by Mg2+. *Cell calcium*, 21(4), 283–290. https://doi.org/10.1016/s0143-4160(97)90116-0

Steele, G. A. (2013). A Novel Explanation for CLIC-2 Induced Subconductance Openings in Cardiac Ryanodine Receptors [Unpublished undergraduate honours thesis]. Australian National University.

Steele, T., & Samsó, M. (2019). The FKBP12 subunit modifies the long-range allosterism of the ryanodine receptor. *Journal of structural biology*, 205(2), 180–188. https://doi.org/10.1016/j.jsb.2018.12.007

Stern, M. D., Pizarro, G., & Ríos, E. (1997). Local control model of excitation-contraction coupling in skeletal muscle. *The Journal of general physiology*, 110(4), 415–440. https://doi.org/10.1085/jgp.110.4.415

Stoyanovsky, D., Murphy, T., Anno, P. R., Kim, Y. M., & Salama, G. (1997). Nitric oxide activates skeletal and cardiac ryanodine receptors. *Cell calcium*, 21(1), 19–29. https://doi.org/10.1016/s0143-4160(97)90093-2

Stutzmann, G. E., Smith, I., Caccamo, A., Oddo, S., Parker, I., & Laferla, F. (2007). Enhanced ryanodine-mediated calcium release in mutant PS1-expressing Alzheimer's mouse models. *Annals of the New York Academy of Sciences*, 1097, 265–277. https://doi.org/10.1196/annals.1379.025

Su, Z., Sugishita, K., Li, F., Ritter, M., & Barry, W. H. (2003). Effects of FK506 on [Ca2+]i differ in mouse and rabbit ventricular myocytes. *The Journal of pharmacology and experimental therapeutics*, 304(1), 334–341. https://doi.org/10.1124/jpet.102.041210

Sun, J., Yamaguchi, N., Xu, L., Eu, J. P., Stamler, J. S., & Meissner, G. (2008). Regulation of the cardiac muscle ryanodine receptor by O(2) tension and S-nitrosoglutathione. *Biochemistry*, 47(52), 13985–13990. https://doi.org/10.1021/bi8012627

Sun, X. H., Protasi, F., Takahashi, M., Takeshima, H., Ferguson, D. G., & Franzini-Armstrong, C. (1995). Molecular architecture of membranes involved in excitation-contraction coupling of cardiac muscle. *The Journal of cell biology*, 129(3), 659–671. https://doi.org/10.1083/jcb.129.3.659

Svedberg, T., Pedersen, K. O., Bauer, J. H., Pickels, E. G., Boestad, G., Kraemer, E. O., Nichols, J. B., ... Smith, E. L. (1940). *The ultracentrifuge*. Oxford: The Clarendon Press.

Szentesi, P., Collet, C., Sárközi, S., Szegedi, C., Jona, I., Jacquemond, V., Kovács, L., & Csernoch, L. (2001). Effects of dantrolene on steps of excitation-

contraction coupling in mammalian skeletal muscle fibers. *The Journal of general physiology*, 118(4), 355–375. https://doi.org/10.1085/jgp.118.4.355

Szent-Györgyi A. G. (1975). Calcium regulation of muscle contraction. *Biophysical journal*, 15(7), 707–723. https://doi.org/10.1016/S0006-3495(75)85849-8

Takasago, T., Imagawa, T., & Shigekawa, M. (1989). Phosphorylation of the cardiac ryanodine receptor by cAMP-dependent protein kinase. *Journal of biochemistry*, 106(5), 872–877. https://doi.org/10.1093/oxfordjournals.jbchem.a122945

Takekura, H., Paolini, C., Franzini-Armstrong, C., Kugler, G., Grabner, M., & Flucher, B. E. (2004). Differential contribution of skeletal and cardiac II-III loop sequences to the assembly of dihydropyridine-receptor arrays in skeletal muscle. *Molecular biology of the cell*, 15(12), 5408–5419. https://doi.org/10.1091/mbc.e04-05-0414

Takeshima, H., Nishi, M., Iwabe, N., Miyata, T., Hosoya, T., Masai, I., & Hotta, Y. (1994). Isolation and characterization of a gene for a ryanodine receptor/calcium release channel in Drosophila melanogaster. *FEBS letters*, 337(1), 81–87. https://doi.org/10.1016/0014-5793(94)80634-9

Takeshima, H., Nishimura, S., Matsumoto, T., Ishida, H., Kangawa, K., Minamino, N., Matsuo, H., Ueda, M., Hanaoka, M., & Hirose, T. (1989). Primary structure and expression from complementary DNA of skeletal muscle ryanodine receptor. *Nature*, 339(6224), 439–445. https://doi.org/10.1038/339439a0

Takizawa, P. (2018). Histology @ Yale, accessed 4 November 2021, <http://medcell.med.yale.edu/histology/histology.php>

Tang, W., Ingalls, C. P., Durham, W. J., Snider, J., Reid, M. B., Wu, G., Matzuk, M. M., & Hamilton, S. L. (2004). Altered excitation-contraction coupling with skeletal muscle specific FKBP12 deficiency. *FASEB journal: official publication of the Federation of American Societies for Experimental Biology*, 18(13), 1597–1599. https://doi.org/10.1096/fj.04-1587fje

Tencerová, B., Zahradníková, A., Gaburjáková, J., & Gaburjáková, M. (2012). Luminal Ca2+ controls activation of the cardiac ryanodine receptor by ATP.

The Journal of general physiology, 140(2), 93–108. https://doi.org/10.1085/jgp.201110708

Terentyev, D., Viatchenko-Karpinski, S., Györke, I., Volpe, P., Williams, S. C., & Györke, S. (2003). Calsequestrin determines the functional size and stability of cardiac intracellular calcium stores: Mechanism for hereditary arrhythmia. *Proceedings of the National Academy of Sciences of the United States of America*, 100(20), 11759–11764. https://doi.org/10.1073/pnas.1932318100

Tian, Q., Katz, A. M., & Kim, D. H. (1991). Effects of azumolene on doxorubicin-induced Ca2+ release from skeletal and cardiac muscle sarcoplasmic reticulum. *Biochimica et biophysica acta*, 1094(1), 27–34. https://doi.org/10.1016/0167-4889(91)90022-p

Tilgen, N., Zorzato, F., Halliger-Keller, B., Muntoni, F., Sewry, C., Palmucci, L. M., Schneider, C., Hauser, E., Lehmann-Horn, F., Müller, C. R., & Treves, S. (2001). Identification of four novel mutations in the C-terminal membrane spanning domain of the ryanodine receptor 1: association with central core disease and alteration of calcium homeostasis. *Human molecular genetics*, 10(25), 2879–2887. https://doi.org/10.1093/hmg/10.25.2879

Timerman, A. P., Ogunbumni, E., Freund, E., Wiederrecht, G., Marks, A. R., & Fleischer, S. (1993). The calcium release channel of sarcoplasmic reticulum is modulated by FK-506-binding protein. Dissociation and reconstitution of FKBP-12 to the calcium release channel of skeletal muscle sarcoplasmic reticulum. *The Journal of biological chemistry*, 268(31), 22992–22999.

Timerman, A. P., Wiederrecht, G., Marcy, A., & Fleischer, S. (1995). Characterization of an exchange reaction between soluble FKBP-12 and the FKBP.ryanodine receptor complex. Modulation by FKBP mutants deficient in peptidyl-prolyl isomerase activity. *The Journal of biological chemistry*, 270(6), 2451–2459. https://doi.org/10.1074/jbc.270.6.2451

Tinker, A., & Williams, A. J. (1992). Divalent cation conduction in the ryanodine receptor channel of sheep cardiac muscle sarcoplasmic reticulum. *The Journal of general physiology*, 100(3), 479–493. https://doi.org/10.1085/jgp.100.3.479

Tinker, A., & Williams, A. J. (1993). Using large organic cations to probe the nature of ryanodine modification in the sheep cardiac sarcoplasmic reticulum calcium release channel. *Biophysical journal*, 65(4), 1678–1683. https://doi.org/10.1016/S0006-3495(93)81201-3

Tiso, N., Stephan, D. A., Nava, A., Bagattin, A., Devaney, J. M., Stanchi, F., Larderet, G., Brahmbhatt, B., Brown, K., Bauce, B., Muriago, M., Basso, C., Thiene, G., Danieli, G. A., & Rampazzo, A. (2001). Identification of mutations in the cardiac ryanodine receptor gene in families affected with arrhythmogenic right ventricular cardiomyopathy type 2 (ARVD2). *Human molecular genetics*, 10(3), 189–194. https://doi.org/10.1093/hmg/10.3.189

Tong, J., McCarthy, T. V., & MacLennan, D. H. (1999). Measurement of resting cytosolic Ca2+ concentrations and Ca2+ store size in HEK-293 cells transfected with malignant hyperthermia or central core disease mutant Ca2+ release channels. *The Journal of biological chemistry*, 274(2), 693–702. https://doi.org/10.1074/jbc.274.2.693

Tonthat, N. K., Juvvadi, P. R., Zhang, H., Lee, S. C., Venters, R., Spicer, L., Steinbach, W. J., Heitman, J., & Schumacher, M. A. (2016). Structures of Pathogenic Fungal FKBP12s Reveal Possible Self-Catalysis Function. *mBio*, 7(2), e00492-16. https://doi.org/10.1128/mBio.00492-16

Towbin, H., Staehelin, T., & Gordon, J. (1979). Electrophoretic transfer of proteins from polyacrylamide gels to nitrocellulose sheets: procedure and some applications. *Proceedings of the National Academy of Sciences of the United States of America*, 76(9), 4350–4354. https://doi.org/10.1073/pnas.76.9.4350

Tripathy, A., & Meissner, G. (1996). Sarcoplasmic reticulum lumenal Ca2+ has access to cytosolic activation and inactivation sites of skeletal muscle Ca2+ release channel. *Biophysical journal*, 70(6), 2600–2615. https://doi.org/10.1016/S0006-3495(96)79831-4

Tripathy, A., Xu, L., Mann, G., & Meissner, G. (1995). Calmodulin activation and inhibition of skeletal muscle Ca2+ release channel (ryanodine receptor). *Biophysical journal*, 69(1), 106–119. https://doi.org/10.1016/S0006-3495(95)79880-0

Valdivia, C., Vaughan, D., Potter, B. V., & Coronado, R. (1992). Fast release of 45Ca2+ induced by inositol 1,4,5-trisphosphate and Ca2+ in the sarcoplasmic reticulum of rabbit skeletal muscle: evidence for two types of Ca2+ release channels. *Biophysical journal*, 61(5), 1184–1193. https://doi.org/10.1016/S0006-3495(92)81927-6

Valdivia, H. H., Kaplan, J. H., Ellis-Davies, G. C., & Lederer, W. J. (1995). Rapid adaptation of cardiac ryanodine receptors: modulation by Mg2+ and phosphorylation. *Science (New York, N.Y.)*, 267(5206), 1997–2000. https://doi.org/10.1126/science.7701323

Van Acker, K., Bultynck, G., Rossi, D., Sorrentino, V., Boens, N., Missiaen, L., De Smedt, H., Parys, J. B., & Callewaert, G. (2004). The 12 kDa FK506-binding protein, FKBP12, modulates the Ca(2+)-flux properties of the type-3 ryanodine receptor. *Journal of cell science*, 117(Pt 7), 1129–1137. https://doi.org/10.1242/jcs.00948

van der Werf, C., Kannankeril, P. J., Sacher, F., Krahn, A. D., Viskin, S., Leenhardt, A., Shimizu, W., Sumitomo, N., Fish, F. A., Bhuiyan, Z. A., Willems, A. R., van der Veen, M. J., Watanabe, H., Laborderie, J., Haïssaguerre, M., Knollmann, B. C., & Wilde, A. A. (2011). Flecainide therapy reduces exercise-induced ventricular arrhythmias in patients with catecholaminergic polymorphic ventricular tachycardia. *Journal of the American College of Cardiology*, 57(22), 2244–2254. https://doi.org/10.1016/j.jacc.2011.01.026

Vassilopoulos, S., Thevenon, D., Rezgui, S. S., Brocard, J., Chapel, A., Lacampagne, A., Lunardi, J., Dewaard, M., & Marty, I. (2005). Triadins are not triad-specific proteins: two new skeletal muscle triadins possibly involved in the architecture of sarcoplasmic reticulum. *The Journal of biological chemistry*, 280(31), 28601–28609. https://doi.org/10.1074/jbc.M501484200

Venturi, E., Galfré, E., O'Brien, F., Pitt, S. J., Bellamy, S., Sessions, R. B., & Sitsapesan, R. (2014). FKBP12.6 activates RyR1: investigating the amino acid residues critical for channel modulation. *Biophysical journal*, 106(4), 824–833. https://doi.org/10.1016/j.bpj.2013.12.041

Volpe, P., Salviati, G., Di Virgilio, F., & Pozzan, T. (1985). Inositol 1,4,5-trisphosphate induces calcium release from sarcoplasmic reticulum of skeletal muscle. *Nature*, 316(6026), 347–349. https://doi.org/10.1038/316347a0

Vukcevic, M., Broman, M., Islander, G., Bodelsson, M., Ranklev-Twetman, E., Müller, C. R., & Treves, S. (2010). Functional properties of RYR1 mutations identified in Swedish patients with malignant hyperthermia and central core disease. *Anesthesia and analgesia*, 111(1), 185–190. https://doi.org/10.1213/ANE.0b013e3181cbd815

Wagner, L. E., 2nd, Groom, L. A., Dirksen, R. T., & Yule, D. I. (2014). Characterization of ryanodine receptor type 1 single channel activity using "on-nucleus" patch clamp. *Cell calcium*, 56(2), 96–107. https://doi.org/10.1016/j.ceca.2014.05.004

Walweel, K., Molenaar, P., Imtiaz, M. S., Denniss, A., Dos Remedios, C., van Helden, D. F., Dulhunty, A. F., Laver, D. R., & Beard, N. A. (2017). Ryanodine receptor modification and regulation by intracellular Ca2+ and Mg2+ in healthy and failing human hearts. *Journal of molecular and cellular cardiology*, 104, 53–62. https://doi.org/10.1016/j.yjmcc.2017.01.016

Walweel, K., Gomez-Hurtado, N., Rebbeck, R. T., Oo, Y. W., Beard, N. A., Molenaar, P., Dos Remedios, C., van Helden, D. F., Cornea, R. L., Knollmann, B. C., & Laver, D. R. (2019). Calmodulin inhibition of human RyR2 channels requires phosphorylation of RyR2-S2808 or RyR2-S2814. *Journal of molecular and cellular cardiology*, 130, 96–106. https://doi.org/10.1016/j.yjmcc.2019.03.018

Wang, J., & Best, P. M. (1992). Inactivation of the sarcoplasmic reticulum calcium channel by protein kinase. *Nature*, 359(6397), 739–741. https://doi.org/10.1038/359739a0

Wang, Y. X., Zheng, Y. M., Mei, Q. B., Wang, Q. S., Collier, M. L., Fleischer, S., Xin, H. B., & Kotlikoff, M. I. (2004). FKBP12.6 and cADPR regulation of Ca2+ release in smooth muscle cells. American journal of physiology. *Cell physiology*, 286(3), C538–C546. https://doi.org/10.1152/ajpcell.00106.2003

Wang, Y., Li, X., Duan, H., Fulton, T. R., Eu, J. P., & Meissner, G. (2009). Altered stored calcium release in skeletal myotubes deficient of triadin and junctin. *Cell calcium*, 45(1), 29–37. https://doi.org/10.1016/j.ceca.2008.05.006

Ward, A., Chaffman, M. O., & Sorkin, E. M. (1986). Dantrolene. A review of its pharmacodynamic and pharmacokinetic properties and therapeutic use in malignant hyperthermia, the neuroleptic malignant syndrome and an update of its use in muscle spasticity. *Drugs*, 32(2), 130–168. https://doi.org/10.2165/00003495-198632020-00003

Watanabe, H., Chopra, N., Laver, D., Hwang, H. S., Davies, S. S., Roach, D. E., Duff, H. J., Roden, D. M., Wilde, A. A., & Knollmann, B. C. (2009). Flecainide prevents catecholaminergic polymorphic ventricular tachycardia in mice and humans. *Nature medicine*, 15(4), 380–383. https://doi.org/10.1038/nm.1942

Wehrens, X. H., Lehnart, S. E., & Marks, A. R. (2005). Ryanodine receptor-targeted anti-arrhythmic therapy. *Annals of the New York Academy of Sciences*, 1047, 366–375. https://doi.org/10.1196/annals.1341.032

Wehrens, X. H., Lehnart, S. E., Huang, F., Vest, J. A., Reiken, S. R., Mohler, P. J., Sun, J., Guatimosim, S., Song, L. S., Rosemblit, N., D'Armiento, J. M., Napolitano, C., Memmi, M., Priori, S. G., Lederer, W. J., & Marks, A. R. (2003). FKBP12.6 deficiency and defective calcium release channel (ryanodine receptor) function linked to exercise-induced sudden cardiac death. *Cell*, 113(7), 829–840. https://doi.org/10.1016/s0092-8674(03)00434-3

Wehrens, X. H., Lehnart, S. E., Reiken, S. R., & Marks, A. R. (2004a). Ca2+/calmodulin-dependent protein kinase II phosphorylation regulates the cardiac ryanodine receptor. *Circulation research*, 94(6), e61–e70. https://doi.org/10.1161/01.RES.0000125626.33738.E2

Wehrens, X. H., Lehnart, S. E., Reiken, S. R., Deng, S. X., Vest, J. A., Cervantes, D., Coromilas, J., Landry, D. W., & Marks, A. R. (2004b). Protection from cardiac arrhythmia through ryanodine receptor-stabilizing protein calstabin2. *Science (New York, N.Y.)*, 304(5668), 292–296. https://doi.org/10.1126/science.1094301

Wehrens, X. H., Lehnart, S. E., Reiken, S., Vest, J. A., Wronska, A., & Marks, A. R. (2006). Ryanodine receptor/calcium release channel PKA phosphorylation: a critical mediator of heart failure progression. *Proceedings of the National Academy of Sciences of the United States of America*, 103(3), 511–518. https://doi.org/10.1073/pnas.0510113103

Wei, L., Hanna, A. D., Beard, N. A., & Dulhunty, A. F. (2009). Unique isoform-specific properties of calsequestrin in the heart and skeletal muscle. *Cell calcium*, 45(5), 474–484. https://doi.org/10.1016/j.ceca.2009.03.006

Wei, L., Varsányi, M., Dulhunty, A. F., & Beard, N. A. (2006). The conformation of calsequestrin determines its ability to regulate skeletal ryanodine receptors. *Biophysical journal*, 91(4), 1288–1301. https://doi.org/10.1529/biophysj.106.082610

Weidelt, T., & Isenberg, G. (2000). Augmentation of SR Ca(2+) release by rapamycin and FK506 causes K(+)-channel activation and membrane hyperpolarization in bladder smooth muscle. *British journal of pharmacology*, 129(7), 1293–1300. https://doi.org/10.1038/sj.bjp.0703223

Wen, H., Kang, S., Song, Y., Song, Y., Yang, H. J., Kim, M. H., & Park, S. (2012). Characterization of the binding sites for the interactions between FKBP12 and intracellular calcium release channels. *Archives of biochemistry and biophysics*, 517(1), 37–42. https://doi.org/10.1016/j.abb.2011.11.004

Wilson, K. P., Yamashita, M. M., Sintchak, M. D., Rotstein, S. H., Murcko, M. A., Boger, J., Thomson, J. A., Fitzgibbon, M. J., Black, J. R., & Navia, M. A. (1995). Comparative X-ray structures of the major binding protein for the immunosuppressant FK506 (tacrolimus) in unliganded form and in complex with FK506 and rapamycin. *Acta crystallographica. Section D, Biological crystallography*, 51(Pt 4), 511–521. https://doi.org/10.1107/S0907444994014514

Wium, E., Dulhunty, A. F., & Beard, N. A. (2012). A skeletal muscle ryanodine receptor interaction domain in triadin. *PloS one*, 7(8), e43817. https://doi.org/10.1371/journal.pone.0043817

Wright, N. T., Prosser, B. L., Varney, K. M., Zimmer, D. B., Schneider, M. F., & Weber, D. J. (2008). S100A1 and calmodulin compete for the same binding site on ryanodine receptor. *The Journal of biological chemistry*, 283(39), 26676–26683. https://doi.org/10.1074/jbc.M804432200

Wu, J., Yan, Z., Li, Z., Yan, C., Lu, S., Dong, M., & Yan, N. (2015). Structure of the voltage-gated calcium channel Cav1.1 complex. *Science (New York, N.Y.)*, 350(6267), aad2395. https://doi.org/10.1126/science.aad2395

Wu, X., Wang, L., Han, Y., Regan, N., Li, P. K., Villalona, M. A., Hu, X., Briesewitz, R., & Pei, D. (2011). Creating diverse target-binding surfaces on FKBP12: synthesis and evaluation of a rapamycin analogue library. *ACS combinatorial science*, 13(5), 486–495. https://doi.org/10.1021/co200057n

Xiao, B., Jiang, M. T., Zhao, M., Yang, D., Sutherland, C., Lai, F. A., Walsh, M. P., Warltier, D. C., Cheng, H., & Chen, S. R. (2005). Characterization of a novel PKA phosphorylation site, serine-2030, reveals no PKA hyperphosphorylation of the cardiac ryanodine receptor in canine heart failure. Circulation research, 96(8), 847–855. https://doi.org/10.1161/01.RES.0000163276.26083.e8

Xiao, B., Zhong, G., Obayashi, M., Yang, D., Chen, K., Walsh, M. P., Shimoni, Y., Cheng, H., Ter Keurs, H., & Chen, S. R. (2006). Ser-2030, but not Ser-2808, is the major phosphorylation site in cardiac ryanodine receptors responding to protein kinase A activation upon beta-adrenergic stimulation in normal and failing hearts. *The Biochemical journal*, 396(1), 7–16. https://doi.org/10.1042/BJ20060116

Xiao, J., Tian, X., Jones, P. P., Bolstad, J., Kong, H., Wang, R., Zhang, L., Duff, H. J., Gillis, A. M., Fleischer, S., Kotlikoff, M., Copello, J. A., & Chen, S. R. (2007). Removal of FKBP12.6 does not alter the conductance and activation of the cardiac ryanodine receptor or the susceptibility to stress-induced ventricular arrhythmias. *The Journal of biological chemistry*, 282(48), 34828–34838. https://doi.org/10.1074/jbc.M707423200

Xiao, R. P., Valdivia, H. H., Bogdanov, K., Valdivia, C., Lakatta, E. G., & Cheng, H. (1997). The immunophilin FK506-binding protein modulates Ca2+ release

channel closure in rat heart. *The Journal of physiology*, 500 (Pt 2)(Pt 2), 343–354. https://doi.org/10.1113/jphysiol.1997.sp022025

Xin, H. B., Senbonmatsu, T., Cheng, D. S., Wang, Y. X., Copello, J. A., Ji, G. J., Collier, M. L., Deng, K. Y., Jeyakumar, L. H., Magnuson, M. A., Inagami, T., Kotlikoff, M. I., & Fleischer, S. (2002). Oestrogen protects FKBP12.6 null mice from cardiac hypertrophy. *Nature*, 416(6878), 334–338. https://doi.org/10.1038/416334a

Xu, L., & Meissner, G. (2004). Mechanism of calmodulin inhibition of cardiac sarcoplasmic reticulum Ca2+ release channel (ryanodine receptor). *Biophysical journal*, 86(2), 797–804. https://doi.org/10.1016/S0006-3495(04)74155-7

Xu, L., Tripathy, A., Pasek, D. A., & Meissner, G. (1998). Potential for pharmacology of ryanodine receptor/calcium release channels. *Annals of the New York Academy of Sciences*, 853, 130–148. https://doi.org/10.1111/j.1749-6632.1998.tb08262.x

Yamaguchi, N., Chakraborty, A., Huang, T. Q., Xu, L., Gomez, A. C., Pasek, D. A., & Meissner, G. (2013). Cardiac hypertrophy associated with impaired regulation of cardiac ryanodine receptor by calmodulin and S100A1. *American journal of physiology. Heart and circulatory physiology*, 305(1), H86–H94. https://doi.org/10.1152/ajpheart.00144.2013

Yamaguchi, N., Prosser, B. L., Ghassemi, F., Xu, L., Pasek, D. A., Eu, J. P., Hernández-Ochoa, E. O., Cannon, B. R., Wilder, P. T., Lovering, R. M., Weber, D., Melzer, W., Schneider, M. F., & Meissner, G. (2011). Modulation of sarcoplasmic reticulum Ca2+ release in skeletal muscle expressing ryanodine receptor impaired in regulation by calmodulin and S100A1. American journal of physiology. *Cell physiology*, 300(5), C998–C1012. https://doi.org/10.1152/ajpcell.00370.2010

Yamaguchi, N., Xu, L., Pasek, D. A., Evans, K. E., Chen, S. R., & Meissner, G. (2005). Calmodulin regulation and identification of calmodulin binding region of type-3 ryanodine receptor calcium release channel. *Biochemistry*, 44(45), 15074–15081. https://doi.org/10.1021/bi051251t

Yan, Z., Bai, X., Yan, C., Wu, J., Li, Z., Xie, T., Peng, W., Yin, C., Li, X., Scheres, S., Shi, Y., & Yan, N. (2015). Structure of the rabbit ryanodine receptor RyR1 at near-atomic resolution. *Nature*, 517(7532), 50–55. https://doi.org/10.1038/nature14063

Yano, M., Kobayashi, S., Kohno, M., Doi, M., Tokuhisa, T., Okuda, S., Suetsugu, M., Hisaoka, T., Obayashi, M., Ohkusa, T., Kohno, M., & Matsuzaki, M. (2003). FKBP12.6-mediated stabilization of calcium-release channel (ryanodine receptor) as a novel therapeutic strategy against heart failure. *Circulation*, 107(3), 477–484. https://doi.org/10.1161/01.cir.0000044917.74408.be

Yano, M., Ono, K., Ohkusa, T., Suetsugu, M., Kohno, M., Hisaoka, T., Kobayashi, S., Hisamatsu, Y., Yamamoto, T., Kohno, M., Noguchi, N., Takasawa, S., Okamoto, H., & Matsuzaki, M. (2000). Altered stoichiometry of FKBP12.6 versus ryanodine receptor as a cause of abnormal Ca(2+) leak through ryanodine receptor in heart failure. *Circulation*, 102(17), 2131–2136. https://doi.org/10.1161/01.cir.102.17.2131

Ye, Y., & Godzik, A. (2003). Flexible structure alignment by chaining aligned fragment pairs allowing twists. *Bioinformatics (Oxford, England)*, 19 Suppl 2, ii246–ii255. https://doi.org/10.1093/bioinformatics/btg1086

Yuan, Q., Deng, K. Y., Sun, L., Chi, S., Yang, Z., Wang, J., Xin, H. B., Wang, X., & Ji, G. (2016). Calstabin 2: An important regulator for learning and memory in mice. *Scientific reports*, 6, 21087. https://doi.org/10.1038/srep21087

Yuan, Q., Fan, G. C., Dong, M., Altschafl, B., Diwan, A., Ren, X., Hahn, H. H., Zhao, W., Waggoner, J. R., Jones, L. R., Jones, W. K., Bers, D. M., Dorn, G. W., 2nd, Wang, H. S., Valdivia, H. H., Chu, G., & Kranias, E. G. (2007). Sarcoplasmic reticulum calcium overloading in junctin deficiency enhances cardiac contractility but increases ventricular automaticity. *Circulation*, 115(3), 300–309. https://doi.org/10.1161/CIRCULATIONAHA.106.654699

Yuchi, Z., Yuen, S. M., Lau, K., Underhill, A. Q., Cornea, R. L., Fessenden, J. D., & Van Petegem, F. (2015). Crystal structures of ryanodine receptor SPRY1 and tandem-repeat domains reveal a critical FKBP12 binding determinant. *Nature communications*, 6, 7947. https://doi.org/10.1038/ncomms8947

Zable, A. C., Favero, T. G., & Abramson, J. J. (1997). Glutathione modulates ryanodine receptor from skeletal muscle sarcoplasmic reticulum. Evidence for redox regulation of the Ca2+ release mechanism. *The Journal of biological chemistry*, 272(11), 7069–7077. https://doi.org/10.1074/jbc.272.11.7069

Zaharieva, I. T., Sarkozy, A., Munot, P., Manzur, A., O'Grady, G., Rendu, J., Malfatti, E., Amthor, H., Servais, L., Urtizberea, J. A., Neto, O. A., Zanoteli, E., Donkervoort, S., Taylor, J., Dixon, J., Poke, G., Foley, A. R., Holmes, C., Williams, G., Holder, M., … Muntoni, F. (2018). STAC3 variants cause a congenital myopathy with distinctive dysmorphic features and malignant hyperthermia susceptibility. *Human mutation*, 39(12), 1980–1994. https://doi.org/10.1002/humu.23635

Zahradník, I., Györke, S., & Zahradníková, A. (2005). Calcium activation of ryanodine receptor channels--reconciling RyR gating models with tetrameric channel structure. *The Journal of general physiology*, 126(5), 515–527. https://doi.org/10.1085/jgp.200509328

Zalk, R., Clarke, O. B., des Georges, A., Grassucci, R. A., Reiken, S., Mancia, F., Hendrickson, W. A., Frank, J., & Marks, A. R. (2015). Structure of a mammalian ryanodine receptor. *Nature*, 517(7532), 44–49. https://doi.org/10.1038/nature13950

Zhang, J., Liu, Z., Masumiya, H., Wang, R., Jiang, D., Li, F., Wagenknecht, T., & Chen, S. R. (2003). Three-dimensional localization of divergent region 3 of the ryanodine receptor to the clamp-shaped structures adjacent to the FKBP binding sites. *The Journal of biological chemistry*, 278(16), 14211–14218. https://doi.org/10.1074/jbc.M213164200

Zhang, L., Kelley, J., Schmeisser, G., Kobayashi, Y. M., & Jones, L. R. (1997). Complex formation between junctin, triadin, calsequestrin, and the ryanodine receptor. Proteins of the cardiac junctional sarcoplasmic reticulum membrane. *The Journal of biological chemistry*, 272(37), 23389–23397. https://doi.org/10.1074/jbc.272.37.23389

Zhang, Y., Chen, H. S., Khanna, V. K., De Leon, S., Phillips, M. S., Schappert, K., Britt, B. A., Browell, A. K., & MacLennan, D. H. (1993). A mutation in the

human ryanodine receptor gene associated with central core disease. *Nature genetics*, 5(1), 46–50. https://doi.org/10.1038/ng0993-46

Zhao, H., Piszczek, G., & Schuck, P. (2015). SEDPHAT--a platform for global ITC analysis and global multi-method analysis of molecular interactions. *Methods (San Diego, Calif.)*, 76, 137–148. https://doi.org/10.1016/j.ymeth.2014.11.012

Zhao, M., Li, P., Li, X., Zhang, L., Winkfein, R. J., & Chen, S. R. (1999). Molecular identification of the ryanodine receptor pore-forming segment. *The Journal of biological chemistry*, 274(37), 25971–25974. https://doi.org/10.1074/jbc.274.37.25971

Zheng, J., Wenzhi, B., Miao, L., Hao, Y., Zhang, X., Yin, W., Pan, J., Yuan, Z., Song, B., & Ji, G. (2010). Ca(2+) release induced by cADP-ribose is mediated by FKBP12.6 proteins in mouse bladder smooth muscle. *Cell calcium*, 47(5), 449–457. https://doi.org/10.1016/j.ceca.2010.03.006

Zhou, H., Lillis, S., Loy, R. E., Ghassemi, F., Rose, M. R., Norwood, F., Mills, K., Al-Sarraj, S., Lane, R. J., Feng, L., Matthews, E., Sewry, C. A., Abbs, S., Buk, S., Hanna, M., Treves, S., Dirksen, R. T., Meissner, G., Muntoni, F., & Jungbluth, H. (2010). Multi-minicore disease and atypical periodic paralysis associated with novel mutations in the skeletal muscle ryanodine receptor (RYR1) gene. *Neuromuscular disorders: NMD*, 20(3), 166–173. https://doi.org/10.1016/j.nmd.2009.12.005

Zima, A. V., & Blatter, L. A. (2004). Inositol-1,4,5-trisphosphate-dependent Ca(2+) signalling in cat atrial excitation-contraction coupling and arrhythmias. *The Journal of physiology*, 555(Pt 3), 607–615. https://doi.org/10.1113/jphysiol.2003.058529

Zissimopoulos, S., & Lai, F. A. (2005). Interaction of FKBP12.6 with the cardiac ryanodine receptor C-terminal domain. *The Journal of biological chemistry*, 280(7), 5475–5485. https://doi.org/10.1074/jbc.M412954200

Zissimopoulos, S., Seifan, S., Maxwell, C., Williams, A. J., & Lai, F. A. (2012). Disparities in the association of the ryanodine receptor and the FK506-binding proteins in mammalian heart. *Journal of cell science*, 125(Pt 7), 1759–1769. https://doi.org/10.1242/jcs.098012

Zissimopoulos, S., Thomas, N. L., Jamaluddin, W. W., & Lai, F. A. (2009). FKBP12.6 binding of ryanodine receptors carrying mutations associated with arrhythmogenic cardiac disease. *The Biochemical journal*, 419(2), 273–278. https://doi.org/10.1042/BJ20082324

Zorzato, F., Fujii, J., Otsu, K., Phillips, M., Green, N. M., Lai, F. A., Meissner, G., & MacLennan, D. H. (1990). Molecular cloning of cDNA encoding human and rabbit forms of the Ca2+ release channel (ryanodine receptor) of skeletal muscle sarcoplasmic reticulum. *The Journal of biological chemistry*, 265(4), 2244–2256.